# EXTENSION OF EFFORT FOR LUNAR FLIGHT HANDBOOK

## Detailed Technical Report

**ER 13550-III**

**December 1964**

Prepared by

F. A. Santora
R. G. Salinger
G. Kovatch
J. G. Gegner

MARTIN
BALTIMORE DIVISION
BALTIMORE, MARYLAND 21203

## FOREWORD

This report has been prepared by the Baltimore Division of the Martin Company under Contract NAS 8-5031 with George C. Marshall Space Flight Center of the National Aeronautics and Space Administration. The primary purpose of this report is to extend the effort of the Orbital and Lunar Flight Handbooks (NASA SP 33 & 34, 1963) that were issued under the same contract; the results are to be incorporated into the subject manuals at a later date.

Symbols and terminology used in this report agree as closely as possible to the nomenclature adopted in the referenced handbooks.

The Martin Company Program Manager for this project has been Mr. Leonard Sternfield, and Mr. Frank Santora has been Technical Director.

The MSFC contract management panel consisted of the following members:

Conrad D. Swanson (Chairman)
Edward E. Waggoner (Cochairman)
William R. Perry (Chairman Pro Tem)
Harry O. Ruppe (Director)
James W. Russel
Rodney D. Wood
Joseph C. King
Daniel T. Martin
Robert M. Coulter

CONTENTS


| | | Page |
|---|---|---|
| | Foreword | iii |
| | Contents | v |
| I. | "Moon-to-Earth" Orbital Departure Windows | I-1 |
| | A. Introduction | I-1 |
| | B. Problem Definition | I-6 |
| | C. Method of Approach | I-14 |
| | D. Results | I-26 |
| | E. Mission Implications | I-57 |
| | F. References | I-60 |
| II. | Stability and Mission Potential of the Libration Points in the Earth-Moon System | II-1 |
| | A. Introduction | II-1 |
| | B. General Discussion | II-3 |
| | C. Stability of Libration Points in the Restricted Three-Body Problem | II-5 |
| | D. The Elliptic Restricted Three-Body Problem | II-14 |
| | E. Numerical Study of Perturbations on the Restricted Three-Body Problem | II-21 |
| | F. References | II-26 |
| III. | Lunar Orbit Estimation | III-1 |
| | Summary | III-1 |
| | A. Introduction | III-1 |
| | B. Observation Matrix | III-5 |
| | C. State Transition Matrix | III-8 |

CONTENTS (continued)


Page

D. Starting the Estimation Procedure . . . . . III-9

E. Confidence Hyperellipses and the Covariance Matrix P . . . . . III-11

F. Onboard Versus Earth Based Computations . . . . . III-16

G. Digital Program Logic . . . . . III-17

H. Results and Conclusions . . . . . III-18

I. Supplementary Derivations . . . . . III-19

J. References . . . . . III-26

IV. Lunar Orbiter Theory . . . . . IV-1

A. Introduction . . . . . IV-1

B. Secular Perturbations . . . . . IV-3

C. Results . . . . . IV-8

D. Orbital Stability . . . . . IV-8

E. Lunar Satellite Data . . . . . IV-10

F. References . . . . . IV-11

V. Orbital Operations (Prepared as an addenda to the Lunar Flight Handbook) . . . . . V-1

A. Earth Orbit Operations . . . . . V-2

B. Lunar Orbit Operations . . . . . V-13

C. Mission Implications . . . . . V-25

# I. MOON-TO-EARTH ORBITAL DEPARTURE WINDOWS

by R. G. Salinger

## A. INTRODUCTION

Future manned missions, such as lunar logistics, lunar exploration and lunar surveillance, now envision extended stay times in parking orbits both at earth and at the moon. The use of such parking orbits depends on the mode of operation for conducting the missions. For example, rendezvous and assembly may be required prior to departing for the moon; then, upon arrival at the moon, supplies and personnel may have to be transferred to the lunar surface. The questions arise, in normal operations, what is the available time to complete work tasks? What is the wait time before the next opportune go time if tasks cannot be completed on time, etc. ? Naturally, the questions also arise as to what are the consequences if the time in parking orbit must be prolonged in the event of an unplanned delay or malfunction? Can the mission be successfuly carried through and at what cost?

Thus, the problem at hand is to determine mission departure windows and their requirements. Departure windows connote the available length of time that missions can be originated from a parking orbit with a given propulsion allowance.

For lunar missions, departure window studies can be divided into two areas: those related to earth departures and those associated with lunar departures.

Reference 1 presents a detailed study of earth departure windows and their requirements as affected by various mission constraints. Investigations were conducted for the years 1969 to 1978 in which the number of windows and their sizes, wait times between windows, and the number of possible injections within a window were ascertained.

The purpose of the following discussion is to present a complementary study to Ref. 1 by investigating those requirements associated with lunar departures. In fact, end point conditions of the Ref. 1 study, such as the approach geometry at the moon, are taken as initial conditions in the present study to assure continuity.

Chapter IX of Ref. 2 discusses the injection requirements for returning to earth from the moon. In the referenced chapter, it is recognized that there are two basic methods for achieving the required injection conditions: first, by means of a direct departure, wherein the spacecraft is "boosted" directly from the lunar surface to the transearth injection point; and, secondly, by the "orbital departure" method. This latter method employs the use of a parking orbit prior to injection. However, Chapter IX (Ref. 2) assumes that injection takes place during the first parking orbit and consequently does not consider ramifications of a "missed" or delayed injection explicitly. At present, the consequences

of a "missed" injection can be determined with hand computations by utilizing the transearth trajectory catalog (Chapter IX) together with appropriate charts in Chapter XI (Ref. 2). This approach is most lengthy and tedious and somewhat difficult if some of the facets of the planning charts and the physical picture are unknown. Thus, a person experienced to only a small degree with the aspects of the entire problem would certainly encounter trouble in attempting to resolve it. Therefore, the purpose of the study presented in this chapter is twofold:

(1) To perform a detailed study which investigates the consequences of a "missed" injection, thereby clearly determining effective orbital operation and serving as an aid to develop future mission concepts.

(2) To provide a source of information to be incorporated at a later date. The object is to eliminate the existing weakness of the need of tedious calculations by presenting specific results and a simple means of obtaining them.

It is important to note that a "missed" injection can be unintentional or completely deliberate. In the former case, it may be impossible to inject at the proper moment because of system malfunctions, incomplete checkouts, etc., and the spacecraft must wait until the next opportune go time. Deliberate postponement of injection may be dictated by the mission itself. For example, consider a logistics vehicle that arrived from earth and entered a lunar orbit. While in this orbit, the "shuttling" of supplies to the lunar surface may take longer than anticipated, thereby delaying the transearth injection. As another example, assume that the following mission specification exists: "Rendezvous with 'earth orbiting' space station upon return from the moon." It now becomes obvious that injection must be delayed until it is possible to establish a transearth trajectory which arrives coplanar with the space-station's orbit at earth.

In all of the above cases, it becomes mandatory to determine the flexibility of the spacecraft to adjust or compensate for these delays. Thus, departure windows and frequencies must be established which take into account the gravitational and geometrical constraints but which are of such a generalized nature that they represent various types of missions.

## LIST OF SYMBOLS

| | |
|---|---|
| A | True longitude of the moon in the moon's orbital plane measured eastward from $\gamma_{\mathbb{C}}$ (deg) |

| | |
|---|---|
| a | Semimajor axis of the moon's orbit around the earth (km) (60.2665 ER) |
| B | True longitude of descending node of the lunar parking orbit in the moon's orbital plane measured from $\gamma_{\mathbb{C}}$ (deg) |
| ER | Earth radius (6378.165 km) |
| $\overrightarrow{EML}$ | Earth-moon line |
| e | Eccentricity of the moon's orbit around the earth |
| $h_{PE}$ | Perigee altitude of transearth trajectory (km) |
| $h_{PL}$ | Altitude of the lunar parking orbit above the lunar surface (km) |
| $i_{eq\mathbb{C}}$ | Inclination of lunar parking orbit plane to the lunar equatorial plane (deg) |
| $i_{eq\oplus}$ | Inclination of transearth trajectory plane to the earth's equatorial plane (deg) |
| $i_{eqM}$ | Inclination of the lunar equatorial plane to the moon's orbital plane (deg) |
| $i_{MOP}$ | Inclination of the moon's orbital plane to the earth equatorial plane (deg) |
| $i_m$ | Inclination of the lunar parking orbit plane to the moon's orbital plane (deg) |
| $i_{VTE}$ | Inclination of the vehicle's transearth trajectory plane to moon's orbital plane (deg) |
| $i_{\oplus R}$ | $180° - i_{VTE}$ |
| $J_{2\mathbb{C}}$ | Second-order zonal harmonic coefficient in the expansion of the gravitational potential of the moon ($2.1 \times 10^{-4}$) |
| M | Mean anomaly of the moon |
| MOP | Moon's orbital plane |
| $R_{\oplus\mathbb{C}}$ | Earth-moon distance (km) |
| $R_{\mathbb{C}}$ | Moon's equatorial radius (1738.946 km) |
| $t_p$ | Flight time from translunar injection at earth to pericynthion altitude at the moon (hr) |

| | |
|---|---|
| $t_f$ | Flight time from transearth injection to return earth perigee (hr) |
| $t_s$ | Stay time in lunar parking orbit, time between insertion into orbit and ejection from orbit (hr) |
| $V_{\mathbb{C}}$ | Velocity of a spacecraft at the time of transearth injection (km/sec) |
| $V_{\mathbb{C}c}$ | Velocity of a spacecraft in a circular orbit around the moon (km/sec) |
| $V_{\oplus c}$ | Velocity of a vehicle in a circular orbit around the earth (km/sec) |
| $\beta_{\mathbb{C}T}$ | True position of the moon relative to ascending node of the lunar orbit on the earth's equatorial plane (deg) |
| $\beta_{\mathbb{C}\gamma}$ | Angle from the ascending node of the lunar orbit in the earth's equatorial plane to $\gamma_{\mathbb{C}}$ (deg) |
| $\dot{\beta}_M$ | Angular velocity of the spacecraft in the lunar parking orbit (deg/sec) |
| $\beta_{\mathbb{C}}$ | Angular position of the moon measured from the ascending node of the lunar orbit on the earth's equator (deg) |
| $\beta_M$ | Vehicle's injection position in the lunar parking orbit measured positive to the north from the descending node of the lunar parking orbit on the moon's orbital plane (deg) |
| $\beta_{M0}$ | Transearth injection position of vehicle in Lunar parking orbit |
| $\gamma$ | Inclination of the moon's orbital plane to the ecliptic plane (deg) |
| $\gamma_{\mathbb{C}\oplus}$ | Moon's orbital flight path angle relative to the earth (deg) |
| $\Upsilon_{\mathbb{C}}$ | Direction of intersection of descending node of the lunar orbit and the ascending node of lunar equator |
| $\Upsilon_{\oplus}$ | Direction of vernal equinox |
| $\gamma_{\mathbb{C}}$ | Flight path angle of transearth injection velocity vector (deg) |
| $\Delta A_{\mathbb{C}}$ | Azimuth change in lunar parking orbit required to obtain $\theta_{MTE}(go)$ (deg) |

| | |
|---|---|
| $\Delta A_{\oplus}$ | Azimuth change in earth parking orbit required for rendezvous (km/sec) |
| $\Delta V_{m\mathbb{C}}$ | Velocity impulse required to maneuver in lunar parking orbit to perform azimuth change $\Delta A_{\mathbb{C}}$ (km/sec) |
| $\Delta V_{E}$ | Velocity impulse required to enter a circular parking orbit at the return earth perigee (km/sec) |
| $\Delta V_{m\oplus}$ | Velocity impulse required to maneuver in earth parking orbit in order to perform rendezvous (km/sec) |
| $\Delta\theta$ | Angle between earth-moon line and line-of-nodes of the transearth trajectory (deg) |
| $\epsilon$ | Obliquity, inclination of the earth equatorial plane to the ecliptic plane (deg) |
| $\theta_0$ | Angular position of return earth perigee relative to moon's orbital plane measured along return trajectory (deg) |
| $\theta_{MTE\ (go)}$ | Value of $\theta_{MTE}$ at the time of transearth injection (deg) |
| $\theta_{MTE}$ | Longitude angle measured eastward from the $\overrightarrow{MEL}$ to the ascending node of the lunar orbit, or measured eastward from the $\overrightarrow{EML}$ to the descending node of the lunar orbit (deg) |
| $\dot{\theta}_{\oplus\mathbb{C}}$ | Angular velocity of earth-moon line (rad/sec) |
| $\theta_T$ | True anomaly of the moon (deg) |
| $\Lambda_{eq\mathbb{C}}$ | Longitude of the descending node of the lunar parking orbit in the lunar equatorial plane from $\gamma_{\mathbb{C}}$ (deg) |
| $\mu_{\oplus}$ | Gravitational constant of the earth (398,606.4 $km^3/sec^2$) |
| $\Omega_{eq\mathbb{C}} = \frac{d\Lambda_{eq\mathbb{C}}}{dt}$ | Constant nodal regression rate of the lunar parking orbit in the lunar equatorial plane (deg/nodal period) |
| $\Omega_{MOP}$ | Right ascension of the ascending node of the lunar orbit. |
| $\Omega_{\Delta\oplus}$ | Right ascension of the ascending node of the transearth trajectory (deg) |
| $\Omega_{\Delta\mathbb{C}}$ | Longitude of the descending node of the transearth trajectory relative to the ascending node of the moon's orbital plane and measured in the moon's orbital plane (deg) |

| | |
|---|---|
| $\Omega$ | Angle between the right ascension of the ascending node of the lunar orbit and the ascending or descending node of the transearth trajectory on the earth's equatorial plane at perigee (deg) |
| $\Omega_{S\oplus}$ | Right ascension of the ascending node of the earth orbiting station orbit (deg) |
| $\omega_{\oplus}$ | Angle between the moon's orbital plane and earth's equatorial plane along the transearth trajectory at perigee ($0° \leq \omega_{\oplus} \leq 180°$) |
| $\omega_{\Delta\oplus}$ | Argument of perigee of the transearth trajectory relative to earth's equatorial plane |
| $\omega_{\oplus\mathbb{C}}$ | Perpendicular component of angular velocity of earth-moon line (rad/sec) |
| $\omega_{\mathbb{C}\odot}$ | Argument of perigee of moon relative to ecliptic plane (deg) |
| $\omega_{\mathbb{C}\oplus}$ | Argument of perigee of the moon's orbit relative to the earth's equatorial plane (deg) |
| $\mathbb{C}$ | Mean longitude of the moon (deg) |
| $\Gamma'$ | Mean longitude of the lunar orbit perigee (deg) |
| $\Omega$ | Longitude of the mean ascending node of the lunar orbit (deg) |
| $\Omega_{\mathbb{C}}$ | Longitude of the mean descending node of the lunar orbit (deg) |

## B. PROBLEM DEFINITION

The present problem of determining lunar orbiter departure windows is concerned with that class of missions originating from a lunar parking orbit and terminating in an earth re-entry or earth parking orbit. In initiating a transearth mission, the spacecraft must acquire a specific position and velocity vector at the time of injection into a transearth trajectory. After the transearth injection, the vehicle is in ballistic flight until arrival at the earth, at which time all specified mission constraints are met. As mentioned before, delayed transearth injections can be intentional or unintentional. For example, if a system malfunction necessitates postponing the injection, it is obvious that the delay is not by design. In contrast, it can also be foreknowable that completion of certain tasks may not be accurately predictable and delays are to be expected. In either case, mission flexibility can be greatly enhanced if provisions are incorporated to allow for such contingencies.

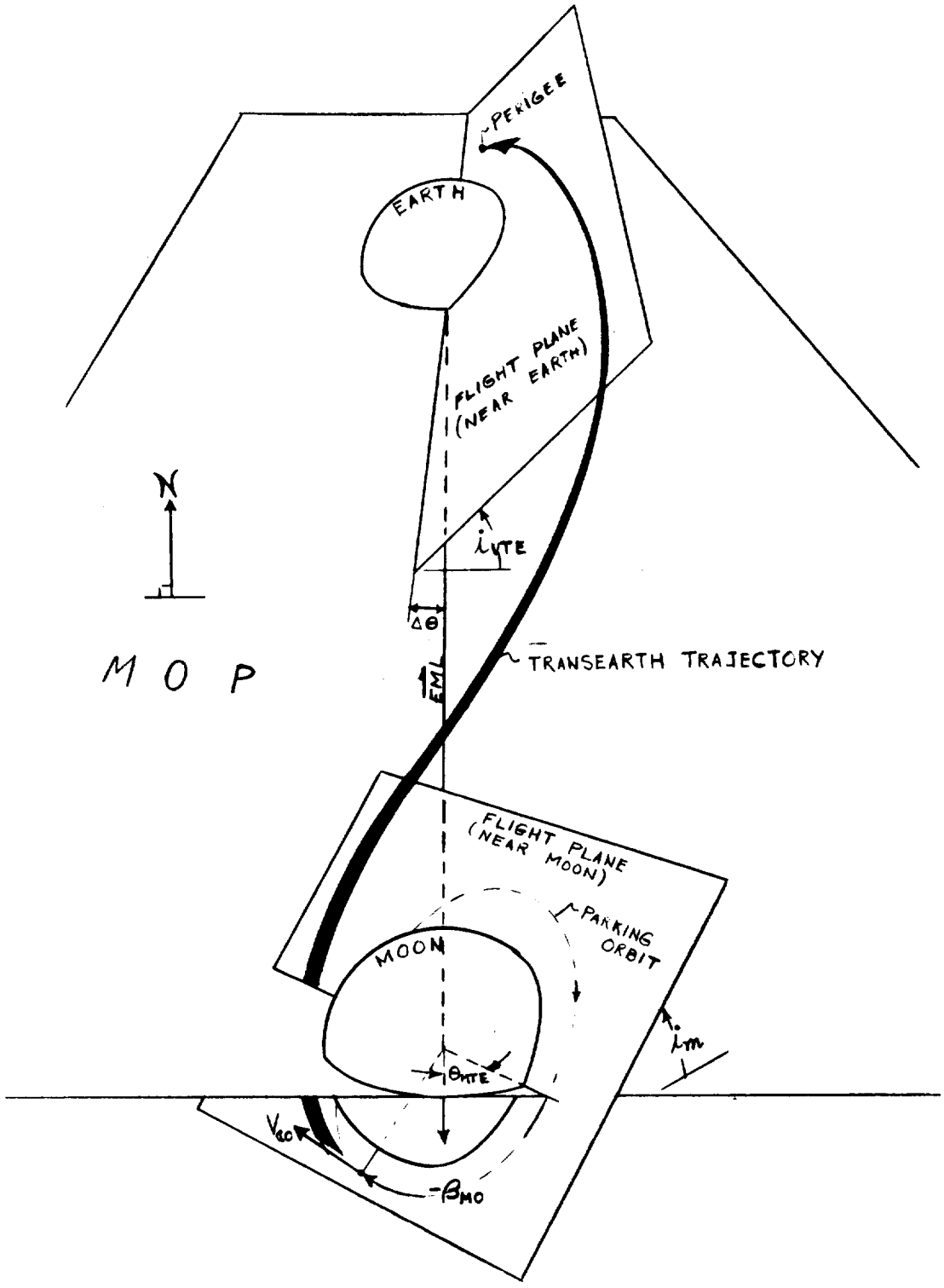


Sketch 1. Transearth Trajectory Geometry

Sketch 1 has been prepared to aid in the visualization of the trajectory parameters associated with transearth missions.

Prior to establishing the transearth trajectory, the spacecraft is located in a lunar parking orbit as shown in Sketch 1. The lunar parking orbit plane (POP) is inclined to the moon's orbital plane (MOP) by an angle $i_m$. The MOP is a plane of symmetry and is chosen as a reference plane because it generalizes trajectory data and lends itself readily to the clarification of the problem. Immediately after injection into the transearth trajectory the transearth flight plane has the same inclination to the MOP as did the POP, i.e., $i_m$. Upon nearing earth, however, the transearth trajectory plane will have a different inclination relative to the MOP, namely, $i_{VTE}$.

An interesting phenomena of transearth trajectories employing this model is the fact that the included angle $\Delta\theta$ (Sketch 1) at the time of arrival ($t_f$) is small in magnitude--approximately 1° for a wide spectrum of missions. This fact was used in the development of iteration schemes, to be discussed presently, for satisfying certain mission constraints.

## 1. Geometrical Considerations

As a first step in defining the departure window problem, consider that the spacecraft is in a circular orbit around the moon. The vehicle may have been placed into this lunar orbit either at the terminal phase of a translunar trajectory, or after ascending from the lunar surface possibly at the conclusion of a lunar landing and exploratory operation.

The orientation of the orbit is illustrated in Sketch 2, which shows the lunar ground trace of the circular orbit, called the "parking orbit." The reference plane is the moon's orbital plane (MOP) and the reference direction is the earth-moon line ($\overline{EML}$). At a given instant, the parking orbit has an inclination of $i_m$ ($0° \leq i_m \leq 90°$) relative to the MOP, and the descending node of the parking orbit is located at an angular distance of $\theta_{MTE}$ measured positively from the $\overline{EML}$ eastward to the descending node of the parking orbit--or eastward from the moon-earth line ($\overline{MEL}$) to the ascending node of the parking orbit. This angle ($\theta_{MTE}$) has been more commonly referred to as the "longitude angle" of the parking orbit. "North" is defined as the direction of the angular momentum vector of the moon's orbital motion around the earth. The parking orbit depicted in Sketch 2 is retrograde (i.e., moving from "east to west," where east is in the direction of the moon's motion in its orbit about the earth. The position of the spacecraft in this orbit at the same instant is given by $\beta_M$ and is measured positively toward the north from the descending node. Thus, the orientation of the parking orbit relative to the MOP is given by $i_m$, $\theta_{MTE}$ and the vehicle's

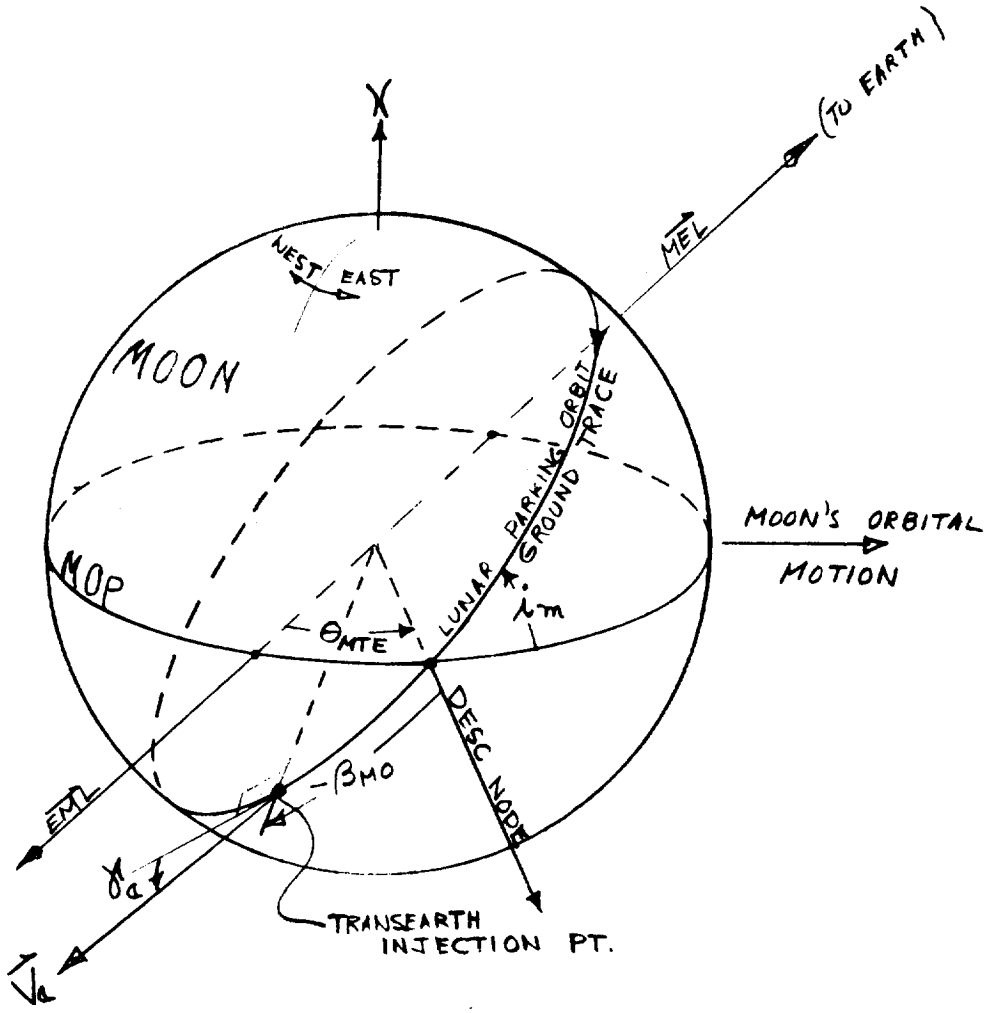


Sketch 2. Lunar Orbit Departure Geometry

position in orbit by $\beta_M$. As the spacecraft progresses in orbit, it will eventually reach a point where injection can be initiated such that the desired return to earth is realized. The complete specification of injection conditions after the spacecraft has been accelerated is given by $\theta_{MTE}$, $i_m$, $\beta_{M0} = \beta_M$ (at injection), $V_{\mathbb{C}0}$ (transearth injection velocity), $h_{PL}$ (injection altitude) and $\gamma_{\mathbb{C}0}$ (elevation of velocity vector).

Thus far, the nomenclature and geometry of the static problem have been given. If, however, a transearth injection does not take place, the possibility of a future injection depends on the future orientation of the moon and of the lunar parking orbit. In order to define the dynamic situation, which is most important in determining departure windows, Sketch 3 has been prepared. Referring to this figure, consider a celestial sphere centered at the earth, with the celestial north pole an extension of the earth's north pole. The moon's orbital plane (MOP) is inclined to the celestial equator by the angle $i_{MOP}$. The moon itself (at a specific time) is located at a central angle $\beta_{\mathbb{C}}$ measured from the ascending node of the moon's orbit. At the same time, the lunar parking orbit has the aforementioned orientation ($i_m$, $\theta_{MTE}$). If injection were to take place at this time, the resultant transearth trajectory plane has its line of nodes displaced from the $\overrightarrow{EML}$ (at injection) by an angular distance $\Delta\theta$.

When the vehicle nears earth, the inclination of its trajectory plane relative to the MOP is $i_{VTE}$; but because of the inclination $i_{MOP}$ and the lunar position ($\beta_{\mathbb{C}}$) at injection, the trajectory plane has a different inclination relative to the equatorial plane--namely, $i_{eq\oplus}$. It is this parameter ($i_{eq\oplus}$) that is a major constraint on the return flight, since the best use of tracking facilities depends on it. Furthermore, specific landing sites for direct reentries may require certain "inclined" approaches, and, most apparent, the establishment of proper inclinations for earth orbit rendezvous purposes.

Now, if the transearth injection does not take place at this time and is delayed, the moon continues to move at a nonlinear rate in its elliptical orbit (eccentricity $\approx 0.0549$) about the earth.

Thus, $\theta_{MTE}$, which is referenced to the $\overrightarrow{EML}$, and $\beta_{\mathbb{C}}$, which defines the position of the moon, will vary in a nonlinear fashion. Simultaneously, the nodal line of the lunar parking orbit regresses at a nonlinear rate, $\dot{\Omega}_{MOP}$, relative to the MOP. This can be better visualized

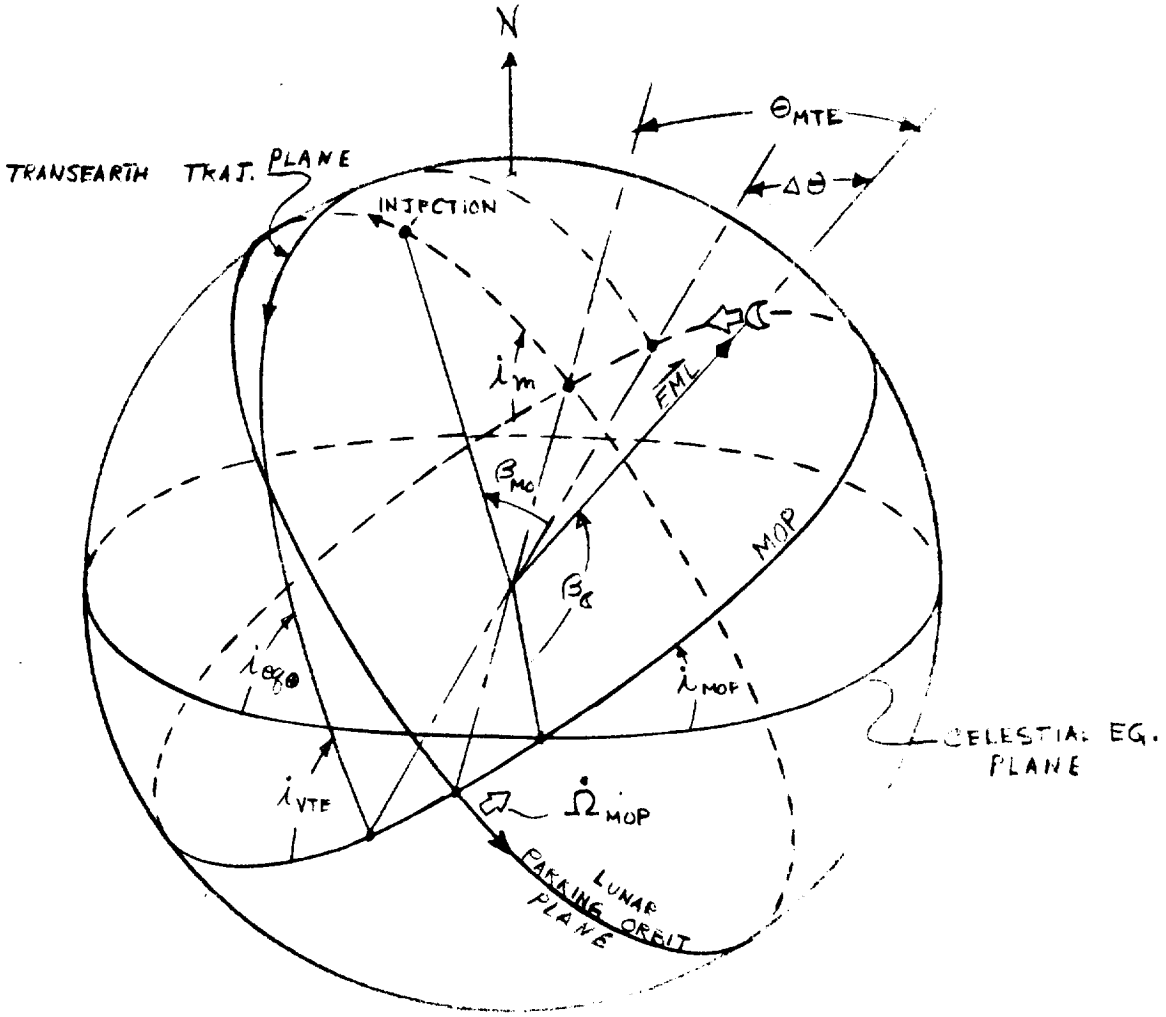


Sketch 3. Problem Geometry

by referring to Sketch 4 which shows the orientation of the true lunar equatorial plane, the lunar parking orbit plane (POP), and the moon's orbital plane (MOP). The lunar parking orbit regresses in the direction shown for a retrograde orbit at a constant average rate, $\dot{\Omega}_{eq\mathbb{C}}$, relative to the lunar equatorial plane (assuming first order secular changes only). However, since the MOP is inclined approximately 6.71° ($i_{eqM}$) to the lunar equator, the nodal regression of the lunar parking orbit is nonlinear relative to the MOP. The first order secular change in the inclination of the parking orbit relative to the lunar equatorial plane, $i_{eq\mathbb{C}}$, is 0, but the inclination $i_m$ relative to the MOP varies nonlinearly due to $i_{eqM}$. Thus, if the injection takes place at a later time, the elements $i_m$, $\theta_{MTE}$, and $\beta_{\mathbb{C}}$ must be updated. It naturally follows that the return earth trajectory inclinations, $i_{VTE}$, relative to the MOP, and $i_{eq\oplus}$, relative to the earth equator also vary. Lunar departure windows are then established by the injection velocity requirements at the moon and the return velocity at earth which vary with these elements and by the practical ranges of the elements.

## 2. Ground Rules

The exactness of any study depends on the stated ground rules and assumptions. Having defined the problem at hand in the above discussion, it now becomes necessary to list the suppositions with which the study was conducted.

(1) The first ground rule specifies that both the lunar parking orbit and the earth return parking orbit are assumed circular, with the lunar altitude ($h_{PL}$) at 185.2 km and the earth altitude ($h_{PE}$) at 588 km. This latter altitude is also equal to the earth return perigee altitude or the altitude of the earth orbiting space station when considered.

(2) It is assumed that the period of the lunar parking orbit ($\tau_{\mathbb{C}}$) is constant which implies that the rate of change of the position of the spacecraft in its orbit ($\dot{\beta}_M$) is also constant.

(3) The transearth injection takes place in the same direction as the spacecraft's motion in its lunar orbit, and, thus, no turns are made during the transearth injection phase. In this study, only retrograde lunar orbits are considered.

(4) The eccentricity of the moon's elliptical orbit about the earth is assumed constant (e = 0.0549). Furthermore, it is assumed that the moon's mean orbital elements as presented in Ref. 3 can be used to adequately describe the moon's motion.

(5) All maneuvers (injection or otherwise) are purely "impulsive" changes.

(6) Once the spacecraft is injected onto the transearth trajectory, inclination changes are prohibited ($\Delta i_{VTE} = 0$) unless a rendezvous with an earth space station is desired. This ground rule assumes that the transearth trajectory satisfies all mission specifications except, possibly, that of "timing" the re-entry point at earth. For the purposes of the study, "timing" maneuvers along the transearth trajectory are also prohibited.

(7) Every transearth trajectory is to satisfy a single specified $i_{eq\oplus}$ and all returns to earth are direct with the earth's rotation. This rule is made to reduce the amount of data output to a practical level; it is for this reason that the selection of $i_{eq\oplus}$ should be of versatile application. At present, it is felt that a value of $i_{eq\oplus} = 30°$ is of most interest. This value is representative of tracking projection for the next decade for flights over the AMR and PMR. In addition, an $i_{eq\oplus}$ of 30° would complement the earth parking orbit used for the translunar launch window study of Ref. 1. An $i_{eq\oplus}$ of 30° will also be used as the inclination of an earth orbiting space station for the rendezvous mission.

(8) Finally, it is assumed that a "patched-conic" trajectory approach which utilizes a spherical earth and a spherical moon and neglects nongravitational forces yields transearth trajectory data of sufficient accuracy for this study.

## 3. Mission Definitions

There are four missions which are of greatest concern to this study and are defined by the constraints imposed on the moon-to-earth trajectory. These constraints are:

(1) A constant inclination of the earth return trajectory relative to the earth equatorial plane ($i_{eq\oplus}$).

(2) A constant flight time from lunar injection to earth return perigee ($t_f$).

(3) An orientation of the earth return trajectory such that a rendezvous is possible with another spacecraft already in an earth parking orbit.

The missions are then defined as:

| Mission | Constraints |
|---|---|
| I | (1) |
| II | (1) and (3) |
| III | (1) and (2) |
| IV | (1), (2) and (3) |

Mission I ($i_{eq\oplus}$ = constant) can also be interpreted as a return to earth with a direct atmospheric re-entry without recourse to an intermediate earth parking orbit. This same interpretation can be applied to Mission III ($i_{eq\oplus}$ = constant; $t_f$ = constant) as well. Missions II and IV require an earth parking orbit in order to satisfy constraint(3). It has been found from previous studies (Ref. 2) that constraint (1) ($i_{eq\oplus}$ = constant) can be satisfied by adjusting the injection position, $\beta_M$. That is, the spacecraft remains in its lunar parking orbit until it reaches the proper $\beta_M$, at which time injection into the transearth trajectory takes place. The particular $\beta_M$ will depend on the desired return inclination ($i_{eq\oplus}$), on the position of the moon ($\beta_{\mathbb{C}}$) (or time of the month), and on the inclination of the moon's orbital plane relative to the earth equatorial plane ($i_{MOP}$ or year). No side-thrust maneuver in the lunar parking orbit is required to satisfy constraint (1). However, for the other two constraints, orbital side-thrust maneuvers are required. For example, in order to satisfy constraint (2), which involves a constant transearth flight time ($t_f$), the longitude of the lunar parking orbit node at injection, $\theta_{MTE}$, must be adjusted by a side-thrust maneuver. Furthermore, upon arrival at earth, the orientation of the earth return orbit may not be coplanar with a rendezvous orbit of another earth orbiting vehicle. Thus, a side-thrust maneuver is similarly required in the earth parking orbit to satisfy constraint (3) and make a rendezvous possible.

Therefore, a general mission sequence of events can now be outlined for clarity and is included in summary form on the next page.

## C. METHOD OF APPROACH

In Chapter IX of Ref. 2, a catalog of moon-to-earth trajectories can be found which was generated with the aid of a "patched-conic"

Sequence of Events

Missions

| Maneuver Impulse Nomenclature | I | II | III | IV |
|---|---|---|---|---|
| $\Delta V_{m\,\mathbb{C}}$ | | | 1. Adjust longitude ($\theta_{MTE}$) of lunar parking orbit node with a side-thrust maneuver. | 1. Adjust longitude ($\theta_{MTE}$) of lunar parking orbit node with a side-thrust maneuver. |
| $\Delta V$ | 1. Inject into transearth trajectory after attaining correct position ($\beta_M$) in the lunar parking orbit. | 1. Inject into transearth trajectory after attaining correct position ($\beta_M$) in the lunar parking orbit. | 2. Inject into transearth trajectory after attaining correct position ($\beta_M$) in the lunar parking orbit. | 2. Inject into transearth trajectory after attaining correct position ($\beta_M$) in the lunar parking orbit. |
| $\Delta V_E$ | *2. Brake into an earth parking orbit upon arrival at earth with a retro-thrust maneuver. | 2. Brake into an earth parking orbit upon arrival at earth with a retro-thrust maneuver. | *3. Brake into an earth parking orbit upon arrival at earth with a retro-thrust maneuver. | 3. Brake into an earth parking orbit upon arrival at earth with a retro-thrust maneuver. |
| $\Delta V_{m\,\oplus}$ | | 3. Adjust longitude of earth parking orbit node with a side-thrust maneuver for rendezvous compatibility with an earth orbiting space station. | | 4. Adjust longitude of earth parking orbit node with a side-thrust maneuver for rendezvous compatibility with an earth orbiting space station. |

*Option: Directly re-enter earth's atmosphere without an intermediate earth parking orbit.

digital computer program entitled "Ejection from Launch Orbit." This program, which utilizes a spherical moon moving in a circular orbit about a spherical earth, has the moon's orbital plane as the plane of reference. In order to adapt this program to the Moon-to-Earth Departure Window Study, several areas of the actual physical situation were approximated and incorporated into the basic program.

## 1. Physical Considerations

The main item incorporated was that of the optical librations of the moon (Chapter III of Ref. 2). The optical libration in longitude is due to the fact that the moon moves in an elliptical orbit about the earth with the result that the earth-moon distance and the angular velocity of the earth-moon line are continuously changing. Thus, an observer on the earth is able to see around the east limb of the moon at one time and around the west limb at some later time. The optical libration in longitude is important in the Departure Window Study since it causes the moon's position, $\beta_{\mathbb{C}}$, and the longitude of the lunar parking orbit, $\theta_{MTE}$, to vary nonlinearly with time. It is apparent from this that the departure windows will not all have the same length in time, nor will they occur at any regular increment in time (i.e., the waiting times between departure windows will vary).

The optical libration in latitude is due to the fact that the lunar equatorial plane is inclined to the moon's orbital plane at a constant angle of 6.71° ($i_{eq_M}$). Thus, it is possible to see beyond the northern and southern limbs of the moon at different times from the earth. The result of this inclination between the two planes is that the inclination of the lunar parking orbit relative to the moon's orbital plane, $i_m$, and longitude of the lunar parking orbit, $\theta_{MTE}$, will both vary nonlinearly with time. These variations in the lunar parking orbit orientation cause variations in the energy required to meet the mission constraints which in turn determine the departure windows.

An approximation to the elliptical motion of the moon about the earth was taken as follows. In Ref. 3, the mean orbital elements of the moon are given as a series function of Julian century after the Epoch Date (1900 January 0.5 E.T. = J.D. 2415020). Therefore, given the date of the initial desired injection, the mean position of the moon can be computed at that time and also at any later time. These mean orbital elements are presented pictorially in Sketch 5 and are defined as follows:

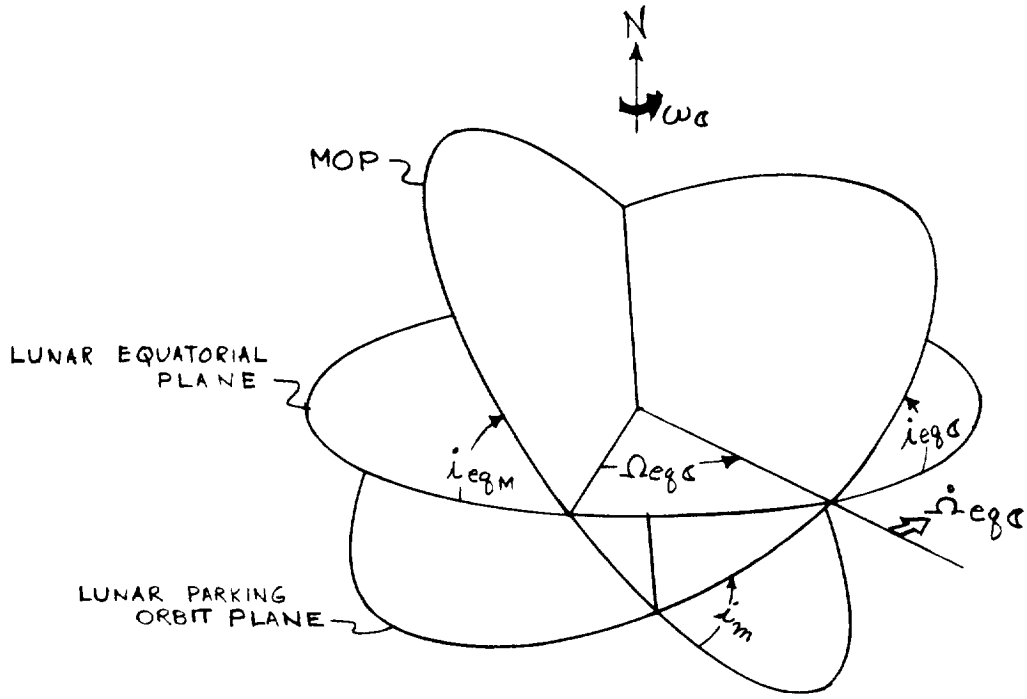


Sketch 4. Principal Reference Plan

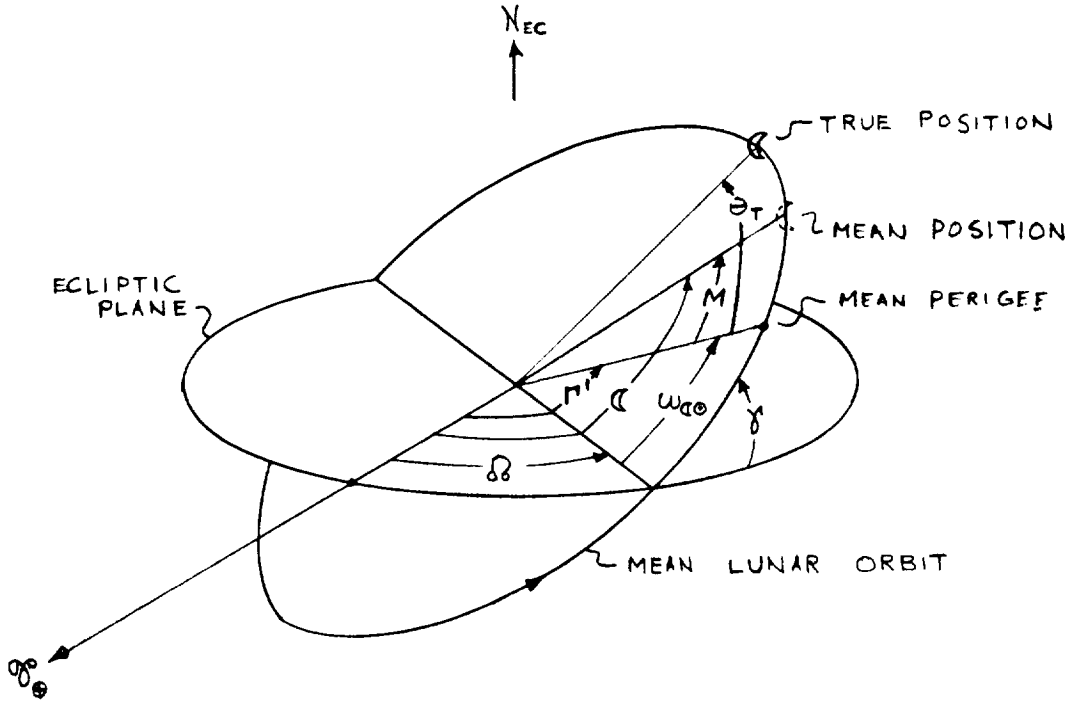


Sketch 5. Mean Lunar Orbital Elements

$\mathbb{C}$ = the mean longitude of the moon, measured in the ecliptic from the mean equinox of date ($\Upsilon_\oplus$) to the ascending node of the lunar orbit, and then along the orbit.

$\Gamma'$ = the mean longitude of the lunar perigee, measured in the ecliptic from the mean equinox of date to the mean ascending node of the lunar orbit, and then along the orbit.

$\Omega$ = the longitude of the mean ascending node of the lunar orbit on the ecliptic measured from the mean equinox of date.

From these three elements, other important elements can be defined:

$\Omega_{\mathbb{C}}$ = $\Omega + 180°$ = longitude of the mean descending node of the lunar orbit measured along the ecliptic from $\Upsilon_\oplus$.

M = $\mathbb{C} - \Gamma'$ = mean anomaly of moon.

$\omega_{\mathbb{C}\odot}$ = $\Gamma' - \Omega$ = argument of perigee of the moon relative to the ecliptic plane.

## 2. Problem Formulation

In the generation of departure windows with specified constraints, it becomes necessary to determine the "true" position of the moon from the near-orbital elements, i.e., $\overrightarrow{EML}$ and $|\overrightarrow{EML}|$. In addition, the orientation of the MOP relative to the earth's equator and the orientation of the lunar equator relative to the MOP must be known. Before proceeding to the derivation of these parameters plus other pertinent geometry, Sketch 6 is presented for clarification and convenience.

This sketch presents the overall problem geometry by giving the orientation of the moon's orbital plane, the earth equatorial plane, the ecliptic plane, the lunar equatorial plane and the lunar parking orbit plane in a moon-centered reference. In addition, the referenced directions used in the study are the mean vernal equinox ($\Upsilon_\oplus$), and $\Upsilon_{\mathbb{C}}$; the common intersection of the lunar equator, ecliptic and MOP; or more precisely, the intersection of the lunar descending node and the ascending node of the lunar equator in the ecliptic plane.

Also included are the previously defined parameters: $I = 1.5639°$ $\gamma = 5.1454°$, $i_{MOP}$, $\mathbb{C} - \Omega$, $\overrightarrow{EML}$, and $\beta_{\mathbb{C}}$.

With reference to Sketch 6, the detailed problem formulation can now be undertaken.

First, the angle $\beta_{\mathbb{C}\Upsilon}$ in the moon's orbital plane measured from the ascending node of the lunar orbit on the earth's equatorial plane to $\Upsilon_{\mathbb{C}}$ is determined from spherical trigonometry:

$$\beta_{\mathbb{C}\Upsilon} = \tan^{-1}\left[\frac{\sin \delta_{\mathbb{C}}}{\cos\gamma\cos\delta_{\mathbb{C}} - \sin\gamma\cot\epsilon}\right] \qquad (1)$$

where $\gamma$ is the almost constant (5.1454°) inclination of the moon's orbital plane relative to the ecliptic and $\epsilon$ is the obliquity (see Sketch 6, $\epsilon \approx 23.4445°$). With $\beta_{\mathbb{C}\Upsilon}$ known, two additional mean elements can be defined:

$\beta'_{\mathbb{C}} = \mathbb{C} - \delta_{\mathbb{C}} + \beta_{\mathbb{C}\Upsilon}$ = mean longitude of the moon measured in the moon's orbital plane from the ascending node of the lunar orbit on the earth's equator

$\omega_{\mathbb{C}\oplus} = \omega_{\mathbb{C}\odot} + \beta_{\mathbb{C}\Upsilon} + 180°$ = argument of perigee of the moon relative to the earth's equator

Assuming that the moon's orbit about the earth has a small constant eccentricity of 0.0549, a true anomaly can be determined by the use of a series expansion involving the mean anomaly, M, and the eccentricity, e. From Chapter III in Ref. 4, a very good approximation to the true anomaly can be obtained from:

$$\theta_T = M + 2e\sin M + \frac{5}{4}e^2\sin 2M + \frac{e^3}{12}(13\sin 3M - 3\sin M) + \ldots \qquad (2)$$

so that the true longitude of the moon is given by:

$$\beta_{\mathbb{C}} = \theta_T + \omega_{\mathbb{C}\oplus} . \qquad (3)$$

The inclination, $i_{MOP}$, and right ascension of the lunar orbit ascending node, $\Omega_{MOP}$, relative to the earth's equatorial plane can also be found with spherical trigonometry:

$$i_{MOP} = \cos^{-1}\left\{\cos\epsilon\cos\gamma + \sin\epsilon\sin\gamma\cos\delta_{\mathbb{C}}\right\} \qquad (4)$$

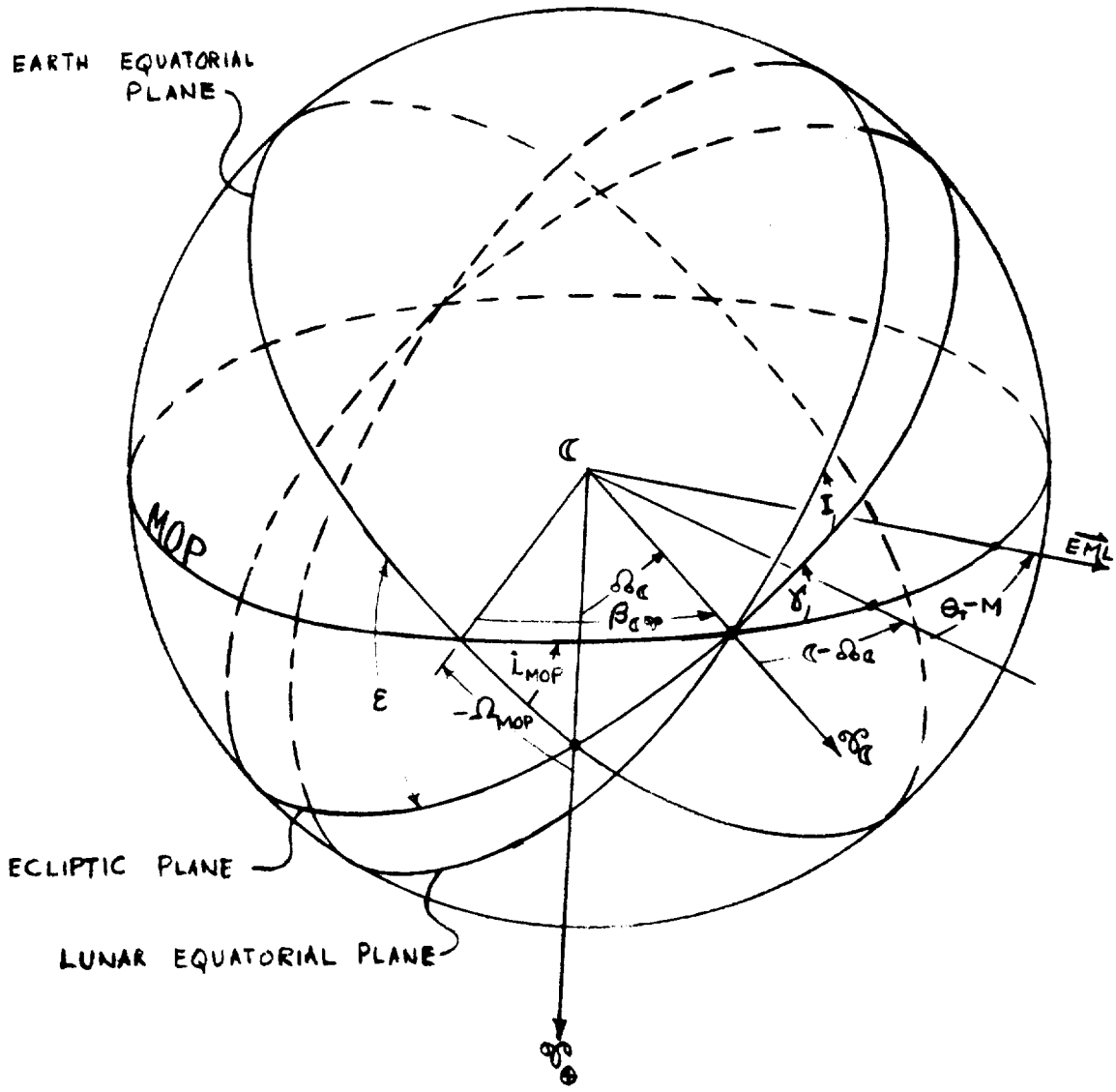


Sketch 6. Problem Geometry (Reference Plan orientations and reference directions)

$$\Omega_{MOP} = \cos^{-1}\left\{\frac{\cos\gamma - \cos i_{MOP}\cos\epsilon}{\sin i_{MOP}\sin\epsilon}\right\} \quad (5)$$

If the semimajor axis (a) of the moon's orbit is taken to be the average earth-moon distance of 60.2665 earth radii (ER), then the instantaneous value for the earth-moon distance is given by:

$$R_{\oplus\mathbb{C}} = \frac{a(1 - e^2)}{1 + e\cos\theta_T} \cdot \quad (6)$$

In addition, if the moon is assumed to be acted upon solely by the earth's gravitational potential, then the instantaneous angular velocity of the earth-moon line is given by

$$\dot{\theta}_{\oplus\mathbb{C}} = \left[\frac{\mu_\oplus(1 + e\cos\theta_T)}{R^3_{\oplus\mathbb{C}}}\right]^{1/2} \quad (7)$$

where $\mu_\oplus$ is the gravitational constant of the earth. Finally, the moon's orbital flight path angle relative to the earth is:

$$\gamma_{\mathbb{C}\oplus} = \cos^{-1}\left\{\left[\frac{a^2(1 - e^2)}{R_{\oplus\mathbb{C}}(2a - R_{\oplus\mathbb{C}})}\right]^{1/2}\right\} \cdot \quad (8)$$

Since the moon-to-earth trajectories were calculated assuming the moon in a circular orbit about the earth, the inputs were the instantaneous value of $R_{\oplus\mathbb{C}}$ and the perpendicular component ($\omega_{\oplus\mathbb{C}}$) of the instantaneous angular velocity, i.e.,

$$\omega_{\oplus\mathbb{C}} = \dot{\theta}_{\oplus\mathbb{C}}\cos\gamma_{\mathbb{C}\oplus} \cdot \quad (9)$$

The error between the elliptical and circular values of these elements exists for the flight time from transearth injection from the lunar parking orbit to the exit from the moon's volume of influence. For practical moon-to-earth flight times (50 to 100 hr), this flight time is between 10 and 20 hr. During this flight time, the earth-moon distance can change by 0.24 ER to 0.48 ER and the moon's angular velocity by 0.044 deg/hr to 0.088 deg/hr. However, as can be seen in Chapter IX of Ref. 2, errors of this magnitude have negligible effects on the energy requirements. The importance of including the variable $R_{\oplus\mathbb{C}}$ and $\omega_{\oplus\mathbb{C}}$ in the Departure Window Study lies in the fact that over an interval of 1 month, $R_{\oplus\mathbb{C}}$ will vary by approximately 8 ER, and $\omega_{\oplus\mathbb{C}}$ will vary by approximately 0.15 deg/hr.

Since this study is concerned with a time interval in a lunar parking orbit of at least 1 month, these variations are not negligible. Non-linearities in the width of departure windows are due in part to these variations.

It has been mentioned previously that the initial orientation of the lunar parking orbit is given by $i_m$, its inclination relative to the moon's orbital plane and by $\theta_{MTE}$, the longitude of its descending node relative to the earth-moon line. However, the orientation of the parking orbit relative to the lunar equatorial plane is also desired. Referring to Sketch 7 which is a repeated portion of Sketch 6, the following angles are defined.

$A = \beta_{\mathbb{C}} - \beta_{\mathbb{C}}\Upsilon$ = true longitude of the moon measured in the moon's orbital plane from $\Upsilon_{\mathbb{C}}$.

$B = A + \theta_{MTE}$ = true longitude of the descending node of the lunar parking orbit measured along the moon's orbital plane from $\Upsilon_{\mathbb{C}}$.

The inclination of the lunar parking orbit plane relative to the lunar equatorial plane can now be found:

$$i_{eq\mathbb{C}} = \cos^{-1}\left\{\begin{matrix}\cos i_m \cos (I+\gamma) \\ + \sin i_m \sin (I+\gamma) \cos B.\end{matrix}\right\} \qquad (10)$$

Next, the longitude of the descending node of the lunar parking orbit measured in the lunar equatorial plane from $\Upsilon_{\mathbb{C}}$ is:

$$\Lambda_{eq\mathbb{C}} = \cos^{-1}\left\{\frac{\cos (I+\gamma) \cos i_{eq\mathbb{C}} - \cos i_m}{\sin (I+\gamma) \sin i_{eq\mathbb{C}}}\right\} \qquad (11)$$

If an injection into a transearth trajectory does not take place at the time the orientation of the lunar parking orbit is known, the orientation must then be computed for the time of the next possible injection. A combination of two motions must be taken into account during this time span. These are the motion of the earth-moon line in the moon's orbital plane and the nodal regression of the lunar parking orbit. Considering only first order secular changes in the nodal regression due to lunar oblateness, the average change in node per nodal period of the lunar parking orbit relative to the lunar equatorial plane is:

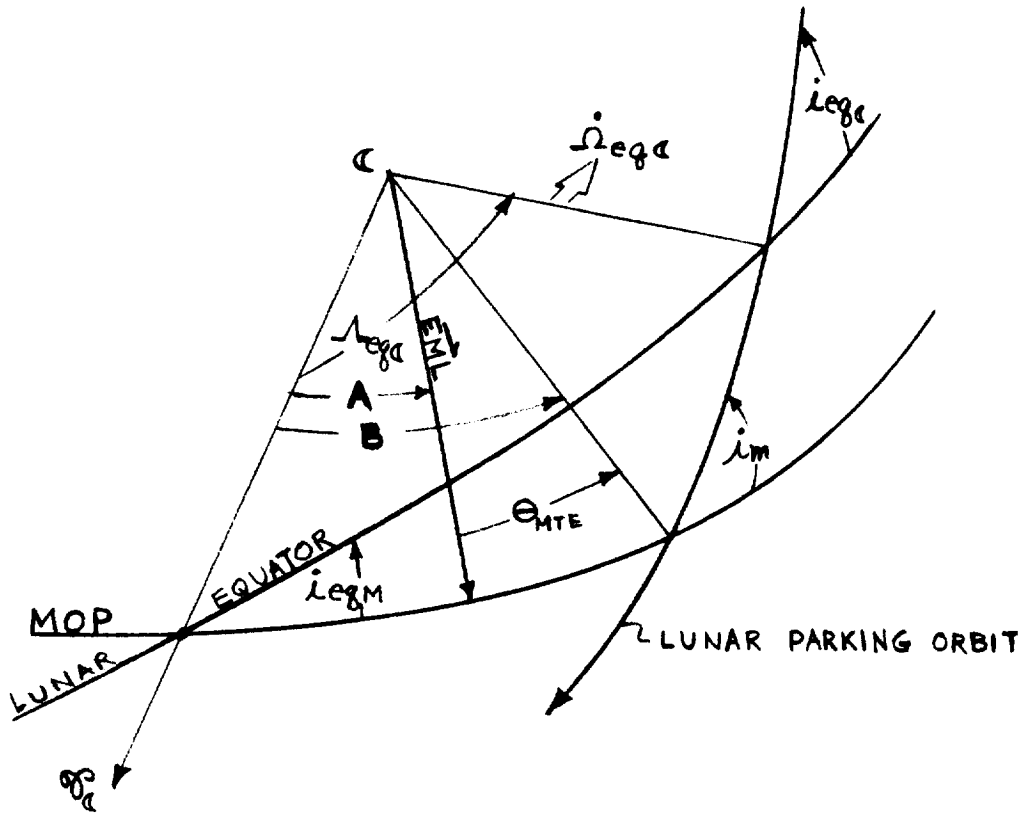


Sketch 7. Lunar Parking Orbit Geometry

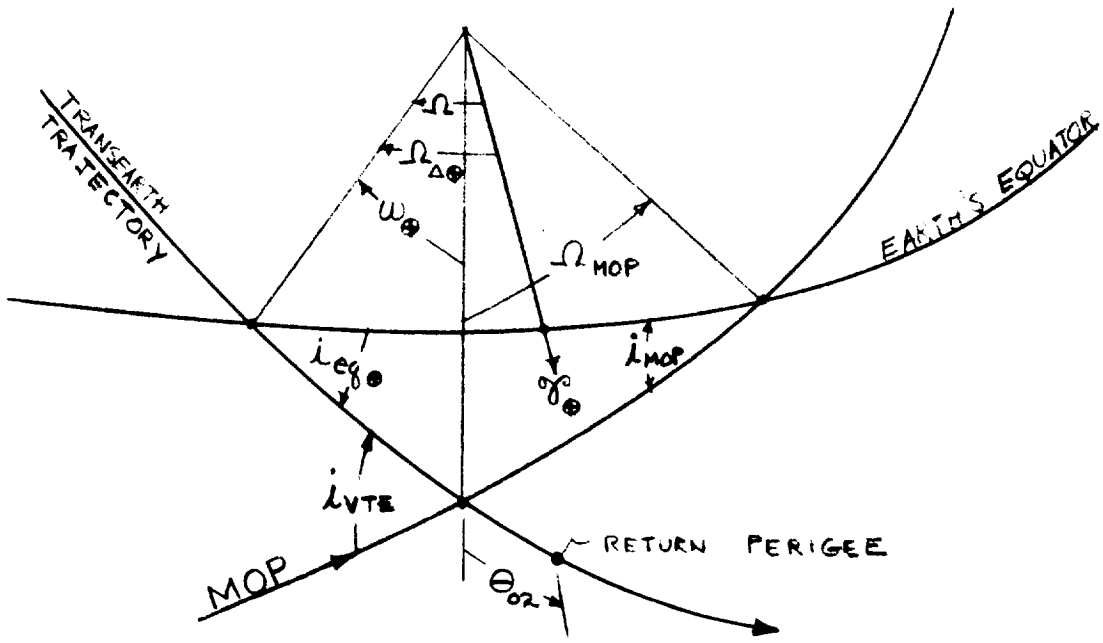


Sketch 8. Transearth Trajectory Geometry

$$\dot{\Omega}_{eq\,\mathbb{C}} = \frac{d\Lambda_{eq\,\mathbb{C}}}{dt} = 540\, J_{2\,\mathbb{C}} \left(\frac{R_{\mathbb{C}}}{h_{PL} + R_{\mathbb{C}}}\right)^2 \cos i_{eq\,\mathbb{C}}$$

(deg/nodal period) (12)

The first order secular change in the inclination $i_{eq\,\mathbb{C}}$ is 0 and, thus, a constant $i_{eq\,\mathbb{C}}$ is established once the initial orientation of the lunar parking orbit is specified. At some time (t) after the initial time ($t_o$), the longitude relative to the lunar equatorial plane becomes:

$$\Lambda'_{eq\,\mathbb{C}} = \Lambda_{eq\,\mathbb{C}} + d\Lambda_{eq\,\mathbb{C}} \tag{13}$$

and the moon's true longitude at a time later than $t_o$ becomes:

$$A' = \beta'_{\mathbb{C}\,T} - \beta'_{\mathbb{C}}\,\gamma \tag{14}$$

which is determined as a function of time. The inclination ($i'_m$ relative to the moon's orbital plane at a later time t is then:

$$i'_m = \cos^{-1}\left\{\cos (I + \gamma) \cos i_{eq\,\mathbb{C}} - \sin (I + \gamma) \sin i_{eq\,\mathbb{C}} \cos \Lambda'_{eq\,\mathbb{C}}\right\} . \tag{15}$$

Let

$$B' = A' + \theta'_{MTE} \tag{16}$$

be the true longitude of the descending node of the lunar parking orbit at time t, then:

$$B' = \cos^{-1}\left\{\frac{\cos i_{eq\,\mathbb{C}} - \cos (I + \gamma) \cos i'_m}{\sin (I + \gamma) \sin i'_m}\right\}. \tag{17}$$

Finally, the longitude of the descending node of the lunar parking orbit relative to the earth-moon line at the later time t is determined as:

$$\theta'_{MTE} = B' - A'. \tag{18}$$

The elements $i_m$, $\theta_{MTE}$, $R_{\oplus \mathbb{C}}$, $\omega_{\oplus \mathbb{C}}$, and $\beta_M$ were used as input to the trajectory computation with the resulting near-earth trajectory specified by a constant perigee altitude, $h_{PE}$, (588 km), the inclination of the trajectory plane relative to the moon's orbital plane, ($i_{VTE}$) and the angular position of perigee relative to the moon's orbital plane ($\theta_0$). These quantities are defined in Sketch 8. It is now desirable to obtain the orientation of the return earth trajectory relative to the earth equatorial plane.

Let

$$i_{\oplus R} = 180^\circ - i_{VTE}. \tag{19}$$

The longitude of the descending node of the earth return trajectory at perigee relative to the ascending node of the lunar orbit is:

$$\Omega_{\Delta \mathbb{C}} = \Delta\theta + \beta_{\mathbb{C}\,T} + 180^\circ \quad \text{(see Sketch 8)} \tag{20}$$

The inclination relative to the earth equatorial plane is then found to be:

$$i_{eq\oplus} = \cos^{-1}\left\{\cos i_{\oplus R} \cos i_{MOP} + \left(\sin i_{\oplus R} \sin i_{MOP} \cdot \cos \Omega_{\Delta \mathbb{C}}\right)\right\} \tag{21}$$

It can be seen that the difference between $i_{VTE}$ and $i_{eq\oplus}$ depends on the year ($i_{MOP}$) and on the time of month ($\beta_{\mathbb{C}\,T}$). The right ascension of the ascending node of the near-earth trajectory is given by:

$$\Omega_{\Delta\oplus} = \Omega_{MOP} + \Omega \qquad \text{if } i_{\oplus R} > 180^\circ$$

or (22)

$$\Omega_{\Delta\oplus} = \Omega_{MOP} + \Omega + 180^\circ \quad \text{if } i_{\oplus R} < 180^\circ$$

where $\Omega$ is computed from:

$$\Omega = \cos^{-1}\left\{\frac{\cos i_{eq\oplus} \cos i_{MOP} - \cos i_{\oplus R}}{\sin i_{eq\oplus} \sin i_{MOP}}\right\}. \tag{23}$$

The argument of perigee of the near-earth trajectory relative to the earth's equatorial plane is given by:

$$\omega_{\Delta\oplus} = \theta_0 + \omega_\oplus \qquad \text{if } i_{\oplus R} > 180^\circ$$

or (24)

$$\omega_{\Delta\oplus} = \theta_0 - \omega_\oplus + 180^\circ \qquad \text{if } i_{\oplus R} < 180^\circ$$

where $\omega$ is computed from:

$$\omega_\oplus = \cos^{-1}\left\{\cos\Omega\cos\Omega_{\Delta\mathbb{C}} + \sin\Omega\sin\Omega_{\Delta\mathbb{C}}\cos i_{MOP}\right\}. \quad (25)$$

All of the above equations have been mechanized into the aforementioned patch-conic digital program together with appropriate iteration schemes that allow easy convergence to satisfy the specified constraints.

## D. RESULTS

An attempt is made to provide sufficient data that is representative of an entire missions spectrum. This is a difficult task since myriad possible conditions present themselves for analyses and therefore a judicious selection is in order.

First, in order to indicate the effects of the varying inclination of the moon's orbital plane relative to the earth's equatorial plane, $i_{MOP}$, two particular dates, April 1969 and July 1978, were selected. During this first date (1969), $i_{MOP}$ has a maximum value of 28.6° while it has a minimum value of 18.3° during the second date (1978). The dependence of the departure windows on the inclination of the lunar parking orbit relative to the lunar equatorial plane, $i_{eq\mathbb{C}}$, was determined by selecting the initial position of the moon in its orbit, $\beta_{\mathbb{C}}$. The moon's position as a function of time for the above dates is given in the following table:

| Julian Date | Universal Time (d,h,m,s,yr) | $\beta_{\mathbb{C}}$ | Lunar Position |
|---|---|---|---|
| 2440326.0968 | 104,14,19,24,1969 | 0.0° | Ascending node |
| 2440333.3580 | 111,20,35,31,1969 | 90.0° | Maximum north declination |
| 2440313.3974 | 91,21,32,15,1969 | 180.0° | Descending node |

| Julian Date | Universal Time (d,h,m,s,yr) | $\beta_{\mathbb{C}}$ | Lunar Position |
|---|---|---|---|
| 2440319.7692 | 98,6,27,39,1969 | 270.0° | Maximum south declination |
| 2443714.0272 | 205,12,39,10,1978 | 0.0° | Ascending node |
| 2443693.7905 | 185,6,58,19,1978 | 90.0° | Maximum north declination |
| 2443701.2475 | 192,17,54,24,1978 | 180.0° | Descending node |
| 2443707.7887 | 199,6,55,44,1978 | 270.0° | Maximum south declination |

The initial orientation of the lunar parking orbit relative to the moon's orbital plane was specified by its inclination $i_m$, and its longitude, $\theta_{MTE}$. The values used in this study for $i_m$ were 20° and 10°, and for $\theta_{MTE}$ 120° and 90°. These orientations are the same as those imposed on the lunar parking orbit in Ref. 1. The inclinations, $i_{eq\mathbb{C}}$, which were dependent upon $i_m$, $\theta_{MTE}$, $\beta_{\mathbb{C}}$, and $i_{MOP}$, were found to be as shown in the following table.

| Year | $\beta_{\mathbb{C}}$ | $\theta_{MTE}$ | $i_m$ | $i_{eq\mathbb{C}}$ |
|---|---|---|---|---|
| April 1969 | 0° | 120° | 20° | 17.51° |
| July 1978 | 0° | 120° | 20° | 24.07° |
| July 1978 | 90° | 120° | 20° | 26.06° |
| July 1978 | 180° | 120° | 20° | 17.65° |
| July 1978 | 270° | 120° | 20° | 14.56° |
| July 1978 | 0° | 120° | 10° | 14.58° |
| July 1978 | 0° | 90° | 20° | 21.09° |

It is to be understood that only delayed injections are considered, i.e., the velocity requirements at any particular time are a function only of the geometrical configuration at that time and the mission constraints and are independent of any previous attempt at injection or maneuvering.

The reader is referred to Ref. 1 for a detailed definition of an alternative method (sequential injections) and its consequences. In brief, sequential injections imply the continuous updating of the geometrical configuration on each parking orbit pass. This continuous updating should be avoided since such maneuvering reduces the number of available departure windows to one.

The quantities of interest which are obtained as a result of a time history of energy requirements for the transearth mission are: departure window size, departure window frequency, injection frequency, and wait time. They are defined as follows:

(1) Departure window size: the time span during which transearth trajectories which satisfy all mission constraints, including propulsion capability are possible.

(2) Departure window frequency: the number of departure windows which occur during any given interval of time. In this study the interval of interest was the time for $\theta_{MTE}$ to rotate through 360°--approximately 30 days. The results for the following interval will be very similiar except for a slight shift due to the nodal regression of the lunar parking orbit.

(3) Injection frequency: the number of satisfactory injections which are possible during a departure window.

(4) Wait time: time span from some initial time to the first departure window or the time between two successive departure windows.

It has been stated in the ground rules that every transearth trajectory, regardless of the mission, is to satisfy a single specified $i_{eq\oplus}$ of 30°. In this study, direct returns to the northern and southern earth hemispheres are denoted by positive (+) and negative (-) values of $i_{eq\oplus}$, respectively. For a given lunar parking orbit orientation ($\theta_{MTE}$, $i_m$) and a given time (Julian date), a single injection position, $\beta_M$, determines a single return inclination, $i_{eq\oplus}$. There are, however, situations such as $\theta_{MTE}$ being in the vicinity of 0° and 180° when a transearth trajectory is not physically possible. Also, the geometrical configuration can be such that the desired return inclination cannot be obtained even though translunar trajectories exist in a neighboring region. In the cases where it is possible, the desired return inclination is obtained by an iteration on $\beta_M$.

A mission which specifies only the return inclination (Mission I or III) results in transearth trajectories of variable flight time. In order to obtain constant flight time trajectories (constraint 2) a side-thrust

maneuver in the lunar parking orbit is required. For a specific return inclination, the flight time depends directly on the longitude of the descending node of the lunar parking orbit ($\theta_{MTE}$), at injection. Thus, missions which satisfy both $i_{eq\oplus}$ and flight time (Missions III and IV) are obtained by means of a double iteration involving both $\beta_M$ and $\theta_{MTE}$. Once the injection longitude is found $\left[\theta_{MTE}\,(go)\right]$, the velocity impulse required to shift the nodal line from the actual longitude ($\theta_{MTE}$), can be calculated. If the inclination is $i_m$, then the required orbital azimuth change is given by

$$\Delta A_{\mathbb{C}} = \cos^{-1}\left\{\cos^2 i_m + \sin^2 i_m \cos\left(\theta_{MTE} - \theta_{MTE}\,(go)\right)\right\} \quad (26)$$

assuming that the maneuver occurs 90° from the moon's orbital plane. Let the velocity of the vehicle in the circular lunar parking orbit be $V_{\mathbb{C}c}$, then the velocity impulse required to perform the maneuver is:

$$\Delta V_{m\mathbb{C}} = 2V_{\mathbb{C}c} \sin\left(\Delta A_{\mathbb{C}}/2\right). \quad (27)$$

In order to limit $\Delta V_{m\mathbb{C}}$, the difference between $\theta_{MTE}$ and $\theta_{MTE}(go)$ is limited to less than 90°. For example, if the difference in longitudes approaches 90° for maneuvers which shift the nodal line to the east, then the maneuver is performed so that the nodal line is shifted to the west when $\theta_{MTE} - \theta_{MTE}\,(go) = 90°$.

For the mission in which a rendezvous is desired (constraint 3) with an earth orbiting space station upon returning to an earth parking orbit, an additional velocity impulse is required. This is due to the fact that the plane of the orbiting space station and the plane of the return earth parking orbit may not be coincident. A side-thrust maneuver is therefore required to make these planes coplanar. The right ascension of the ascending node of the space station orbit is obtained by assuming some value for the nominal earth-to-moon trajectory flight time ($t_p$) and some initial right ascension at the nominal earth injection ($\Omega_{s\oplus 0}$). If the moon-to-earth trajectory flight time is $t_f$, then the right ascension at the time of return is:

$$\Omega_{s\oplus} = \Omega_{s\oplus 0} + d\frac{\Omega_{s\oplus}}{dt}\,(t_p + t_f + t_s) \quad (28)$$

where

$\frac{d\Omega_{s\oplus}}{dt}$ = constant average nodal regression rate

$t_s$ = stay time in the lunar parking orbit

The right ascension of the earth return parking orbit at the time of return earth perigee is $\Omega_{\Delta\oplus}$, and thus a nodal shift of $\Omega_{\Delta\oplus} - \Omega_{s\oplus}$ must be accomplished. The required azimuth change is:

$$\Delta A_\oplus = \cos^{-1} \left\{ \cos^2 i_{eq\oplus} + \sin^2 i_{eq\oplus} \cos (\Omega_{\Delta\oplus} - \Omega_{s\oplus}) \right\} \qquad (29)$$

If the velocity of the vehicle in the circular earth parking orbit is $V_{\oplus c}$, then the velocity impulse required to perform the maneuver is

$$\Delta V_{m\oplus} = V_{\oplus c} \sin (\Delta A_\oplus / 2).$$

In all missions, the constant return inclination is either +30.0° (return to the northern earth hemisphere) or -30.0° (return to the southern earth hemisphere). For the missions in which constraint (2) is involved, the constant moon-to-earth flight time ($t_f$) was taken as either 50 hr or as 90 hr. These are the limits on the range of the most practical flight times.

To satisfy constraint (3), earth rendezvous in the various missions, the orientation of the earth supply parking orbit must be known at the time of arrival back at earth. In order to arrive nominally at the moon when the moon is at one of its nodes, the injection at earth had to occur when the right ascension of the ascending node ($\Omega_{s\oplus 0}$) of the earth parking orbit had a particular value. For the cases in this study, the values of $\Omega_{s\oplus 0}$ were as follows.

| Year | $\beta_{\mathfrak{C}}$ (nominal arrival at moon) | $\Omega_{s\oplus 0}$ |
|---|---|---|
| April 1969 | 0° (ascending node) | 180° |
| July 1978 | 0° (ascending node) | 180° |
| July 1978 | 90° (maximum north declination) | 305° |
| July 1978 | 180° (descending node) | 0° |
| July 1978 | 270° (maximum south declination) | 55° |

These values of $\Omega_{s\oplus 0}$ are for the situation in which only direct-north translunar injections from earth are allowed (see Ref. 2, Chapter 6) and are the only cases considered in this study. It is felt that the resultant windows are representative both in duration and number for the translunar inject-south cases as well. For a general picture, two translunar (earth-to-moon) flight times of 100 hr and of 50 hr were used. The orbital orientation of the earth orbiting space station at the time of return to the earth from the moon was then found by multiplying the sum of the earth-to-moon and the moon-to-earth flight times and the lunar stay time by the nodal regression rate for the earth parking orbit. It was assumed that the inclination ($i_{eq\oplus}$) remained fixed at 30.0° which, with an altitude of 588 km, yields an average nodal regression rate of 0°.6784 per hr for the earth parking orbit. The difference in nodes between the return earth parking orbit and the space station parking orbit then had to be negated for rendezvous to take place.

The various velocity impulses which are required to obtain moon-to-earth departure windows are again defined and summarized here.

$\Delta V$ = velocity impulse to eject from the lunar parking orbit

$\Delta V_{m\mathbb{C}}$ = side-thrust velocity impulse to correct $\theta_{MTE}$ to obtain constant flight time moon-to-earth trajectories

$\Delta V_E$ = velocity impulse to establish an earth circular parking orbit at the return perigee altitude

$\Delta V_{m\oplus}$ = side-thrust velocity impulse to correct the nodal difference in earth parking orbits for rendezvous

1. Departure Windows--Missions Without Flight Time Constraints

Missions I and II represent that class of missions where the return flight time is not a constraint. In the data presented below, the spacecraft is assumed to be in a retrograde lunar parking orbit and the transearth injection position, $\beta_M$, is based on an injection flight path angle of 0° ($\gamma_{\mathbb{C}} = 0°$).

a. Mission I (constraint 1)

This mission specifies that the spacecraft perform a transearth injection which results in arriving at earth with a trajectory inclination of ±30° (constraint 1) relative to the earth's equator. The transearth flight time, as mentioned above, is arbitrary and in addition there is no earth rendezvous requirement. Upon arrival at earth, the spacecraft may make a direct atmospheric re-entry, or may establish a parking

orbit prior to reentry. Figures 1 to 7 present the departure windows for this case, but before proceeding to the discussion of the data, it is most advantageous to first exemplify the reading and use of these charts. Each figure shows the transearth injection impulse requirement, $\Delta V$ (km/sec), as a function of elapsed time (hr) after the nominal arrival at the moon. The sketch below illustrates the shape of the curves and their interpretation.

Department Windows--Mission I

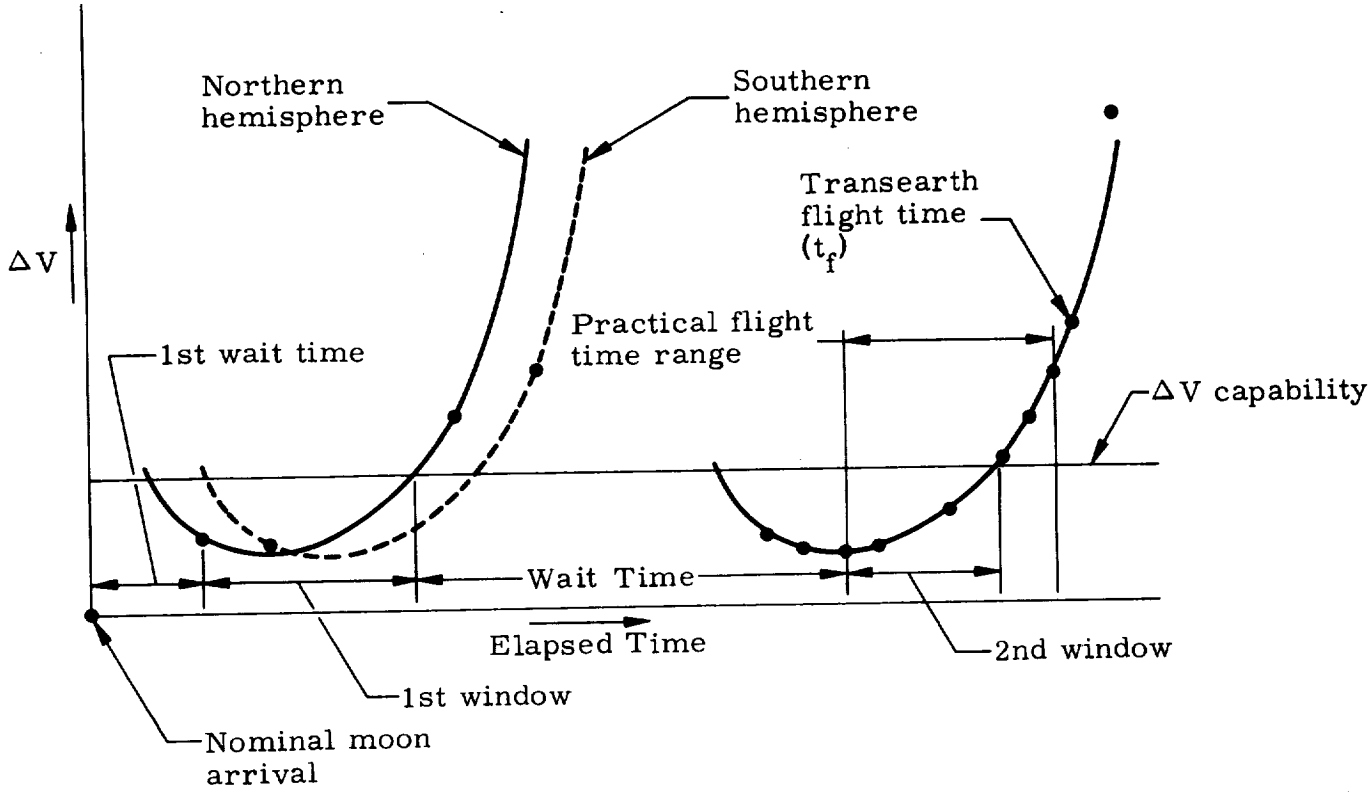


The solid lines denote returning from the north ($i_{eq\oplus} = +30°$); the broken curve represents an earth arrival from the south ($i_{eq\oplus} = -30°$).

The pronounced solid points on each curve mark the return flight times ($t_f$). Let there be a range of practical transearth flight times as noted in the above sketch. Also assume a propulsion capability, $\Delta V$ (horizontal line). The departure windows are then determined by the intersection of the horizontal line ($\Delta V$) and/or practical flight time limits. After arrival at the moon, the spacecraft generally will remain in its lunar parking orbit until the first departure window is entered;

this time interval is referred to specifically as the "first wait time." The time interval between successive departure windows is termed only as "wait time." As can be observed in the above sketch, window sizes can possibly be increased and wait times reduced if both returns ($\pm i_{eq_\oplus}$) are utilized.

Returning to Figs. 1 to 7, it is seen that two departure windows exist for a 1-mo time span. Since there is a large overlap between both northerly and southerly returns, the number of windows remain the same when both returns are permitted. However, there is an accompanied increase in window size.

Figures 1 to 5 record data for an initial lunar parking orbit orientation of $i_m = 20°$ and $\theta_{MTE} = 120°$. Transearth flight times between 40 and 120 hr are indicated in the figures in 10 hr increments. In order to gain an insight into the magnitude of numbers associated with departure windows for Mission I, a velocity capability ($\Delta V$) of 1.0 km/sec is considered reasonable. Furthermore, transearth flight times ($t_f$) between 50 and 100 hr are considered practical. Two different means for determining the departure windows now become apparent.

(1) Flight time restrictions only:

$50 \leq t_f \leq 100$ hr

(2) Flight time and $\Delta V$ restrictions:

$\Delta V \leq 1.0$ km/sec, $50 \leq t_f \leq 100$ hr

The results for the above conditions are presented as a function of year and time of the month (i.e., the position of the moon at the nominal moon arrival). The following codes are used to signify the allowable earth return direction:

$+i_{eq}$: only returns to the northern earth hemisphere ($i_{eq_\oplus} = +30°$) are allowed

$-i_{eq}$: only returns to the southern earth hemisphere ($i_{eq_\oplus} = -30°$) are allowed

$\pm i_{eq}$: returns to either the northern earth hemisphere ($i_{eq_\oplus} = +30°$) or the southern earth hemisphere ($i_{eq_\oplus} = -30°$) are allowed.

Table 1 presents the results for the above specified conditions. For the flight time restriction ($50 \leq t_f \leq 100$ hr), there is little variance in the magnitude of the departure windows from 1969 to 1978. The actual magnitude varies from 54 hr to 144 hr depending on what earth return

## TABLE 1

Mission I
Lunar Departure Windows

| First Departure Window (hr) $i_m = 20°$, $\theta_{MTE} = 120°$ | | | | | | | | | | | | | | | |
|---|---|---|---|---|---|---|---|---|---|---|---|---|---|---|---|
| Year | 1969 | | | 1978 | | | 1978 | | | 1978 | | | 1978 | | |
| Position of moon | AN | | | AN | | | MND | | | DN | | | MSD | | |
| | $+i_{eq}$ | $-i_{eq}$ | $\pm i_{eq}$ | $+i_{eq}$ | $-i_{eq}$ | $\pm i_{eq}$ | $+i_{eq}$ | $-i_{eq}$ | $\pm i_{eq}$ | $+i_{eq}$ | $-i_{eq}$ | $\pm i_{eq}$ | $+i_{eq}$ | $-i_{eq}$ | $\pm i_{eq}$ |
| $50 \leq t_f \leq 100$ hr | 88 | 64 | 100 | 100 | 70 | 132 | 100 | 78 | 134 | 106 | 80 | 138 | 96 | 66 | 130 |
| $50 \leq t_f \leq 100$ hr $\Delta V < 1.0$ km/sec | 68 | 46 | 82 | 80 | 36 | 98 | 72 | 62 | 118 | 86 | 68 | 126 | 84 | 56 | 120 |
| Second Departure Window (hr) | | | | | | | | | | | | | | | |
| | $+i_{eq}$ | $-i_{eq}$ | $\pm i_{eq}$ | $+i_{eq}$ | $-i_{eq}$ | $\pm i_{eq}$ | $+i_{eq}$ | $-i_{eq}$ | $\pm i_{eq}$ | $+i_{eq}$ | $-i_{eq}$ | $\pm i_{eq}$ | $+i_{eq}$ | $-i_{eq}$ | $\pm i_{eq}$ |
| $50 \leq t_f \leq 100$ hr | 60 | 68 | 84 | 62 | 78 | 108 | 90 | 104 | 144 | 86 | 136 | 162 | 54 | 90 | 118 |
| $50 \leq t_f \leq 100$ hr $\Delta V \leq 1.0$ km/sec | 52 | 64 | 80 | 56 | 66 | 102 | 76 | 78 | 130 | 70 | 108 | 146 | 46 | 72 | 110 |

AN, ascending node
MND, maximum north declination
DN, decending node
MSD, maximum south declination

$+i_{eq}$ return to northern hemisphere
$-i_{eq}$ return to southern hemisphere
$\pm i_{eq}$ return to either hemisphere

Note: All returns are posigrade

TABLE 2

Mission I

| Injection Frequency for First Departure Window, $i_m = 20°$, $\theta_{MTE} = 120°$ | | | | | | | | | | | | | | | |
|---|---|---|---|---|---|---|---|---|---|---|---|---|---|---|---|
| Year | 1969 | | | 1978 | | | 1978 | | | 1978 | | | 1978 | | |
| Position of moon | AN | | | AN | | | MND | | | DN | | | MSD | | |
| | $+i_{eq}$ | $-i_{eq}$ | $\pm i_{eq}$ | $+i_{eq}$ | $-i_{eq}$ | $\pm i_{eq}$ | $+i_{eq}$ | $-i_{eq}$ | $\pm i_{eq}$ | $+i_{eq}$ | $-i_{eq}$ | $\pm i_{eq}$ | $+i_{eq}$ | $-i_{eq}$ | $\pm i_{eq}$ |
| $50 \leq t_f \leq 100$ hr | 42 | 30 | 72 | 48 | 33 | 81 | 47 | 37 | 84 | 50 | 38 | 88 | 46 | 31 | 77 |
| $50 \leq t_f \leq 100$ hr $\Delta V \leq 1.0$ km/sec | 32 | 22 | 54 | 38 | 17 | 55 | 34 | 29 | 63 | 41 | 32 | 73 | 40 | 27 | 67 |
| Injection Frequency for Second Departure Window | | | | | | | | | | | | | | | |
| | $+i_{eq}$ | $-i_{eq}$ | $\pm i_{eq}$ | $+i_{eq}$ | $-i_{eq}$ | $\pm i_{eq}$ | $+i_{eq}$ | $-i_{eq}$ | $\pm i_{eq}$ | $+i_{eq}$ | $-i_{eq}$ | $\pm i_{eq}$ | $+i_{eq}$ | $-i_{eq}$ | $\pm i_{eq}$ |
| $50 \leq t_f \leq 100$ hr | 29 | 32 | 61 | 30 | 37 | 67 | 43 | 49 | 92 | 41 | 65 | 106 | 26 | 43 | 69 |
| $50 \leq t_f \leq 100$ hr $\Delta V \leq 1.0$ km/sec | 25 | 30 | 55 | 27 | 31 | 58 | 36 | 37 | 73 | 33 | 51 | 84 | 22 | 34 | 56 |

AN, ascending node
MND, maximum north declination
DN, descending node
MSD, maximum south declination

Note: All returns are posigrade

$+i_{eq}$ return to northern hemisphere
$-i_{eq}$ return to southern hemisphere
$\pm i_{eq}$ return to either hemisphere

directions are allowed. With the $\Delta V$ restriction ($\Delta V \leq 1.0$ km/sec) included, the window sizes are reduced by 5 to 30 hr. In all cases, allowing a return to be from either direction ($\pm i_{eq_\oplus}$) the windows are wider by approximately 12 to 76 hr for the restriction $50 \leq t_f \leq 100$ hr with the greatest change being realized in 1978. With both restrictions ($t_f$ and $\Delta V$) the same trends are exhibited.

The injection frequencies (i.e., the number of possible injections during a departure window) can be immediately found from the previous results and are presented in Table 2.

Note that the injection frequencies follow the same trend as the departure window sizes since the number of possible injections varies directly with window size. Also note from Figs. 1 to 7, that because northerly and southerly return windows do overlap, it is possible to have two transearth injection points on the same orbital pass if either return ($\pm i_{eq}$) is acceptable. In this circumstance, injection frequencies are the sum of the two separate injection frequencies ($+i_{eq}$, $-i_{eq}$). For returning from one direction only ($+i_{eq}$ or $-i_{eq}$), the number of possible injections can range from 17 to 65; and for returns from either direction ($\pm i_{eq}$), possible injections can range from 54 to 106.

Another important variable is the wait time. The first wait time is the time (in hours) from the nominal arrival at the moon to the start of the first departure window. Other wait times are the times between any two successive departure windows. A listing of the wait times from Figs. 1 to 5 is given in Table 3.

The first wait time for both $t_f$ and $\Delta V$ restrictions are the same since the transearth flight time is the determining factor for the first departure window. There is a variance in the first wait times which is a function of year and nominal position of the moon. This is due to the fact that even though the energy requirements for transearth injection are the same, the time at which they occur is dependent on the geometrical configuration of the principal planes and on the position of the moon.

First wait times in 1978 can vary from 38 to 78 hr and wait times between successive windows may vary between 180 and 370 hr.

Thus far, only an $i_m = 20°$ and $\theta_{MTE} = 120°$ has been considered. Figures 6 and 7 have been prepared to show a comparison of different initial conditions in July 1978 when the moon is nominally at its ascending node. These comparison situations had initial orientations of ($i_m = 20°$ and $\theta_{MTE} = 90°$) and of ($i_m = 10°$ and $\theta_{MTE} = 120°$) and yielded the results shown in Table 4.

TABLE 3

Mission I

Wait Times (hr)

| First Wait Time $i_m = 20°, \theta_{MTE} = 120°$ | | | | | | | | | | | | | | | |
|---|---|---|---|---|---|---|---|---|---|---|---|---|---|---|---|
| Year | 1969 | | | 1978 | | | 1978 | | | 1978 | | | 1978 | | |
| Position of moon | AN | | | AN | | | MND | | | DN | | | MSD | | |
| | $+i_{eq}$ | $-i_{eq}$ | $\pm i_{eq}$ | $+i_{eq}$ | $-i_{eq}$ | $\pm i_{eq}$ | $+i_{eq}$ | $-i_{eq}$ | $\pm i_{eq}$ | $+i_{eq}$ | $-i_{eq}$ | $\pm i_{eq}$ | $+i_{eq}$ | $-i_{eq}$ | $\pm i_{eq}$ |
| $50 \leq t_f \leq 100$ hr | 100 | 136 | 100 | 78 | 140 | 78 | 72 | 128 | 72 | 38 | 96 | 38 | 48 | 112 | 48 |
| $50 \leq t_f$ 100 hr $\Delta V \leq 1.0$ km/sec | 100 | 136 | 100 | 78 | 140 | 78 | 72 | 128 | 72 | 38 | 96 | 38 | 48 | 112 | 48 |
| Wait Time Between Windows | | | | | | | | | | | | | | | |
| | $+i_{eq}$ | $-i_{eq}$ | $\pm i_{eq}$ | $+i_{eq}$ | $-i_{eq}$ | $\pm i_{eq}$ | $+i_{eq}$ | $-i_{eq}$ | $\pm i_{eq}$ | $+i_{eq}$ | $-i_{eq}$ | $\pm i_{eq}$ | $+i_{eq}$ | $-i_{eq}$ | $\pm i_{eq}$ |
| $50 \leq t_f \leq 100$ hr | 310 | 234 | 234 | 280 | 244 | 244 | 276 | 188 | 188 | 304 | 196 | 196 | 352 | 254 | 254 |
| $50 \leq t_f \leq 100$ hr $\Delta V \leq 1.0$ km/sec | 332 | 250 | 250 | 300 | 262 | 262 | 304 | 204 | 204 | 324 | 208 | 208 | 364 | 268 | 268 |

AN, ascending node
MND, maximum north declination
DN, descending node
MSD, maximum south declination

Note: All returns are posigrade

$+i_{eq}$ return to northern hemisphere
$-i_{eq}$ return to southern hemisphere
$\pm i_{eq}$ return to either hemisphere

TABLE 4

Mission I

| First Departure Window (hr) April 1978--Moon at AN | | | | | | |
|---|---|---|---|---|---|---|
| Initial lunar orbit orientation | $i_m = 20°$ $\theta_{MTE} = 90°$ | | | $i_m = 10°$ $\theta_{MTE} = 120°$ | | |
| | $+i_{eq}$ | $-i_{eq}$ | $\pm i_{eq}$ | $+i_{eq}$ | $-i_{eq}$ | $\pm i_{eq}$ |
| $50 \leq t_f \leq 100$ hr | 104 | 66 | 130 | 90 | 50 | 145* |
| $50 \leq t_f \leq 100$ hr $\Delta V \leq 1.0$ km/sec | 82 | 56 | 120 | 80 | 38 | 118* |
| Second Departure Window (hr) | | | | | | |
| | $+i_{eq}$ | $-i_{eq}$ | $\pm i_{eq}$ | $+i_{eq}$ | $-i_{eq}$ | $\pm i_{eq}$ |
| $50 \leq t_f \leq 100$ hr | 52 | 80 | 106 | 50 | 80 | 130* |
| $50 \leq t_f \leq 100$ hr $\Delta V \leq 1.0$ km/sec | 48 | 68 | 102 | 46 | 66 | 112* |

*For an initial orientation of $i_m = 10°$ and $\theta_{MTE} = 120°$, the departure windows for northerly and southerly earth returns do not overlap. For the first departure windows there is an additional wait time of 10 hr (included in quoted number) between the north and south returns and for the second departure windows there is an additional wait time of 14 hr (included in quoted number) between the north and south returns.

Comparing this table with Table 1, it is noted that the change in the departure windows sizes due to a change in $\theta_{MTE}$ is from 2 to 20 hr for both single return directions ($+i_{eq}$ or $-i_{eq}$) and for any direction ($\pm i_{eq}$). Thus, a change in $\theta_{MTE}$ in the range considered is not very influential in altering window sizes. The above statement is also true for a change in $i_m$.

Table 5 presents the injection frequency for the above initial conditions and is presented at this time without further discussion.

TABLE 5

Mission I
Injection Frequencies

| First Departure Window (Apr 1978-AN) | | | | | | |
|---|---|---|---|---|---|---|
| Initial lunar orbit orientation | $i_m = 20°$ $\theta_{MTE} = 90°$ | | | $i_m = 10°$ $\theta_{MTE} = 120°$ | | |
| | $+i_{eq}$ | $-i_{eq}$ | $\pm i_{eq}$ | $+i_{eq}$ | $-i_{eq}$ | $\pm i_{eq}$ |
| $50 \leq t_f \leq 100$ hr | 49 | 31 | 80 | 44 | 24 | 68 |
| $50 \leq t_f \leq 100$ hr $\Delta V \leq 1.0$ km/sec | 39 | 27 | 66 | 38 | 18 | 56 |
| Second Departure Window | | | | | | |
| | $+i_{eq}$ | $-i_{eq}$ | $\pm i_{eq}$ | $+i_{eq}$ | $-i_{eq}$ | $\pm i_{eq}$ |
| $50 \leq t_f \leq 100$ hr | 25 | 38 | 63 | 24 | 38 | 62 |
| $50 \leq t_f \leq 100$ hr $\Delta V \leq 1.0$ km/sec | 23 | 32 | 55 | 22 | 31 | 53 |

For an initial $\theta_{MTE} = 90°$, and for northerly returns to earth, there is a small first wait time (12 hr) since the node of the lunar parking orbit is such that satisfactory transearth trajectories can take place sooner than for initial $\theta_{MTE}$ greater than 90°. This can be seen in Table 6 which lists wait times for the above comparison conditions. Note that the wait times between windows are quite comparable to those presented in Table 3.

b. Mission II (constraints 1 and 3)

This mission is a direct extension of Mission I and specifies that the spacecraft, upon arriving at earth with an $i_{eq_\oplus}$ of ±30°, enters into an earth parking orbit, then performs a side-thrust maneuver for rendezvous purposes. This maneuver makes the return parking orbit plane coplanar with a space station orbital plane. The space station has been in orbital flight indefinitely. Possibly the returning spacecraft may have initiated its lunar mission from the space station. Figures 8 to 14 present the departure windows for this case by showing

TABLE 6

Mission I
Wait Times

| First Wait Time (hr) (Apr 1978-AN) | | | | | | |
|---|---|---|---|---|---|---|
| Initial lunar orbit orientation | $i_m = 20°$ $\theta_{MTE} = 90°$ | | | $i_m = 10°$ $\theta_{MTE} = 120°$ | | |
| | $+i_{eq}$ | $-i_{eq}$ | $\pm i_{eq}$ | $+i_{eq}$ | $-i_{eq}$ | $\pm i_{eq}$ |
| $50 \leq t_f \leq 100$ hr | 12 | 76 | 12 | 60 | 178 | 60 |
| $50 \leq t_f \leq 100$ hr $\Delta V \leq 1.0$ km/sec | 12 | 76 | 12 | 60 | 178 | 60 |
| Wait Time Between Windows (hr) | | | | | | |
| | $+i_{eq}$ | $-i_{eq}$ | $\pm i_{eq}$ | $+i_{eq}$ | $-i_{eq}$ | $\pm i_{eq}$ |
| $50 \leq t_f \leq 100$ hr | 330 | 250 | 250 | 362 | 208 | 208 |
| $50 \leq t_f \leq 100$ hr $\Delta V \leq 1.0$ km/sec | 352 | 260 | 260 | 390 | 220 | 220 |

the total velocity requirement ($\Delta V + \Delta V_E + \Delta V_{m\oplus}$) versus elapsed time from date of moon arrival. Again for purposes of clarity, the following sketch is referred to. The maneuver impulse required to enter an earth parking orbit is $\Delta V_E$ and $\Delta V_{m\oplus}$ is the side-thrust maneuver impulse required for rendezvous purposes.

Again, in the following sketch, the solid lines denote a northerly return ($+i_{eq\oplus}$) and the broken lines a southerly return ($-i_{eq\oplus}$). However, for this mission there are two representative lines for a given elapsed time. The two curves for any $i_{eq\oplus}$ are for two translunar flight times ($t_p$) which affect the right ascension of the space station parking orbit at the time of arrival at earth. The two translunar flight times ($t_p$) selected are 50 hr and 100 hr which are considered as practical outbound flight durations. Thus, the effect of flight time ($t_p$) on windows could easily be determined.

Departure Windows--Mission II

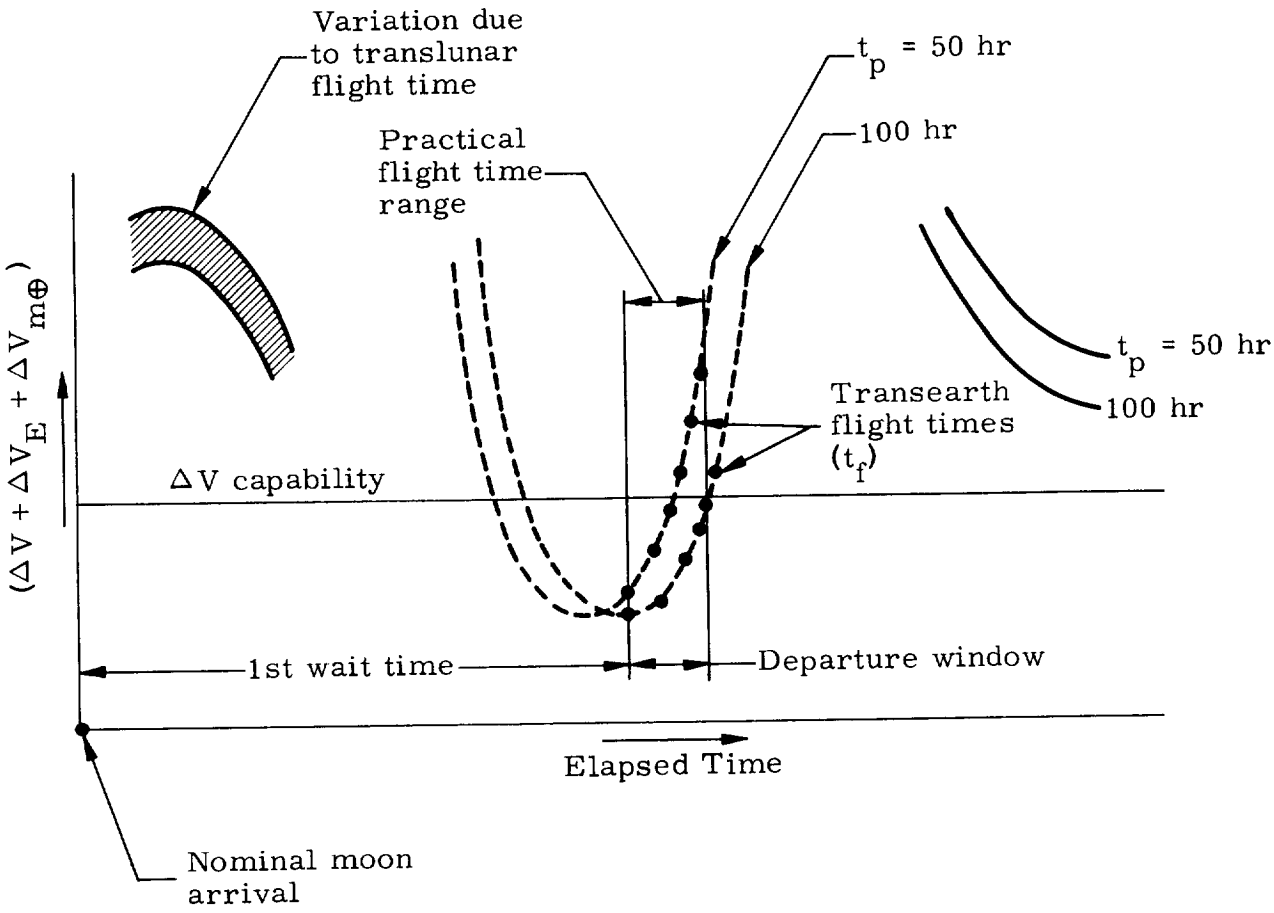


As before (Mission I), the pronounced solid points on each curve mark the return flight times ($t_f$) in 10-hr increments. Assuming a propulsion capability ($\Delta V$ capability), the window width is determined as shown in the above sketch along with the first wait time for a given practical transearth flight time range. For the windows shown below this practical flight range is again 50 to 100 hr.

Referring to Figs. 15 to 21 and assuming a $\Delta V$ (propulsion capability) $\leq$ 5.0 km/sec and allowing both northerly and southerly earth returns, there exists at least one departure window during a 1-mo time interval. Table 7 gives a summary of Figs. 8 to 12 and it is quite evident that in addition to a decrease in departure window frequency, a large reduction in window size is also realized.

TABLE 7

Mission II
Departure Windows (hr)

$\Delta V \leq 5$ km/sec
Translunar flight time between 50 and 100 hr
Transearth flight time between 50 and 90 hr
$i_m = 20°$ ; $\theta_{MTE} = 120°$

| Year | April 1969 | | July 1978 | | July 1978 | | July 1978 | | July 1978 | |
|---|---|---|---|---|---|---|---|---|---|---|
| Initial position of moon | AN | | AN | | MND | | DN | | MSD | |
| | $t_p$=50 | $t_p$=100 | $t_p$=50 | $t_p$=100 | $t_p$=50 | $t_p$=100 | $t_p$=50 | $t_p$=100 | $t_p$=50 | $t_p$=100 |
| $i_{eq_\oplus} = -30°$ | 62 | 60 | 32 | 8 | 32 | 36 | 8 | 0 | 0 | 0 |
| $i_{eq_\oplus} = +30°$ | 0 | 0 | 0 | 0 | 0 | 0 | 16 | 30 | 70 | 68 |
| Injection Frequency--Mission II | | | | | | | | | | |
| | $t_p$=50 | $t_p$=100 | $t_p$=50 | $t_p$=100 | $t_p$=50 | $t_p$=100 | $t_p$=50 | $t_p$=100 | $t_p$=50 | $t_p$=100 |
| $i_{eq_\oplus} = -30°$ | 30 | 29 | 15 | 4 | 15 | 17 | 4 | 0 | 0 | 0 |
| $i_{eq_\oplus} = +30°$ | 0 | 0 | 0 | 0 | 0 | 0 | 8 | 14 | 33 | 32 |

From Table 7 it is observed that the windows are strongly dependent on both year and time of month and in some cases also dependent on translunar flight time ($t_p$). The related injection frequency is shown following Table 7.

Figures 13 and 14 present departure windows for an $i_m = 20°$, $\theta_{MTE} = 90°$ and $i_m = 10°$, $\theta_{MTE} = 120°$. The pertinent data is given in Table 8.

TABLE 8

Mission II

Departure Windows and Injection Frequency
$\Delta V \leq 5$ km/sec

| Year | July 1978 | | July 1978 | |
|---|---|---|---|---|
| Initial position of moon | AN | | AN | |
| $i_m$, $\theta_{MTE}$ | 20° ; 90° | | 10° ; 120° | |
| | $t_p = 50$ | $t_p = 100$ | $t_p = 50$ | $t_p = 100$ |
| $i_{eq_\oplus} = -30°$ | 52 | 68 | 42 | 22 |
| $i_{eq_\oplus} = +30°$ | 0 | 0 | 0 | 26 |
| Injection frequency | 25 | 32 | 20 | 10 |
| | 0 | 0 | 0 | 12 |

As can be seen, the resultant departure windows are sensitive to $i_m$ and $\theta_{MTE}$ variations and can actually be enlarged with a proper selection.

Since there is usually only one departure window per month, the first wait time becomes most important. A summary listing of wait times is given in Table 9 below and when comparing this table with Table 6, the first wait time has increased significantly--on the order of 100 to 400 hr because of the rendezvous requirement (constraint 3).

TABLE 9

Mission II

First Wait Times (hr)

| Year | 1969 | 1978 | 1978 | 1978 | 1978 | 1978 | 1978 |
|---|---|---|---|---|---|---|---|
| Moon position | AN | AN | MND | DN | MSD | AN | AN |
| $i_m$ (deg) | 20 | 20 | 20 | 20 | 20 | 20 | 10 |
| $\theta_{MTE}$ (deg) | 120 | 120 | 120 | 120 | 120 | 90 | 120 |
| First wait time | | | | | | | |
| $t_p$ = 50 hr | 452 | 444 | 440 | 128 | 78 | 420 | 436 |
| $t_p$ = 100 hr | 444 | 444 | 426 | 112 | 54 | 392 | 436 |

c. Auxiliary data for Missions I and II

Figures 1 to 7 presented the Mission I velocity requirement, $\Delta V$, and Figs. 8 to 14 presented the total velocity requirements for Mission II ($\Delta V + \Delta V_E + \Delta V_{m\oplus}$). For the departure windows of these missions, it is desirable to know explicitly what $\Delta V_E$ and $\Delta V_{m\oplus}$ are. To this end, Figs. 15 to 21 have been prepared so that $\Delta V_E$ and $\Delta V_{m\oplus}$ can be determined independently. These figures are quite similar to the departure windows with rendezvous constraints (Figs. 8 to 14) and in fact have the same nomenclature and constraints except for two variables, namely $\Delta V_E$ and ($\Delta V_E + \Delta V_{m\oplus}$). A sketch of a typical chart is included on the following page in order to point out the use of the chart. Basically these figures give the energy requirements associated with establishing a earth parking orbit upon return to earth.

If only the return inclination ($i_{eq\oplus}$) is restricted (Mission I), then the only required velocity impulse is $\Delta V_E$, the difference between the trajectory velocity at perigee and the circular parking orbit velocity at the same altitude. This impulse is essentially constant at 3.05 km/sec, since it is heavily dependent on the perigee altitude which is held constant.

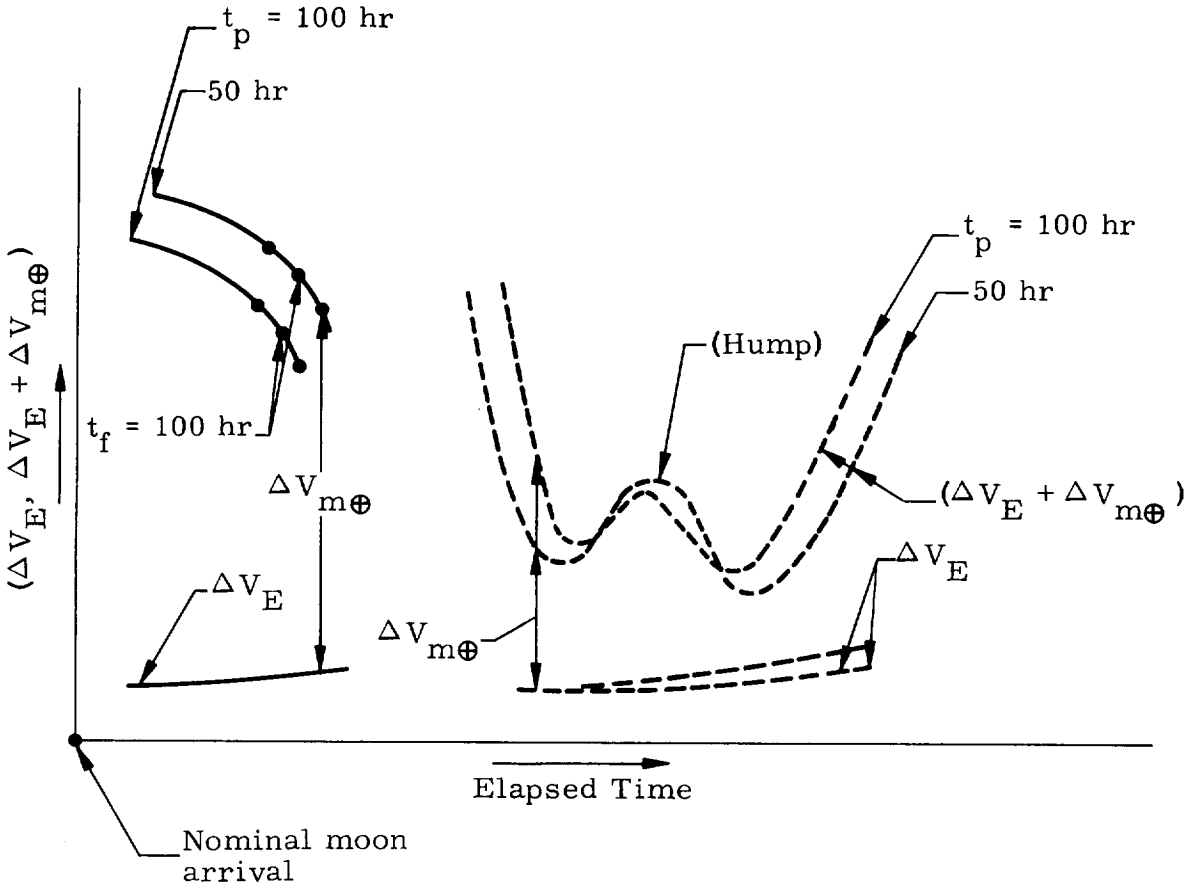


If a rendezvous with an earth orbiting space station is desired, then an additional velocity impulse of $\Delta V_{m\oplus}$ (see sketch above) is required to make the two orbits coplanar. This impulse is periodic due to the nodal regression of the space station's parking orbit and to the time at which ejection from the lunar parking orbit actually takes place.

In Figs. 15 to 21, minimum values of ($\Delta V_E$ and $\Delta V_{m\oplus}$) are found which are quite close together and which occur near a "hump" region (see sketch). This is due to the fact that in some regions the transearth trajectory flight times decrease as the elapsed time increases. Thus, it becomes possible to return earlier to the earth by delaying the time at which transearth injection takes place. Several of the curves in these figures are shown to be abruptly terminated before they reach a minimum. This occurs at the times when the required nodal change in the earth parking orbit is small but when transearth injections become physically impossible.

## 2. Departure Windows--Missions with Flight Time Constraints

Missions III and IV represent that class of missions where the transearth flight time is a specified constraint. Major maneuvers during transearth flight are prohibited; only minor midcourse corrections are assumed to take place. No allowance is made for these corrections in the data to be presented below.

a. Mission III (constraints 1 and 2)

This mission specifies that the spacecraft perform a transearth injection which results in arriving at earth in a prespecified flight time (constraint 2) and with a trajectory inclination of ±30° ($i_{eq\oplus}$, constraint 1). At arrival, the spacecraft may make a direct atmospheric re-entry, or may establish an earth parking orbit.

Figures 22 to 28 show graphically the departure windows for this case. The following sketch and subsequent discussion describe the use of these figures.

Departure Windows--Mission III

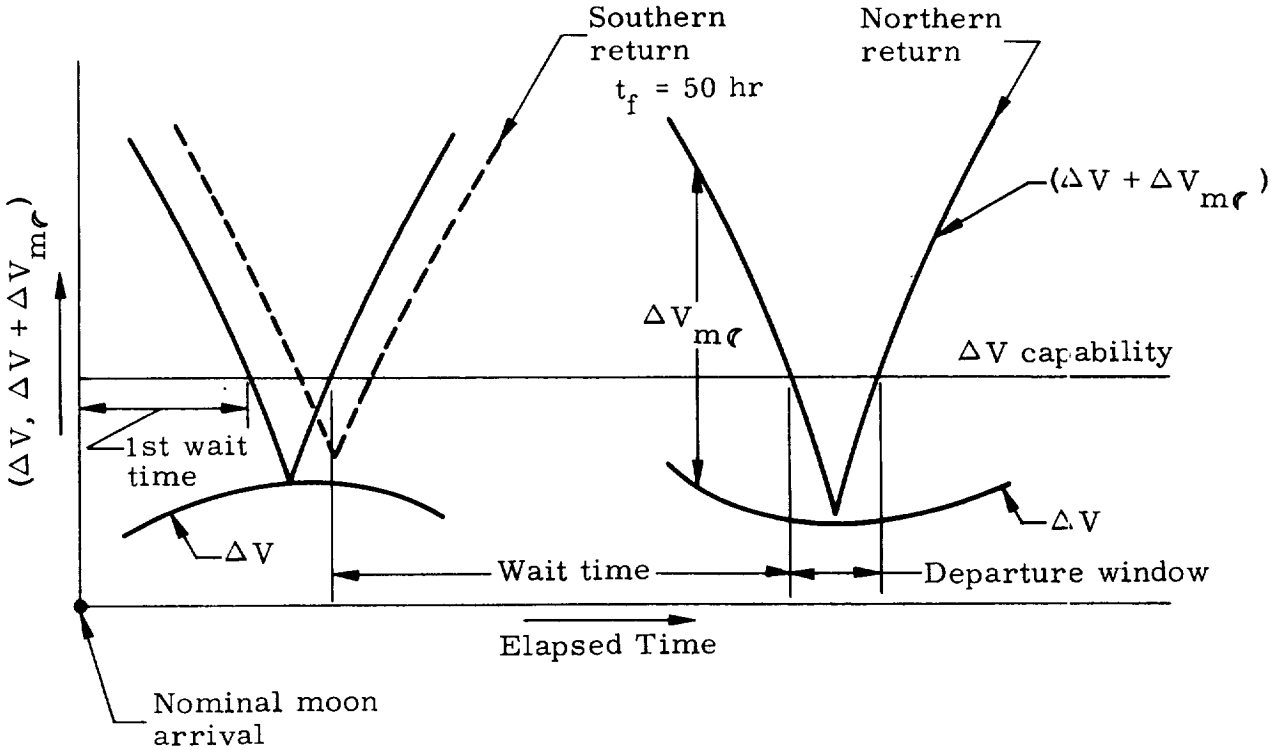

The above mentioned figures show the transearth injection requirement ($\Delta V$ km/sec) and the maneuver requirement ($\Delta V_{m\,\mathbb{C}}$ km/sec) to adjust the parking orbit node as a function of elapsed time (hr) after the nominal arrival at the moon.

The solid lines denote returning from the north ($i_{eq\,\oplus} = +30°$) while the dashed lines represent a southerly return ($i_{eq\,\oplus} = -30°$). Each figure depicts a window for a constant transearth flight time ($t_f$). Two extreme values of $t_f$ are used as criteria in establishing the windows, namely, $t_f = 50$ hr and $t_f = 90$ hr. The departure windows are determined by the intersection of the $\Delta V$ (propulsion capability) line and ($\Delta V + \Delta V_{m\,\mathbb{C}}$) curves as demonstrated in the sketch on the preceding page. The wait times are also defined in the sketch on the preceding page. Referring to the above referenced figures, there are two departure windows for both northerly and southerly earth returns during the one month time span. Assuming a $\Delta V$ capability of 1.5 km/sec, Table 10 lists window sizes for an initial lunar parking orbit orientation of $i_m = 20°$ and $\theta_{MTE} = 120°$.

TABLE 10

Mission III

Departure Windows (hr)
$\Delta V = 1.5$ km/sec

| Year | 1969 | | | 1978 | | | 1978 | | |
|---|---|---|---|---|---|---|---|---|---|
| Lunar Position | AN | | | AN | | | MND | | |
| | $+i_{eq}$ | $-i_{eq}$ | $\pm i_{eq}$ | $+i_{eq}$ | $-i_{eq}$ | $\pm i_{eq}$ | $+i_{eq}$ | $-i_{eq}$ | $\pm i_{eq}$ |
| 1st window | | | | | | | | | |
| $t_f = 50$ hr | 88 | 100 | 112 | 92 | 114 | 150 | 110 | 122 | 150 |
| $t_f = 90$ hr | 242 | 276 | 284 | 256 | 584* | U** | -- | -- | -- |
| 2nd window | | | | | | | | | |
| $t_f = 50$ hr | 120 | 110 | 130 | 144 | 132 | 172 | 134 | 134 | 166 |
| $t_f = 90$ hr | 196 | 214 | 248 | 592 | 584* | U** | -- | -- | -- |

*The first and second departure windows overlap to give a total window as quoted.

**Unlimited windows--capable of returning to earth at any time.

The table on the preceding page emphasizes the effect of transearth flight time on window size. Essentially, for longer flight times ($t_f$), the $\Delta V$ to perform a transearth injection diminishes and therefore additional $\Delta V$ can be allocated for maneuvering purposes. Note also in the table that the year and time of month do not influence the window sizes to any significant degree.

In the next table, Table 11, the corresponding injection frequencies to Table 10 are tabulated. It is worthy to note again the direct additive nature of the frequencies when either return is allowed.

TABLE 11

Mission III

Injection Frequency
$\Delta V$ = 1.5 km/sec

| Year | 1969 | | | 1978 | | | 1978 | | |
|---|---|---|---|---|---|---|---|---|---|
| Lunar Position | AN | | | AN | | | MND | | |
| | $+i_{eq}$ | $-i_{eq}$ | $\pm i_{eq}$ | $+i_{eq}$ | $-i_{eq}$ | $\pm i_{eq}$ | $+i_{eq}$ | $-i_{eq}$ | $\pm i_{eq}$ |
| 1st window | | | | | | | | | |
| $t_f$ = 50 hr | 42 | 48 | 90 | 44 | 54 | 98 | 52 | 58 | 110 |
| $t_f$ = 90 hr | 115 | 131 | 246 | 122 | 278 | 697 | -- | -- | -- |
| 2nd window | | | | | | | | | |
| $t_f$ = 50 hr | 57 | 52 | 109 | 68 | 63 | 131 | 64 | 64 | 128 |
| $t_f$ = 90 hr | 93 | 102 | 195 | 282 | 278 | 697 | -- | -- | -- |

As pointed out above, since the longer flight times provide wider windows, it is to be expected that the wait times involved will be shortened. Table 12 verifies this statement and shows that the wait times are to a high degree independent of year or time of the month.

TABLE 12

Mission III

Wait Time (hr)
$\Delta V$ = 1.5 km/sec

| Year | 1969 | | | 1978 | | | 1978 | | |
|---|---|---|---|---|---|---|---|---|---|
| Lunar Position | AN | | | AN | | | MND | | |
| | $+i_{eq}$ | $-i_{eq}$ | $\pm i_{eq}$ | $+i_{eq}$ | $-i_{eq}$ | $\pm i_{eq}$ | $+i_{eq}$ | $-i_{eq}$ | $\pm i_{eq}$ |
| 1st wait time | | | | | | | | | |
| $t_f$ = 50 hr | 140 | 152 | 140 | 116 | 152 | 116 | 122 | 150 | 122 |
| $t_f$ = 90 hr | 0 | 8 | 0 | 0 | 0 | 0 | -- | -- | -- |
| Wait time between windows | | | | | | | | | |
| $t_f$ = 50 hr | 244 | 210 | 210 | 260 | 194 | 194 | 230 | 158 | 158 |
| $t_f$ = 90 hr | 138 | 52 | 52 | 118 | 0 | 0 | -- | -- | -- |

Although independent of year and time of month, they are however, sensitive to both the initial $i_m$ and $\theta_{MTE}$ as is evidenced in Figs. 27 and 28. These figures graphically display the same information as the preceding, but for an $i_m = 20°$ and $\theta_{MTE} = 90°$, and also for $i_m = 10°$ and $\theta_{MTE} = 120°$. Essentially, lower values of $i_m$ shift the available windows toward the nominal arrival time as did longer flight times. Lower values of $i_m$ do not shift the windows but rather lower $\Delta V + \Delta V_{mc}$ requirements which effectively increase window size. The latter point is due to the fact that the required azimuth change (to change nodal position) is much more efficiently obtained with lower values of $i_m$.

b. Mission IV (constraints 1, 2 and 3)

Mission IV is basically an extension to Mission III in the sense that, upon arrival at earth, the spacecraft establishes a parking orbit; then performs a maneuver to establish a coplanar orbit with an earth orbiting station.

The total velocity required to eject from a lunar parking orbit and return to an earth parking orbit is presented as a function of elapsed

time in Figs. 29 to 35 for constant flight times of 50 and 90 hr. This total velocity is the sum ($\Delta V + \Delta V_{m\,\mathbb{C}} + \Delta V_E + \Delta V_{m\oplus}$) and is dominated by $\Delta V_{m\oplus}$, the impulse to perform the earth parking orbit maneuver.

The next sketch is provided as an aid in the interpretation of Figs. 29 to 35.

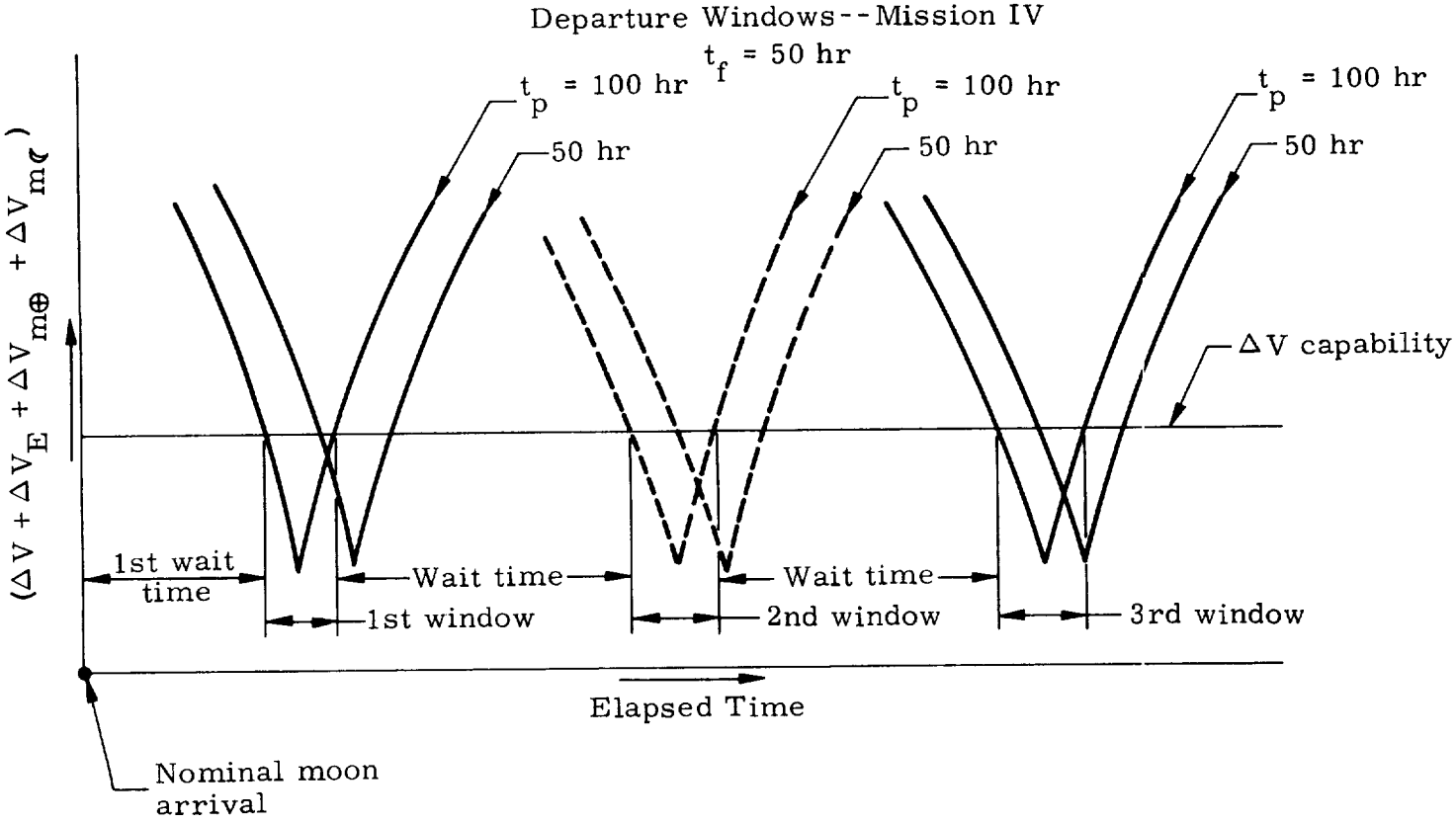


As before, the solid and broken curves represent northerly ($+i_{eq}$) and southerly ($-i_{eq}$) returns, respectively. Departure windows and wait times are determined by the $\Delta V$ intersections with ($\Delta V + \Delta V_{m\,\mathbb{C}} + \Delta V_E + \Delta V_{m\oplus}$) as illustrated in the above sketch. Observe from the sketch, and also from Figs. 29 to 35, that there are three potential windows during a month. The cycling of the windows is: northerly returns ($+i_{eq}$), southerly ($-i_{eq}$) and again, northerly.

Table 13 has been prepared from the referenced figures assuming a $\Delta V$ of 5.0 km/sec. This table gives the departure windows (in hours) and the corresponding injection frequency (enclosed in parentheses). As was the case for Mission III, longer transearth flight times ($t_f$) can increase the windows significantly. However, contrary to the Mission III results, reducing $\theta_{MTE}$ or $i_m$ does not increase the window sizes nor reduce the wait times because the impulse ($\Delta V_E + \Delta V_{m\oplus}$) completely dominates the width of the windows.

The related first wait times are shown in Table 14. With the rendezvous requirement, the first wait time is on the order of 200 hr.

TABLE 14

Mission IV

$\Delta V$ = 5.0 km/sec

1st Wait Time (hr)

| Year | Lunar Position | $i_m$ (deg) | $\theta_{MTE}$ (deg) | $t_f$ | Wait Time $t_p$ = 50 | Wait Time $t_p$ = 100 |
|---|---|---|---|---|---|---|
| 1969 | AN | 20 | 120 | 50 | 248 | 236 |
| 1978 | AN | 20 | 120 | 50 | 226 | 212 |
| 1978 | MND | 20 | 120 | 50 | 222 | 208 |
| 1969 | AN | 20 | 120 | 90 | 240 | 228 |
| 1978 | AN | 20 | 120 | 90 | 210 | 196 |
| 1978 | AN | 20 | 90 | 90 | 212 | 196 |
| 1978 | AN | 10 | 120 | 90 | 208 | 188 |

c. Auxiliary data for Missions III and IV

Figures 36 to 42 present auxiliary data for Missions III and IV which are intended to fulfill the same purpose as the auxiliary data for Missions I and II, namely, to enable the determination of $\Delta V_E$ and $\Delta V_{m\oplus}$ explicitly. The use of these figures is identical to that of Figs. 15 to 21 and therefore their explanation and discussion are not repeated here.

TABLE 13

Mission IV

Departure Windows and Injection Frequencies

$t_f$ = 50 hr

| Year, Lunar Position, $i_m$, $\theta_{MTE}$ | 1st Window Northerly Return ($+i_{eq}$) | | 2nd Window Southerly Return ($-i_{eq}$) | | 3rd Window Northerly Return ($\pm i_{eq}$) | |
|---|---|---|---|---|---|---|
| | $t_p$ = 50 hr | $t_p$ = 100 hr | $t_p$ = 50 hr | $t_p$ = 100 hr | $t_p$ = 50 hr | $t_p$ = 100 hr |
| April 1969, AN, 20°, 120° | 6 (3) | 8 (4) | 24 (11) | 26 (12) | 36 (17) | 50 (24) |
| July 1978, AN, 20°, 120° | 12 (6) | 14 (7) | 16 (8) | 16 (8) | 28 (13) | 36 (17) |
| July 1978, MND, 20°, 120° | 10 (5) | 14 (7) | 16 (8) | 12 (6) | 0 (0) | 0 (0) |

$t_f$ = 90 hr

| | | | | | | |
|---|---|---|---|---|---|---|
| April 1969, AN, 20°, 120° | 9 (4) | 12 (6) | 48 (23) | 68 (32) | 50 (24) | 40 (19) |

TABLE 13 (continued)

$t_f$ = 90 hr

| Year, Lunar Position, $i_m$, $\theta_{MTE}$ | 1st Window Northerly Return ($+i_{eq}$) | | 2nd Window Southerly Return ($-i_{eq}$) | | 3rd Window Northerly Return ($\pm i_{eq}$) | |
|---|---|---|---|---|---|---|
| | $t_p$ = 50 hr | $t_p$ = 100 hr | $t_p$ = 50 hr | $t_p$ = 100 hr | $t_p$ = 50 hr | $t_p$ = 100 hr |
| July 1978, AN, 20°, 120° | 18 (8) | 20 (9) | 50 (24) | 52 (25) | 36 (17) | 36 (17) |
| July 1978, AN, 20°, 90° | 14 (7) | 16 (8) | 48 (23) | 56 (27) | 34 (16) | 26 (12) |
| July 1978, AN, 10°, 120° | 28 (13) | 32 (15) | 56 (27) | 56 (27) | 54 (26) | 50 (24) |

## 3. Departure Window Sensitivities

It is advantageous to qualitatively summarize what effect certain parameters have on departure window sizes and wait times. The table on the following page gives a brief description of window sensitivity due to year, lunar position, lunar parking orbit orientation and flight times. The window variations are described as being minor, moderate or major in nature, as assessed from Figs. 1 through 42.

Aside from the above, window sizes and delay times can also be affected by the governing constraints of $i_{eq\oplus}$, $t_f$, $h_{PL}$ and $h_{PE}$. It has been found during the course of the study that a tolerance of $\pm 0.5°$ on the earth return inclination ($i_{eq\oplus}$) has negligible effect on window sizes and wait times. It is felt that the data presented herein is representative of tolerances of $\pm 1°$ to $\pm 3°$ or in other words $i_{eq\oplus} = \pm 27°$ to $\pm 33°$.

It has also been demonstrated that a flight time tolerance of $\pm 0.5$ hr on the transearth flight time ($t_f$) is quite acceptable. In fact, it can be confidently stated that this tolerance could be extended to $\pm 1.5$ hr without seriously detracting from the study results.

Variations in the lunar parking orbit altitude ($h_{PL}$) and earth perigee altitude ($h_{PE}$) have not been specifically investigated. However, from the experience gained in Chapters VI and IX of Ref. 2 and in Chapter I of Ref. 1, it can be said with assurance that variations of $\pm 100$ km in $h_{PE}$ and $\pm 10$ km in $h_{PL}$ will not alter the data to any significant degree.

## 4. Inject-on-Time Window

In each successive orbital phase during a possible departure window, there is a specific point at which injection can nominally take place. For this study, this point is associated with a nominal injection flight path angle ($\gamma_c$) of zero degree. Actually, the instant of time at which this point is encountered can be enlarged by controlling the injection velocity vector to different directions before and after arrival at the nominal point. In other words, there exists a secondary departure window for each orbital pass, hereafter termed as the "inject-on-time" window.

Since the inject-on-time window is of shorter duration, several assumptions can be made which simplify the problem considerably, but which can be shown to have a very small effect on the actual physical situation. These assumptions are:

| | Mission I | | | Mission II | | | Mission III | | | Mission IV | | |
|---|---|---|---|---|---|---|---|---|---|---|---|---|
| | Window | 1st Wait Time | Wait Time | Window | 1st Wait Time | Wait Time | Window | 1st Wait Time | Wait Time | Window | 1st Wait Time | Wait Time |
| Year | Minor | Moderate | Minor | Moderate | Minor | Moderate | Minor | Minor | Minor | Minor | Minor | Major |
| Lunar position | Minor | Moderate | Minor | Moderate | Major | Major | Minor | Minor | Minor | Moderate | Minor | Moderate |
| $i_m$ | Minor | Minor | Minor | Minor | Minor | Moderate | Major | Major | Major | Minor | Minor | Minor |
| $\theta_{MTE}$ | Minor | Major | Minor | Minor | Minor | Minor | Minor | Major | Major | Minor | Minor | Minor |
| $t_f$ | -- | -- | -- | -- | -- | -- | Major | Major | Major | Minor | Minor | Moderate |
| $t_p$ | -- | -- | -- | Minor | Minor | Minor | -- | -- | -- | Minor | Minor | Minor |

(1) The lunar parking orbit and the initial transearth trajectory lie in the same plane.

(2) The plane of the parking orbit does not change due to nodal regression during the secondary departure window.

(3) The time to traverse the nominal and the off-nominal transearth trajectories is the same.

(4) The maneuver is impulsive (zero burning time).

Now, it is possible to inject earlier at a negative flight path angle and later at a positive flight angle with an accompanying velocity loss. The velocity loss is due to the requirement of deflecting the parking orbit velocity vector to a desired $\gamma_{\mathbb{C}}$ and increasing the velocity magnitude to $V_{\mathbb{C}}$ when using "impulsive" corrections.

If the nominal altitude and circular parking orbit velocity are kept the same, then the energy will remain the same, and only the flight path angle $\gamma_{\mathbb{C}}$ will change with the central angle ($\beta_M$). The problem thus reduces to determining ($\beta_M$) as a function of $\gamma_{\mathbb{C}}$ and relating these two parameters to the injection velocity and time.

Since the transearth trajectory relative to the moon just after ejection is a hyperbola, the relation between $\gamma_{\mathbb{C}}$ and $\beta_M$ for constant energy trajectories (i.e., constant eccentricity, e) is (Chapter III of Ref. 4)

$$\gamma_{\mathbb{C}} = \cos^{-1}\left\{\frac{1 + e\cos\beta_M}{\left[1 + 2e\cos\beta_M + e^2\right]^{1/2}}\right\} . \qquad (31)$$

Thus, if either $\gamma_{\mathbb{C}}$ or $\beta_M$ is known, the other is readily calculated. In this study, $\beta_M$ is determined by assuming values for $\gamma_{\mathbb{C}}$ and the transearth injection time is found by multiplying $\beta_M$ by the constant angular velocity $\dot{\beta}_M$. Time equal to zero is defined as the time at which $\beta_M = \gamma_{\mathbb{C}} = 0$.

The impulsive velocity increment, $\Delta V_i$, required above the lunar parking orbit velocity, $V_{\mathbb{C}c}$, due to the change in $\gamma_{\mathbb{C}}$ is found from the law of cosines in terms of the circular parking orbit velocity, $V_{\mathbb{C}c}$

$$\left(\frac{\Delta V_i}{V_{\mathbb{C}c}}\right)^2 = 1 + \left(\frac{V_{\mathbb{C}o}}{V_{\mathbb{C}c}}\right)^2 - 2\left(\frac{V_{\mathbb{C}o}}{V_{\mathbb{C}c}}\right) \cos \gamma_{\mathbb{C}} . \qquad (32)$$

The graph shown in Fig. 43 presents the velocity requirements for a typical inject-on-time window as a function of time and of flight path angle, $\gamma_{\mathbb{C}}$. The velocity impulse $\Delta(\Delta V)$ is defined as the difference between $\Delta V_i$ and $\Delta V$ where $\Delta V$ is the velocity impulse required above the lunar parking orbit velocity, $V_{\mathbb{C}c}$ when $\gamma_{\mathbb{C}} = 0$. These requirements are for a 70-hr transearth trajectory flight time (eccentricity $\approx 1.422$).

The positive and negative limits of $\gamma_{\mathbb{C}}$ about the nominal $\gamma_{\mathbb{C}} = 0$ are subject to the following constraints:

(1) Negative $\gamma_{\mathbb{C}}$ constraint = minimum pericynthion to avoid impact with the lunar surface.

(2) Negative and positive $\gamma_{\mathbb{C}}$ constraints = maximum practical $\Delta(\Delta V)$ velocity impulse limitation.

For the situation depicted in the graph, the minimum $\gamma_{\mathbb{C}}$ was found to be -19.3° which corresponded to a time of -11.1 min. If the maximum velocity impulse $[\Delta(\Delta V)]$ available is 0.1 km/sec, then this secondary departure window at a lunar altitude of 185.2 km yields a window size of 17 min. As was shown in Ref. 1 of Chapter I, the $\Delta(\Delta V)$ requirements will increase because of finite burning and the optimum $\gamma_{\mathbb{C}}$ will shift from 0° to some positive value.

## E. MISSION IMPLICATIONS

The above sections have discussed in detail the various methods which can be employed to generate departure windows from a lunar parking orbit. Also included are numerical results for departure window sizes, injection frequencies, and waiting times for these methods which reflect various imposed constraints. It is the intent of this section to give an insight to the philosophy that is presently associated with lunar missions and their related windows. This can be best accomplished by depicting sample missions and the circumstances that may be present during their execution.

First, the spacecraft may originally leave the earth's vicinity either from an "independent" parking orbit or from a "dependent" parking orbit. The former implies a convenient orbit established at the end of boost and the latter refers to a parking orbit of an earth orbiting space station. It may be necessary to transfer additional personnel and supplies and also assemble necessary "space structure" in the independent orbit prior to embarking on the translunar trip. Likewise, supplies and personnel may have to be "shuttled" to the space station if the station is being used as a "jumping off" point. In either case, there may be extensive waiting in the earth parking orbit before the lunar mission is initiated. Once all the tasks are complete and the spacecraft makes an entrance into an earth-to-moon departure window, the spacecraft then injects into a translunar trajectory that arrives at the moon with a specific orientation.

Upon arrival at the moon, the vehicle then establishes a lunar parking orbit and the next phase of the mission commences. This phase may be a photographic or surveillance operation or perhaps supplies and personnel are "shuttled" to and from a lunar base. Or, possibly, a separate vehicle module is used to descend to the lunar surface for surface exploration and upon completion of its mission rejoins the orbiting module. All of these possible mission phases utilize a lunar parking orbit which is regressing with time because of the moon's triaxiality. In addition, the parking orbit orientation is changing rapidly because of the moon's travel around the earth. As soon as the lunar mission phase is completed and the spacecraft enters a moon-to-earth departure window, the transearth injection maneuver is executed.

The transearth trajectory will have stringent requirements depending on the operational concept. For instance, by timing the arrival at earth, the spacecraft may directly re-enter the earth's atmosphere and be recovered at a landing site. An alternative that eliminates the timing consideration is to enter an earth parking orbit and allow the earth to rotate underneath it until a proper orientation is attained that allows shuttle service from the earth's surface. It may be required to rendezvous with the earth orbiting space station for resupply and to initiate another logistics mission from this station. In any event, the inclination and flight time of the transearth trajectory is most important and must be considered the prime criteria for defining the transearth injection requirements. However, the translunar injection requirements are dependent on the wait time in lunar orbit that is required to complete the lunar tasks and also to allow for contingencies. This wait time is referred to as the first wait time and also has frequently been termed the lunar stay time when there is a specific mission in mind. Therefore, it is very logical to have a moon-to-earth departure window located immediately after this stay time to minimize life-support requirements and space-exposure time. However, depending on the complexity

of the mission, it may be desirable to provide ample life support capability until the next launch window, e.g., in the event a malfunction exceedingly delays the transearth injection.

In order to gain a firmer grasp of the data presented in the previous sections, it will be specified, as part of a sample operational concept, that maneuvers other than the transearth injection maneuver are not permitted in the lunar parking orbit (Missions I and II). With this restriction transearth flight time is not readily controllable and is a function of the time since entering the departure window. The placement of the departure window itself and consequently the duration of the lunar stay time is realized by planning the lunar mission for a given time during the month and/or by controlling the parking orbit longitude ($\theta_{MTE}$) at the nominal lunar arrival. Generally there are two departure windows per month for this case and returns to earth can be from the southerly or northerly direction (relative to earth's equator).

Although a window may exist for a considerable length of time, it must be realized that there are some practical problems associated with this case. For example, if a direct atmospheric re-entry is to be made, there is the necessary timing requirement that allows recovery to take place on a given land mass. Since the transearth flight time is not controllable at the time of transearth injection, then two choices present themselves. First, although within a departure window, the transearth injection must be delayed until the timing requirement is met or, secondly, perform the transearth injection with a subsequent timing maneuver along the transearth trajectory prior to reaching earth. With either choice or even a combination of choices, only portions of the windows will actually be available. The full window could be realized only if the spacecraft returns to an independent parking orbit (no timing or rendezvous restrictions).

If the spacecraft must return and rendezvous with the orbiting space station, with which it had originated the lunar mission, there generally will be one transearth departure window per month. The first wait time (or stay time) associated with this requirement is usually of a much longer duration than without the rendezvous requirement. The date of translunar departure is the controlling variable to effectively regulate the stay time. Normally, the entire window is available for earth departures, but, in the event of an extremely long unscheduled delay, there is usually a very long wait time (as long as a month) until entrance into the next departure window. The spacecraft may have to revert, in this circumstance, to returning to earth into an independent parking orbit which can be supplied by earth shuttle until rendezvous with the space station can be effected.

Next, assume an operational concept that allows maneuvers to take place in the lunar parking orbit. This mission flexibility now enables the spacecraft to control its transearth flight time as well as its return inclination. If there are no rendezvous requirements (Mission III) at earth, there are again two transearth departure windows per month that allow both northerly and southerly returns to earth. Since flight time can be controlled, the entire transearth departure window is usually available. However, the exact use of the window depends on the required transearth flight time, which may be continually changing. Thus, it cannot be expected to have a specific value of flight time that is held constant throughout the window. Instead, the return time will be variable according to the geometry of the earth and transearth trajectory plane and therefore the windows may actually be larger than those presented for one constant return flight time.

The width of the windows for this case is controlled by lunar parking orbit inclination ($i_m$) and the transearth flight time, especially when the required flight time can be preplanned to have higher values consistently throughout the window. The placement of the windows is governed by the above mentioned factors plus the initial lunar parking orbit orientation, $\theta_{MTE}$.

When a rendezvous requirement is present, there are usually three windows in a month's span, but the return direction is not arbitrary. Control of the initial wait time (stay time) is not readily accomplished, and the window sizes are nearly invariant regardless of initial conditions.

From the above discussion and the previous data, it can be seen that if maneuvers are allowed in the lunar parking orbit, operations can be made more flexible, especially when an earth rendezvous must be conducted. Furthermore, there are complications that arise when mission details are considered. Examination of these details and their effect on the above windows is beyond the scope of this report.

## F. REFERENCES


1. "Extension of Effort for Orbital and Lunar Flight Handbooks," Vol. II, Martin Company, Space Systems Division, Baltimore, Maryland, ER 13189-II, 1963.

2. "Lunar Flight Handbook," Martin Company, Space Systems Division, Baltimore, Maryland, ER 12685, 1963.

3. "Explanatory Supplement to the Astronomical Ephemeris and the American Ephemeris and Nautical Almanac," Her Majesty's Stationery Office, London, 1961.

4. "Orbital Flight Handbook," Martin Company, Space Systems Division, Baltimore, Maryland, ER 12684, 1963.

MISSION I

Departure Windows

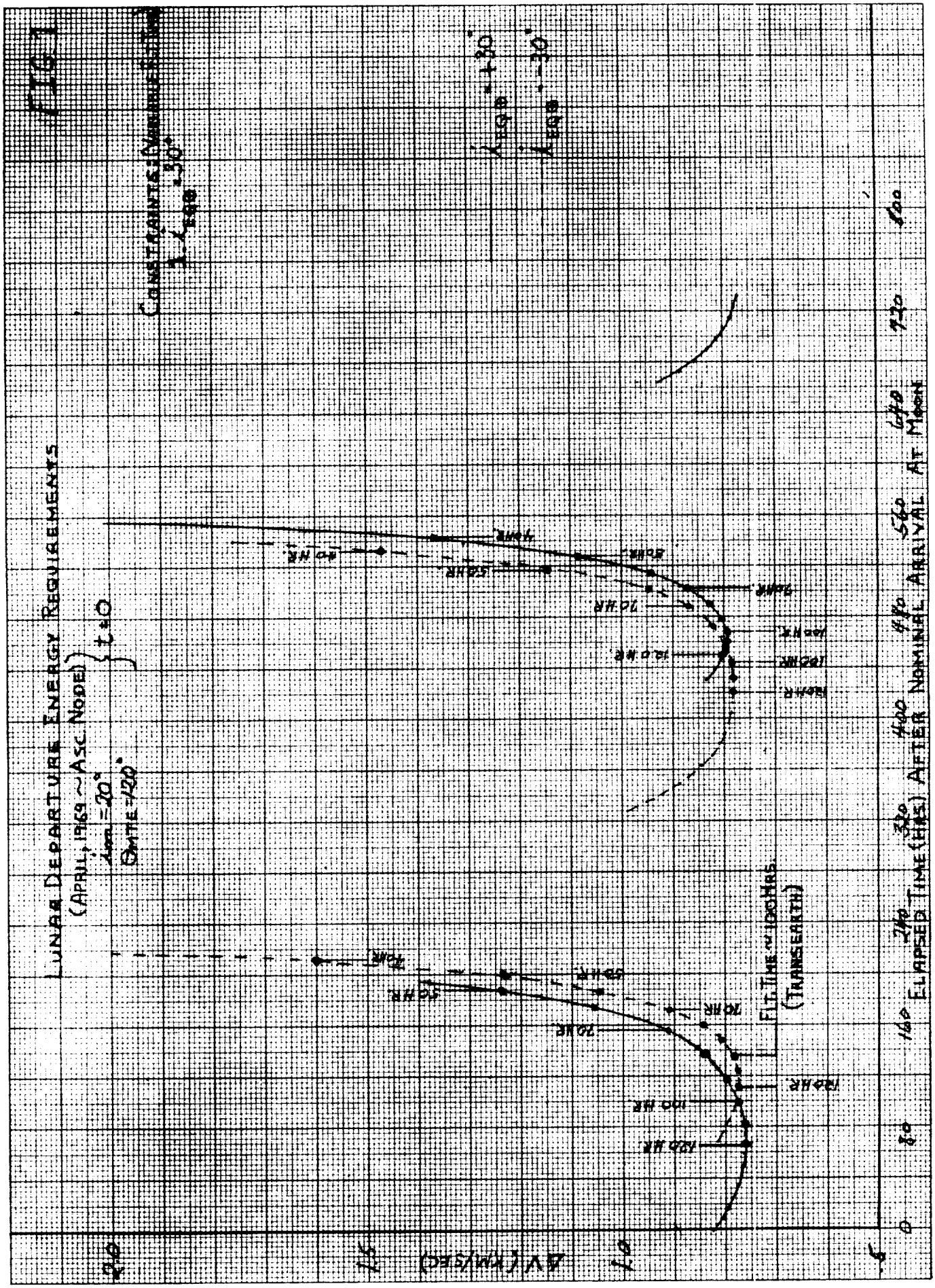
FIG. 1
LUNAR DEPARTURE ENERGY REQUIREMENTS
(APRIL, 1969 ~ ASC. NODE)
$\lambda_{asc} = 20°$
$\Omega_{MTE} = 120°$
$i \pm 0$
CONSTRAINTS: VARIABLE $\lambda_{EQB}$
1. $\lambda_{EQB} \pm 30°$
$\lambda_{EQB} = +30°$
$\lambda_{EQB} = -30°$
$\Delta V$ (FPS/SEC)
FLT. TIME (HRS) (TRANSEARTH)
ELAPSED TIME (HRS) AFTER NOMINAL ARRIVAL AT MOON
0
60
120
180
240
300
360
420
480
540
600
660
720
780
840
900
960
1000
40 HR
45 HR
50 HR
55 HR
60 HR
70 HR
80 HR
90 HR
100 HR
120 HR
140 HR
160 HR
180 HR
200 HR

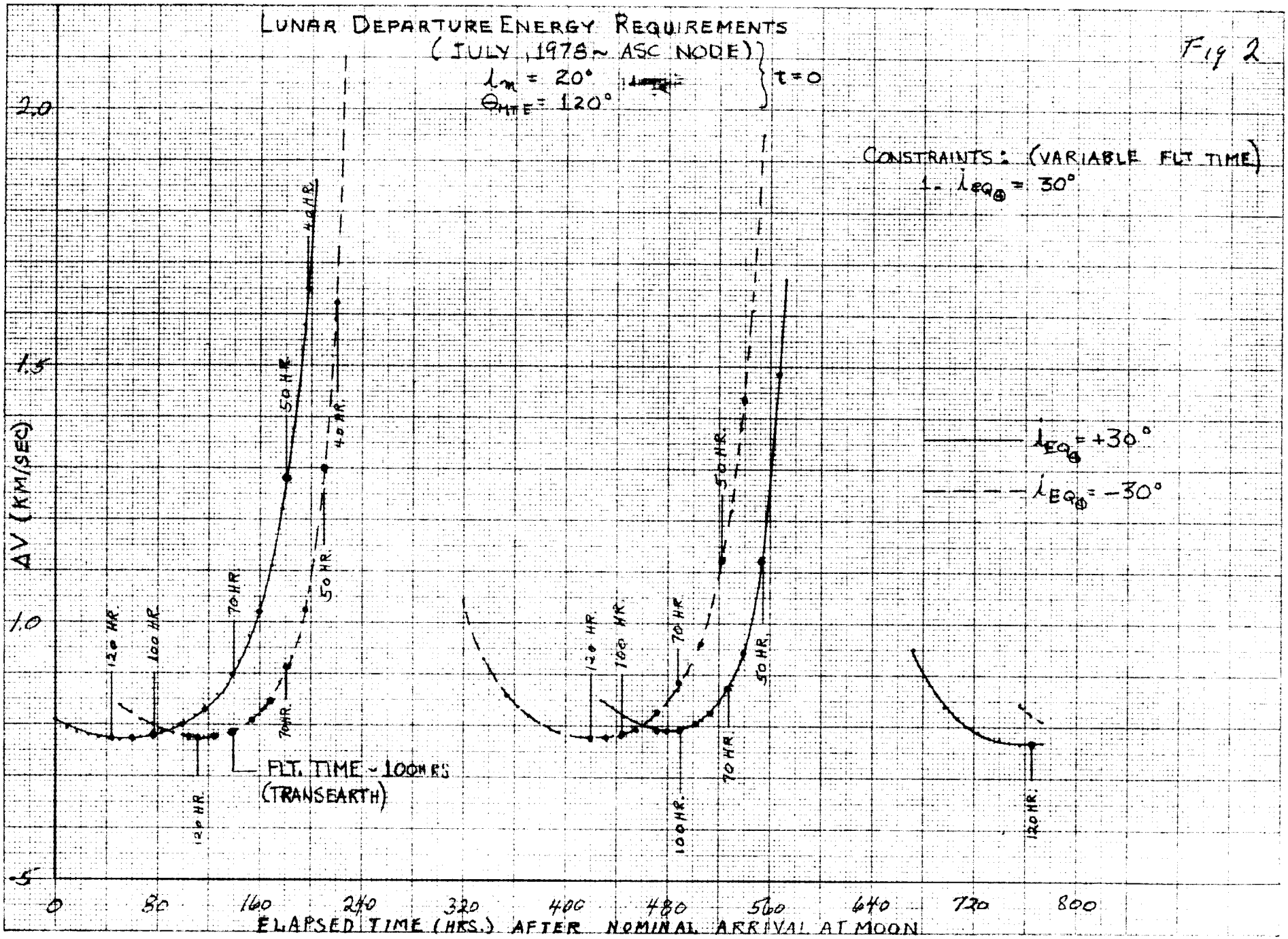
LUNAR DEPARTURE ENERGY REQUIREMENTS
(JULY, 1978 ~ ASC NODE)
$i_m$ = 20°
$\Theta_{MTE}$ = 120°
t = 0
Fig 2
CONSTRAINTS: (VARIABLE FLT TIME)
1. $i_{EQ_\oplus}$ = 30°
$i_{EQ_\oplus}$ = +30°
$i_{EQ_\oplus}$ = -30°
ΔV (KM/SEC)
2.0
1.5
1.0
.5
120 HR.
100 HR.
70 HR.
50 HR.
40 HR.
FLT. TIME ~ 100 HRS
(TRANSEARTH)
0
80
160
240
320
400
480
560
640
720
800
ELAPSED TIME (HRS.) AFTER NOMINAL ARRIVAL AT MOON

FIG. 3

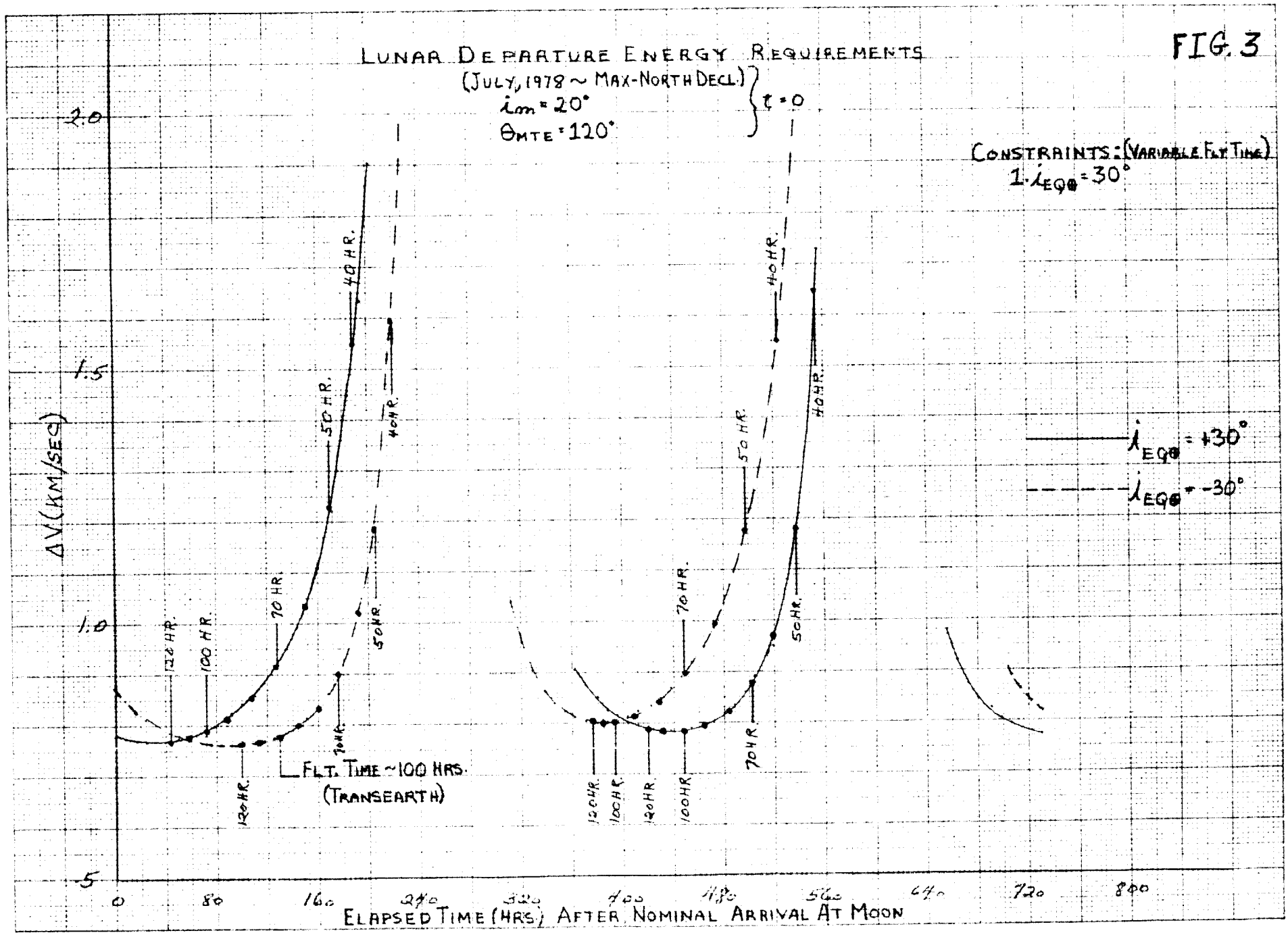
LUNAR DEPARTURE ENERGY REQUIREMENTS
(JULY, 1978 ~ MAX-NORTH DECL.)
$i_m = 20°$
$\theta_{MTE} = 120°$
$t = 0$
CONSTRAINTS: (VARIABLE FLT TIME)
1. $\lambda_{EQ\oplus} = 30°$
$\lambda_{EQ\oplus} = +30°$
$\lambda_{EQ\oplus} = -30°$
$\Delta V$ (KM/SEC)
2.0
1.5
1.0
.5
0
80
160
240
320
400
480
560
640
720
800
ELAPSED TIME (HRS) AFTER NOMINAL ARRIVAL AT MOON
120 HR.
100 HR.
70 HR.
50 HR.
40 HR.
FLT. TIME ~ 100 HRS.
(TRANSEARTH)

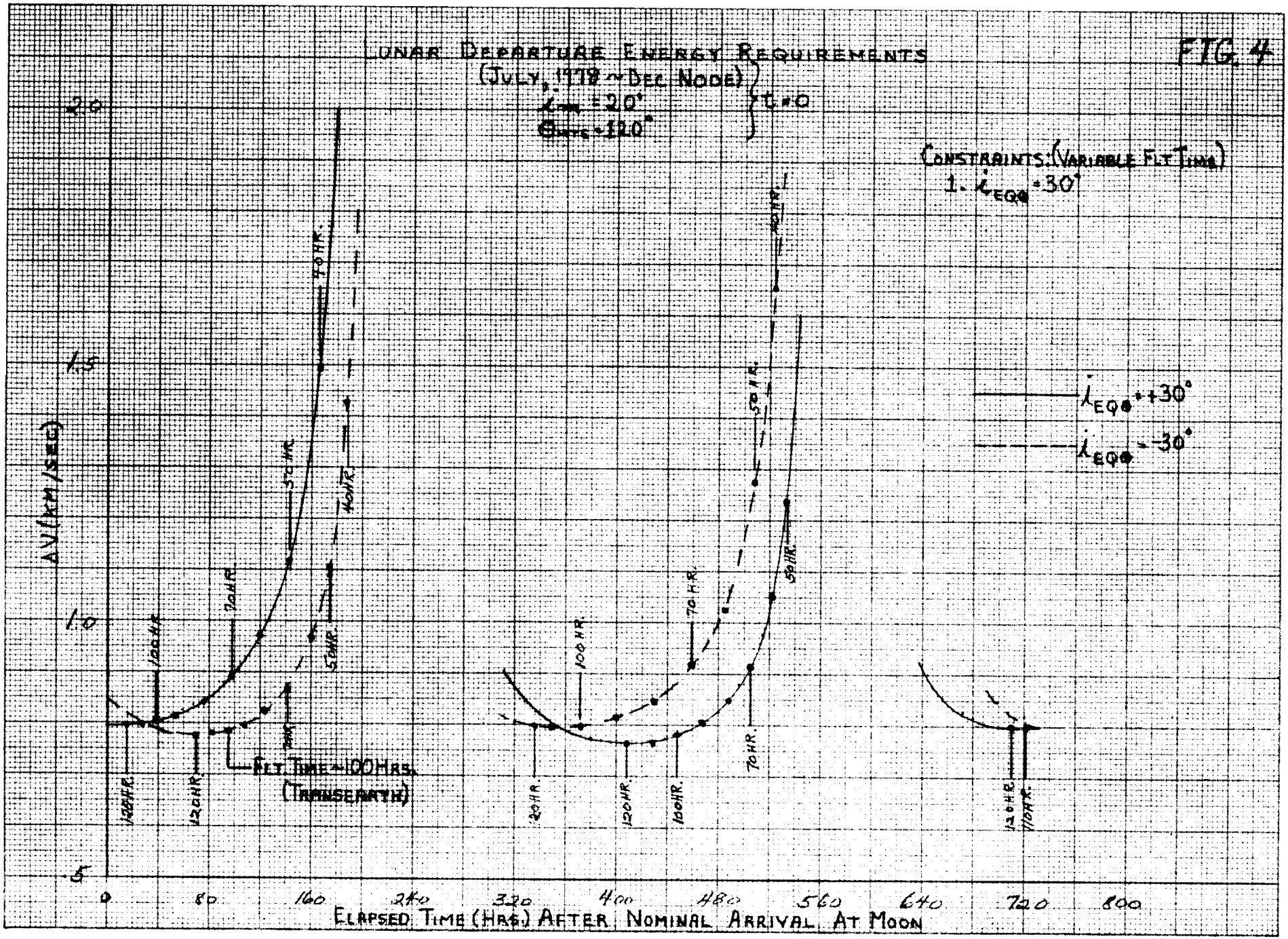
LUNAR DEPARTURE ENERGY REQUIREMENTS
(JULY, 1979 ~ DEC. NODE)
$\lambda_{EQ\oplus} = 20°$
$\Theta_{MCC} = 120°$
t=0
FIG. 4
CONSTRAINTS: (VARIABLE FLT TIME)
1. $\lambda_{EQ\oplus} = 30°$
$\lambda_{EQ\oplus} = +30°$
$\lambda_{EQ\oplus} = -30°$
ΔV (KM/SEC)
2.0
1.5
1.0
.5
0
80
160
240
320
400
480
560
640
720
800
ELAPSED TIME (HRS.) AFTER NOMINAL ARRIVAL AT MOON
FLT. TIME = 100 HRS.
(TRANSEARTH)
120HR.
100HR.
80HR.
70HR.
60HR.
50HR.
40HR.
30HR.
20HR.

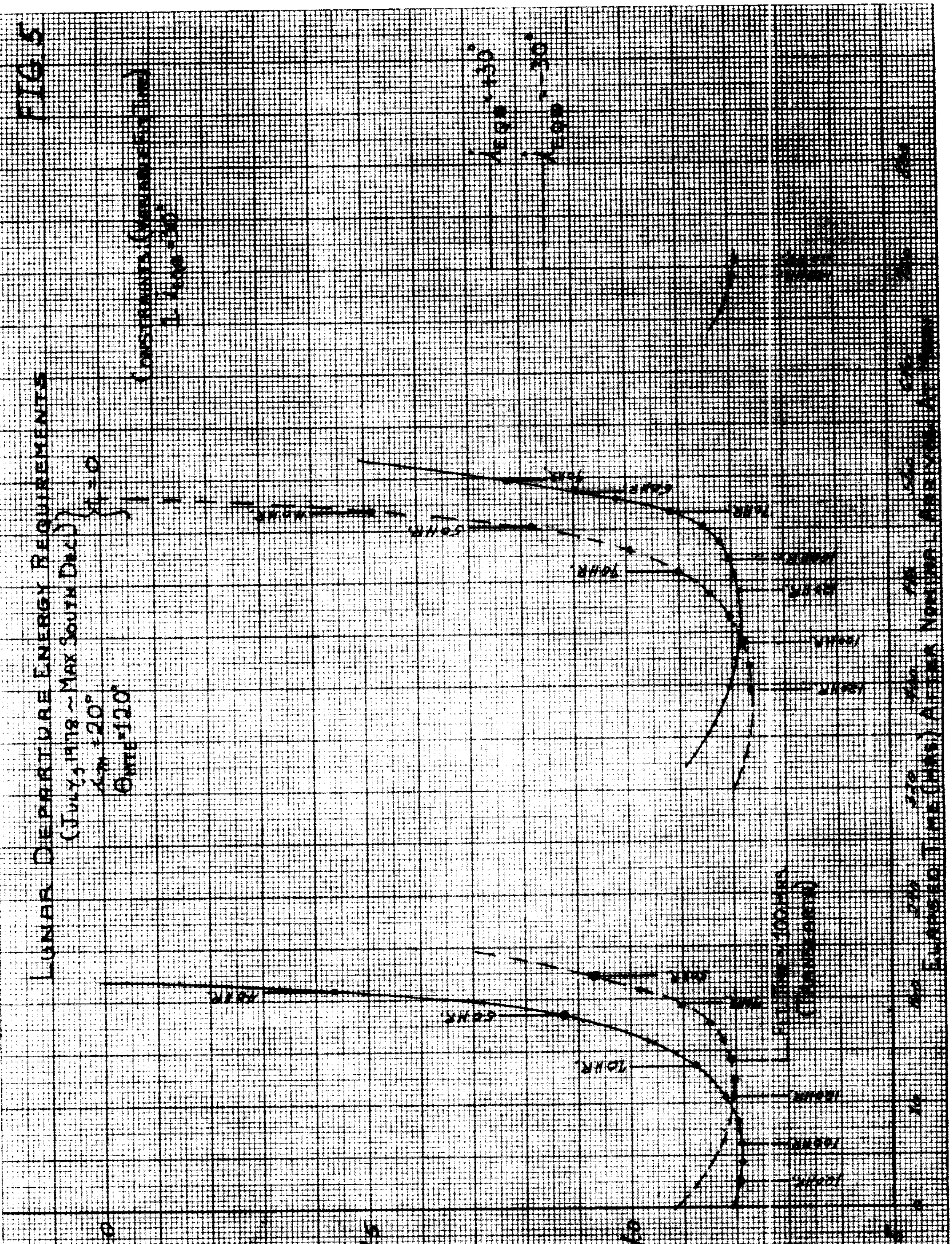
FIG 5
LUNAR DEPARTURE ENERGY REQUIREMENTS
(JULY, 1978 ~ MAX SOUTH DEC.)
θ = 120°
ΔV (KM/SEC)
ELAPSED TIME (HRS) AFTER NODAL ARRIVAL
2.0
1.5
1.0

FIG 6

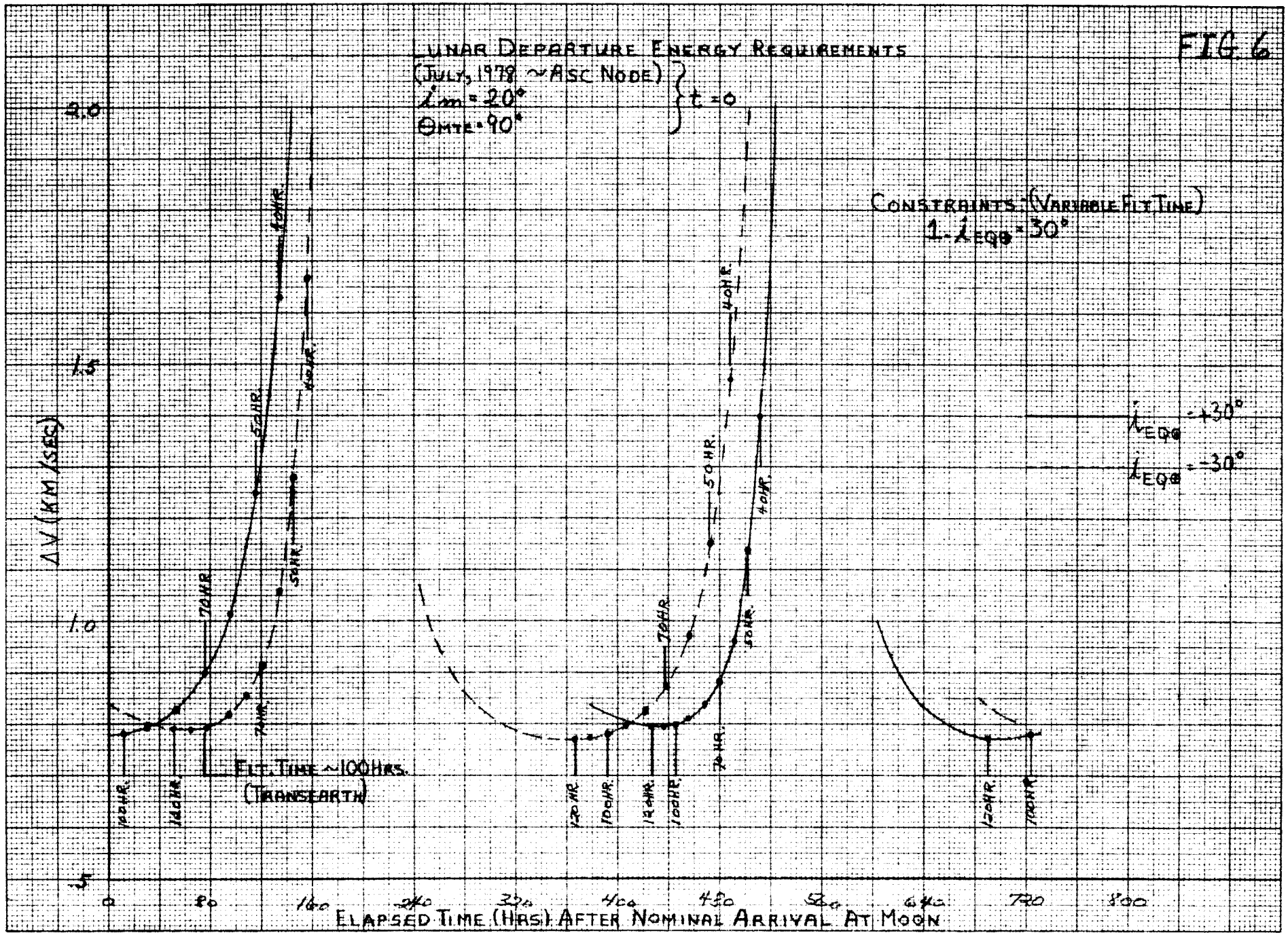
LUNAR DEPARTURE ENERGY REQUIREMENTS
(JULY, 1978 ~ ASC NODE)
$i_m = 20°$
$\Theta_{MTE} = 90°$
t = 0
CONSTRAINTS: (VARIABLE FLT. TIME)
1. $\lambda_{EQ\Theta} = 30°$
$\lambda_{EQ\Theta} = +30°$
$\lambda_{EQ\Theta} = -30°$
ΔV (KM/SEC)
3.0
2.5
2.0
1.5
1.0
.5
0
80
160
240
320
400
480
560
640
720
800
ELAPSED TIME (HRS) AFTER NOMINAL ARRIVAL AT MOON
FLT. TIME ~ 100 HRS.
(TRANSEARTH)
40HR.
50HR.
70HR.
72HR.
100HR.
120HR.
140HR.
160HR.

FIG. 7

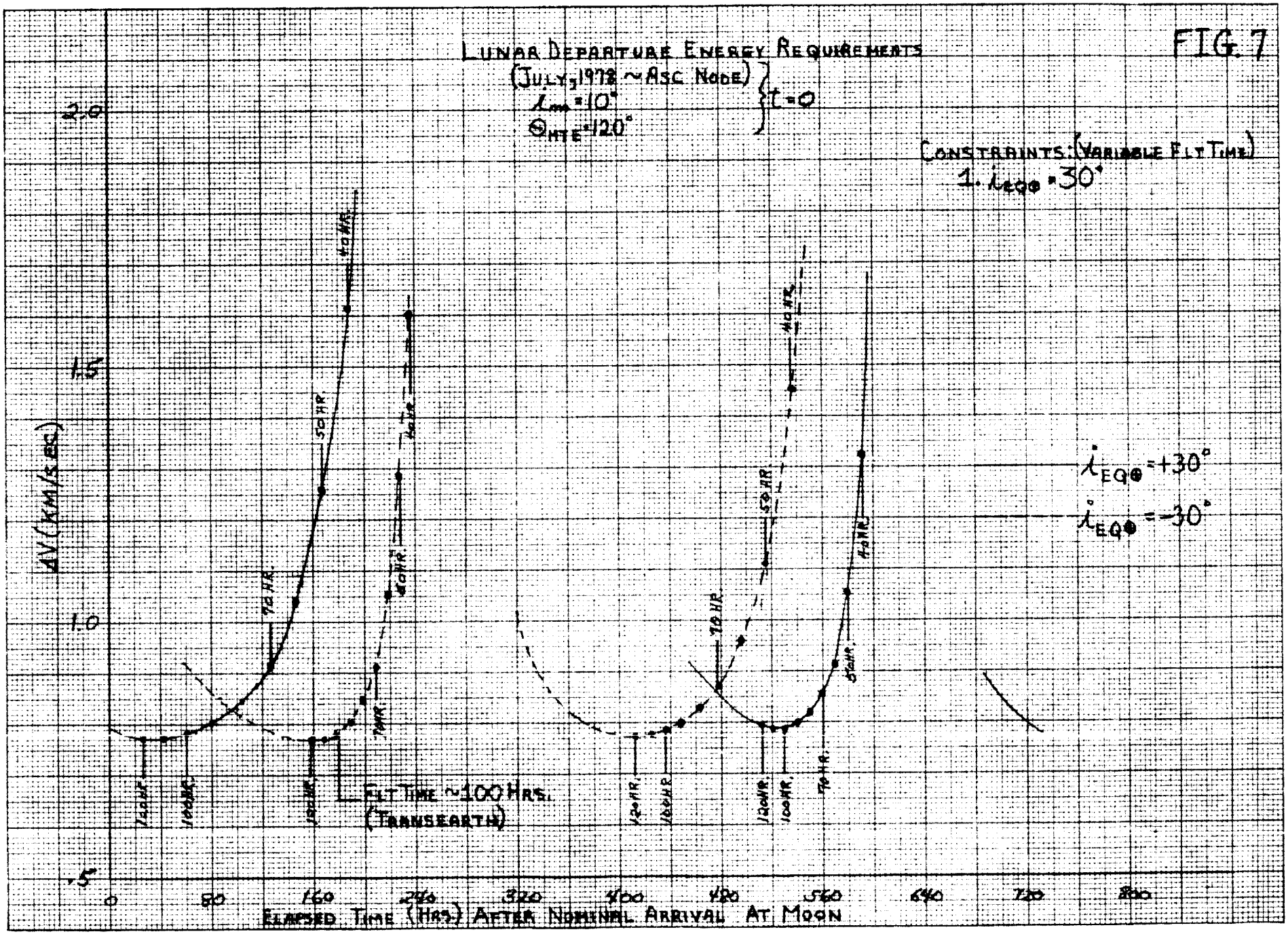
LUNAR DEPARTURE ENERGY REQUIREMENTS
(JULY, 1972 ~ ASC. NODE)
$i_{MS}$ = 10°
$\Theta_{MTE}$ = 120°
t = 0
CONSTRAINTS: (VARIABLE FLT TIME)
1. $i_{EQ\oplus}$ = 30°
$i_{EQ\oplus}$ = +30°
$i_{EQ\oplus}$ = -30°
ΔV (KM/SEC)
2.0
1.5
1.0
.5
0
80
160
240
320
400
480
560
640
720
800
ELAPSED TIME (HRS.) AFTER NOMINAL ARRIVAL AT MOON
FLT TIME ~100 HRS.
(TRANSEARTH)
72 HR.
56 HR.
40 HR.
24 HR.
16 HR.
120 HR.
140 HR.
160 HR.
180 HR.
200 HR.

MISSION II

Departure Windows

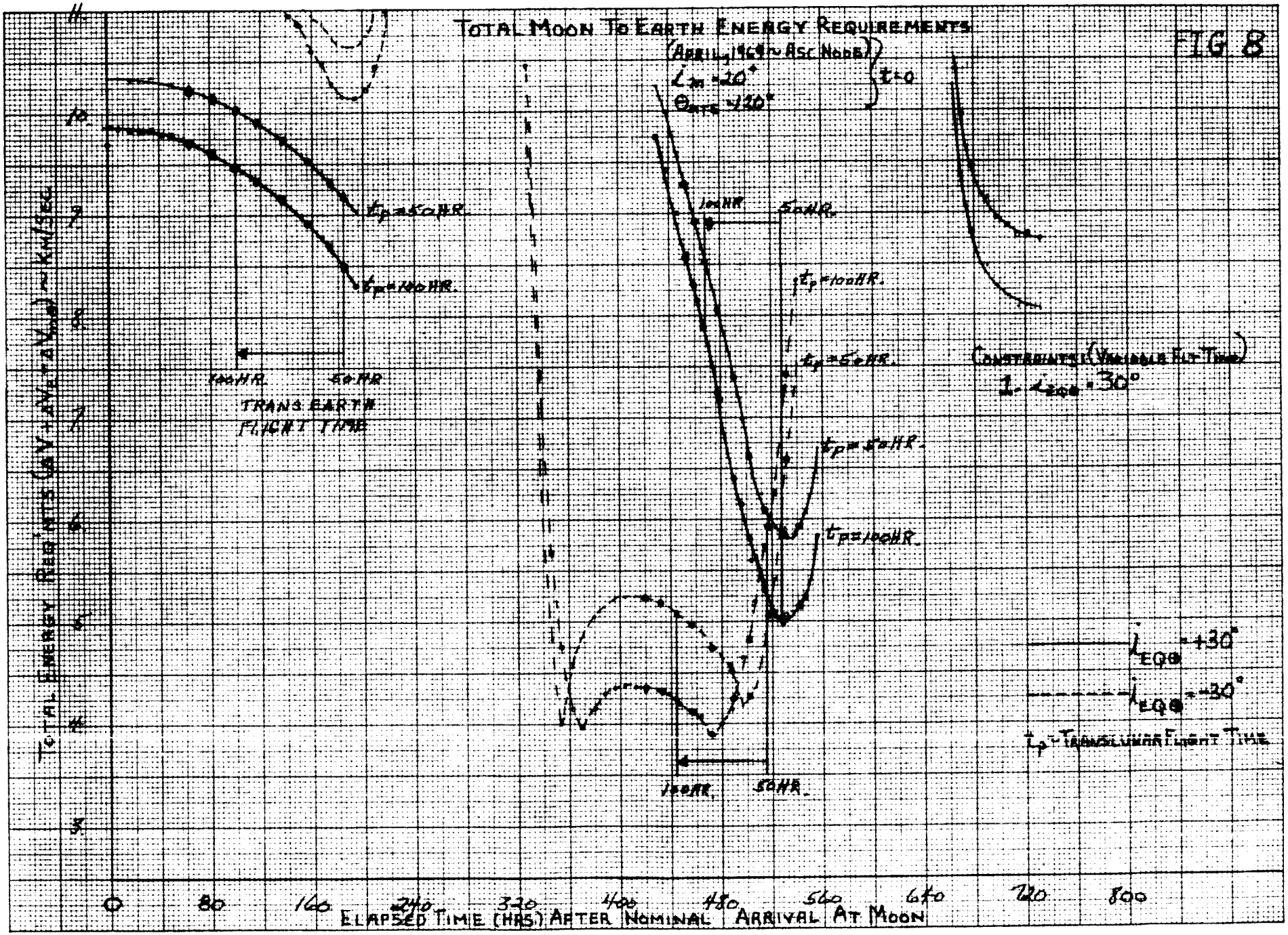
TOTAL MOON TO EARTH ENERGY REQUIREMENTS
(APRIL 1969 ~ ASC NODE)
$i_m$ = 20°
$\Theta_{MTE}$ = 120°
t=0
FIG 8
$t_p$ = 150 HR.
$t_p$ = 100 HR.
100 HR
50 HR
TRANS EARTH FLIGHT TIME
$t_p$ = 100 HR.
$t_p$ = 50 HR.
CONSTRAINTS (VARIABLE FLT TIME)
1. $i_{EQ\Phi}$ = 30°
$t_p$ = 50 HR.
$t_p$ = 100 HR.
100 HR
50 HR
$i_{EQ\Phi}$ = +30°
$i_{EQ\Phi}$ = -30°
$t_p$ = TRANSLUNAR FLIGHT TIME
TOTAL ENERGY REQUIREMENTS (ΔV · ΔV_MAG) - KM/SEC
10
9
8
7
6
5
0
80
160
240
320
400
480
560
640
720
800
ELAPSED TIME (HRS) AFTER NOMINAL ARRIVAL AT MOON

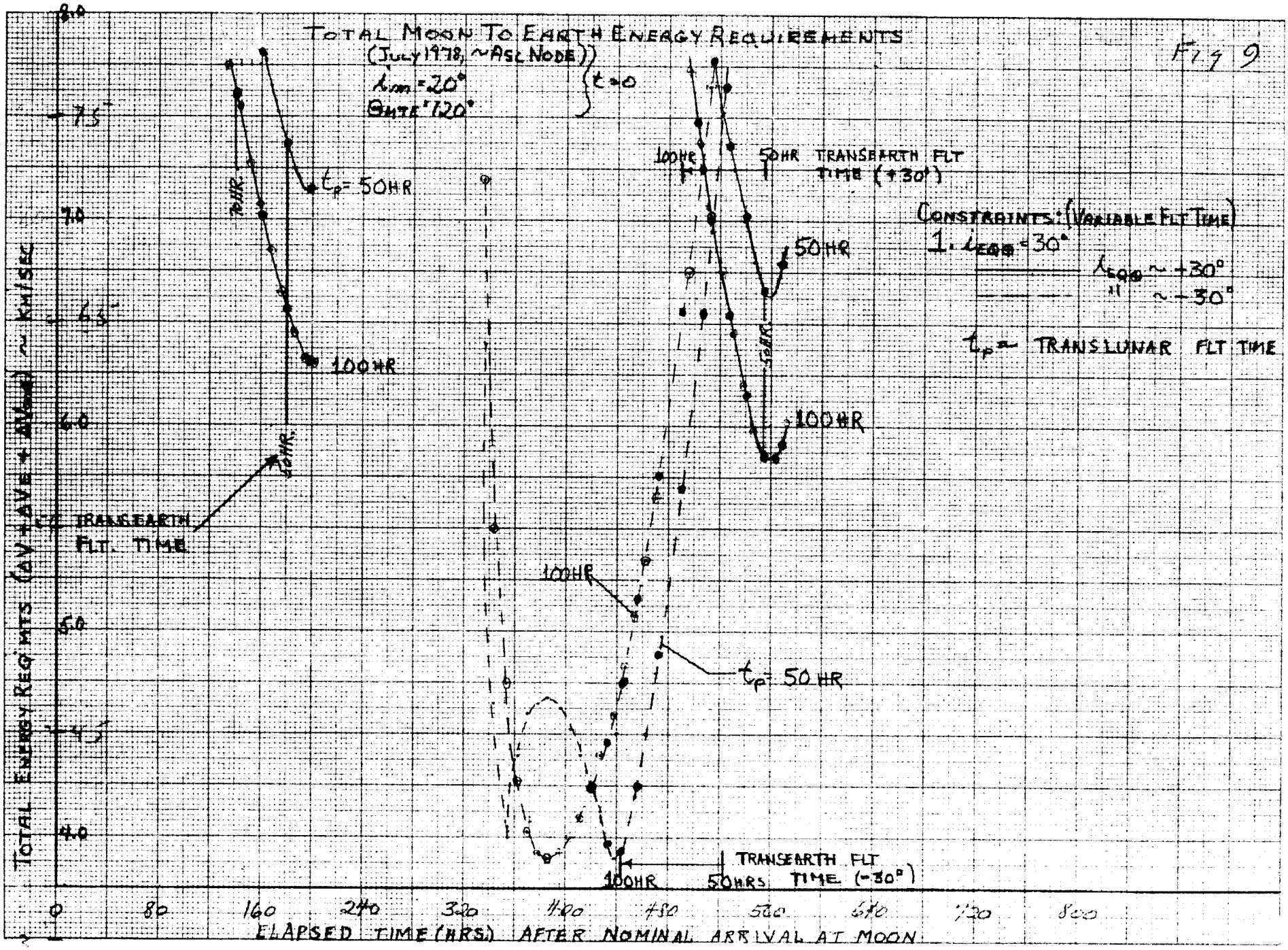
TOTAL MOON TO EARTH ENERGY REQUIREMENTS
(JULY 1978, ~ASC. NODE)
$i_{VM} = 20°$
$\Theta_{MTE} = 120°$
Fig 9
$t_p$= 50HR
100HR
24HR
48HR
TRANSEARTH FLT. TIME
50HR TRANSEARTH FLT TIME (+30°)
CONSTRAINTS: (VARIABLE FLT TIME)
1. $i_{EQ\Phi} = 30°$
$i_{EQ\Phi} \sim +30°$
$\sim -30°$
$t_p$ = TRANSLUNAR FLT TIME
50HR
100HR
TRANSEARTH FLT TIME (-30°)
50HRS
TOTAL ENERGY REQ'MTS ($\Delta V + \Delta V_{EC} + \Delta V_{LOI}$) ~ KM/SEC
7.5
7.0
6.5
6.0
5.5
5.0
4.5
4.0
0
80
160
240
320
400
480
560
640
720
800
ELAPSED TIME (HRS.) AFTER NOMINAL ARRIVAL AT MOON

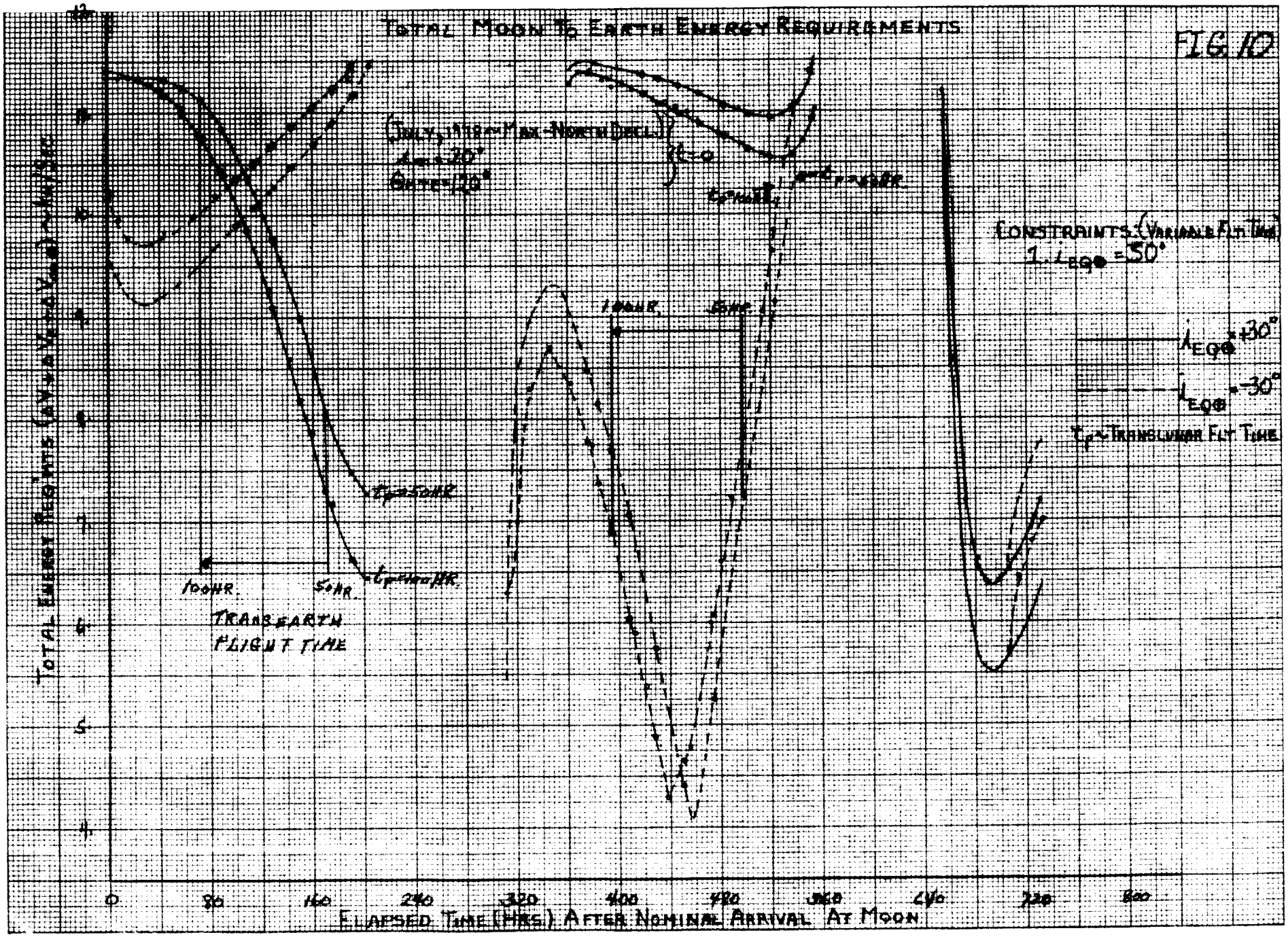
TOTAL MOON TO EARTH ENERGY REQUIREMENTS
FIG. 10
TOTAL ENERGY REQUIREMENTS (KM²/SEC²) VARIATION WITH
(ONLY WHEN MAX NORTH DECL.)
$\lambda_{max}=20°$
$\theta_{MPE}=120°$
$t_f=0$
$t_f=t_{f_{MIN}}$
$t_f=t_{f_{MAX}}$
CONSTRAINTS (VARIABLE FLT TIME)
1. $\lambda_{EQ\oplus}=50°$
$\lambda_{EQ\oplus}=+30°$
$\lambda_{EQ\oplus}=-30°$
$t_f$ = TRANSLUNAR FLT TIME
100HR.
50HR.
$t_f=250HR$
$t_f=160HR$
100HR.
50HR.
TRANSEARTH FLIGHT TIME
0
80
160
240
320
400
480
560
640
720
800
ELAPSED TIME (HRS.) AFTER NOMINAL ARRIVAL AT MOON

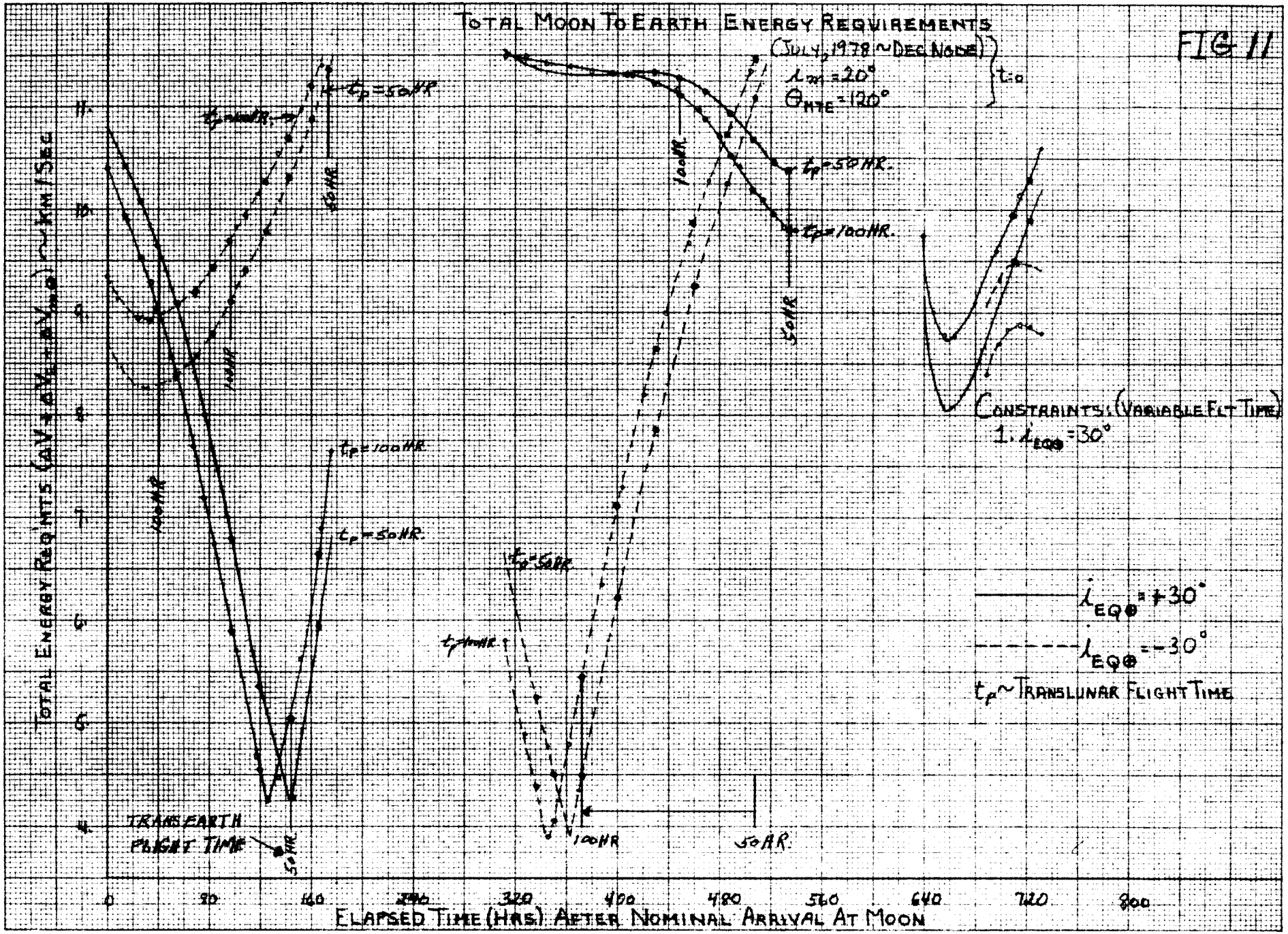
TOTAL MOON TO EARTH ENERGY REQUIREMENTS
(JULY, 1978 ~ DEC NODE)
$\lambda_m = 20°$
$\theta_{MTE} = 120°$
$t_{i=0}$
FIG 11
TOTAL ENERGY REQ'MTS ($\Delta V^2 + \Delta V_{LOI}^2 = \Delta V_{TOT}^2$) ~ KM/SEC
$t_p$=100HR.
$t_p$=50HR.
TRANS EARTH FLIGHT TIME
CONSTRAINTS: (VARIABLE FLT TIME)
1. $i_{EQ\oplus} = 30°$
$i_{EQ\oplus} = +30°$
$i_{EQ\oplus} = -30°$
$t_p$ ~ TRANSLUNAR FLIGHT TIME
0
80
160
240
320
400
480
560
640
720
800
ELAPSED TIME (HRS) AFTER NOMINAL ARRIVAL AT MOON

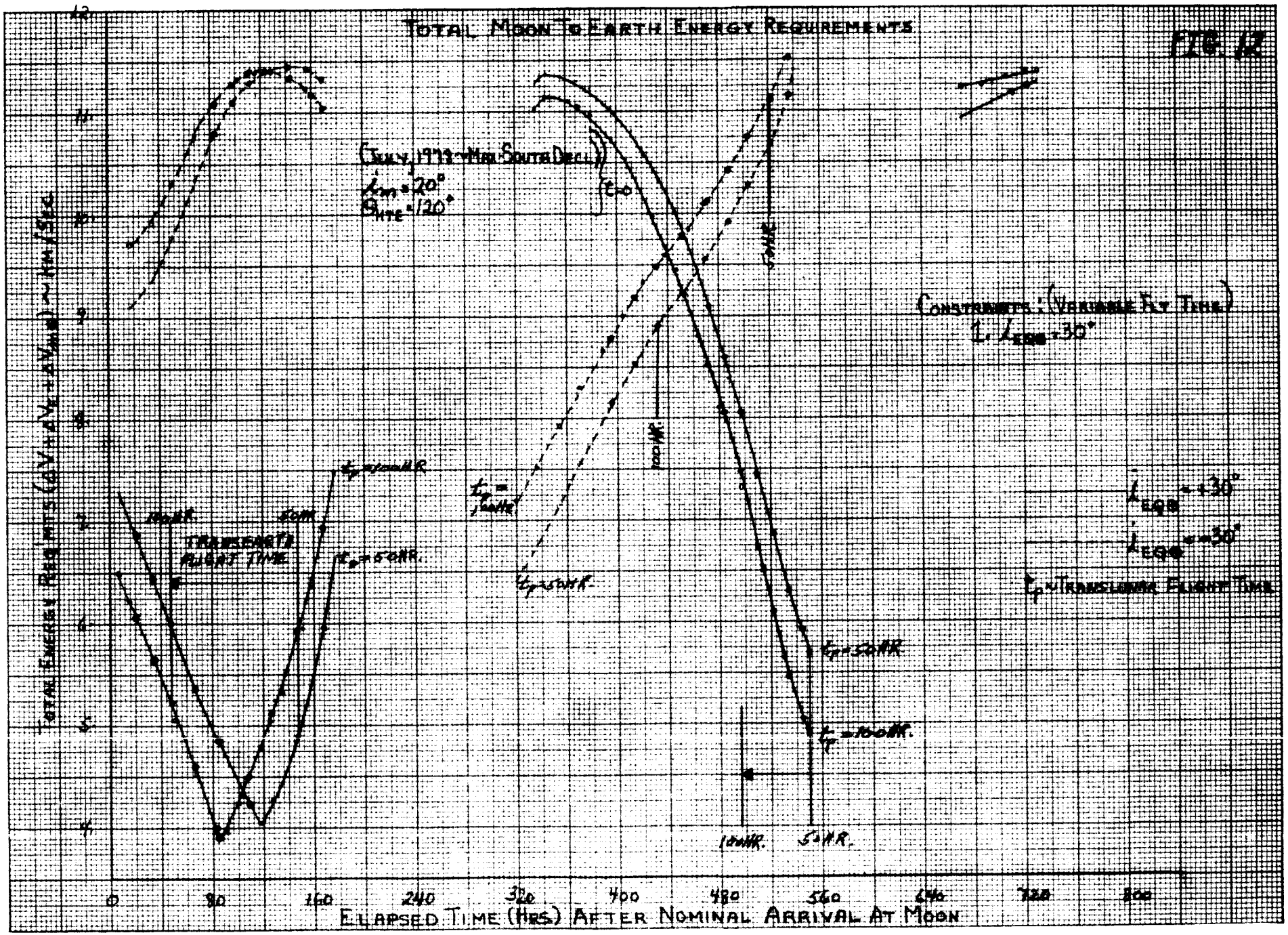
TOTAL MOON TO EARTH ENERGY REQUIREMENTS
FIG. 42
(JULY, 1977 - MID SOUTH DECL.)
$i_{MM}$ = 20°
$\Theta_{MTE}$ = 120°
$t_F$ = TRANSLUNAR FLIGHT TIME
$i_{EQB}$ = +30°
$i_{EQA}$ = -30°
CONSTRAINTS: (VARIABLE FLY TIME)
1. $i_{EQB}$ = 30°
$t_F$ = 10 DAYS
$t_F$ = 5 DAYS
$t_F$ = 5.0 HR.
$t_F$ = 10.0 HR.
TRANSLUNAR FLIGHT TIME
10 HR.
60 HR.
$t_F$ = 5.0 HR.
$t_F$ = 5.0 HR.
$t_F$ = 10.0 HR.
10 HR.
5 HR.
TOTAL ENERGY REQUIREMENTS (ΔV + ΔV) FT/SEC x 10³
0
80
160
240
320
400
480
560
640
720
800
ELAPSED TIME (HRS.) AFTER NOMINAL ARRIVAL AT MOON

FIG. 13

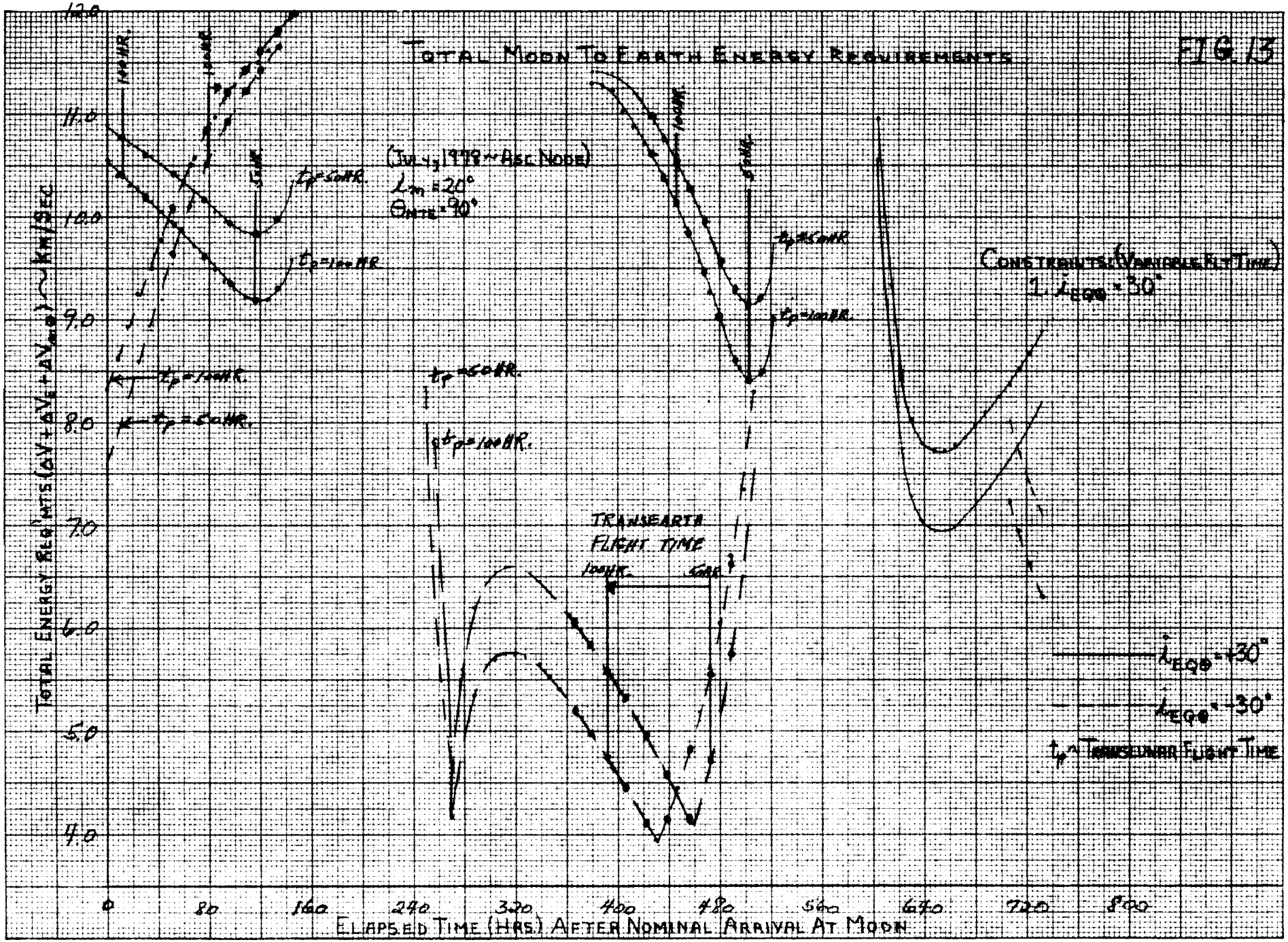
TOTAL MOON TO EARTH ENERGY REQUIREMENTS
(JULY 4, 1979 ~ ASC. NODE)
$L_m = 20°$
$\Theta_{INTR} = 90°$
CONSTRAINTS: (VARIABLE FLT TIME)
1. $\lambda_{EQ\Phi} = 30°$
$\lambda_{EQ\Phi} = +30°$
$\lambda_{EQ\Phi} = -30°$
$t_p$ = TRANSEARTH FLIGHT TIME
TRANSEARTH FLIGHT TIME
100HR.
60HR.
$t_p$=60HR.
$t_p$=100HR.
TOTAL ENERGY $KLB^2$ MTS $(\Delta V + \Delta V_E + \Delta V_{m\Phi})^2$ — $KM^2/SEC^2$
12.0
11.0
10.0
9.0
8.0
7.0
6.0
5.0
4.0
0
80
160
240
320
400
480
560
640
720
800
ELAPSED TIME (HRS.) AFTER NOMINAL ARRIVAL AT MOON

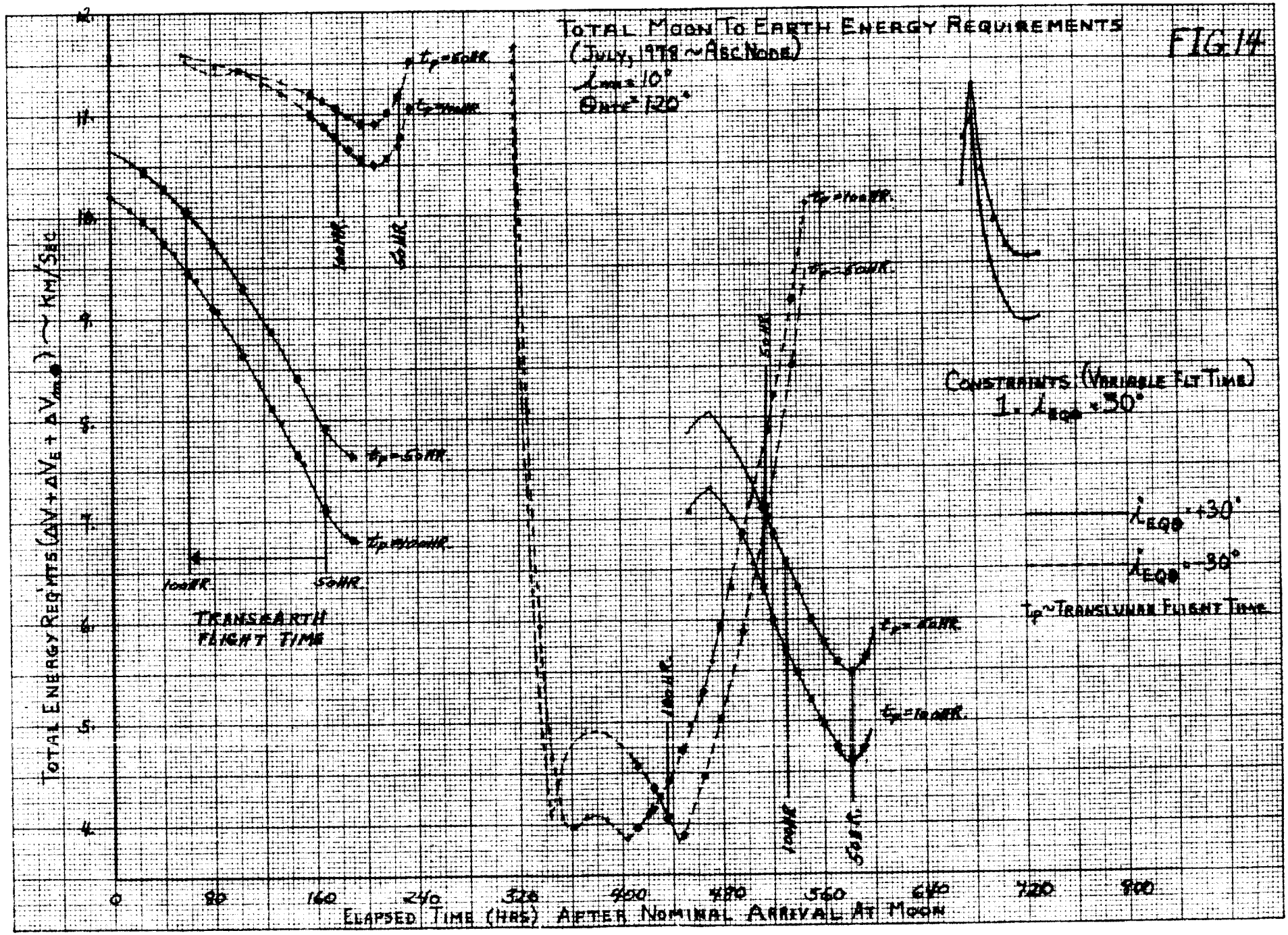
TOTAL MOON TO EARTH ENERGY REQUIREMENTS
(JULY, 1978 ~ ASC. NODE)
$\lambda_{min} = 10°$
$\Theta_{ARC} = 120°$
FIG. 14
CONSTRAINTS: (VARIABLE FLT TIME)
1. $\lambda_{EQ\oplus} \leq 30°$
$\lambda_{EQ\oplus} = +30°$
$\lambda_{EQ\oplus} = -30°$
$t_F$ ~ TRANSLUNAR FLIGHT TIME
TOTAL ENERGY REQ'MTS ($\Delta V + \Delta V_E + \Delta V_{m\oplus}$) ~ KM/SEC
TRANSEARTH FLIGHT TIME
ELAPSED TIME (HRS) AFTER NOMINAL ARRIVAL AT MOON
0
80
160
240
320
400
480
560
640
720
800

MISSIONS I AND II

Auxiliary Data for Missions I and II

FIG. 15

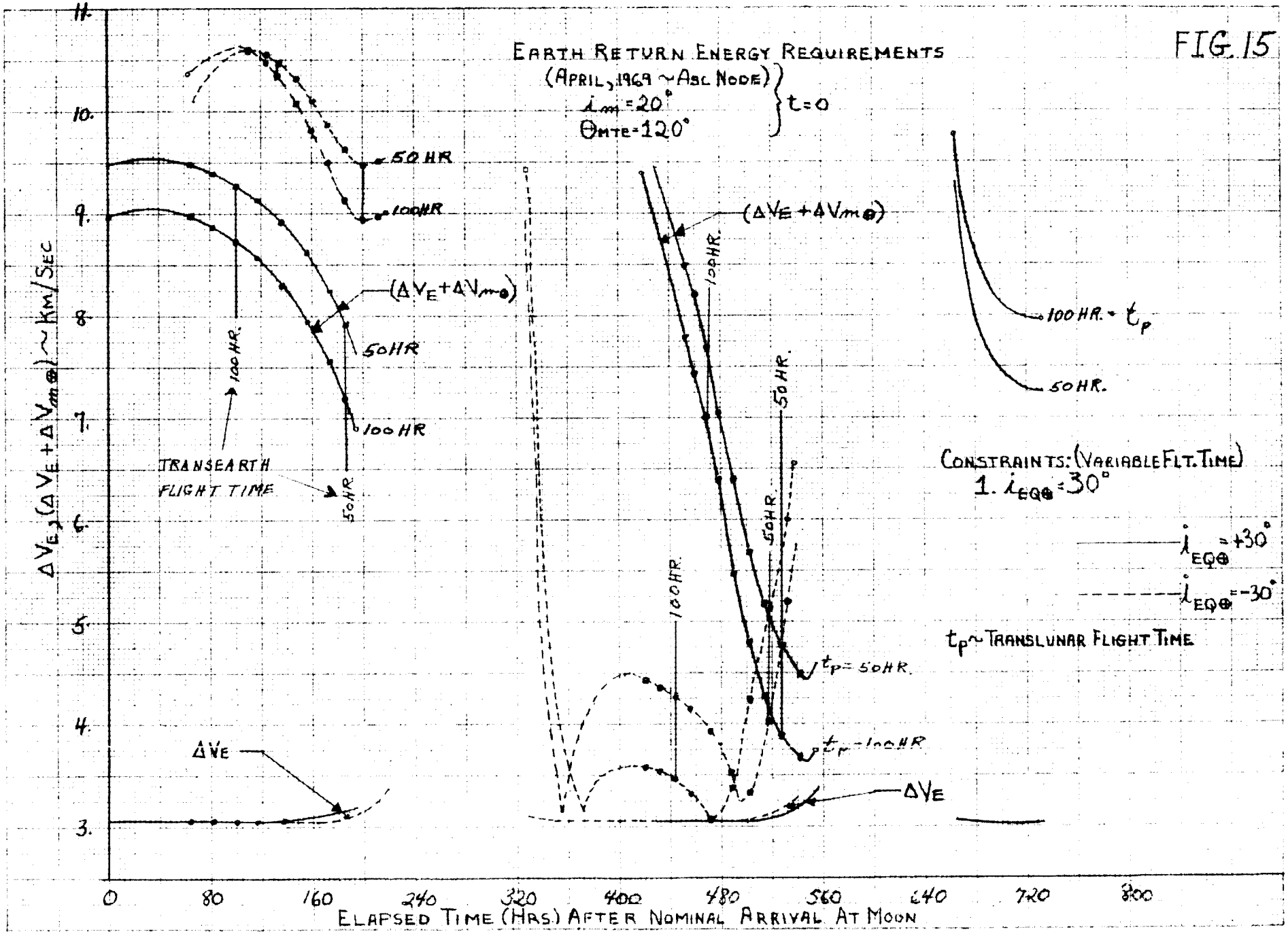
EARTH RETURN ENERGY REQUIREMENTS
(APRIL, 1969 ~ ASC NODE)
$i_m = 20°$
$\Theta_{MTE} = 120°$
t=0
$\Delta V_E, (\Delta V_E + \Delta V_{m\oplus}) \sim$ KM/SEC
11.
10.
9.
8
7
6
5
4
3.
50 HR
100 HR
$(\Delta V_E + \Delta V_{m\oplus})$
50 HR
100 HR
TRANSEARTH FLIGHT TIME
100 HR.
50 HR.
$\Delta V_E$
$(\Delta V_E + \Delta V_{m\oplus})$
100 HR.
50 HR.
50 HR.
100 HR.
$t_p$ = 50 HR.
$t_p$ = 100 HR
$\Delta V_E$
100 HR. = $t_p$
50 HR.
CONSTRAINTS: (VARIABLE FLT. TIME)
1. $i_{EQ\oplus} = 30°$
$i_{EQ\oplus} = +30°$
$i_{EQ\oplus} = -30°$
$t_p$ ~ TRANSLUNAR FLIGHT TIME
0
80
160
240
320
400
480
560
640
720
800
ELAPSED TIME (HRS) AFTER NOMINAL ARRIVAL AT MOON

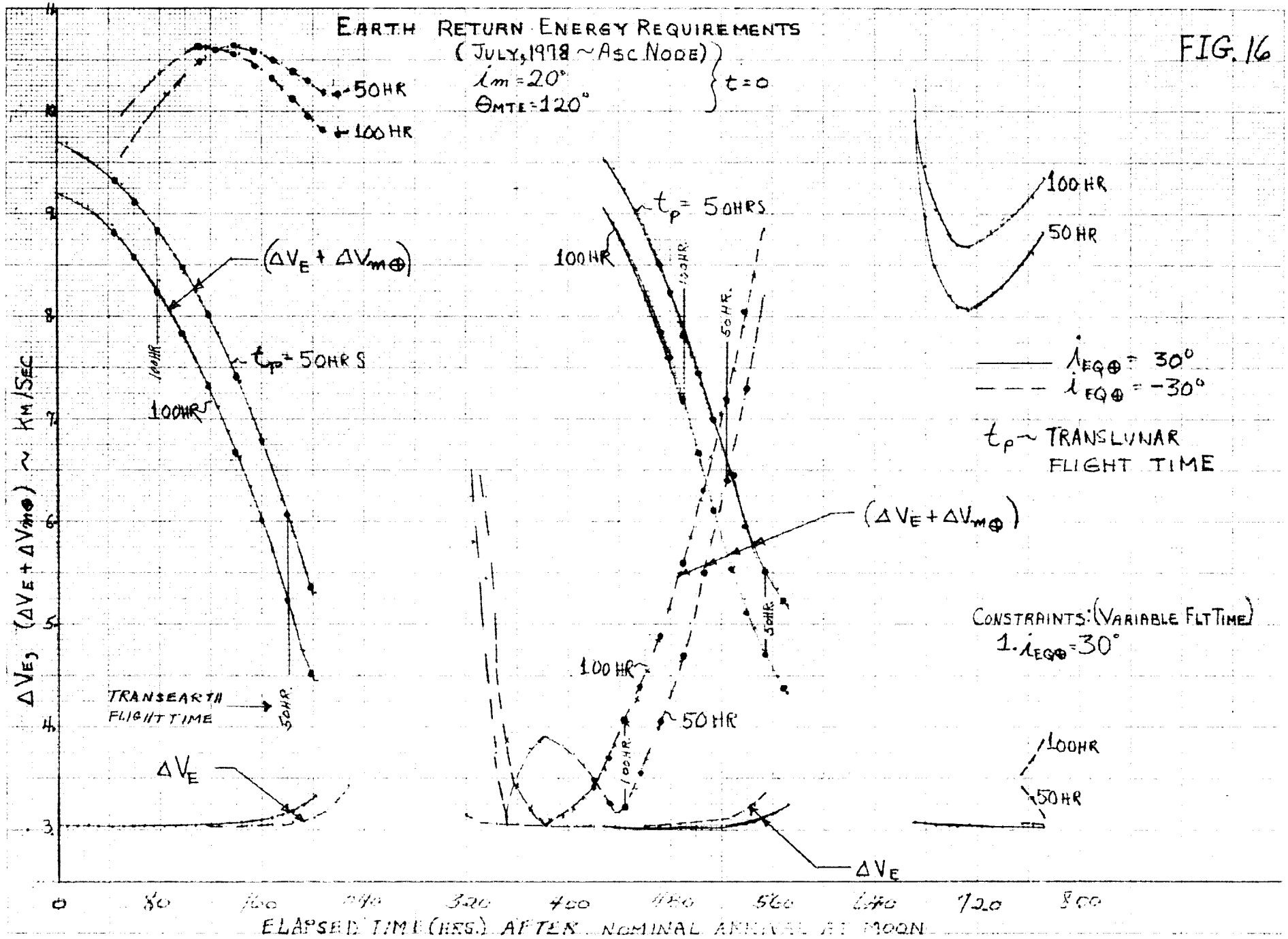
EARTH RETURN ENERGY REQUIREMENTS
(JULY, 1978 ~ ASC. NODE)
$i_m = 20°$
$\theta_{MTE} = 120°$
$t = 0$
FIG. 16
50 HR
100 HR
$(\Delta V_E + \Delta V_{m\oplus})$
$t_p$ = 50 HRS
100 HR
50 HR
$i_{EQ\oplus} = 30°$
$i_{EQ\oplus} = -30°$
$t_p$ ~ TRANSLUNAR FLIGHT TIME
CONSTRAINTS: (VARIABLE FLT TIME)
1. $i_{EQ\oplus} = 30°$
TRANSEARTH FLIGHT TIME
50 HR
$\Delta V_E$
$\Delta V_{E_3}$ $(\Delta V_E + \Delta V_{m\oplus})$ ~ KM/SEC
ELAPSED TIME (HRS.) AFTER NOMINAL ARRIVAL AT MOON

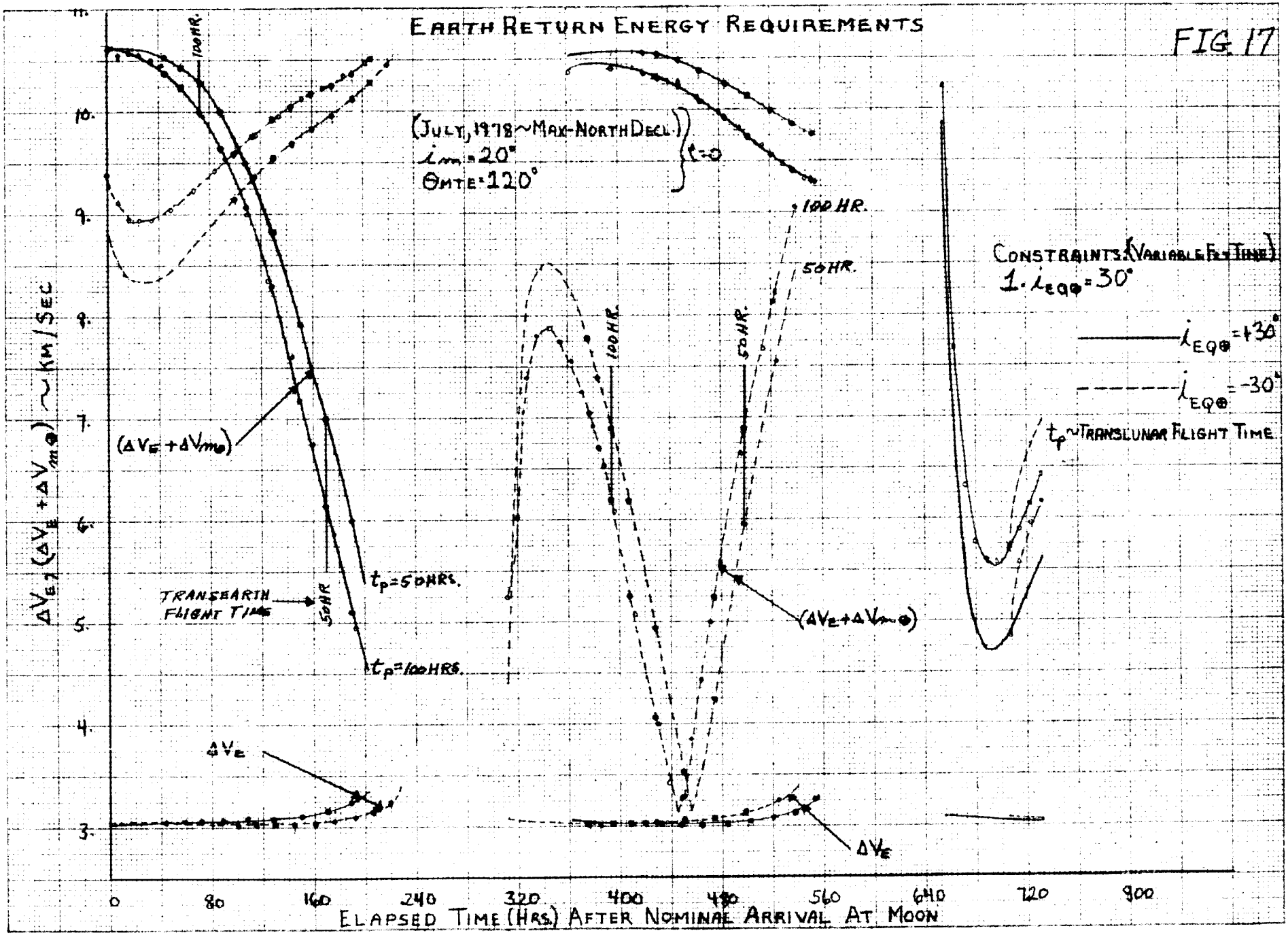
EARTH RETURN ENERGY REQUIREMENTS
FIG 17
(JULY, 1978 ~ MAX-NORTH DECL.)
$i_m$ = 20°
$\Theta_{MTE}$ = 120°
t=0
100 HR.
50 HR.
CONSTRAINTS: (VARIABLE FREE TIME)
1. $i_{EQ\oplus}$ = 30°
$i_{EQ\oplus}$ = +30°
$i_{EQ\oplus}$ = -30°
$t_p$ ~ TRANSLUNAR FLIGHT TIME
$(\Delta V_E + \Delta V_{m\oplus})$
$t_p$ = 50 HRS.
$t_p$ = 100 HRS.
TRANSEARTH FLIGHT TIME
50 HR
$\Delta V_E$
$\Delta V_{E1}$ $(\Delta V_E + \Delta V_{m\oplus})$ ~ KM/SEC
ELAPSED TIME (HRS.) AFTER NOMINAL ARRIVAL AT MOON
0
80
160
240
320
400
480
560
640
720
800
3.
4.
5.
6.
7.
8.
9.
10.
11.

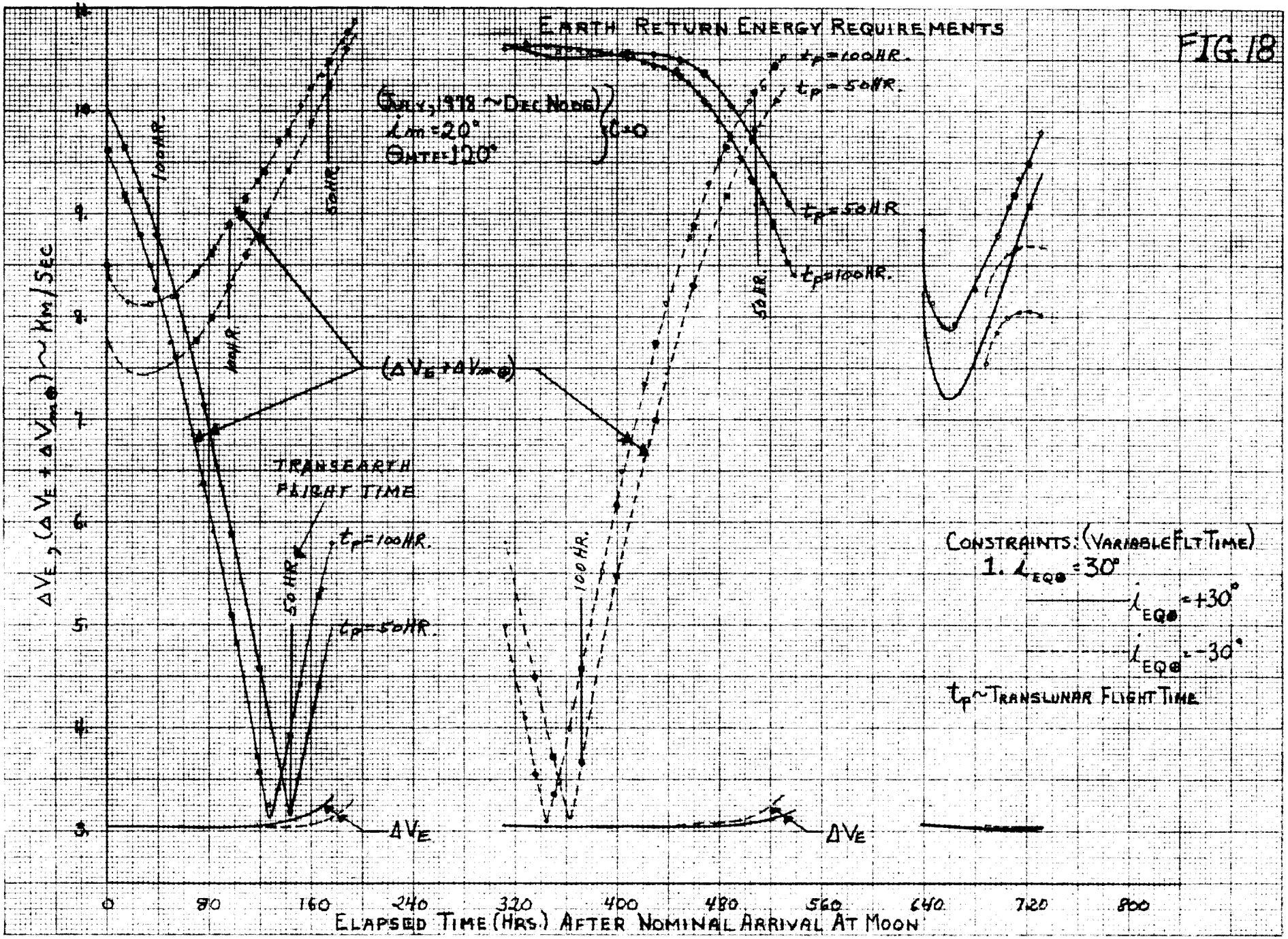
EARTH RETURN ENERGY REQUIREMENTS
FIG. 18
$\Delta V_E$ , $(\Delta V_E + \Delta V_{em\oplus})$ ~ KM/SEC
$(\Delta V_E + \Delta V_{em\oplus})$
$\Delta V_E$
TRANSEARTH FLIGHT TIME
$t_p$=100HR.
$t_p$=50HR.
100 HR.
50 HR.
CONSTRAINTS: (VARIABLE FLT TIME)
1. $i_{EQ\oplus}$ = 30°
$i_{EQ\oplus}$ = +30°
$i_{EQ\oplus}$ = -30°
$t_p$ ~ TRANSLUNAR FLIGHT TIME
ELAPSED TIME (HRS.) AFTER NOMINAL ARRIVAL AT MOON
0
80
160
240
320
400
480
560
640
720
800

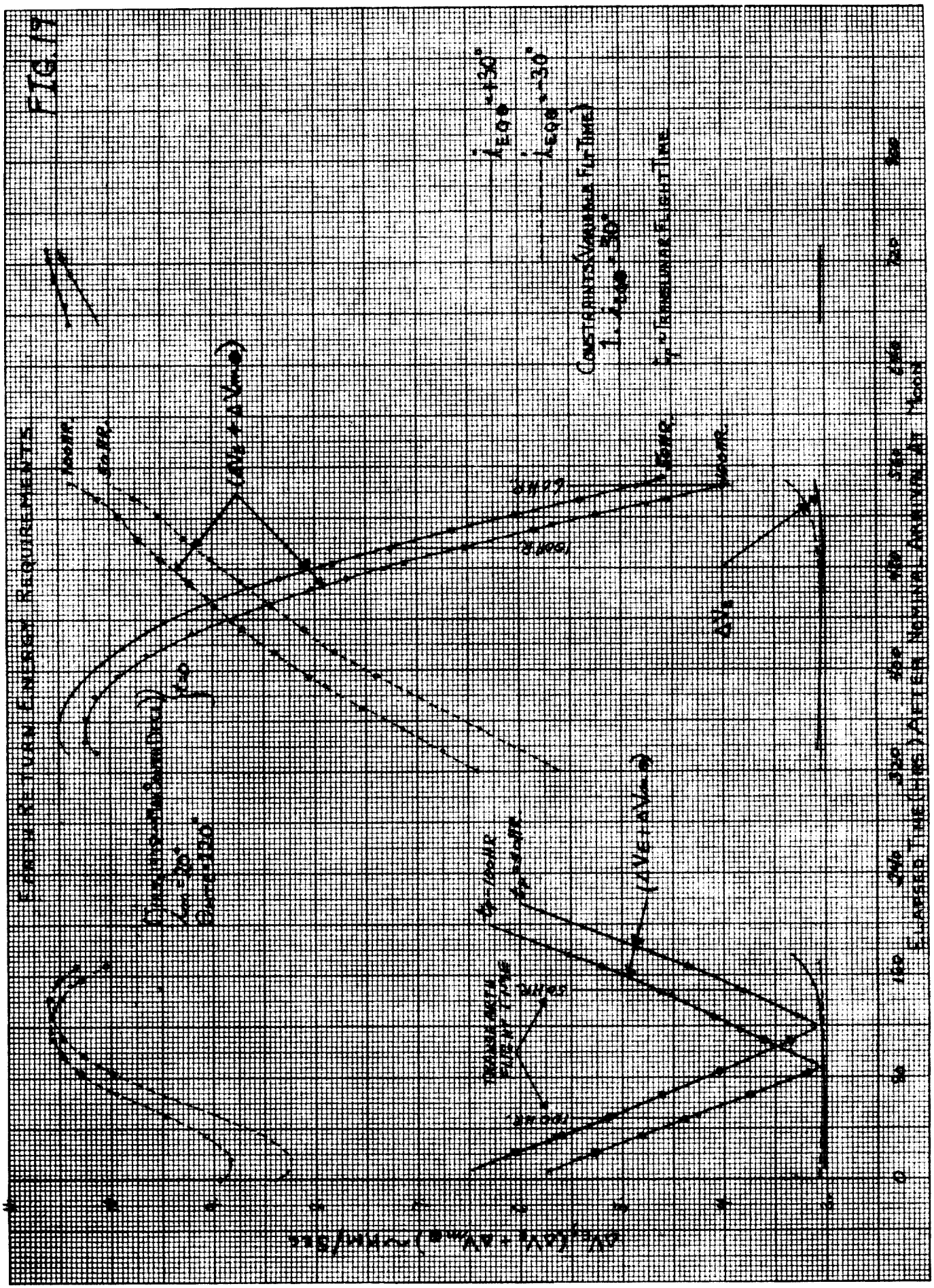

ER 13550-III
I-82

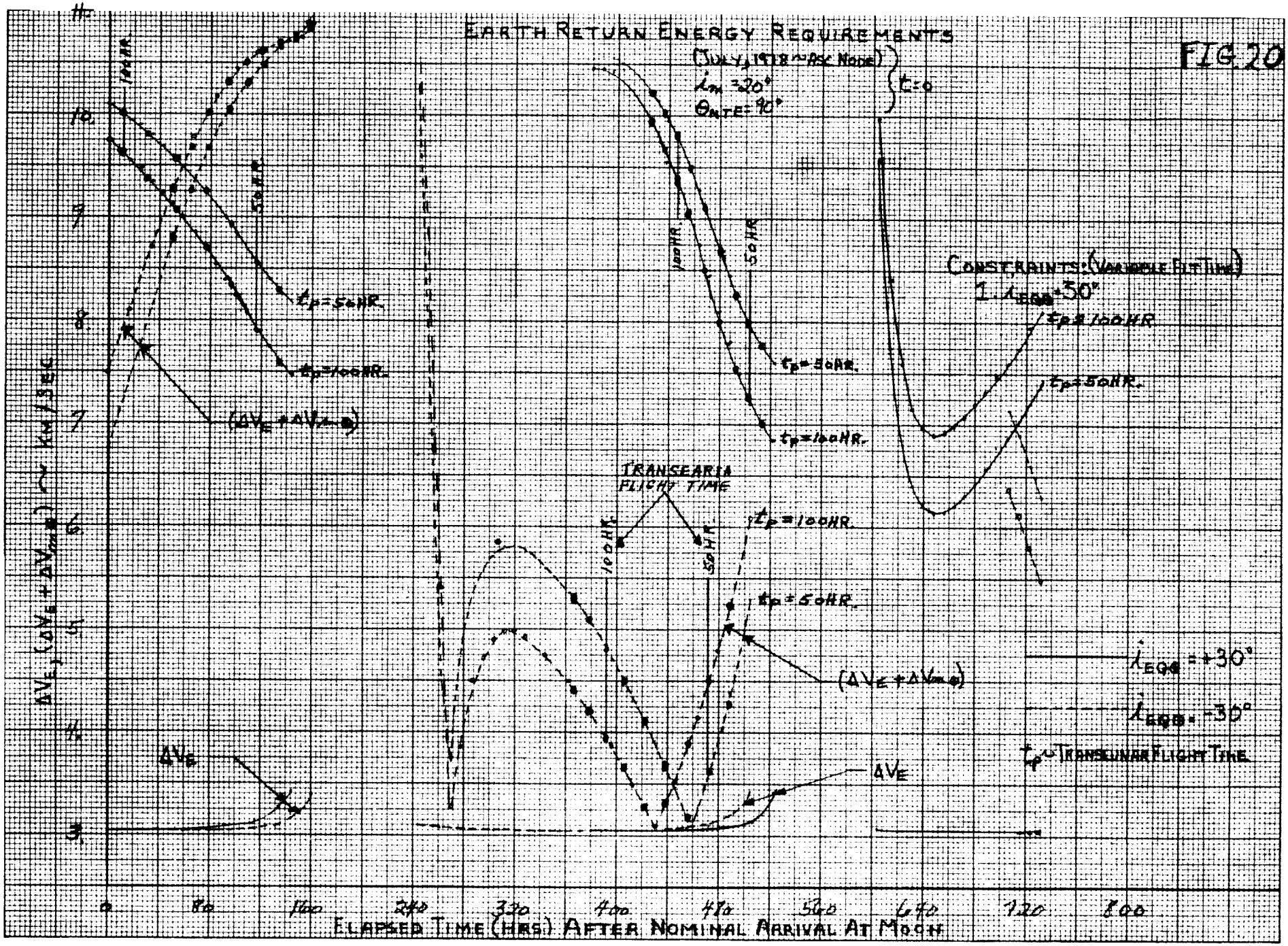
EARTH RETURN ENERGY REQUIREMENTS
(JULY, 1978 ASC NODE)
$\lambda_{EM} = 20°$
$\theta_{INTE} = 90°$
$t_c = 0$
FIG. 20
CONSTRAINTS: (VARIABLE FLIGHT TIME)
1. $\lambda_{EOM} = 30°$
$t_p = 100$ HR.
$t_p = 50$ HR.
$t_p = 100$ HR.
$t_p = 50$ HR.
$t_p = 100$ HR.
$t_p = 50$ HR.
TRANSEARTH FLIGHT TIME
100 HR.
50 HR.
$(\Delta V_E + \Delta V_{MCC})$
$\Delta V_E$
$\lambda_{EOM} = +30°$
$\lambda_{EOM} = -30°$
$t_p$ = TRANSLUNAR FLIGHT TIME
$\Delta V_E + \Delta V_{MCC}$ (KM/SEC)
ELAPSED TIME (HRS.) AFTER NOMINAL ARRIVAL AT MOON

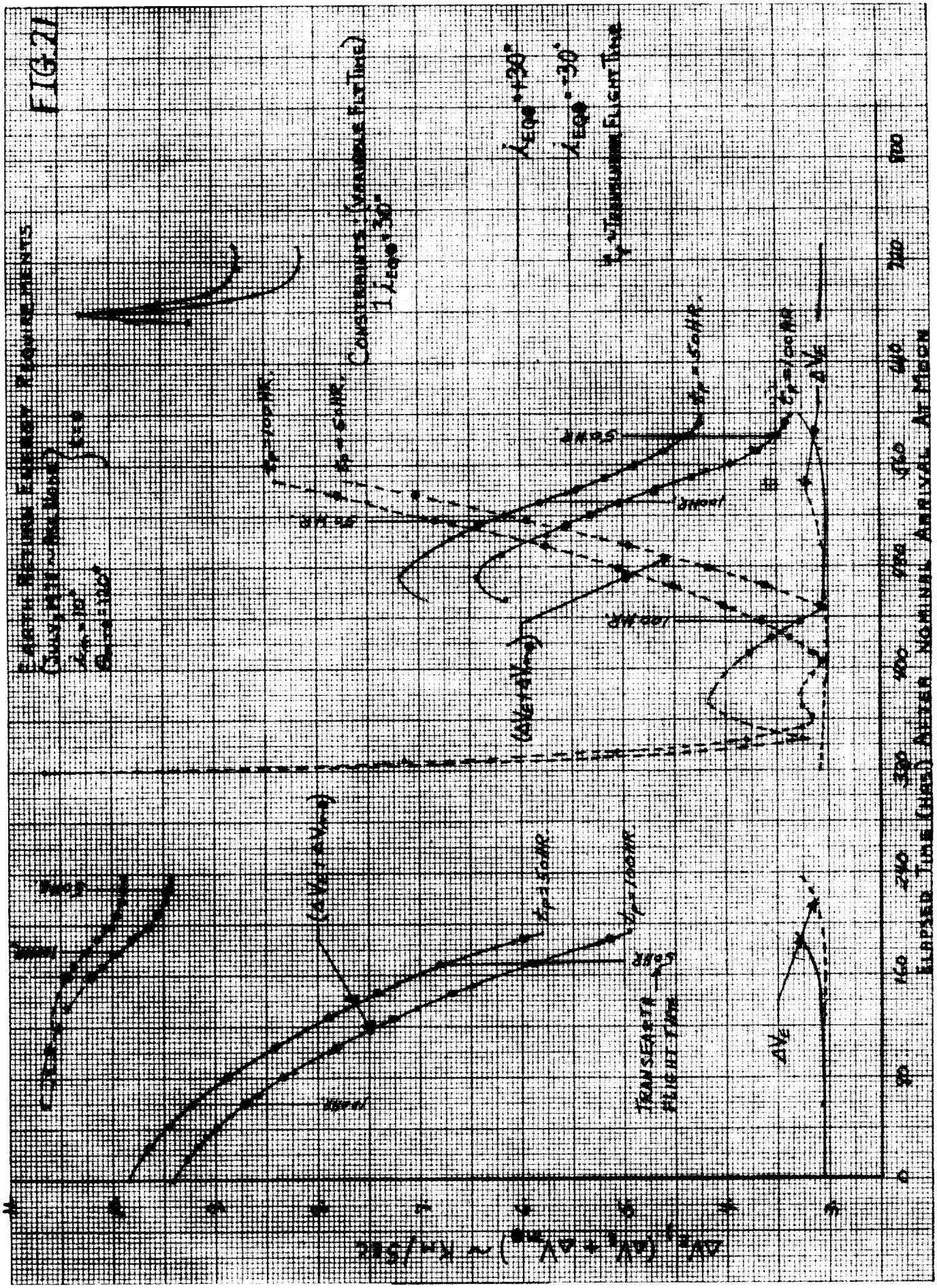
FIG 21
ELAPSED TIME (HRS) AFTER NOMINAL ARRIVAL AT MOON
TRANSEARTH FLIGHT TIME
Translunar Flight Time

MISSION III

Departure Windows

FIG 22

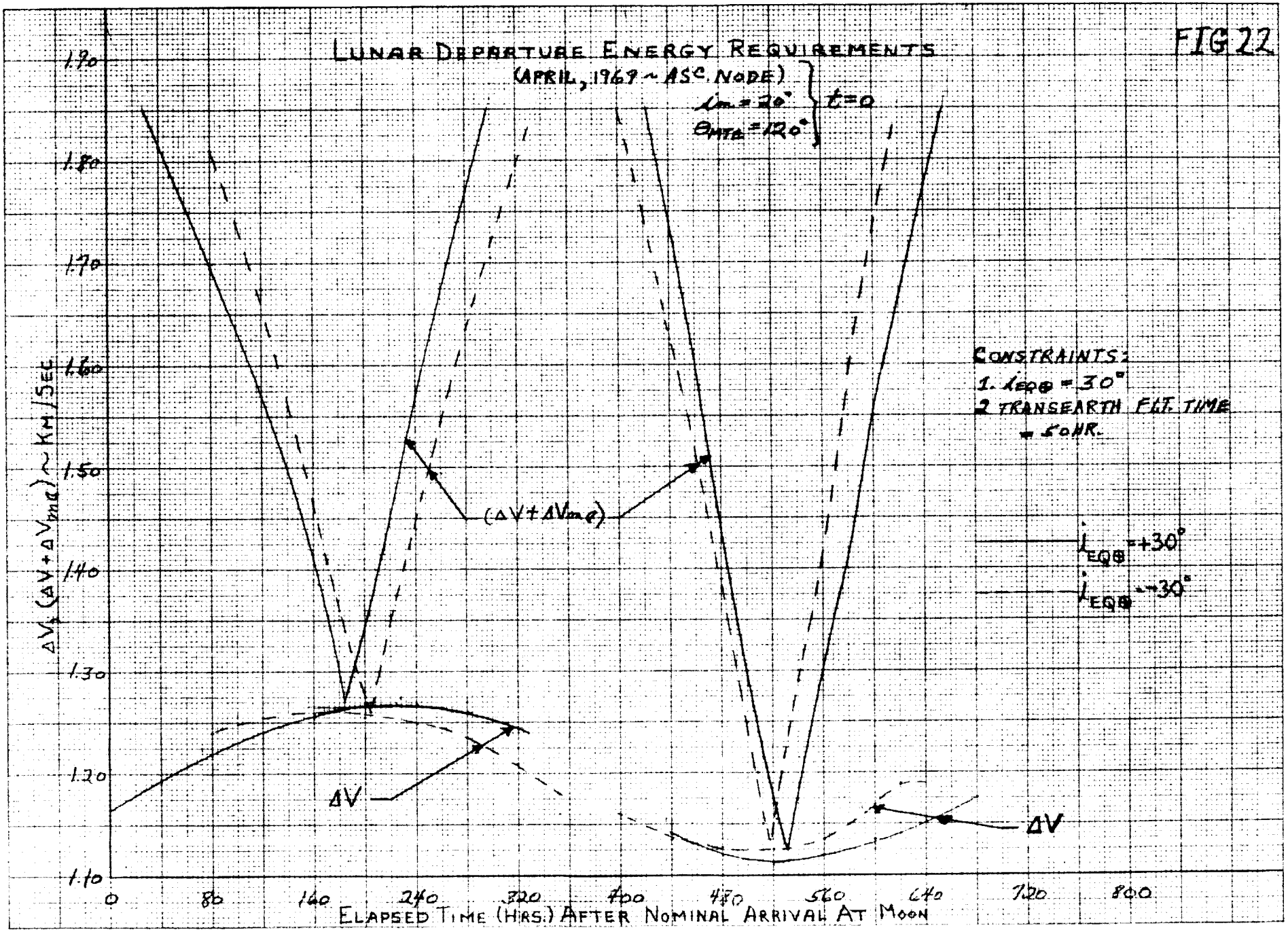
LUNAR DEPARTURE ENERGY REQUIREMENTS
(APRIL, 1969 ~ ASC. NODE)
$i_m = 20°$
$\theta_{MTE} = 120°$
t=0
CONSTRAINTS:
1. $i_{EQ\oplus} = 30°$
2 TRANSEARTH FLT TIME = 50 HR.
$i_{EQ\oplus} = +30°$
$i_{EQ\oplus} = -30°$
$\Delta V_t (\Delta V + \Delta V_{mcc}) \sim$ KM/SEC
1.90
1.80
1.70
1.60
1.50
1.40
1.30
1.20
1.10
$(\Delta V + \Delta V_{mcc})$
$\Delta V$
$\Delta V$
0
80
140
240
320
400
480
560
640
720
800
ELAPSED TIME (HRS.) AFTER NOMINAL ARRIVAL AT MOON

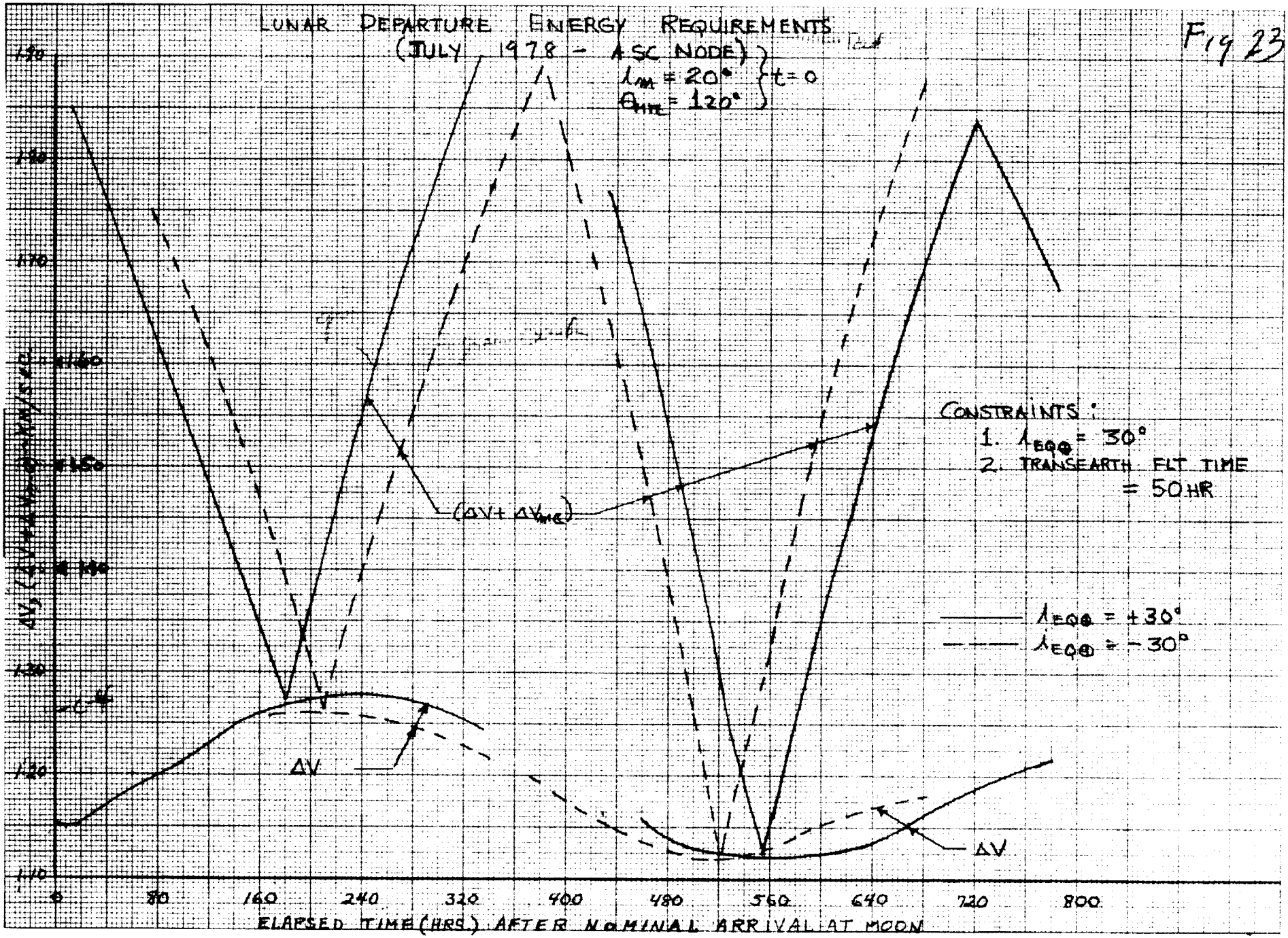
LUNAR DEPARTURE ENERGY REQUIREMENTS
(JULY 1978 - ASC NODE)
$\lambda_M = 20°$
$\theta_{MTE} = 120°$
t = 0
Fig 23
CONSTRAINTS:
1. $\lambda_{EQ\oplus} = 30°$
2. TRANSEARTH FLT TIME = 50 HR
$(\Delta V + \Delta V_{MTE})$
$\lambda_{EQ\oplus} = +30°$
$\lambda_{EQ\oplus} = -30°$
ΔV
ΔV
120
110
0
80
160
240
320
400
480
560
640
720
800
ELAPSED TIME (HRS.) AFTER NOMINAL ARRIVAL AT MOON

FIG. 24

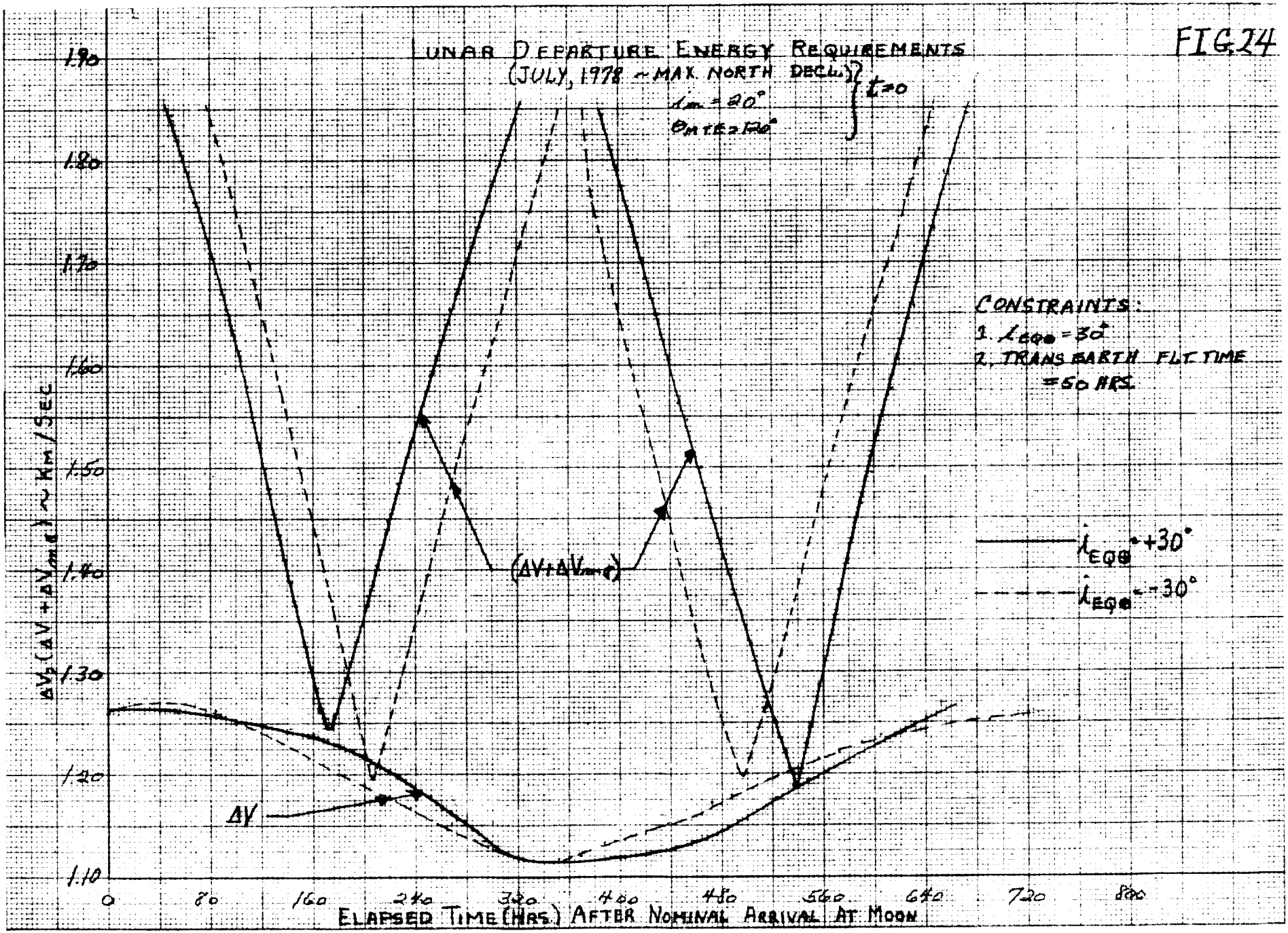
LUNAR DEPARTURE ENERGY REQUIREMENTS
(JULY, 1978 ~ MAX. NORTH DECL.)
$i_m = 20°$
$\theta_{MTE} = 140°$
$t_{\pi}=0$
CONSTRAINTS:
1. $i_{EQ\oplus} = 30°$
2. TRANS EARTH FLT. TIME = 50 HRS.
$i_{EQ\oplus} = +30°$
$i_{EQ\oplus} = -30°$
$(\Delta V + \Delta V_{mcc})$
$\Delta V$
$\Delta V (\Delta V + \Delta V_{mcc})$ ~ KM/SEC
1.90
1.80
1.70
1.60
1.50
1.40
1.30
1.20
1.10
0
80
160
240
320
400
480
560
640
720
800
ELAPSED TIME (HRS.) AFTER NOMINAL ARRIVAL AT MOON

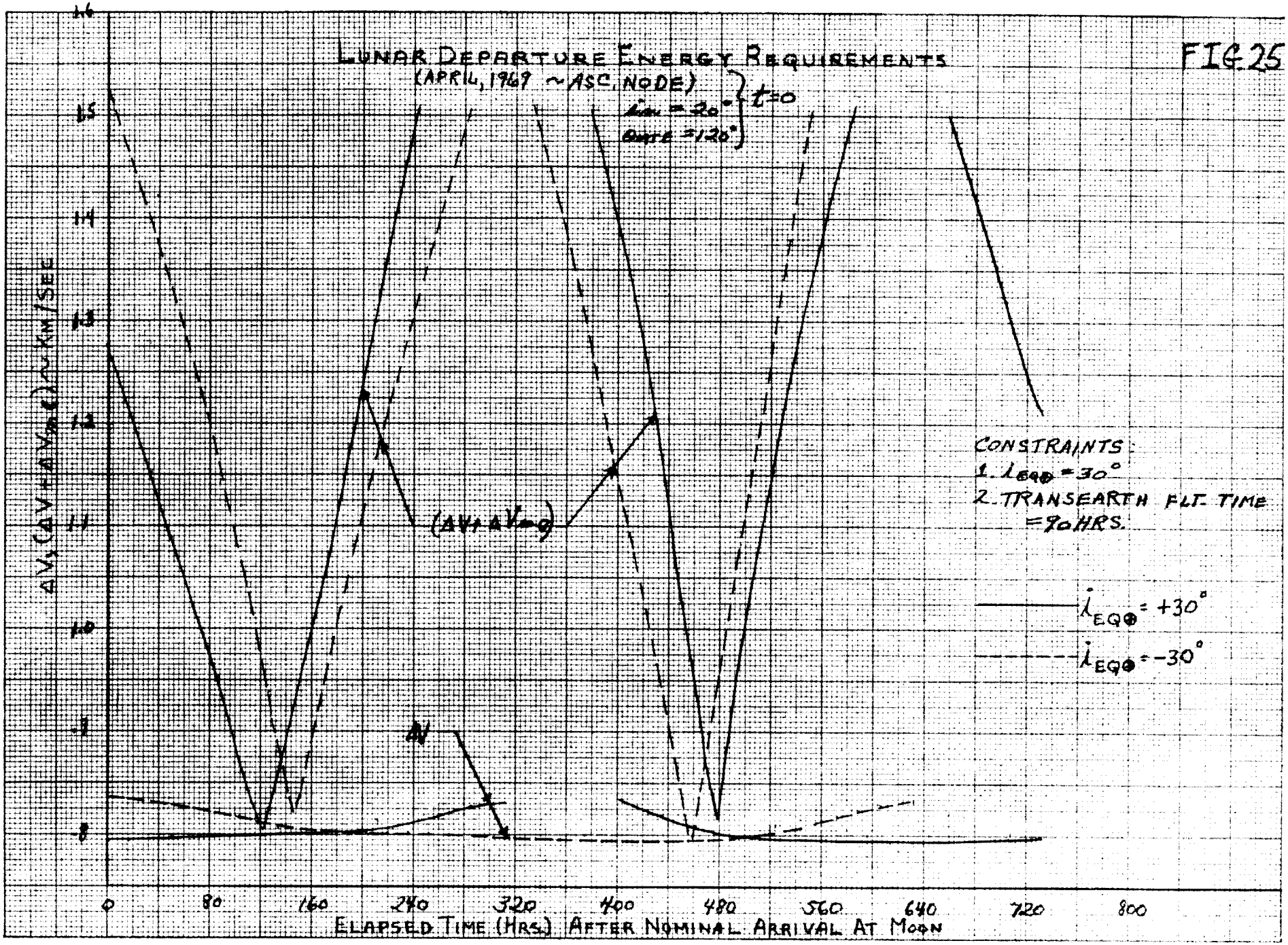
LUNAR DEPARTURE ENERGY REQUIREMENTS
(APRIL 4, 1969 ~ ASC. NODE)
$i_{EQ\oplus} = 30°$
$\Omega_{MOON} = 120°$
$t = 0$
FIG. 25
CONSTRAINTS:
1. $i_{EQ\oplus} = 30°$
2. TRANSEARTH FLT. TIME = 70 HRS.
$i_{EQ\oplus} = +30°$
$i_{EQ\oplus} = -30°$
$(\Delta V_1 + \Delta V_2)$
$\Delta V_2$
$\Delta V_1 + \Delta V_2$ (FEET/SEC) X $10^{-3}$
16
15
14
13
12
11
10
9
8
0
80
160
240
320
400
480
560
640
720
800
ELAPSED TIME (HRS.) AFTER NOMINAL ARRIVAL AT MOON

FIG 26

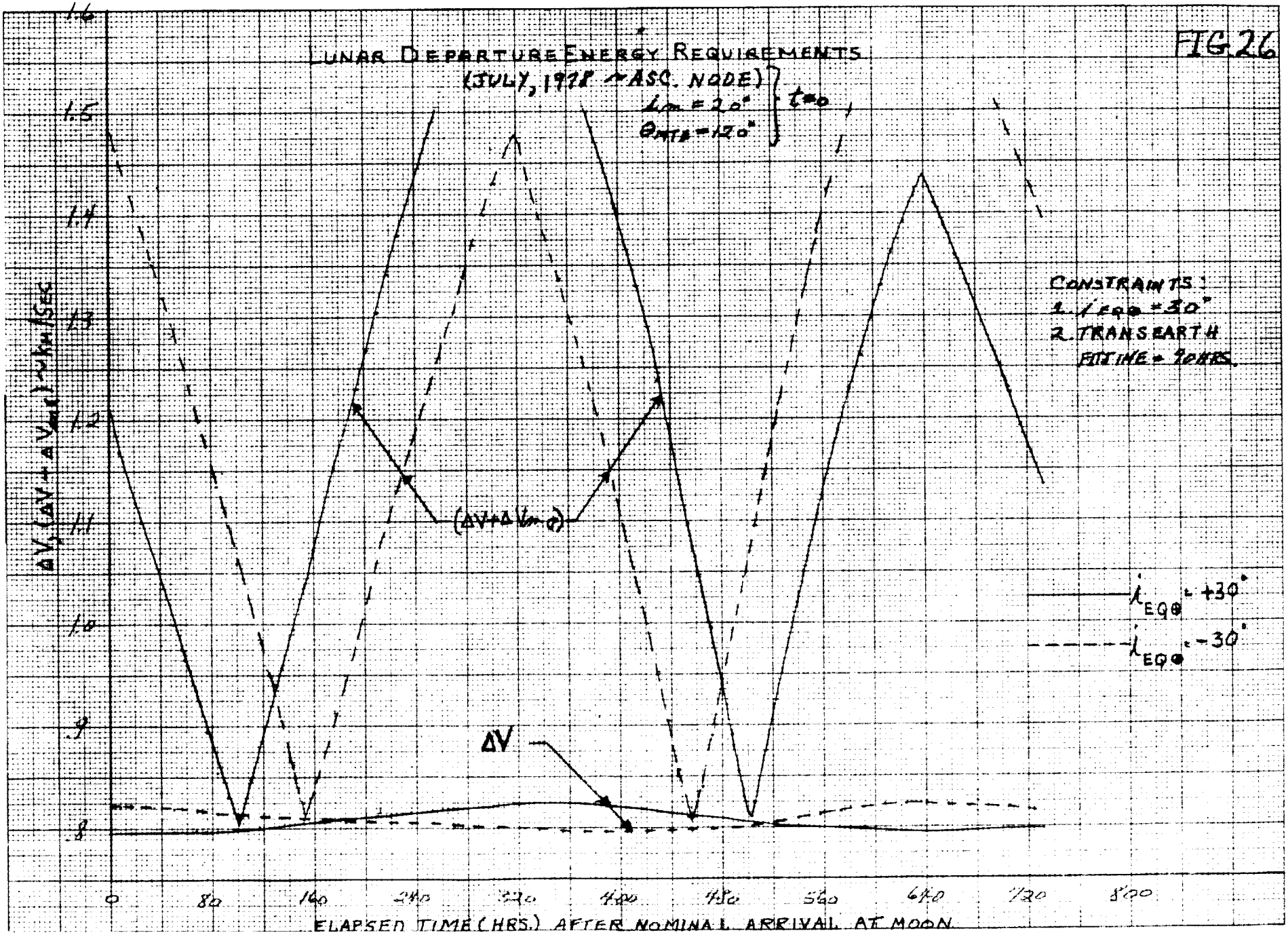
LUNAR DEPARTURE ENERGY REQUIREMENTS
(JULY, 1978 ↑ASC. NODE)
$L_{Sun} = 20°$
$\theta_{MTE} = 120°$
$t=0$
CONSTRAINTS:
1. $i_{EQ\oplus} = 30°$
2. TRANSEARTH FLTIME = 90 HRS.
$i_{EQ\oplus} = +30°$
$i_{EQ\oplus} = -30°$
$(\Delta V + \Delta V_{m-d})$
$\Delta V$
$\Delta V, (\Delta V + \Delta V_{m-d})$ km/sec
1.6
1.5
1.4
1.3
1.2
1.1
1.0
.9
.8
0
80
160
240
320
400
480
560
640
720
800
ELAPSED TIME (HRS.) AFTER NOMINAL ARRIVAL AT MOON

FIG 27

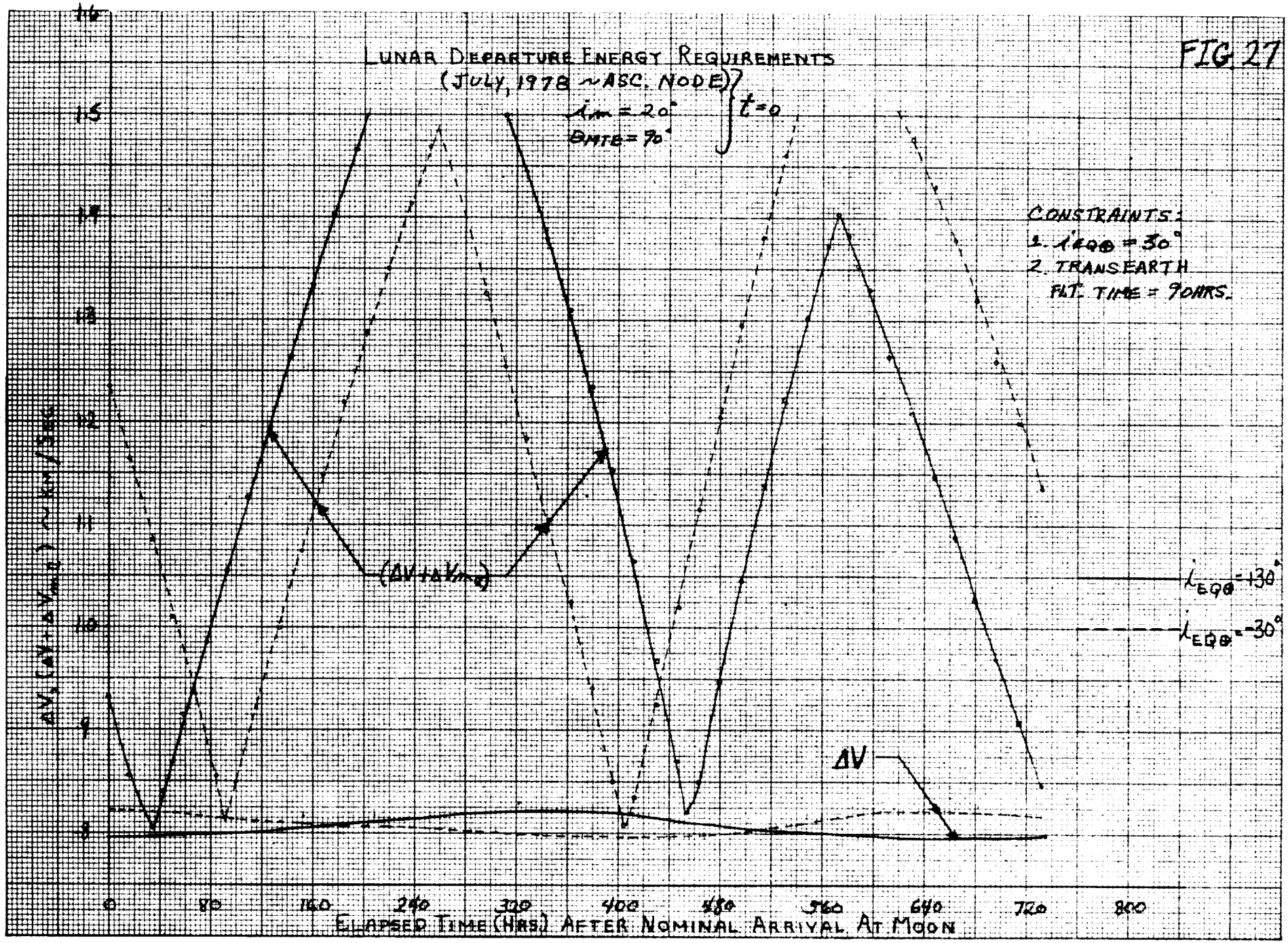
LUNAR DEPARTURE ENERGY REQUIREMENTS
(JULY, 1978 ~ASC. NODE)
$i_m = 20°$
$\theta_{MTE} = 70°$
$t=0$
CONSTRAINTS:
1. $i_{EQ\oplus} = 30°$
2. TRANSEARTH FLT. TIME = 90HRS.
$i_{EQ\oplus} = +30°$
$i_{EQ\oplus} = -30°$
$\Delta V$
$(\Delta V + \Delta V_{mc})$
$\Delta V, (\Delta V + \Delta V_{mc})$ KM/SEC
16
15
14
13
12
11
10
9
8
0
80
160
240
320
400
480
560
640
720
800
ELAPSED TIME (HRS) AFTER NOMINAL ARRIVAL AT MOON

FIG 28

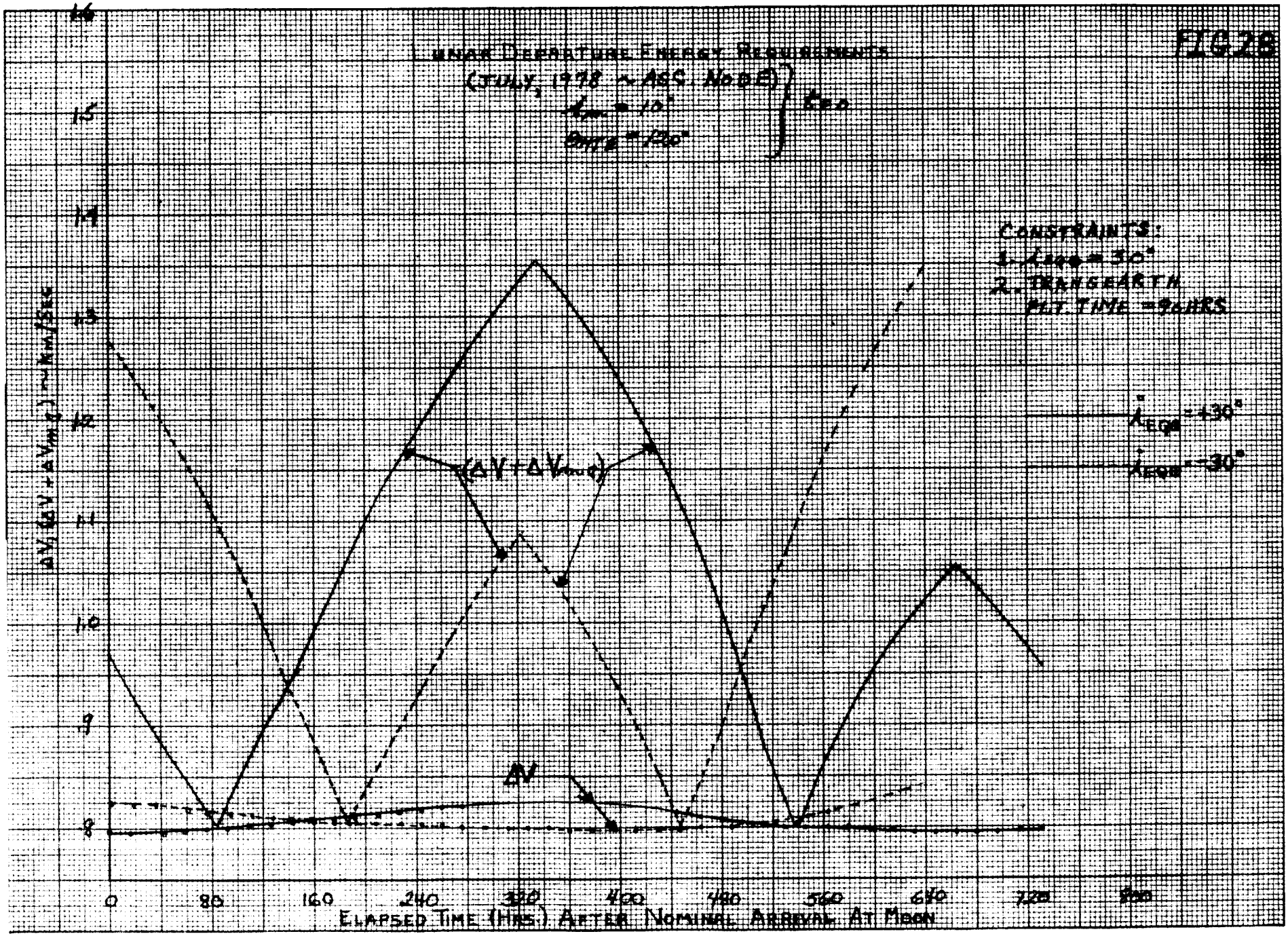
LUNAR DEPARTURE ENERGY REQUIREMENTS
(JULY, 1978 — ASC. NODE)
CONSTRAINTS:
1. $\lambda_{MOON} = 30°$
2. TRANSEARTH FLT. TIME = 96 HRS.
$\lambda_{EQ\oplus} = +30°$
$\lambda_{EQ\oplus} = -30°$
$(\Delta V + \Delta V_{MCC})$
$\Delta V$
$\Delta V$ (KM/SEC) + $\Delta V_{MCC}$ (KM/SEC)
16
15
14
13
12
11
10
9
8
0
80
160
240
320
400
480
560
640
720
800
ELAPSED TIME (HRS.) AFTER NOMINAL ARRIVAL AT MOON

MISSION IV

Departure Windows

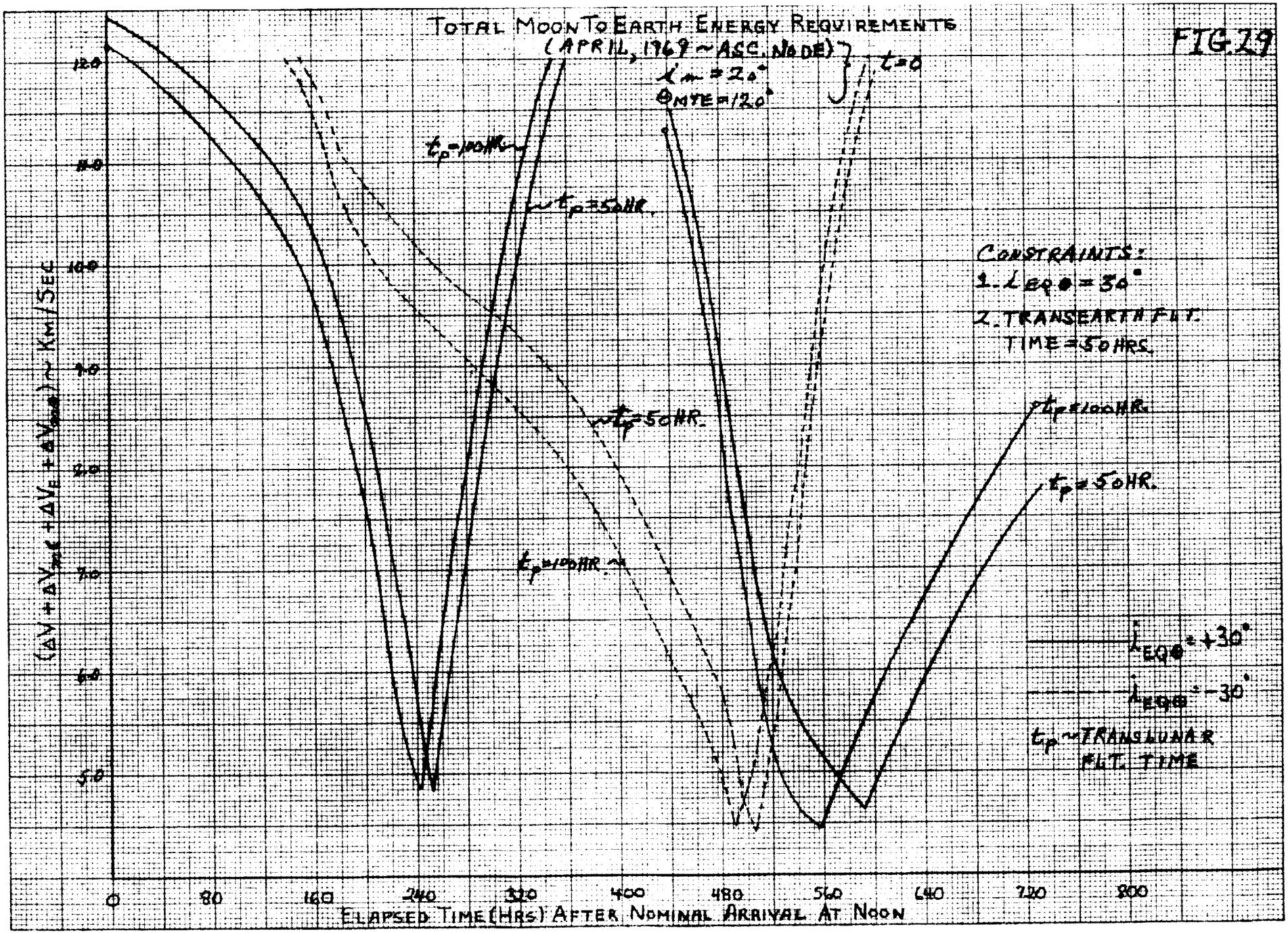
TOTAL MOON TO EARTH ENERGY REQUIREMENTS
(APRIL, 1969 ~ ASC. NODE)
FIG. 19
$i_m = 20°$
$\Theta_{MTE} = 120°$
$t=0$
$t_p = 100$ HR.
$t_p = 50$ HR.
$t_p = 50$ HR.
$t_p = 100$ HR.
CONSTRAINTS:
1. $i_{EQ\oplus} = 30°$
2. TRANSEARTH FLT. TIME = 50 HRS.
$t_p = 100$ HR.
$t_p = 50$ HR.
$i_{EQ\oplus} = +30°$
$i_{EQ\oplus} = -30°$
$t_p$ ~ TRANSLUNAR FLT. TIME
$(\Delta V) + \Delta V_{MCC} + \Delta V_{INS} + \Delta V_{EOI} + \Delta V_{TEI}$ ~ KM/SEC
120
110
100
90
80
70
60
50
0
80
160
240
320
400
480
560
640
720
800
ELAPSED TIME (HRS) AFTER NOMINAL ARRIVAL AT NOON

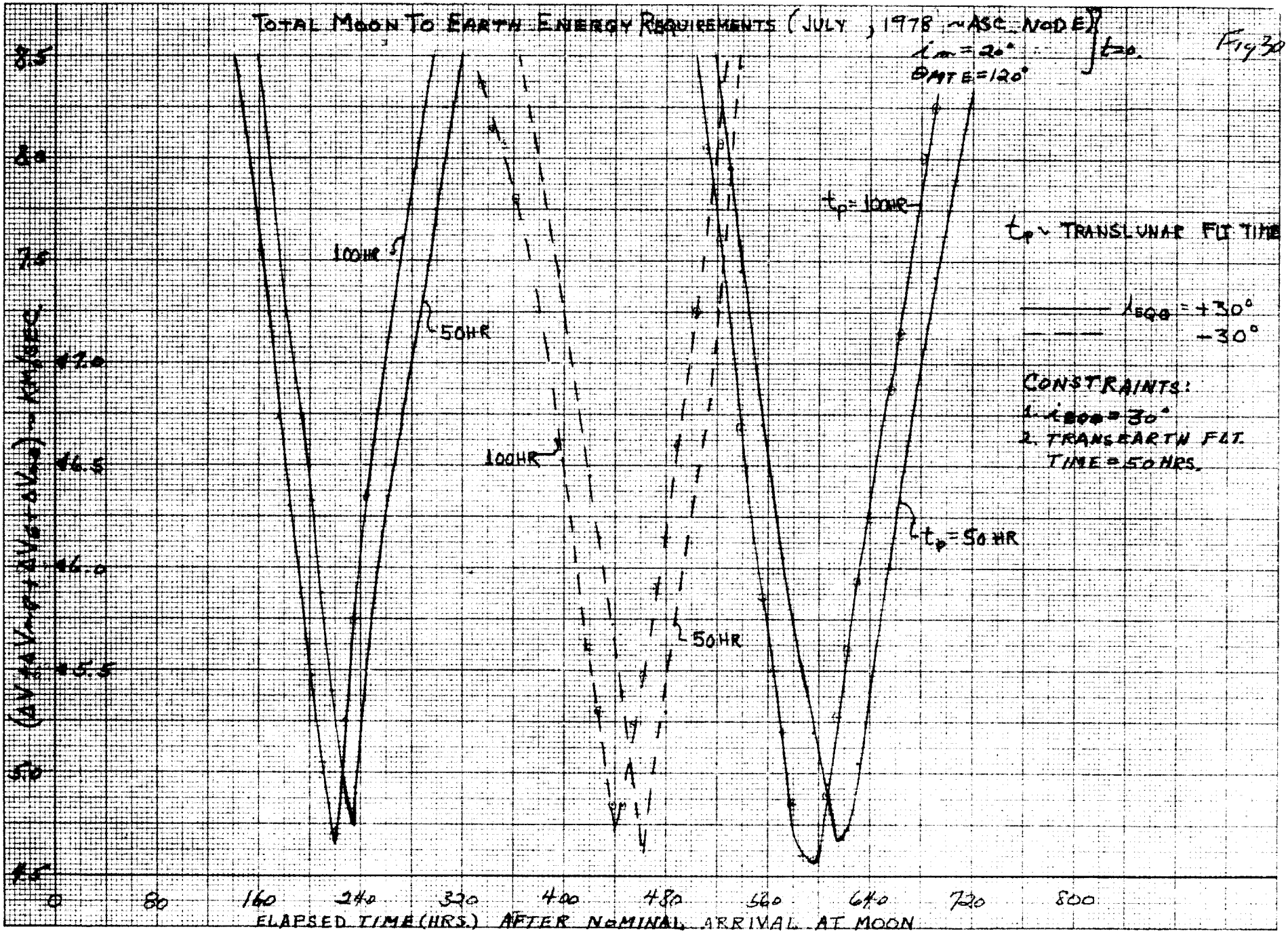
TOTAL MOON TO EARTH ENERGY REQUIREMENTS (JULY, 1978 ~ASC. NODE)
Fig 30
$i_m = 20°$
$\Theta_{MTE} = 120°$
$t_p$ = TRANSLUNAR FLT TIME
$i_{SOO} = +30°$
$-30°$
CONSTRAINTS:
1. $i_{SOO} = 30°$
2. TRANSEARTH FLT. TIME = 50 HRS.
$t_p$ = 100 HR
100 HR
50 HR
$t_p$ = 50 HR
50 HR
$(\Delta V_{MTE})^2$ (FT/SEC)$^2$
8.5
8.0
7.5
7.0
6.5
6.0
5.5
5.0
4.5
0
80
160
240
320
400
480
560
640
720
800
ELAPSED TIME (HRS.) AFTER NOMINAL ARRIVAL AT MOON

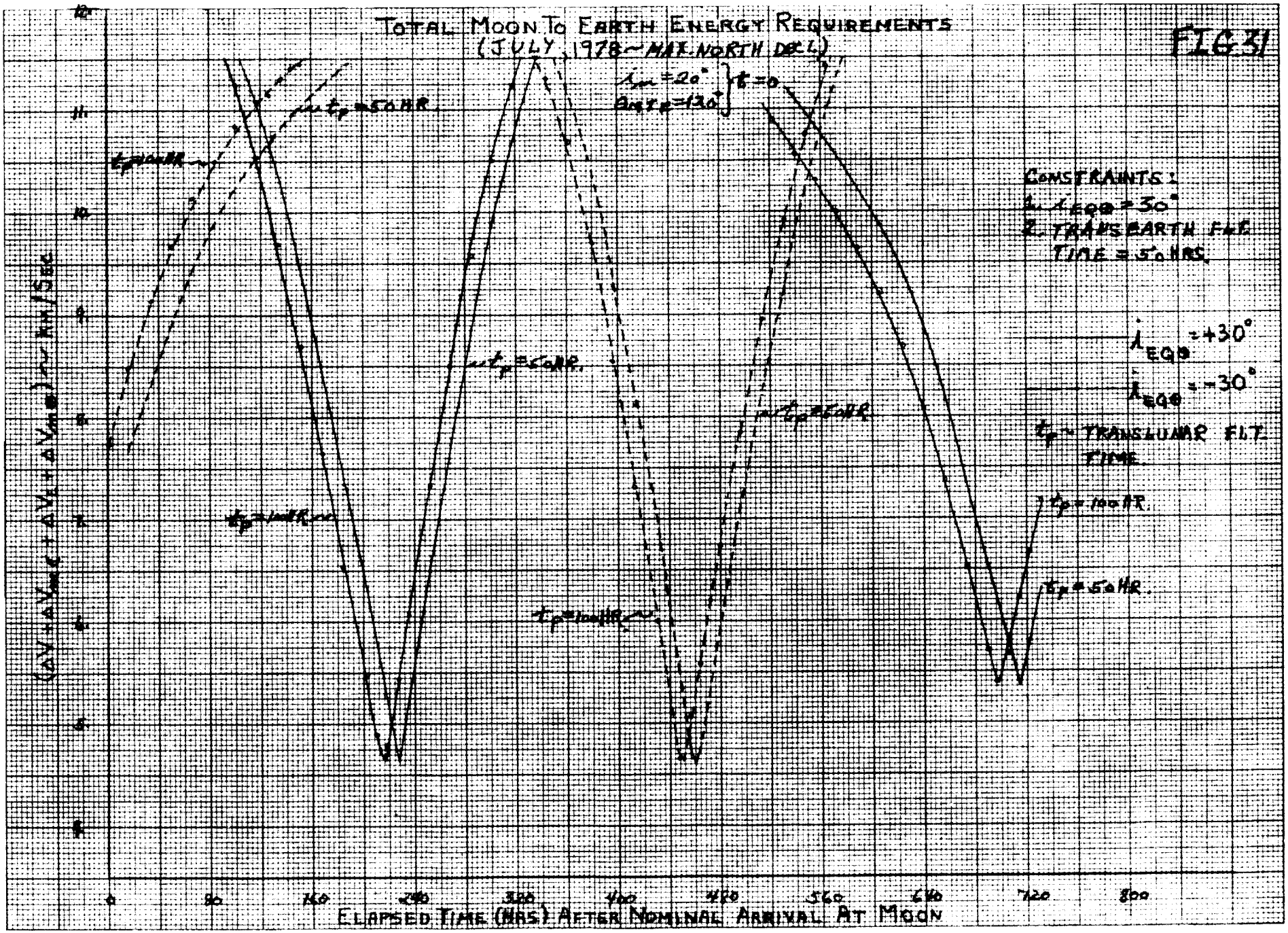
TOTAL MOON TO EARTH ENERGY REQUIREMENTS
(JULY 1978 ~ MAX. NORTH DECL)
FIG 31
$\lambda_{EQ\oplus} = +20°$
$\theta_{MT_F} = 130°$
$t = 0$
CONSTRAINTS:
1. $\lambda_{EQ\oplus} \geq 30°$
2. TRANSEARTH F.F.
TIME = 50 HRS.
$\lambda_{EQ\oplus} = +30°$
$\lambda_{EQ\oplus} = -30°$
$t_p$ = TRANSLUNAR F.F. TIME
$t_p$ = 100 HR.
$t_p$ = 50 HR.
$t_p$ = 50 HR.
$t_p$ = 100 HR.
$t_p$ = 100 HR.
$t_p$ = 50 HR.
$(\Delta V_1 + \Delta V_2 + \Delta V_{MCC} + \Delta V_3)$ FT/SEC
0
80
160
240
320
400
480
560
640
720
800
ELAPSED TIME (HRS) AFTER NOMINAL ARRIVAL AT MOON

FIG 32

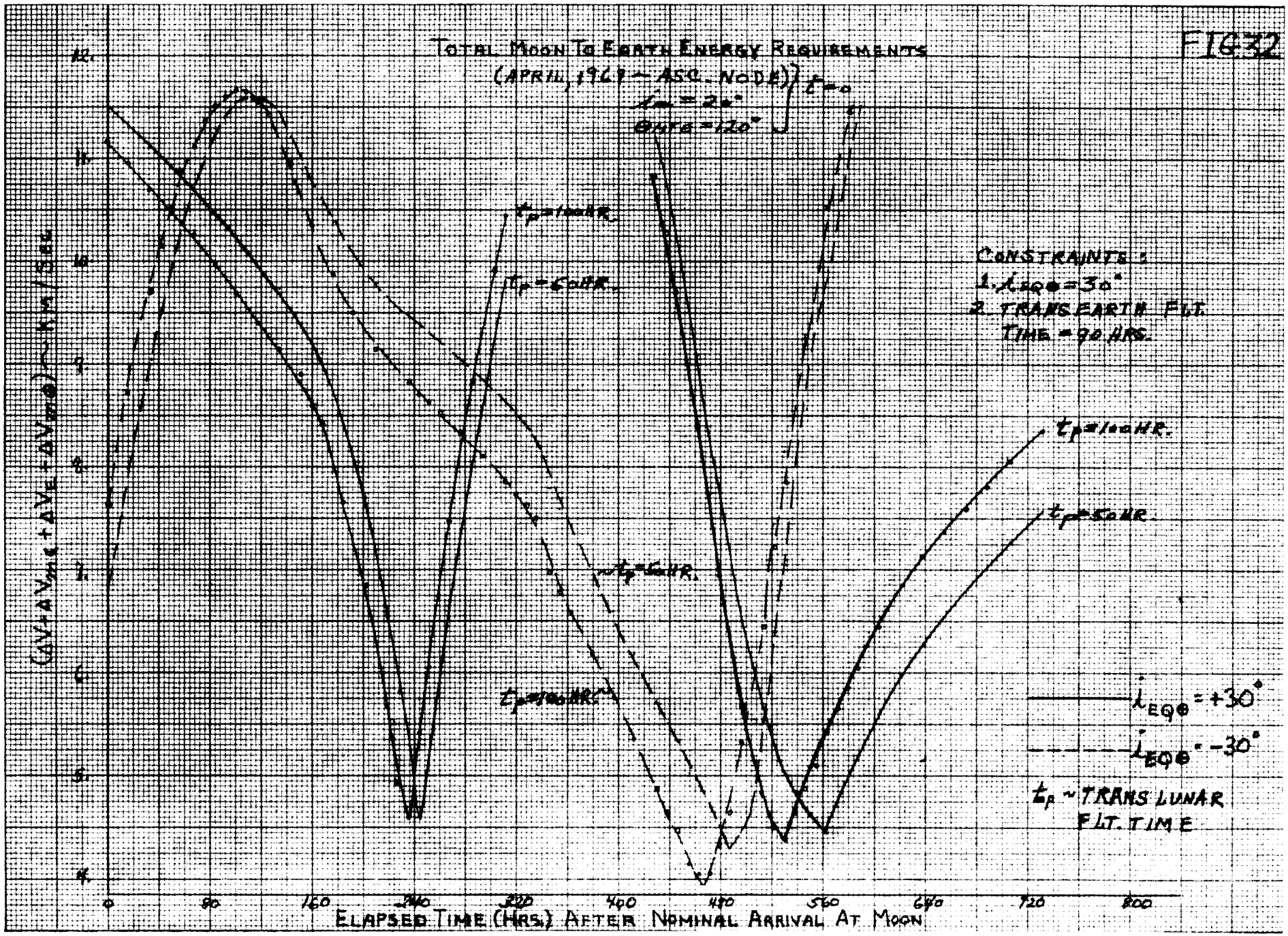
TOTAL MOON TO EARTH ENERGY REQUIREMENTS
(APRIL, 1969 – ASC. NODE)
$i_m = 2°$
$\Phi_{MFA} = 120°$
$t_p = 0$
CONSTRAINTS:
1. $i_{EQ\oplus} = 30°$
2. TRANS EARTH FLT. TIME = 90 HRS.
$t_p$ = 100 HR.
$t_p$ = 50 HR.
$t_p$ = 100 HR.
$t_p$ = 50 HR.
$i_{EQ\oplus} = +30°$
$i_{EQ\oplus} = -30°$
$t_p$ ~ TRANS LUNAR FLT. TIME
$(\Delta V_{TA} + \Delta V_{MF} + \Delta V_{EF} + \Delta V_{MP\oplus})$ (KM/SEC)
12.
10.
8.
6.
4.
0
80
160
240
320
400
480
560
640
720
800
ELAPSED TIME (HRS.) AFTER NOMINAL ARRIVAL AT MOON

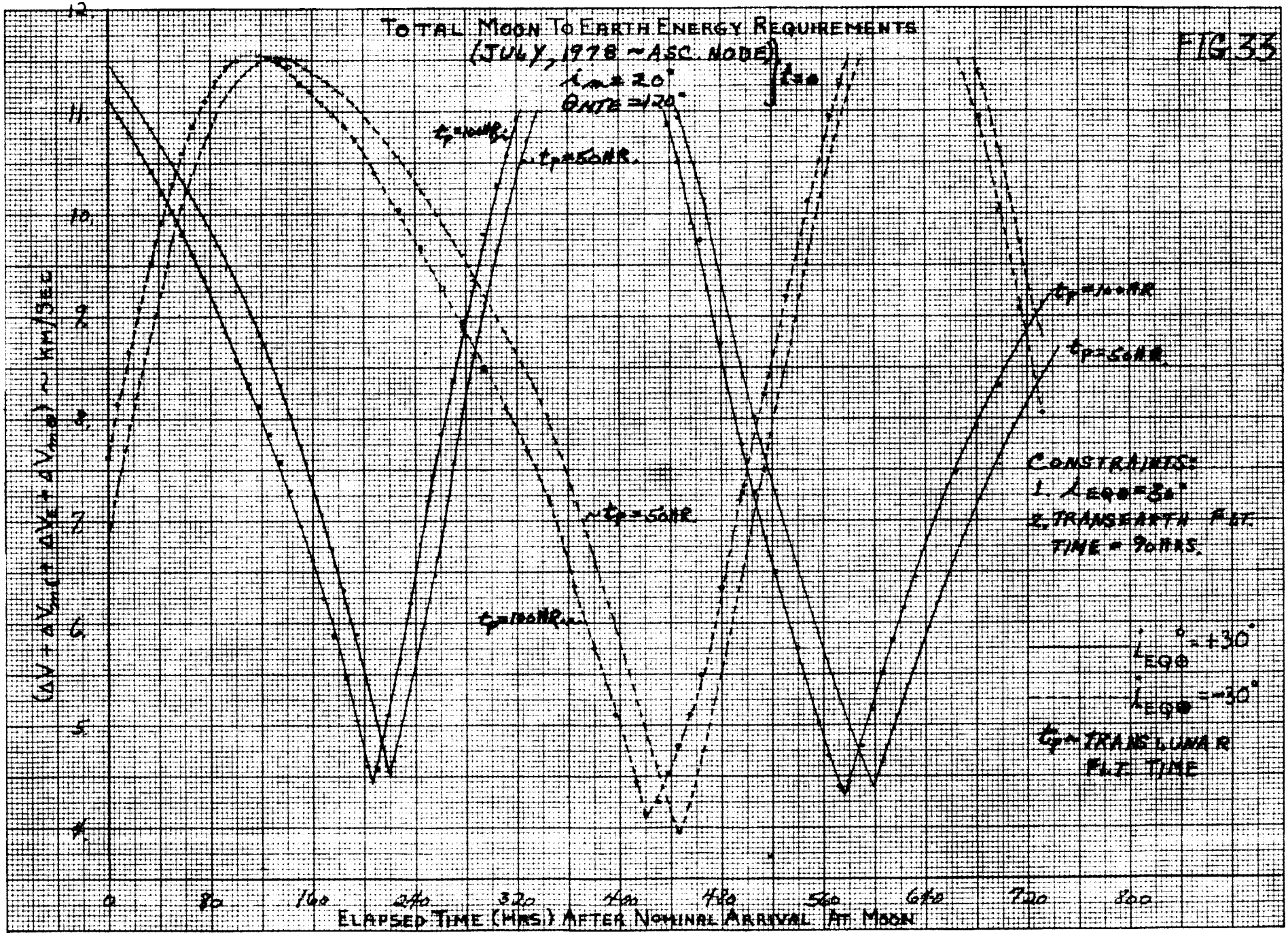
TOTAL MOON TO EARTH ENERGY REQUIREMENTS
(JULY, 1978 ~ ASC. NODE)
FIG 35
$\lambda_m = 20°$
$\theta_{INT} = 120°$
$t_p = 100$ HR.
$t_p = 50$ HR.
$t_p = 100$ HR.
$t_p = 50$ HR.
$t_p = 100$ HR.
$t_p = 50$ HR.
CONSTRAINTS:
1. $\lambda_{EQ\oplus} = 28°$
2. TRANSEARTH FLT. TIME = 90 HRS.
$\lambda_{EQ\oplus} = +30°$
$\lambda_{EQ\oplus} = -30°$
$t_p$ = TRANSLUNAR FLT. TIME
(V + AV) - (V + AV)$^2$ km$^2$/sec$^2$
ELAPSED TIME (HRS.) AFTER NOMINAL ARRIVAL AT MOON

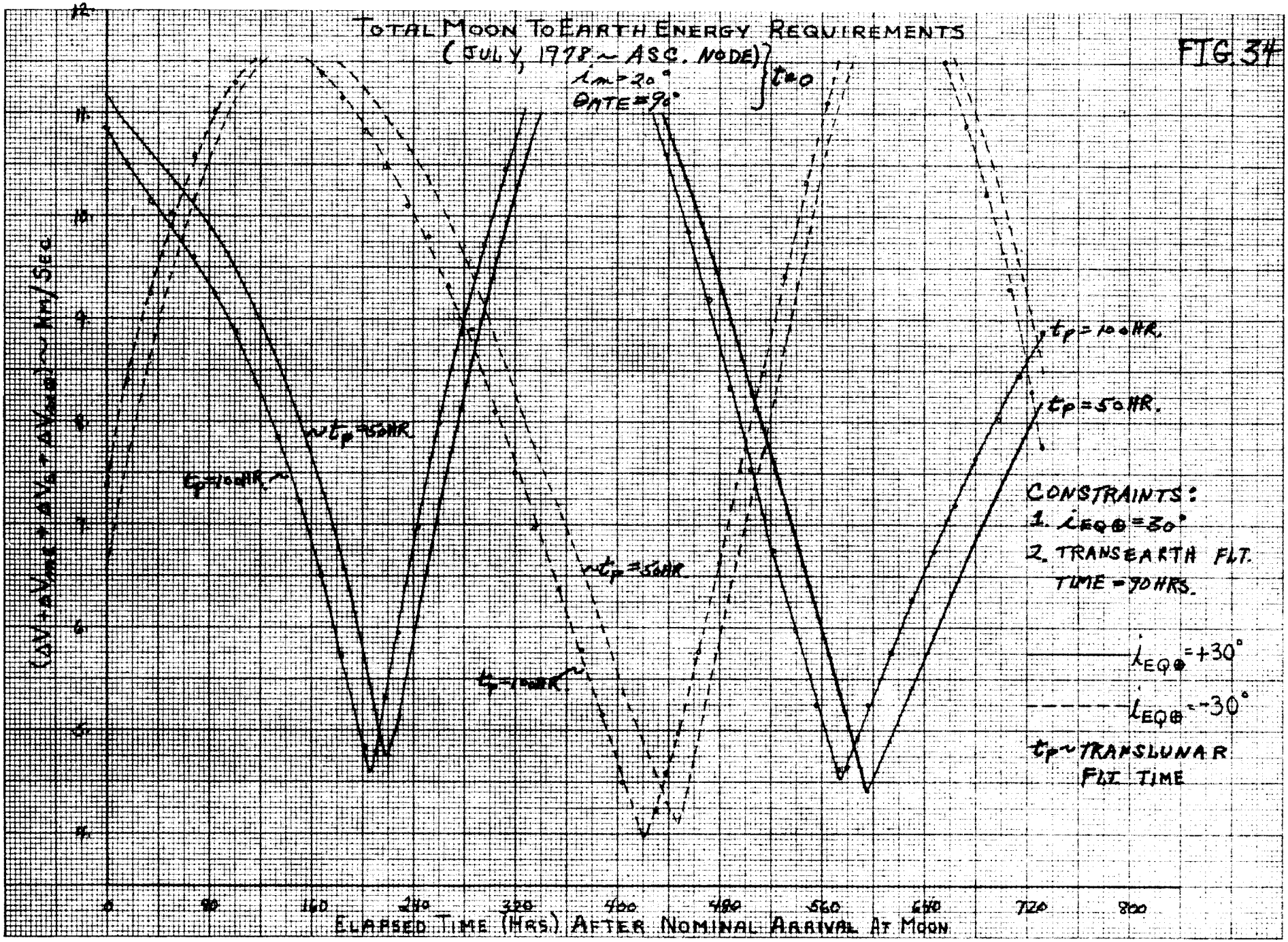
TOTAL MOON TO EARTH ENERGY REQUIREMENTS
(JULY, 1978 ~ ASC. MODE)
FIG 34
$i_m = 30°$
$\Theta_{ATE} = 90°$
$t=0$
$t_p = 100$ HR.
$t_p = 50$ HR.
CONSTRAINTS:
1. $i_{EQ\oplus} = 30°$
2. TRANSEARTH FLT. TIME = 70 HRS.
$i_{EQ\oplus} = +30°$
$i_{EQ\oplus} = -30°$
$t_p$ ~ TRANSLUNAR FLT. TIME
$(\Delta V)_{TOT} = \Delta V_{MCC} + \Delta V_{LOI} + \Delta V_{TEI}$ (KM/SEC)
12
11
10
9
8
7
6
5
4
0
80
160
240
320
400
480
560
640
720
800
ELAPSED TIME (HRS.) AFTER NOMINAL ARRIVAL AT MOON

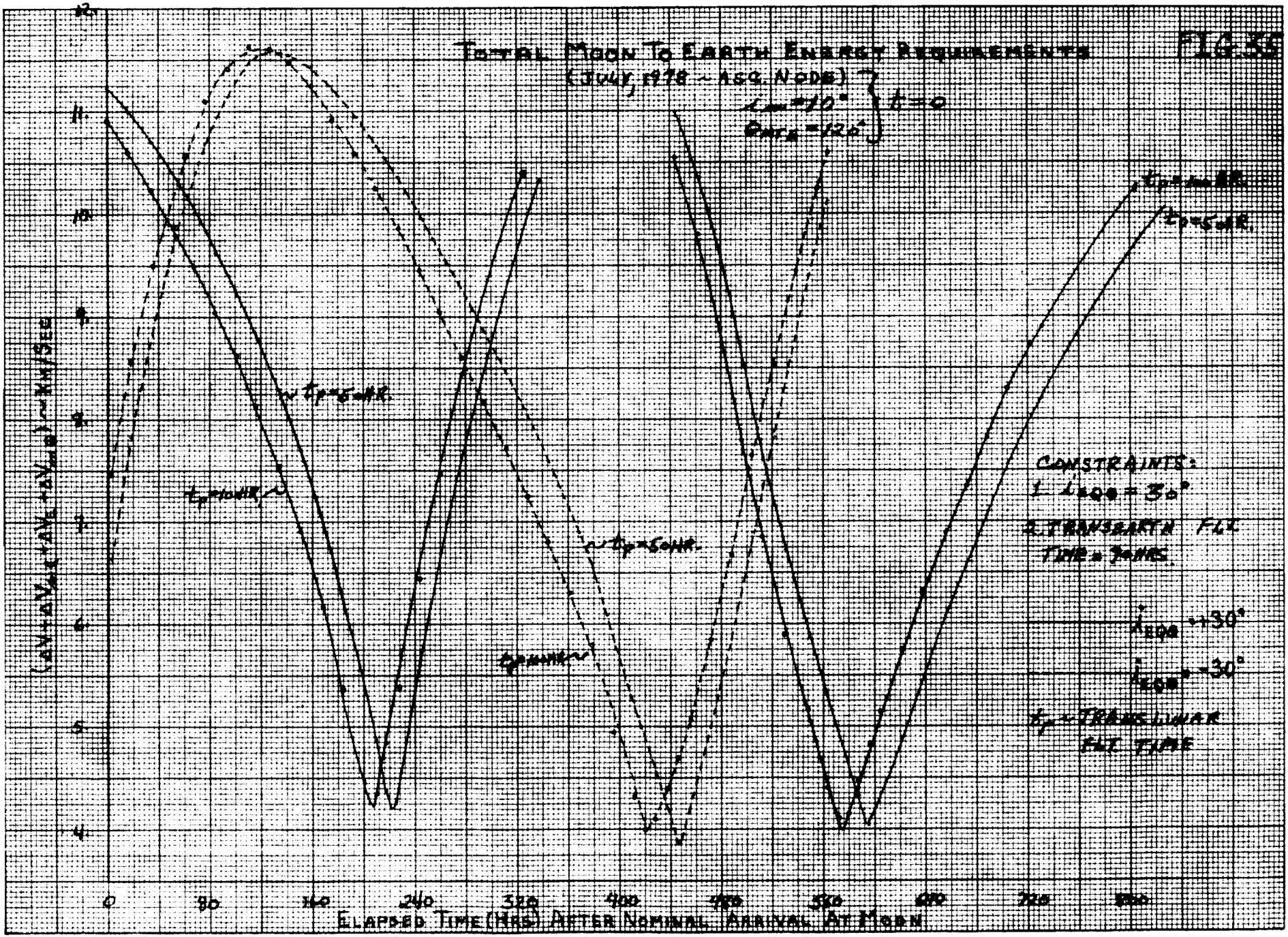
TOTAL MOON TO EARTH ENERGY REQUIREMENTS
(JULY, 1978 – ASC. NODE)
$\lambda_{asc} = 10°$
$\Omega_{MES} = 120°$
$t = 0$
$t_p = 6$ HR.
$t_p = 5$ HR.
$t_p = 6$ HR.
$t_p = 5$ HR.
CONSTRAINTS:
1. $\lambda_{ASC} = 30°$
2. TRANSEARTH FLT TIME = 3 DAYS
$\lambda_{ASC} = +30°$
$\lambda_{ASC} = -30°$
$t_p$ = TRANSLUNAR FLT. TIME
ΔV + ΔV* + ΔV** (FT/SEC)
ELAPSED TIME (HRS) AFTER NOMINAL ARRIVAL AT MOON

FIG 35

MISSIONS III AND IV

Auxiliary Data for Missions III and IV

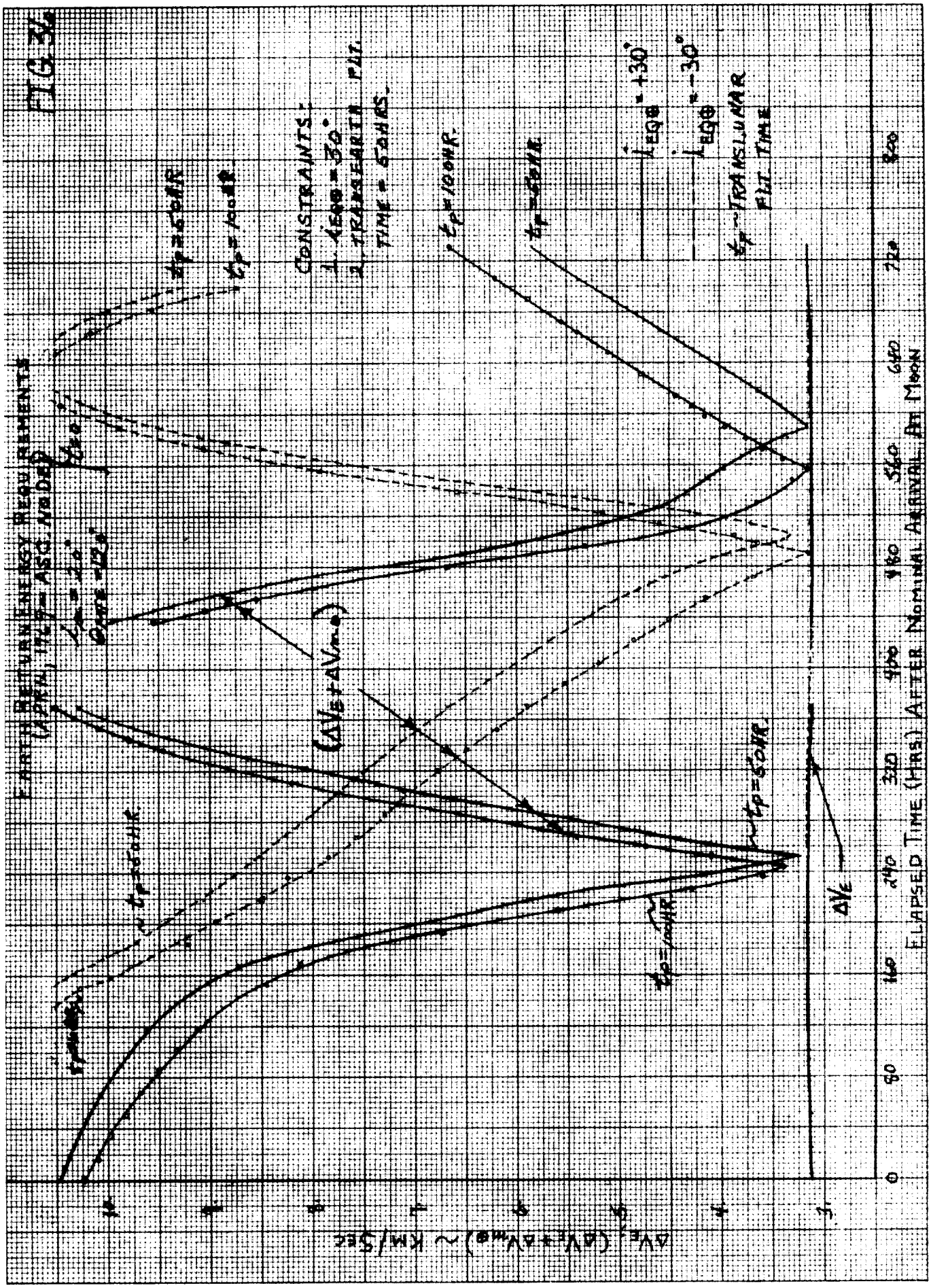
FIG 3.4
EARTH RETURN ENERGY REQUIREMENTS
(APRIL 1976 ASC. ARIDE)
CONSTRAINTS:
1. $\lambda_{EQ\oplus} = 30°$
2. TRAJECTORY FLT. TIME = 5 DAYS
$\lambda_{EQ\oplus} = +30°$
$\lambda_{EQ\oplus} = -30°$
$\Sigma_p$ = TRANSLUNAR FLT. TIME
$\Sigma_p$ = 10 HR.
$\Sigma_p$ = 5 HR.
$\Sigma_p$ = 2 HR.
$\Sigma_p$ = 1 HR.
$\Sigma_p$ = 0.5 HR.
$\Sigma_p$ = 0.25 HR.
$\Sigma_p$ = 0.1 HR.
$\Sigma_p$ = 0.05 HR.
$\Sigma_p$ = 0.01 HR.
$\Delta V_E$
$(\Delta V_E + \Delta V_{m\text{-}e})$
$\Delta V_E$, $(\Delta V_E + \Delta V_{m\text{-}e})$ ~ KM/SEC
ELAPSED TIME (HRS) AFTER NOMINAL ARRIVAL AT MOON
0
80
240
320
400
480
560
640
720
800

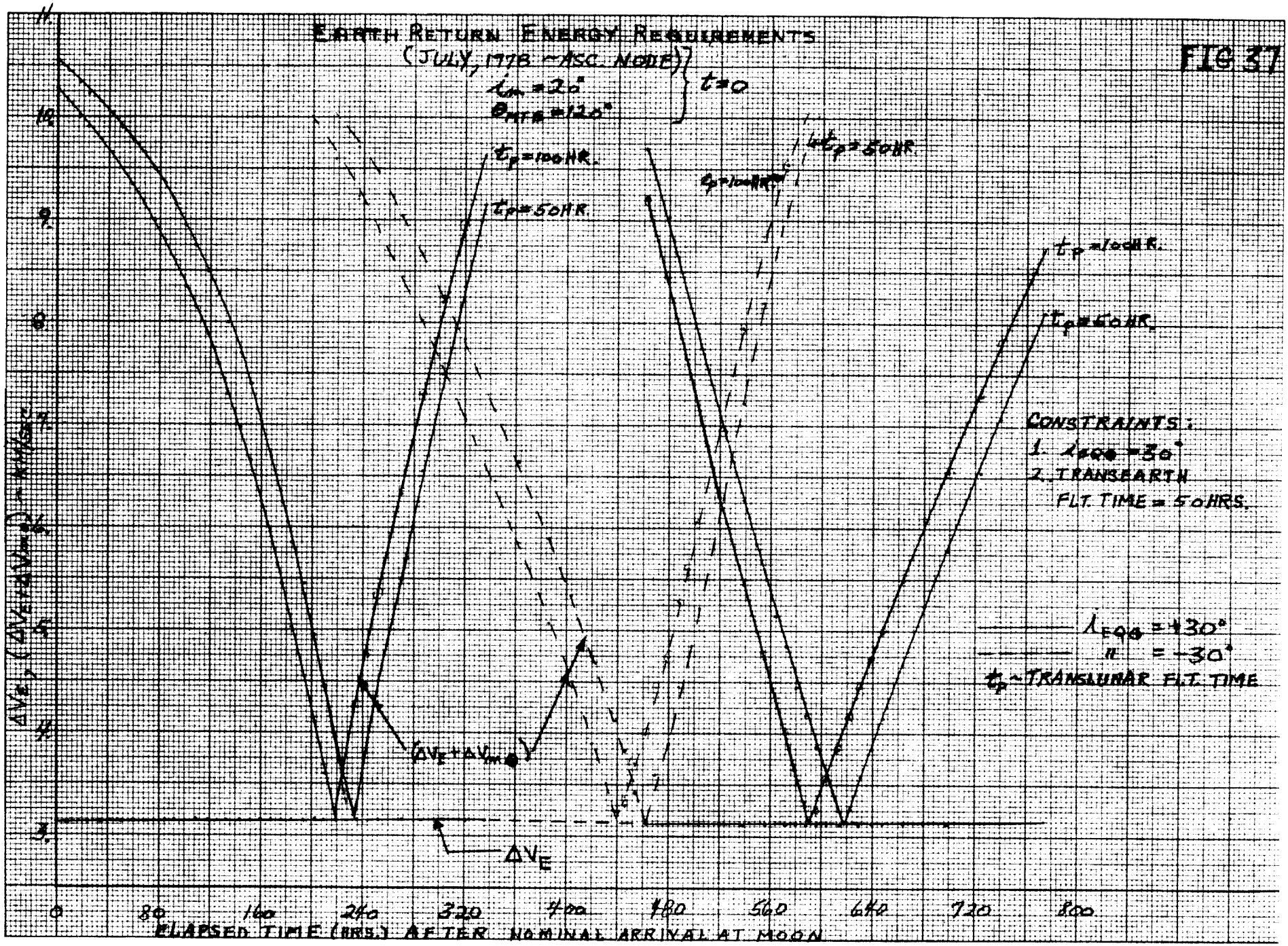
EARTH RETURN ENERGY REQUIREMENTS
(JULY, 1978 - ASC. NODE)
FIG 37
$t_{LO}$ = 20°
$\theta_{MTR}$ = 120°
$t_p$ = 100 HR.
$t_p$ = 50 HR.
$t_p$ = 100 HR.
$t_p$ = 50 HR.
$t_p$ = 100 HR.
$t_p$ = 50 HR.
$t = 0$
CONSTRAINTS:
1. $\lambda_{EQ\oplus}$ = 30°
2. TRANSEARTH FLT. TIME = 50 HRS.
$\lambda_{EQ\oplus}$ = +30°
$\pi$ = -30°
$t_p$ - TRANSLUNAR FLT. TIME
$\Delta V_E + \Delta V_{LOI}$
$\Delta V_E$
$\Delta V_E + \Delta V_{LOI}$ - (KM/SEC)
0
80
160
240
320
400
480
560
640
720
800
ELAPSED TIME (HRS.) AFTER NOMINAL ARRIVAL AT MOON

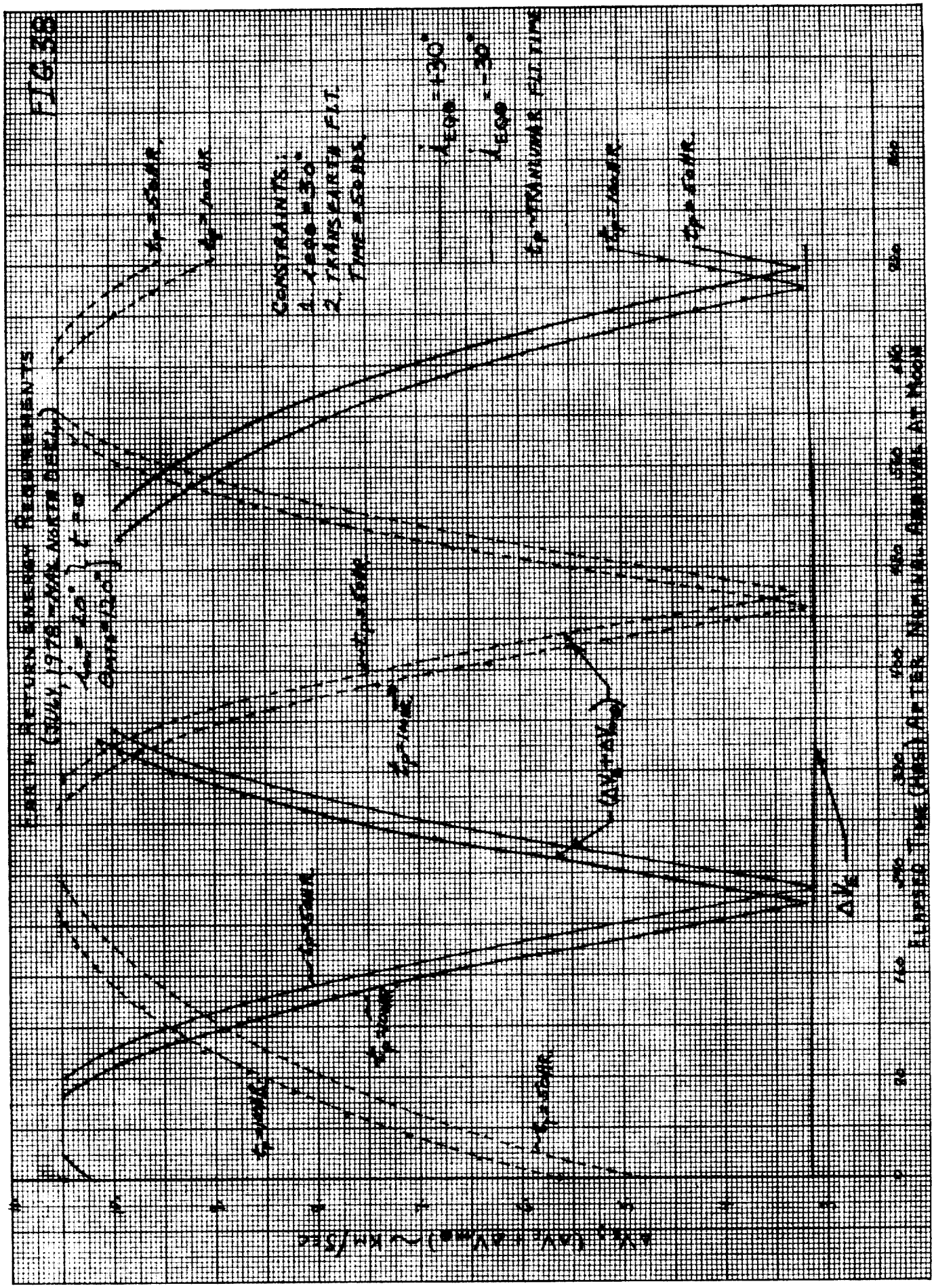

ER 13550-III
I-104

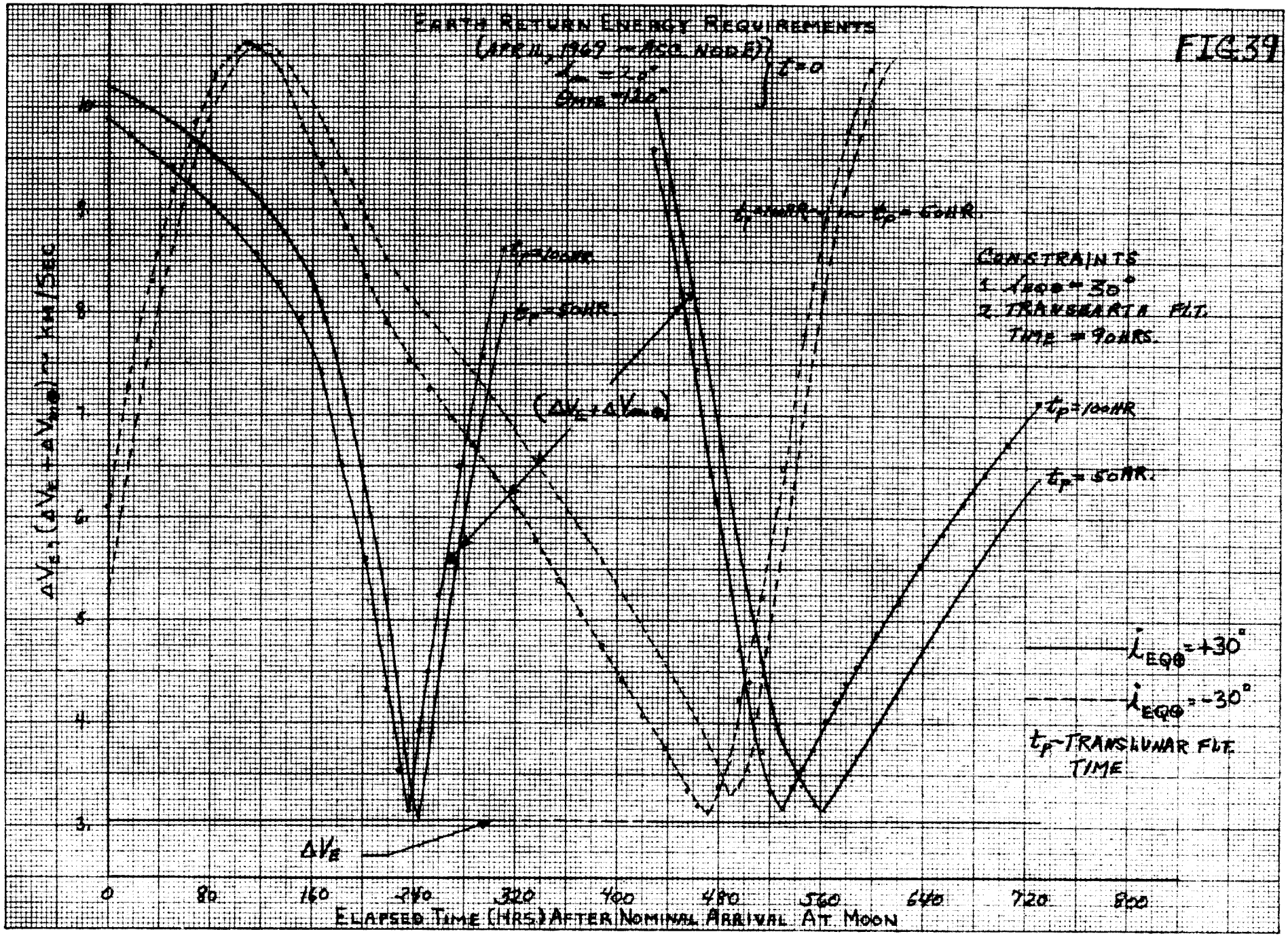
EARTH RETURN ENERGY REQUIREMENTS
(APR 11, 1969 — ASC. NODE)
$i_{EQ\oplus} = i_{\oplus}$
$\Omega_{MOON} = 112°$
$t=0$
FIG 39
$t_p$=100HR
$t_p$=50HR.
$t_p$=100HR
$t_p$=60HR.
$t_p$=50HR.
CONSTRAINTS
1. $i_{EQ\oplus} = 30°$
2. TRANSEARTH FLT. TIME = 90HRS.
$(\Delta V_E + \Delta V_{MOON})$
$\Delta V_E$
$i_{EQ\oplus} = +30°$
$i_{EQ\oplus} = -30°$
$t_p$ - TRANSLUNAR FLT. TIME
$\Delta V$'s $(\Delta V_E + \Delta V_{MOON})$ - KM/SEC
3
4
5
6
7
8
9
10
0
80
160
240
320
400
480
560
640
720
800
ELAPSED TIME (HRS) AFTER NOMINAL ARRIVAL AT MOON

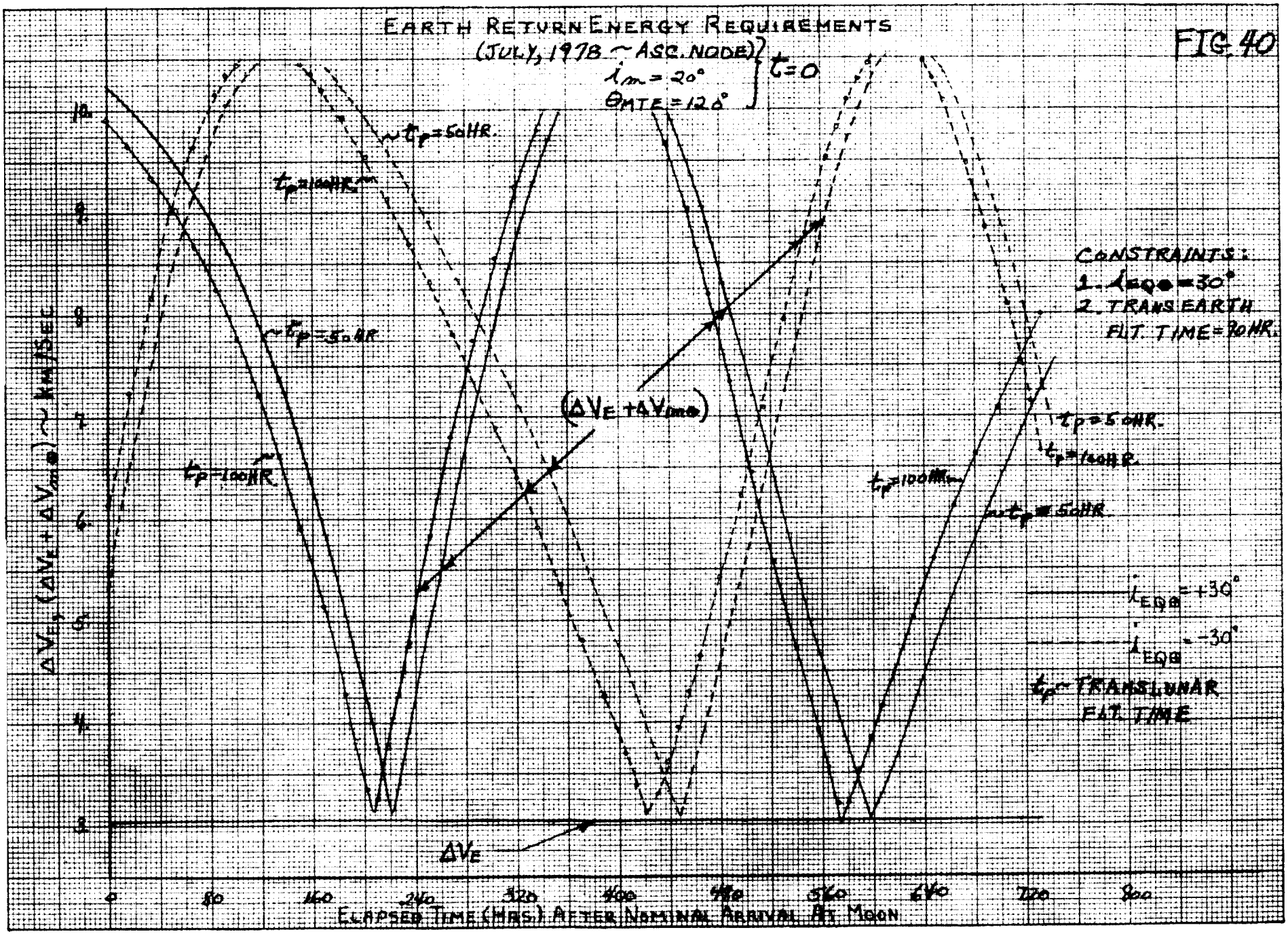
EARTH RETURN ENERGY REQUIREMENTS
(JULY, 1978 ~ ASC. NODE)
$i_m = 20°$
$\theta_{MTE} = 120°$
$t=0$
FIG. 40
$t_p = 50$ HR.
$t_p = 100$ HR.
$t_p = 150$ HR.
$t_p = 200$ HR.
$(\Delta V_E + \Delta V_{lmo})$
$\Delta V_E$
CONSTRAINTS:
1. $i_{EQB} = 30°$
2. TRANS EARTH FLT. TIME = 70 HR.
$i_{EQB} = +30°$
$i_{EQB} = -30°$
$t_p$ = TRANSLUNAR FLT. TIME
$\Delta V_E, (\Delta V_E + \Delta V_{lmo}) \sim$ KM/SEC
ELAPSED TIME (HRS.) AFTER NOMINAL ARRIVAL AT MOON
0
80
160
240
320
400
480
560
640
720
800
2
3
4
5
6
7
8
9
10

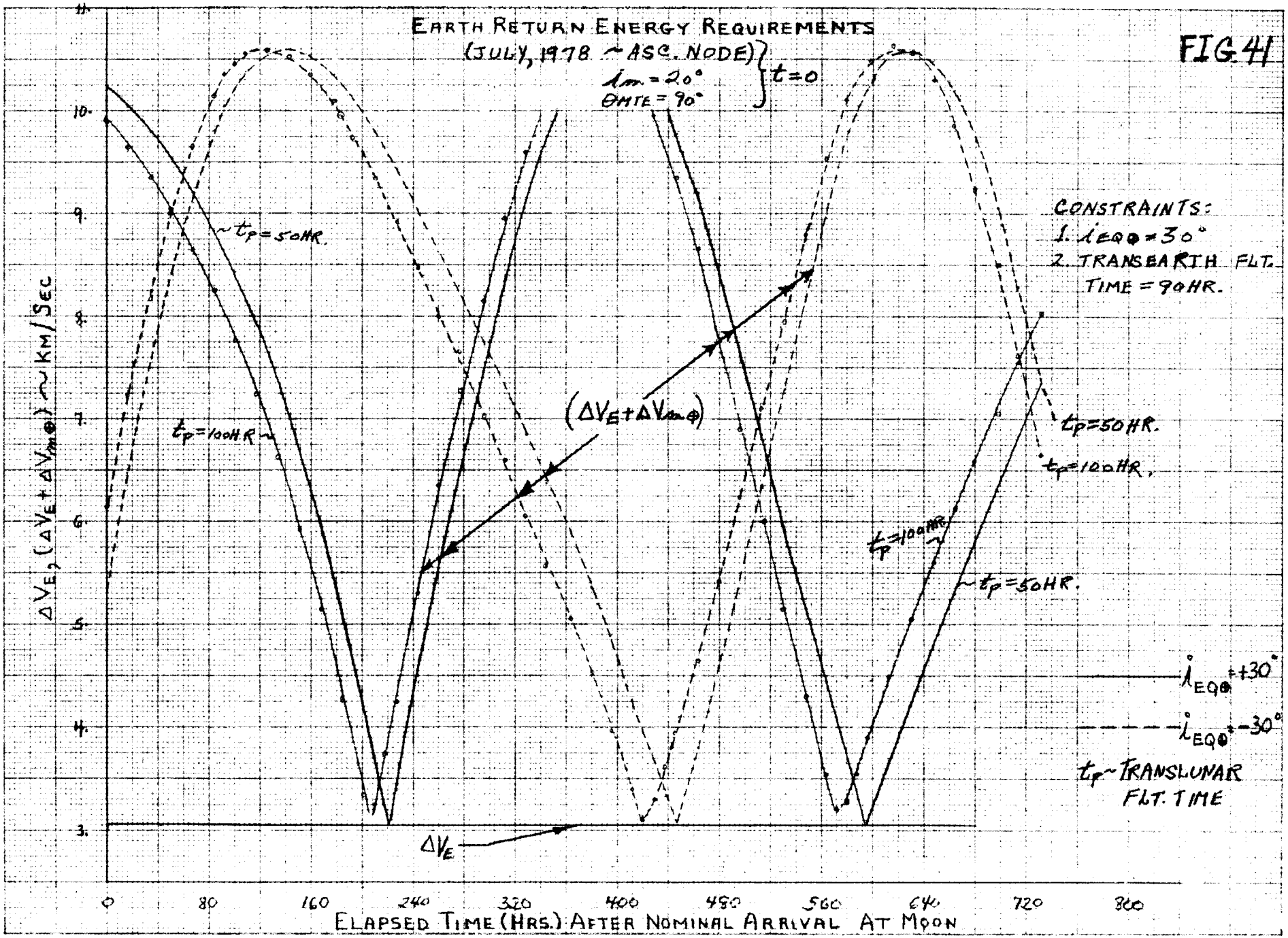
EARTH RETURN ENERGY REQUIREMENTS
(JULY, 1978 ~ ASC. NODE)
$i_m = 20°$
$\theta_{MTE} = 90°$
$t=0$
FIG. 4
CONSTRAINTS:
1. $i_{EQ\oplus} = 30°$
2. TRANSEARTH FLT. TIME = 90 HR.
$\Delta V_E, (\Delta V_E + \Delta V_{m\oplus})$ ~ KM/SEC
$t_p$ = 50 HR.
$t_p$ = 100 HR.
$(\Delta V_E + \Delta V_{m\oplus})$
$\Delta V_E$
$i_{EQ\oplus} = +30°$
$i_{EQ\oplus} = -30°$
$t_p$ ~ TRANSLUNAR FLT. TIME
ELAPSED TIME (HRS.) AFTER NOMINAL ARRIVAL AT MOON

FIG. 42

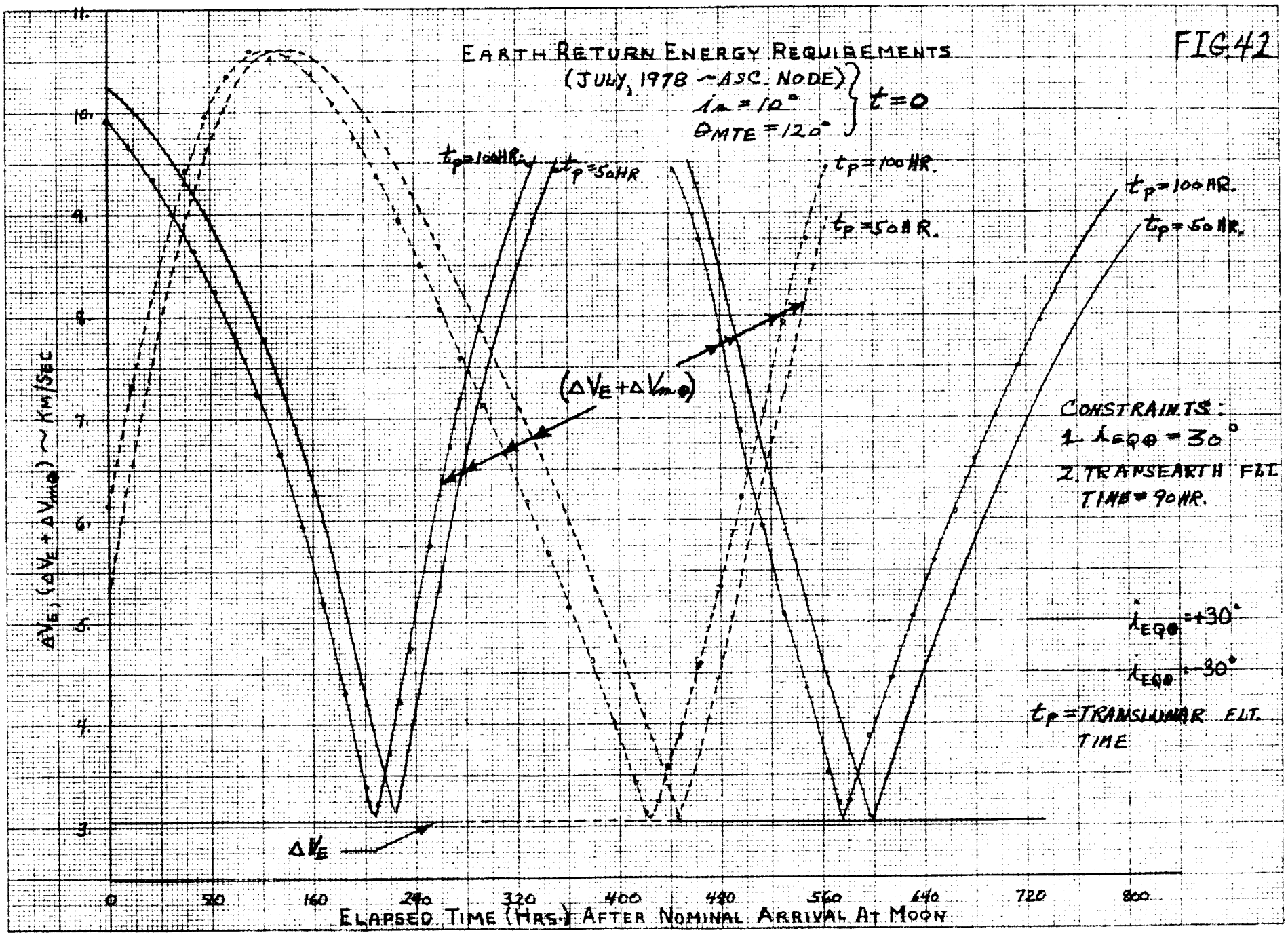
EARTH RETURN ENERGY REQUIREMENTS
(JULY, 1978 ~ ASC. NODE)
$i_m = 10°$
$\theta_{MTE} = 120°$
$t = 0$
$t_p = 100$ HR.
$t_p = 50$ HR.
$(\Delta V_E + \Delta V_{m\theta})$
$\Delta V_E$
CONSTRAINTS:
1. $i_{EQ\theta} = 30°$
2. TRANSEARTH FLT TIME = 90 HR.
$i_{EQ\theta} = +30°$
$i_{EQ\theta} = -30°$
$t_p$ = TRANSLUNAR FLT. TIME
$\Delta V_E, (\Delta V_E + \Delta V_{m\theta}) \sim$ KM/SEC
ELAPSED TIME (HRS.) AFTER NOMINAL ARRIVAL AT MOON
0
80
160
240
320
400
480
560
640
720
800

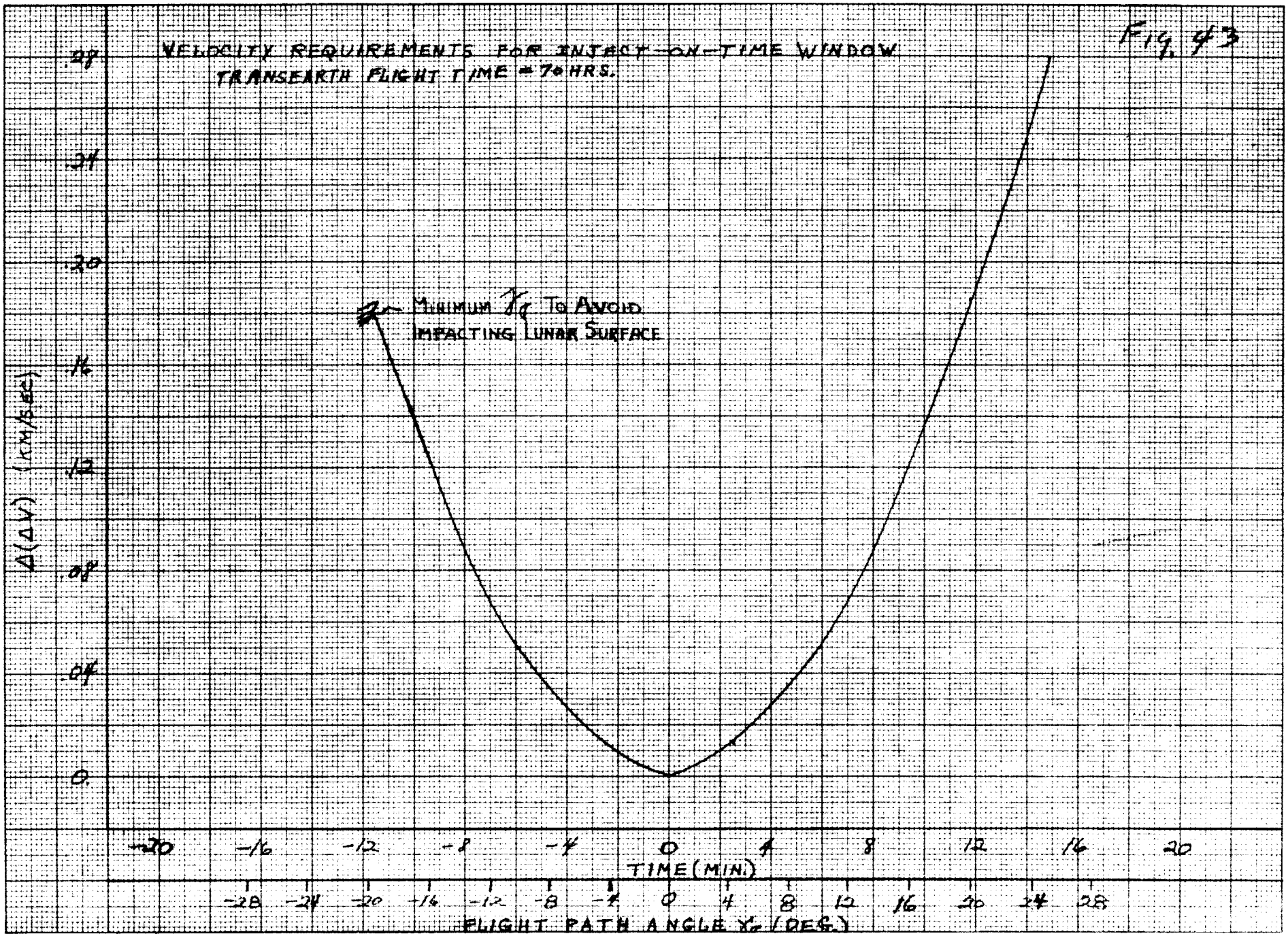
VELOCITY REQUIREMENTS FOR INJECT-ON-TIME WINDOW
TRANSEARTH FLIGHT TIME = 70 HRS.
Fig. 4-3
MINIMUM $\gamma_f$ TO AVOID IMPACTING LUNAR SURFACE
$\Delta(\Delta V)$ (KM/SEC)
TIME (MIN.)
FLIGHT PATH ANGLE $\gamma_f$ (DEG.)

# II. STABILITY AND MISSION POTENTIAL OF THE LIBRATION POINTS IN THE EARTH-MOON SYSTEM

by R. G. Salinger

## A. INTRODUCTION

It is the purpose of this chapter to update and strengthen the discussion of the libration points in the earth-moon system as presented in Chapter III of Ref. 1. A study of the stability of these points under various models of the earth-moon system is presented. If the libration points are to be utilized for purposes such as navigation, storage depots and way stations, confinement of a vehicle to the near vicinity of the point becomes a mission constraint. The station-keeping requirements for these type missions have been determined over a period of 1 yr for a particular libration point and a particular injection date in this study. Wherever possible, excerpts from the stated references are used to relate a complete, accurate and concise treatment.

## SYMBOLS

| | |
|---|---|
| A | Acceleration |
| a | Semimajor axis |
| C | Jacobi's constant |
| e | Eccentricity |
| G | Universal gravitational constant |
| M | Mass |
| m | Body mass in the restricted elliptical problem |
| p | Semiparameter |
| $R_{\oplus\mathbb{C}}$ | Earth-moon distance |
| r | Distance of vehicle from reference body |
| t | Time |
| u | Ratio of the mass of the smaller primary body to the sum of the masses of the primary bodies |
| V | Velocity of vehicle relative to a rotating coordinate system ($X_R$, $Y_R$, $Z_R$) |
| $X_R$, $Y_R$, $Z_R$ | Orthogonal coordinate system center at the earth-moon barycenter with the $X_R$-axis rotating with the earth-moon line |
| $X_{RL}$, $Y_{RL}$, $Z_{RL}$ | Rotating coordinate system centered at a libration point |
| x, y, z | Dimensionless rectangular coordinates in restricted elliptic three-body problem |
| $\tau$ | |
| ($\xi$, $\eta$, $\zeta$) | Displacement of a vehicle from a libration point in the ($X_R$, $Y_R$, $Z_R$) coordinate system |
| $\theta$ | True anomaly |
| $\omega_{\oplus\mathbb{C}}$ | Angular velocity of earth-moon line |

SYMBOLS (continued)

Subscripts

| | |
|---|---|
| i, j | Arbitrary indices |
| L | Libration point |
| R | Rotating system |
| T | Total |
| V | Vehicle |
| X | Partial derivative with respect to $X_{R\Delta}$ |
| Y | Partial derivative with respect to $Y_{R\Delta}$ |
| Z | Partial derivative with respect to $Z_{R\Delta}$ |
| x | Component along x coordinate |
| y | Component along y coordinate |
| $\Delta$ | Vehicle |
| $\theta$ | Component along $\theta$ coordinate |
| 0 | Initial value |
| 1, 2 | Arbitrary indices |
| $\oplus$ | Earth |
| $\mathbb{C}$ | Moon |

## B. GENERAL DISCUSSION

The restricted three-body problem involves the motion of two bodies of finite mass which revolve around one another in circular orbits and of a third body of infinitesimal mass moving in their field. This problem, as it applies to the earth-moon system, has been treated in Ref. 1 where the equations of motion in a rotating coordinate system were derived, Jacobi's integral was

obtained and the regions of possible motion were studied. The coordinate system referred to ($X_R$, $Y_R$, $Z_R$) has its origin at the center of mass of the earth-moon system; the $X_R$-axis lies along the earth-moon line, the $Z_R$-axis is perpendicular to the moon's orbital plane and the system rotates in the same direction as the earth-moon system with the uniform angular velocity $\omega_{\oplus\mathbb{C}}$. In this coordinate system the equations of motion do not involve time explicitly.

In the space that surrounds the two primary bodies there are five points at which a third body will remain in equilibrium under the gravitational attractions of the other two bodies. These points are denoted by various names: libration points, stationary points, or double points. As shown in Fig. 1, three of the points lie on a straight line that joins the mass centers of the first two bodies. The two remaining points lie at the vertices of two equilateral triangles which have the line joining the two bodies as a mutual base. In the circular orbit model, a vehicle will remain in equilibrium if placed at one of the libration points with zero velocity relative to the rotating coordinate system. The question of stability of these five points is of importance; i.e., will the vehicle stay near the point if given a small displacement and velocity (stable solution) or will it rapidly depart from that point (unstable solution)? These small displacements and velocities may be regarded as due to insertion errors or to forces neglected in the circular orbit model. For the earth-moon system these forces are due to the eccentric lunar orbit, the gravitational attractions of the sun and planets, solar radiation pressure and the effects arising from the nonsphericity of the moon and earth.

It is the aim of this chapter to present a study of the stability of motion near the libration points in the earth-moon system under various approximations. The first approximation will be the restricted three-body circular orbit model in which it will be shown that the straight-line solutions are unstable while the equilateral triangle solutions are stable. Next, the stability of the triangular points in the elliptic restricted problem of three bodies will be considered. In the elliptic restricted problem of three bodies, the relative orbit of the two primary bodies is an ellipse of eccentricity e, and the third body, of negligible mass, moves in their field. Possible positions of equilibrium occur when the three bodies form equilateral triangles. Finally, numerical studies of other perturbations on the triangular libration points will be presented. In the first of these the influence of the sun's gravitational potential and of solar radiation pressure using a circular earth-moon model is determined. In the second numerical study an n-body integrated trajectory program was utilized to simulate the actual physical system. Included in this program were the gravitational potentials of the sun and planets, the nonspherical effects of the moon and the earth, the eccentricity of the moon's orbit and solar radiation pressure.

## C. STABILITY OF THE LIBRATION POINTS IN THE RESTRICTED THREE-BODY PROBLEM

It has been shown in Ref. 2 and Ref. 3 that the straight line solutions of the restricted three-body problem are unstable, whereas the equilateral triangle solutions are stable. In this section a derivation of the stability of these points will be presented.

The equations of motion of a vehicle in the rotating $(X_R, Y_R, Z_R)$ coordinate system were found in Ref. 1 to be

$$\left.\begin{aligned}
\ddot{X}_{R\Delta} - 2\omega_{\oplus\mathbb{C}}\dot{Y}_{R\Delta} &= \omega^2_{\oplus\mathbb{C}} X_{R\Delta} - \frac{GM_{\oplus}(X_{R\Delta} - X_{R\oplus})}{r^3_{\oplus\Delta}} - \frac{GM_{\mathbb{C}}(X_{R\Delta} - X_{R\oplus})}{r^3_{\mathbb{C}\Delta}} \\
\ddot{Y}_{R\Delta} + 2\omega_{\oplus\mathbb{C}}\dot{X}_{R\Delta} &= \omega^2_{\oplus\mathbb{C}} Y_{R\Delta} - \frac{GM_{\oplus} Y_{R\Delta}}{r^3_{\oplus\Delta}} - \frac{GM_{\mathbb{C}} Y_{R\Delta}}{r^3_{\mathbb{C}\Delta}} \\
\ddot{Z}_{R\Delta} &= - \frac{GM_{\oplus} Z_{R\Delta}}{r^3_{\oplus\Delta}} - \frac{GM_{\mathbb{C}} Z_{R\Delta}}{r^3_{\mathbb{C}\Delta}}
\end{aligned}\right\} \quad (1)$$

where

$$r_{\oplus\Delta} = \left[(X_{R\Delta} - X_{R\oplus})^2 + Y^2_{R\Delta} + Z^2_{R\Delta}\right]^{1/2} \quad (2)$$

and

$$r_{\mathbb{C}\Delta} = \left[(X_{R\Delta} - X_{R\mathbb{C}})^2 + Y^2_{R\Delta} + Z^2_{R\Delta}\right]^{1/2} \quad (3)$$

The symbols $\Delta$, $\oplus$, and $\mathbb{C}$ denote the vehicle, the earth and the moon, respectively.

Equations (1) admit an integral first given by Jacobi and which has been discussed by Hill in his lunar theory.

Let

$$W = 1/2\ \omega^2_{\oplus\mathbb{C}}\ (X^2_{R\Delta} + Y^2_{R\Delta}) + \frac{GM_{\oplus}}{r_{\oplus\Delta}} + \frac{GM_{\mathbb{C}}}{r_{\mathbb{C}\Delta}} \quad (4)$$

then Eqs (1) can be written in the form

$$\left.\begin{aligned}
\ddot{X}_{R\Delta} - 2\omega_{\oplus\mathbb{C}}\dot{Y}_{R\Delta} &= \frac{\partial W}{\partial X_{R\Delta}} \\
\ddot{Y}_{R\Delta} + 2\omega_{\oplus\mathbb{C}}\dot{X}_{R\Delta} &= \frac{\partial W}{\partial Y_{R\Delta}} \\
\ddot{Z}_{R\Delta} &= \frac{\partial W}{\partial Z_{R\Delta}}
\end{aligned}\right\} \quad (5)$$

If these equations are multiplied by $2\dot{X}_{R\Delta}$, $2\dot{Y}_{R\Delta}$ and $2\dot{Z}_{R\Delta}$, respectively, and added, the resulting equation can be integrated, since W is a function of $X_{R\Delta}$, $Y_{R\Delta}$, and $Z_{R\Delta}$ alone, and this gives Jacobi's integral:

$$(\dot{X}_{R\Delta})^2 + (\dot{Y}_{R\Delta})^2 + (\dot{Z}_{R\Delta})^2 = V_{R\Delta}^2 = 2W\text{-}C$$

$$V_{R\Delta}^2 = \omega_{\oplus\mathbb{C}}^2 (X_{R\Delta}^2 + Y_{R\Delta}^2) + \frac{2\,GM_{\oplus}}{r_{\oplus\Delta}} + \frac{2\,GM_{\mathbb{C}}}{r_{\mathbb{C}\Delta}} - C \tag{6}$$

where $V_{R\Delta}$ is the magnitude of the velocity of the vehicle in the rotating coordinate system and C is the Jacobian constant.

The libration points occur at stationary values of the surfaces of zero relative velocity $F(X_{R\Delta}, Y_{R\Delta}, Z_{R\Delta})$, where

$$F(X_{R\Delta}, Y_{R\Delta}, Z_{R\Delta}) = W + 1/2\,C = 0 \tag{7}$$

Now, from the condition

$$\frac{\partial F}{\partial X_{R\Delta}} = \frac{\partial F}{\partial Y_{R\Delta}} = \frac{\partial F}{\partial X_{R\Delta}} = 0 \tag{8}$$

there results

$$\frac{\partial F}{\partial Z_{R\Delta}} = Z_{R\Delta} \left( \frac{GM_{\oplus}}{r_{\oplus\Delta}^3} + \frac{GM_{\mathbb{C}}}{r_{\mathbb{C}\Delta}^3} \right) \tag{9}$$

so that any libration point lies in the $X_R$ - $Y_R$ plane for there $Z_{R\Delta} = 0$. Putting $Z_{R\Delta} = 0$, the conditions for $\frac{\partial F}{\partial X_{R\Delta}} = 0$ and $\frac{\partial F}{\partial Y_{R\Delta}} = 0$ can be found. They are

$$\omega_{\oplus\mathbb{C}}^2 X_{R\Delta} - \frac{GM_{\oplus}(X_{R\Delta} - X_{R\oplus})}{r_{\oplus\Delta}^3} - \frac{GM_{\mathbb{C}}(X_{R\Delta} - X_{R\mathbb{C}})}{r_{\mathbb{C}\Delta}^3} = 0 \tag{10}$$

and

$$\omega_{\oplus\mathbb{C}}^2 Y_{R\Delta} - \frac{GM_{\oplus}\, Y_{R\Delta}}{r_{\oplus\Delta}^3} - \frac{GM_{\mathbb{C}}\, Y_{R\Delta}}{r_{\mathbb{C}\Delta}^3} = 0 \tag{11}$$

Equation (11) is satisfied if $Y_{R\Delta} = 0$, and in this case Eq (10) becomes

$$\omega^2_{\oplus\mathbb{C}} X_{R\Delta} - \frac{GM_{\oplus}(X_{R\Delta} - X_{R\oplus})}{\left|X_{R\Delta} - X_{R\oplus}\right|^3} - \frac{GM_{\mathbb{C}}(X_{R\Delta} - X_{R\mathbb{C}})}{\left|X_{R\Delta} - X_{R\mathbb{C}}\right|^3} = 0 \quad (12)$$

Equation (12) yields the libration points on the $X_R$ - axis or the straight line solutions to the problem.

Consider the case when $Y_{R\Delta} \neq 0$, then Eq (11) becomes

$$\omega^2_{\oplus\mathbb{C}} - \frac{GM_{\oplus}}{r^3_{\oplus\Delta}} - \frac{GM_{\mathbb{C}}}{r^3_{\mathbb{C}\Delta}} = 0 \quad (13)$$

Multiply this by $(X_{R\Delta} - X_{R\oplus})$ and $(X_{R\Delta} - X_{R\mathbb{C}})$ and subtract the products separately from Eq (10). Then

$$\omega^2_{\oplus\mathbb{C}} X_{R\oplus} - \frac{GM_{\mathbb{C}}}{r^3_{\mathbb{C}\Delta}}(X_{R\oplus} - X_{R\mathbb{C}}) = 0$$

and (14)

$$\omega^2_{\oplus\mathbb{C}} X_{R\mathbb{C}} - \frac{GM_{\oplus}}{r^3_{\oplus\Delta}}(X_{R\mathbb{C}} - X_{R\oplus}) = 0$$

But $X_{R\oplus} = -\frac{M_{\mathbb{C}}}{M_{\oplus} + M_{\mathbb{C}}}(R_{\oplus\mathbb{C}})$ and $X_{R\mathbb{C}} = R_{\oplus\mathbb{C}} + X_{R\oplus}$ since the origin is at the center of mass of the primary bodies, so that these equations reduce to

$$r_{\mathbb{C}\Delta} = r_{\oplus\Delta} = R_{\oplus\mathbb{C}}.$$

These points of equilibrium form equilateral triangles in the $X_R$ - $Y_R$ plane with the earth and the moon.

In order to determine whether the positions of equilibrium found above are stable, the motion of the infinitesimal body if it is slightly displaced from that

position must be investigated. Unless the three bodies are assumed to be totally isolated, this will be constantly happening as a result of perturbations.

Let the origin again be at the earth-moon barycenter and take the $X_R$-axis along the earth-moon line. Take the unit of mass to be the sum $(M_\oplus + M_\leftmoon)$ and let the separate masses be $u$ and $(1 - u)$. The axes will be rotating with constant angular velocity, $\omega_{\oplus\leftmoon}$, and the bodies will be fixed at $(X_{R\leftmoon}, 0, 0)$ and $(X_{R\oplus}, 0, 0)$ where $X_{R\oplus}$ is negative. Let the unit of distance be $(-X_{R\oplus} + X_{R\leftmoon})$ and let the unit of time be such as to make $\omega_{\oplus\leftmoon} = 1$. With these definitions the equations of motion become

$$\begin{aligned} \ddot{X}_{R\Delta} - 2\dot{Y}_{R\Delta} &= \frac{\partial W'}{\partial X_{R\Delta}} \\ \ddot{Y}_{R\Delta} + 2\dot{X}_{R\Delta} &= \frac{\partial W'}{\partial Y_{R\Delta}} \\ \ddot{Z}_{R\Delta} &= \frac{\partial W'}{\partial Z_{R\Delta}} \end{aligned} \tag{15}$$

where

$$W' = 1/2\,(X^2_{R\Delta} + Y^2_{R\Delta}) + \frac{(1-u)}{r_{\oplus\Delta}} + \frac{u}{r_{\leftmoon\Delta}} \tag{16}$$

Let the position of equilibrium be at $(X_{R\Delta}, Y_{R\Delta}, Z_{R\Delta})$, and let the body be displaced to $(X_{R\Delta} + \xi, Y_{R\Delta} + \eta, Z_{R\Delta} + \zeta)$ where $\xi$, $\eta$, and $\zeta$ are assumed small. If their squares and products are neglected and if it is remembered that $\frac{\partial W'}{\partial X_{R\Delta}} = 0$, etc. at $(X_{R\Delta}, Y_{R\Delta}, Z_{R\Delta})$, then the equations of motion are

$$\ddot{\xi} - 2\dot{\eta} = -\xi W'_{XX} - \eta W'_{XY} - \zeta W'_{XZ}$$

$$\ddot{\eta} + 2\dot{\xi} = -\xi W'_{YX} - \eta W'_{YY} - \zeta W'_{YZ} \tag{17}$$

$$\ddot{\zeta} = -\xi W'_{ZX} - \eta W'_{ZY} - \zeta W'_{ZZ}$$

where $W'_{YZ}$ stands for $\delta^2 W' / \delta Y_{R\Delta}\, \delta Z_{R\Delta}$, etc., and these quantities are evaluated at the point of equilibrium so that they have constant values.

Now

$$-W' = \frac{1}{2}\left(X^2_{R\Delta} + Y^2_{R\Delta}\right) + (1-u)\left\{\left(X_{R\Delta} - X_{R\oplus}\right)^2 + Y^2_{R\Delta} + Z^2_{R\Delta}\right\}^{-1/2}$$

$$+ u\left\{\left(X_{R\Delta} - X_{R\mathbb{C}}\right)^2 + Y^2_{R\Delta} + Z^2_{R\Delta}\right\}^{-1/2} \tag{18}$$

Define $\alpha$ and $\beta$ by

$$\alpha = \frac{1-u}{r^3_{\oplus\Delta}} + \frac{u}{r^3_{\mathbb{C}\Delta}} \tag{19}$$

and

$$\beta = \frac{1-u}{r^5_{\oplus\Delta}} + \frac{u}{r^5_{\mathbb{C}\Delta}} \tag{20}$$

then it is found that

$$W'_{XX} = -1 + \alpha - 3(1-u)\frac{\left(X_{R\Delta} - X_{R\oplus}\right)^2}{r^5_{\oplus\Delta}} - 3u\frac{\left(X_{R\Delta} - X_{R\mathbb{C}}\right)^2}{r^5_{\mathbb{C}\Delta}}$$

$$W'_{YY} = -1 + \alpha - 3\, Y^2_{R\Delta}\, \beta$$

$$W'_{ZZ} = +\alpha - 3\, Z^2_{R\Delta}\beta$$

$$W'_{YZ} = -3\, Y_{R\Delta} Z_{R\Delta}\beta,\quad W'_{ZX} = -3\, Z_{R\Delta} X_{R\Delta}\beta,\quad W'_{XY} = -3 X_{R\Delta} Y_{R\Delta}\beta$$

For a straight-line solution for which $Y_{R\Delta} = Z_{R\Delta} = 0$ and $X_{R\Delta} = X_{R\Delta 0}$, there results

$$r^2_{\oplus\Delta} = (X_{R\Delta 0} - X_{R\oplus}) \text{ and } r^2_{\mathbb{C}\Delta} = (X_{R\Delta 0} - X_{R\mathbb{C}})^2$$

Also

$$W'_{YZ} = W'_{ZX} = W'_{XY} = 0,$$

so the equations of motion following a small displacement are

$$\begin{aligned} \ddot{\xi} - 2\dot{\eta} &= \xi(1 + 2\alpha) \\ \ddot{\eta} + 2\dot{\xi} &= \eta(1 - \alpha) \\ \ddot{\zeta} &= -\zeta\alpha \end{aligned} \tag{21}$$

Since $\alpha$ is positive, the oscillations in the $Z_R$-direction are finite and small, and therefore stable, and thus only the first two equations of (21) must be studied.

Try a solution $\xi = Ke^{\lambda t}$, $\eta = Le^{\lambda t}$. If $\lambda$ is purely imaginary, then the solution can be put entirely in the form of sines and cosines, and the motion, consisting of finite oscillations, will be stable. Otherwise the solution must involve hyperbolic functions; then $\xi$ and $\eta$ will increase without limit, and the motion is unstable. Substituting the trial solutions into the equations of motion yields

$$K\lambda^2 - 2L\lambda = K(1 + 2\alpha)$$

and

$$L\lambda^2 + 2K\lambda = L(1 - \alpha)$$

Eliminating K and L, it is found that

$$\begin{vmatrix} \lambda^2 - (1 + 2\alpha) & -2\lambda \\ 2\lambda & \lambda^2 - (1 - \alpha) \end{vmatrix} = 0$$

or:

$$\lambda^4 + \lambda^2 (2 - \alpha) + (1 + 2\alpha)(1 - \alpha) = 0$$

For stability $\lambda$ must be purely imaginary so that there must be two real negative roots for $\lambda^2$, for this to be so,

$$1 - \alpha > 0$$

since the product of the roots must be positive, or

$$1 - \frac{1}{r^3_{\oplus\Delta}} + u\left(\frac{1}{r^3_{\oplus\Delta}} - \frac{1}{r^3_{\mathbb{C}\Delta}}\right) > 0$$

Equation (11) can be written in nondimensional form as

$$X_{R\Delta} - (1 - u)\frac{(X_{R\Delta} - X_{R\oplus})}{\left|X_{R\Delta} - X_{R\oplus}\right|^3} - u\frac{(X_{R\Delta} - X_{R\mathbb{C}})}{\left|X_{R\Delta} - X_{R\mathbb{C}}\right|^3} = 0 \qquad (22)$$

It can be shown that Eq (22) has:

a positive root greater than $X_{R\mathbb{C}}$, when $r_{\oplus\Delta}$ is greater than $r_{\mathbb{C}\Delta}$;

a positive root between $X_{R\oplus}$ and $X_{R\mathbb{C}}$, when $r_{\oplus\Delta}$ is greater than $r_{\mathbb{C}\Delta}$;

a negative root less than $X_{R\oplus}$, when $r_{\oplus\Delta}$ is less than $r_{\mathbb{C}\Delta}$.

Now Eq (22) can be written in the form

$$X_{R\Delta 0}(1 - \alpha) + (1 - u)\frac{X_{R\oplus}}{r^3_{\oplus\Delta}} + u\frac{X_{R\mathbb{C}}}{r^3_{\mathbb{C}\Delta}} = 0 \qquad (23)$$

or, since $X_{R\oplus} = -u$ and $X_{R\mathbb{C}} = 1 - u$,

$$X_{R\Delta 0}(1 - \alpha) - u(1 - u)\left\{\frac{1}{r^3_{\oplus\Delta}} - \frac{1}{r^3_{\mathbb{C}\Delta}}\right\} = 0 \qquad (24)$$

So that

$$(1 - \alpha) = \frac{u(1 - u)}{X_{R\Delta 0}}\left\{\frac{1}{r^3_{\oplus\Delta}} - \frac{1}{r^3_{\mathbb{C}\Delta}}\right\} \qquad (25)$$

It is clear from inspection that for each solution $(1 - \alpha)$ is negative. Therefore the straight-line solutions are unstable.

Next consider the stability of the triangular solutions, in terms of the earth-moon distance, $r_{\oplus\Delta} = r_{\mathbb{C}\Delta} = 1$, so that

$$X_{R\Delta} = \frac{1}{2}(1 - 2u),\ Y_{R\Delta} = \pm\sqrt{\frac{3}{2}},\ \text{and}\ Z_{R\Delta} = 0$$

The positive sign for $Y_{R\Delta}$ can be taken without loss of generality. The values of $W'_{i,j}$ that are not zero are

$$W'_{XX} = -\frac{3}{4},\ W'_{YY} = -\frac{9}{4},$$

$$W'_{ZZ} = 1,\ W'_{XY} = -\frac{3\sqrt{3}}{4}(1 - 2u)$$

The equations of motion are:

$$\begin{aligned}
\ddot{\xi} - 2\dot{\eta} &= \frac{3}{4}\xi + \frac{3\sqrt{3}}{4}(1 - 2u)\eta, \\
\ddot{\eta} + 2\dot{\xi} &= \frac{9}{4}\eta + \frac{3\sqrt{3}}{4}(1 - 2u)\xi \qquad (26) \\
\ddot{\zeta} &= -\zeta
\end{aligned}$$

The oscillations in the $Z_R$-direction are stable, the period being the same as that of the revolution of the finite bodies. To investigate the first two equations, again try $\xi = Ke^{\lambda t}$, and $\eta = Le^{\lambda t}$. Substituting, and eliminating K and L as before, it is found that

$$\lambda^4 + \lambda^2 + \frac{27}{4}u(1 - u) = 0 \qquad (27)$$

Considered as a quadratic for $\lambda^2$, this equation must have real negative roots for stability. Since the sum of the roots is negative and their product is positive, they must be negative provided the roots are real. To find the condition for stability, it is sufficient to find the condition for real roots. This is

$$1 - 27\,u\,(1 - u) > 0$$

Putting the left-hand side equal to $\epsilon$, and solving the resulting quadratic for u, it is found:

$$u = \frac{1}{2} \pm \sqrt{\frac{23 + 4\epsilon}{108}} \tag{28}$$

Since $u \leq \frac{1}{2}$, the minus sign is taken. The condition for stability is $\epsilon > 0$, or

$$u < 0.0385$$

This criteria is satisfied for the earth-moon system where $u = \frac{M_{\mathbb{C}}}{M_{\oplus} + M_{\mathbb{C}}} \approx 0.01213$.

In Ref. 2, a study is presented of typical orbits about the stable libration points in the earth-moon system.

## D. THE ELLIPTIC RESTRICTED THREE-BODY PROBLEM

The principal reason why the circular three-body formulation is unable to describe the long-time behavior of important dynamical systems in astronomy is the neglect of the eccentricity of the orbits of the primary bodies. Introducing elliptic orbits generalizes the original restricted problem and significantly improves its applicability. In this section, Ref. 3 is used to show that the equations of motion for the case of eccentricity $\neq 0$ can be written in a form identical with the form of the equations for the circular case. Then the stability of the triangular libration points in the elliptic case are discussed according to the results of Ref. 4.

The elliptic restricted problem is described by

$$\begin{aligned} x'' - 2y' &= \omega_x \\ y'' + 2x' &= \omega_y \end{aligned} \tag{29}$$

where: primes denote derivations with respect to the true anomaly ($\theta$) of the primaries; x and y are the Cartesian rectangular dimensionless coordinates of the third body in a nonuniformly rotating system (mean motion = 1); and

$$\omega(\rho_1, \rho_2) = \frac{\Omega(\rho_1, \rho_2)}{(1 + e\cos\theta)} \tag{30}$$

$$\text{where } \Omega(\rho_1, \rho_2) = \frac{1}{2}\left[(1-u)\rho_1^2 + u\rho_2^2\right] + \frac{1-u}{\rho_1} + \frac{u}{\rho_2} \tag{31}$$

$$\text{with } \rho_1^2(x, y) = (x-u)^2 + y^2$$

$$\rho_2^2(x, y) = (x-u+1)^2 + y^2 \tag{32}$$

and where $u = m_2/(m_1 + m_2)$; $m_2 \leq m_1$, $m_1$ and $m_2$ are the masses of the primary bodies.

The (x, y) coordinates are obtained by dividing the dimensional position coordinates of the elliptic problem (x*, y*) by the variable distance between the primaries. Therefore

$$z = \frac{1 + e\cos\theta}{a(1-e^2)}\, z^*, \tag{33}$$

where $z = x + iy$, $z^* = x^* + iy^*$, $i^2 = -1$, a is the semimajor axis of the elliptic orbit of the second primary body with respect to the first, and e is the common eccentricity of the primaries.

The derivation of Eq (29) starts with the dimensional description of the elliptic problem:

$$\frac{d^2x^*}{dt^2} - 2\frac{d\theta}{dt}\frac{dy^*}{dt} = \frac{-Gm_1(x^* - x_1^*)}{P_1^3} - \frac{Gm_2(x^* - x_2^*)}{P_2^3} + y^*\frac{d^2\theta}{dt^2} + x^*\left(\frac{d\theta}{dt}\right)^2 \tag{34}$$

$$\frac{d^2 y^*}{dt^2} + 2\,\frac{d\theta}{dt}\,\frac{dx^*}{dt} = -\,\frac{Gm_1 y^*}{P_1^3} - \frac{Gm_2 y^*}{P_2^3} - x^*\,\frac{d^2\theta}{dt^2} + y^*\left(\frac{d\theta}{dt}\right)^2$$

where $x^*$ and $y^*$ are the dimensional coordinates of the third body in the elliptic problem, G is the universal gravitational constant and $P_1$, $P_2$ are given as:

$$P_1^2 = (x^* - x_1^*)^2 + y^{*2} \qquad (35)$$

$$P_2^2 = (x^* - x_2^*)^2 + y^{*2}$$

The origin of the system $(x^*, y^*)$ is at the mass center of the primaries which move on ellipses. The masses are located on the $x^*$-axis whose rotation is not uniform, and the $x_1^*$, $x_2^*$ abscissas of these masses are not constant. In fact

$$x_1^* = \frac{p_1}{1 + e\cos\theta}$$

$$x_2^* = \frac{-p_2}{1 + e\cos\theta} \qquad (36)$$

with

$$\frac{p_1}{p_2} = \frac{a_1}{a_2} = \frac{m_2}{m_1}$$

where $a_1$ and $a_2$ are the semimajor axes of the elliptic orbits of $m_1$ and $m_2$ described around their center of mass.

The terms on the left side of Eq (34) are the total accelerations and the Coriolis effects. The first and second terms on the right side represent the gravitational forces; the last two terms are the centrifugal force (radial acceleration) and the force occurring because the system is not rotating with a uniform angular velocity (acceleration normal to the radius vector).

Equation (29) can now be obtained from Eq (34) by using the true anomaly as the independent variable instead of the time t and by introducing dimensionless variables. The transformation of the independent variable is given by

$$\frac{d}{dt} = \frac{d\theta}{dt}\,\frac{d}{d\theta} \tag{37}$$

It is noted that the following four orbits all have the same eccentricity: the orbit of $m_1$ relative to $m_2$, the orbit of $m_2$ relative to $m_1$, the orbit of $m_1$ with respect to the center of mass and the orbit of $m_2$ with respect to the center of mass. The semimajor axes are different, in fact, $a_1 = au$ and $a_2 = a(1 - u)$, where a is the semimajor axis of the ellipse described by the relative motion.

The dimensionless variables are the $(x^*, y^*)$ variables divided by the variable distance between the primaries:

$$\begin{aligned} x &= x^* \frac{(1 + e\cos\theta)}{a(1 - e^2)} \\ y &= y^* \frac{(1 + e\cos\theta)}{a(1 - e^2)} \end{aligned} \tag{38}$$

The masses of the primaries are made dimensionless, u and 1 - u, and the location of the primaries becomes fixed since $x_1^*$ and $x_2^*$ are made dimensionless by division by their variable distance.

$$x_1 = \frac{x_1^*(1 + e\cos\theta)}{a(1 - e^2)} = \frac{p_1}{a(1 - e^2)} = \frac{a_1}{a} = u \tag{39}$$

and similarly

$$x_2 = u - 1.$$

With the above remarks Eq (29) can be obtained from Eq (34).

The circular restricted problem in a rotating coordinate system has the property that the energy does not depend explicitly on the time; therefore the problem possesses an integral, namely, Jacobi's integral, Eq (6). A similar expression can be obtained for the elliptic problem by multiplying the first of Eq (29) by $x'$, the second by $y'$, adding the resulting equations, and integrating with respect to the independent variable. This results in

$$x'^2 + y'^2 = 2 \int (\omega_x \, dx + \omega_y dy) \tag{40}$$

The integrand is now not a total differential, since $\omega$ depends on the independent variable ($\theta$) explicitly.

In fact:

$$d\omega = \omega_x \, dx + \omega_y dy + \omega_\theta \, d\theta \tag{41}$$

therefore, the integral can be written as

$$2 \int (d\omega - \omega_\theta \, d\theta) = 2\omega - 2 \int \omega_\theta \, d\theta - C \tag{42}$$

Since $\omega(x, y, \theta) = \frac{\Omega(x, y)}{1 + e \cos\theta}$ the integral can also be expressed as

$$\frac{2\Omega}{1 + e\cos\theta} - 2e \int \frac{\Omega \sin\theta}{(1 + e\cos\theta)^2} \, d\theta - C \tag{43}$$

and the form of the Jacobi integral corresponding to the circular situation becomes

$$x'^2 + y'^2 = 2\omega(x, y, \theta) - C - 2e \int_0^\theta \frac{\Omega \sin\theta}{(1 + e\cos\theta)^2} \, d\theta \tag{44}$$

The left side and the first two terms on the right side in Eq (44) show complete analogy to the Jacobi integral of the circular problem since zero velocity curves

can be constructed for any fixed value of $\theta$. At $\theta = t = 0$ the Hill curves of the elliptic problem are identical to the Hill curves of the circular problem, but in general the expression

$$2\omega - C = 2\Omega/(1 + e\cos\theta) - C \tag{45}$$

shows that, still neglecting the last term in Eq (44), the zero-velocity curves pulsate. That is, a fixed Hill curve will have a variable value of C attached to it. The variation during one revolution of the primaries is between $\frac{\Omega}{1+e}$ and $\frac{\Omega}{1-e}$ and it amounts to $2e\Omega$ (for small e). Equation (45) describes a dynamical quasi-steady effect, since at every instant (i.e., at every value of $\theta$) the relation holds and it is meaningful. The true and essential "unsteady" effects appear with the inclusion of the last term in Eq (44). The interpretation of this term and its evaluation is as follows.

Along an orbit for given $\theta$ values the x and y coordinates of the third body are to be substituted in $\Omega(x, y)$ and the resulting expression

$$2e \int_0^\theta \frac{\Omega(\theta)\sin\theta}{(1 + e\cos\theta)^2}\, d\theta$$

is to be evaluated. An expansion of this expression to the second order in the eccentricity gives

$$2e \int_0^\theta \Omega(\theta)\sin\theta\, d\theta - 2e^2 \int_0^\theta \Omega(\theta)\sin 2\theta\, d\theta$$

This shows that the quasi-steady approach, by neglecting the integral in Eq (44), errs in first order. For orbits of brief duration, that is, when interest in an orbit is only from some initial point to a point which is reached in a time during which $\theta$ changes little, the unsteady effect represented by the integral might be a small contribution.

In Ref. 4 the stability of the equilateral triangular configurations in the elliptic restricted problem is investigated for general u and e, and the region in the u - e plane in which there is stability is found. Here stability is investigated using only the first-order, linear equations for displacements from the points of equilibrium. A point is considered to be stable only if an arbitrary but infinitesimal displacement from the point is followed by motion that forever remains infinitesimally close to the point.

From general arguments it is reasonable to expect that for very small eccentricity the stability of the triangular points would be preserved. For the differential equations of motion very close to the libration points will then consist, first, of a part applying to circular motion, and second, of a part that takes the eccentricity into account. Since the eccentricity is small, these two parts will not be coupled; the latter will have the eccentricity as a factor, and the variable terms in it will be evaluated along the circular orbit and will therefore be known functions of the time. Therefore, the second part can be considered as a "forcing function" added to the equations of displaced motion around the libration points in the circular case. The solution will consist of a complementary function, which will be the known solution for oscillations around the circular libration points, and a particular integral that can be any solution that takes the forcing function into account. But such a solution is known, namely, the libration point corresponding to the elliptic orbit. Since the complete solution remains bounded, the motion should be stable.

In this referenced paper, Danby derives the first variational equations of the general equations of motion and analytical solutions for the cases of small e and

of small u. In Fig. 2 the shaded area is the region of the u - e plane in which the triangular points are stable.

The boundary of the region of stability tends to e = 1 as u tends to zero, although the point e = 1, u = 0 cannot be included. At point 1, one of the two periods of oscillation is equal to twice the period of the massive bodies and e = 0, u = 0.0285. At point 2, the coordinates are roughly u = 0.04698, e = 0.3143.

For the earth-moon system, u = 0.01213 and e = 0.0549 and from Fig. 2 it is seen that stability for motion about the triangular points does exist.

## E. NUMERICAL STUDY OF PERTURBATIONS ON THE RESTRICTED THREE-BODY PROBLEM

### 1. Solar Influence on the Circular Three-Body Model

The motion of a vehicle in the vicinity of the triangular earth-moon libration points has been studied in Ref. 5 using a model which includes the perturbing effects of the gravitational attraction and the radiation pressure of the sun. The model used to describe the motion was such that the earth and the moon moved in circular orbits about their mass center and the mass center, in turn, moved in a circular orbit about the sun. The earth-moon orbit plane was inclined at an angle of 5°9' to the ecliptic plane and each of the bodies was treated as a mass point.

The equations of motion were written in a coordinate system centered at the earth-moon barycenter and rotating with the same angular velocity as the earth-moon line. These equations were then transformed to a libration-point-centered coordinate system ($X_{RL}$, $Y_{RL}$, $Z_{RL}$) and were numerically integrated to determine

the behavior of the vehicle. The initial conditions now contained the angular positions of the sun and the earth-moon line with respect to some reference direction, in this case, vernal equinox.

In this study the initial position of the sun was on the extended earth-moon line with the moon between the earth and sun and the vehicle was placed at one of the triangular libration points with zero relative velocity. For a vehicle originally at $L_4$, the triangular libration point leading the earth-moon line, the envelope of motion after 8 mo exceeded 48,000 km in the $X_{RL}$ direction and 32,000 km in the $Y_{RL}$ direction. The envelope of motion continued to grow and, even after 700 days, a limiting value for the envelope was not being approached. It was noted that the envelope of motion was warped around a circle centered at the earth-moon barycenter. The displacement in the $Z_{RL}$ direction was found to be periodic with the amplitude of motion increasing with time. The period of motion in the $Z_{RL}$-direction was about 27.6 days and the amplitude at 250 days was about 7500 km. Several area-to-mass ratios for the vehicle were assumed in order to take account of the solar radiation pressure. In general, it was found that the solar radiation pressure caused the vehicle to move farther away from $L_4$ in a given time. The larger area-to-mass ratios were associated with larger envelopes of motion.

When the effects of the sun are included, the triangular points are no longer equilibrium points, and thus new equilibrium points were located for various orientations of the earth, moon and sun. These equilibrium points are points where a vehicle at rest with respect to the triangular points will have zero acceleration in the ($X_{RL}$, $Y_{RL}$, $Z_{RL}$) coordinate system. It was found that these

equilibrium points lie along a circle whose center is at the earth-moon mass center. The equilibrium point is at times more than 200,000 km from a triangular point. The solar-radiation pressure changes the locations of the equilibrium points, but they still lie very near to the same circle. If the solar radiation pressure is neglected, the points move along the circle with a period of about 14.7 days.

Several sets of initial conditions were tried in an effort to find a set which would result in a small envelope of motion. For initial positions chosen to coincide with the equilibrium points it was found that the resulting motion was less stable than the motion when the initial position was at the triangular point. For the cases of an initial displacement of zero, the smallest envelope of motion was obtained for an initial velocity of 3.05 m/sec normal to the barycenter - $L_4$ line in the opposite direction of rotation of the coordinate system.

In order to force the vehicle to stay precisely at the triangular point $L_4$, the perturbing force due to the sun must be nulled by application of a continuous thrust. The area under the thrust-time curve represents the magnitude of the specific impulse per unit mass of the vehicle required to force the vehicle to remain at $L_4$. The value of the impulse required is 720 newton-sec/kgm-year. The impulse requirements necessary to force a vehicle to remain at any point around $L_4$ is greater than this amount.

2. Actual Motion of a Vehicle Near a Triangular Point in the Earth-Moon System

In order to obtain the most physically representative model of the earth-moon system, a study has been carried out at the Martin Company utilizing an integrated trajectory program (Ref. 6) which includes ephermeris data for the moon,

sun and planets and also the effects of solar radiation pressure. For the present study, an area-to-mass ratio of 6.37 $\frac{cm^2}{gm}$ was assumed. The purpose of this study was to determine the motion of a vehicle for a period of a year having initially been placed with zero relative velocity at the earth-moon triangular point, $L_4$. In addition, it was desired to calculate the energy for station keeping requirements over the same span of time.

As a comparison for Ref. 5 the initial time was chosen such that the moon is between the earth and the sun along the earth-sun line and the moon is at apogee. The time selected was 51d, 6h, 50m, 1966.

Since the moon moves in an approximately elliptical orbit about the earth, the earth-moon distance varies with time and the triangular points are not fixed. However, if at any instant of time the earth-moon distance is known, then the position of the triangular points is readily determined. If the earth-moon distance is denoted by $R_{\oplus\mathbb{C}}$, the position of the triangular point $L_4$ in a coordinate system rotating with the earth-moon line ($X_R$-axis) is given by

$$X_{RL} = R_{\oplus\mathbb{C}} \cos 60°$$

$$Y_{RL} = R_{\oplus\mathbb{C}} \sin 60°$$

$$Z_{RL} = 0$$

The ($X_R$ - $Y_R$) coordinate plane lies in the instantaneous moon orbital plane and the $Z_R$-axis is perpendicular to this plane. The $X_R$-axis lies along the earth-moon line and rotates with the same instantaneous angular velocity. If the position of the vehicle in this coordinate system ($X_{RV}$, $Y_{RV}$, $Z_{RV}$) is known as a function of time, then the position of the vehicle relative to the instantaneous triangular point is given by

$$X_{RVL} = X_{RV} - X_{RL}$$
$$Y_{RVL} = Y_{RV} - Y_{RL}$$
$$Z_{RVL} = Z_{RV}$$

At the previously mentioned initial time, a vehicle was placed at the instantaneous triangular point, $L_4$, with zero relative velocity and the motion of the vehicle for a period of one year was computed. The $X_{RVL}$, $Y_{RVL}$ components of the vehicle's position are presented for three separated periods during that year in Fig. 3. The number of days elapsed since the initial time is indicated along the curves. There is seen to be wide excursions of motion of the vehicle, even during the first month when the motion exceeds 50,000 km in the $X_R$ direction and 30,000 km in the $Y_R$ direction. For the other two months shown, the motion is of the same order of magnitude. The periods of linear and constricted motions seen in Fig. 3 correspond to the times during the year when the moon is at its apogee.

Figure 4 presents the $Z_{RVL}$ coordinate of the vehicle as a function of time for a period of one year. The amplitude of motion increases and decreases with time, with the largest amplitude approximately 800 km. The period of the motion in the $Z_R$ direction is about 28 days.

Although definite regional instability is not proved by the previous figures, it is reasonable to expect that unless the trend indicated in these results is reversed, the vehicle will ultimately escape from the vicinity of the osculating triangular points.

The wide excursions of the vehicle from the triangular point indicate the need for active station keeping when nearness to the point itself is to be considered as a mission constraint. This station keeping can be accomplished in

either of two ways: application of a continuous thrust or application of an impulse at specified intervals of time. The total accelerations of the vehicle

$$A_T = \left[(\ddot{X}_{RVL})^2 + (\ddot{Y}_{RVL})^2 + (\ddot{Z}_{RVL})^2\right]^{1/2}$$

relative to the osculating triangular point is presented in Fig. 5 as a function of time for a period of 1 yr. The area beneath this curve yields a velocity impulse requirement of 1323 m/sec-yr for active station keeping requirements. This is a higher value than that quoted in Ref. 5 and reflects the additional effects of the eccentricity of the moon's orbit. As an example of intermittent pulsing, if the motion of the vehicle is confined to a tolerance radius of 200 km from the triangular point, then at least one correction impulse per day is required.

## F. REFERENCES


1. "Lunar Flight Handbook," Martin Company, Space Systems Division, Baltimore, Maryland, ER 12685, 1963 or NASA SP34.
2. Michael, W. H., Jr., "Considerations of the Motion of a Small Body in the Vicinity of the Stable Libration Points of the Earth-Moon System," NASA TR R-160, 1963.
3. Szebehely, V., and Giacaglia, G., "On the Elliptic Restricted Problem of Three Bodies," Astron. J. 69, 230, April 1964.
4. Danby, J. M. A., "Stability of the Triangular Points in the Elliptic Restricted Problem of Three Bodies," Astron. J. 69, 165, March 1964.
5. Tapley, B. D., and Lewallen, J. M., "Solar Influence on Satellite Motion Near the Stable Earth-Moon Libration Points," AIAA Journal Vol. 2, p 728, 1964.
6. Shaffer, F., "Interplanetary Trajectory Encke Method (ITEM) Program Manual," NASA X-640-63-71, 1 May 1963.

ILLUSTRATIONS

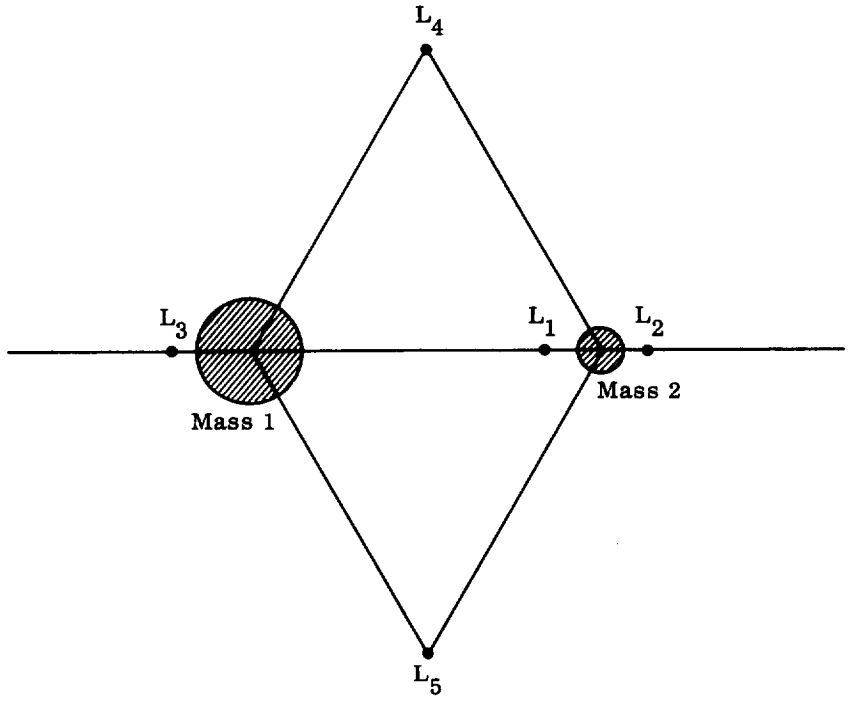


Fig. 1. Libration Points in the Restricted Three-Body Problem

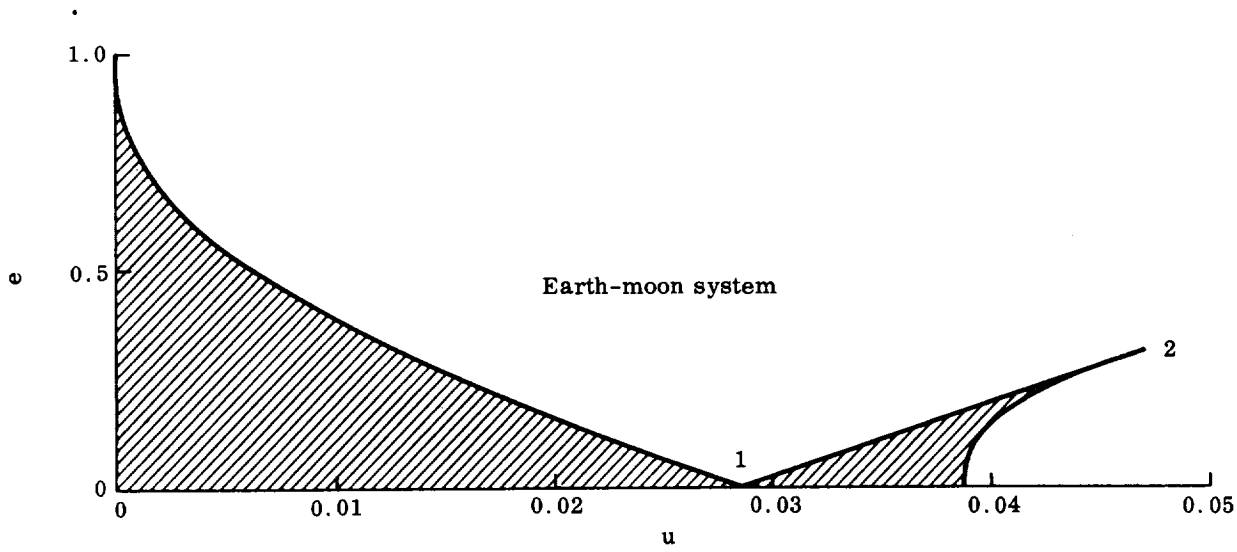


Fig. 2. System Boundary for Stable Libration Points

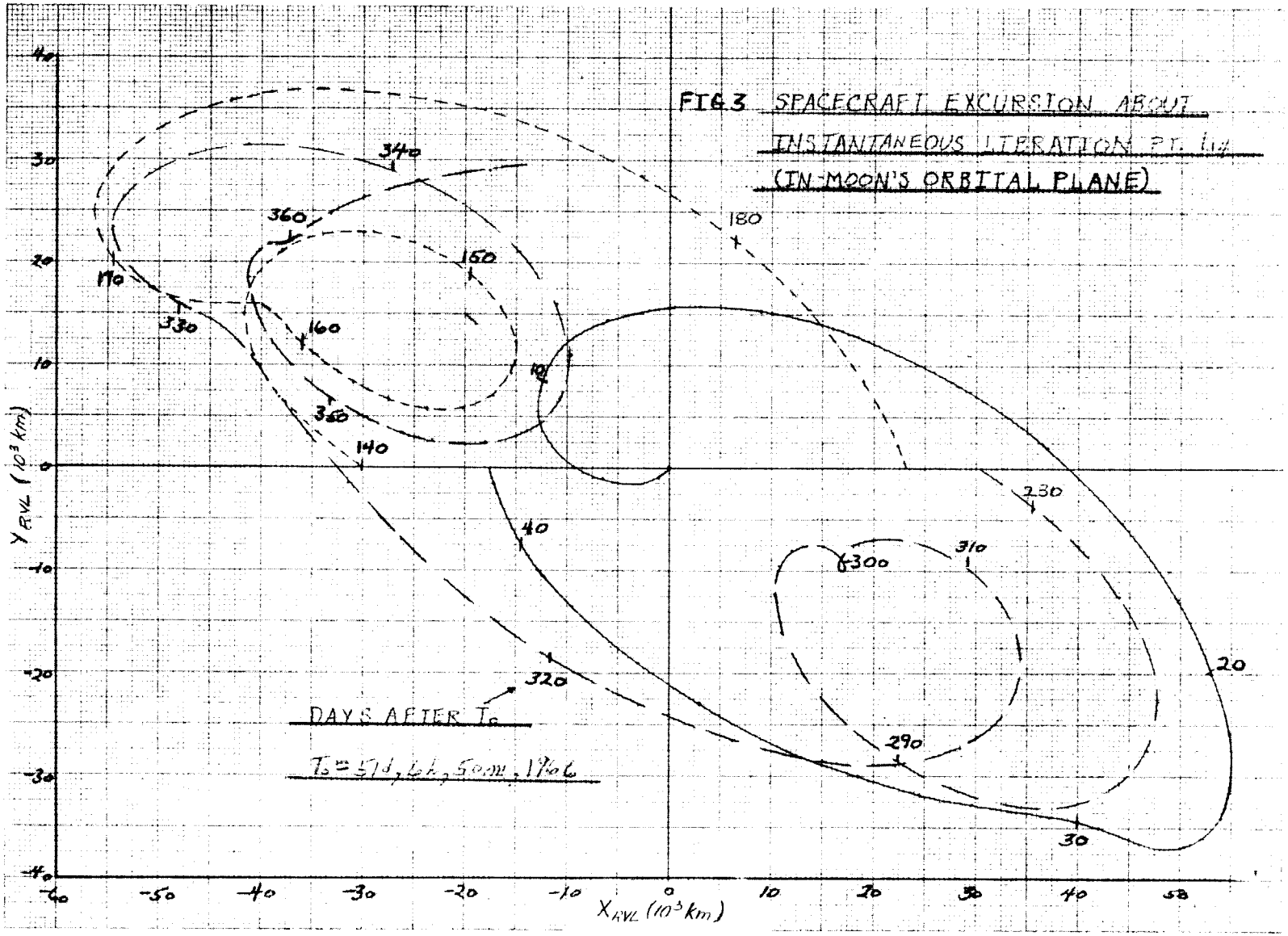
FIG 3 SPACECRAFT EXCURSION ABOUT
INSTANTANEOUS ITERATION PT. L4
(IN MOON'S ORBITAL PLANE)
180
340
360
160
170
330
160
10
360
140
40
230
310
300
320
20
290
30
DAYS AFTER $T_0$
$T_0$ = 5 d, 6 h, 50 m, 17 s
$Y_{RVL}$ ($10^3$ km)
$X_{RVL}$ ($10^3$ km)
40
30
20
10
0
-10
-20
-30
-40
-60
-50
-40
-30
-20
-10
0
10
20
30
40
50

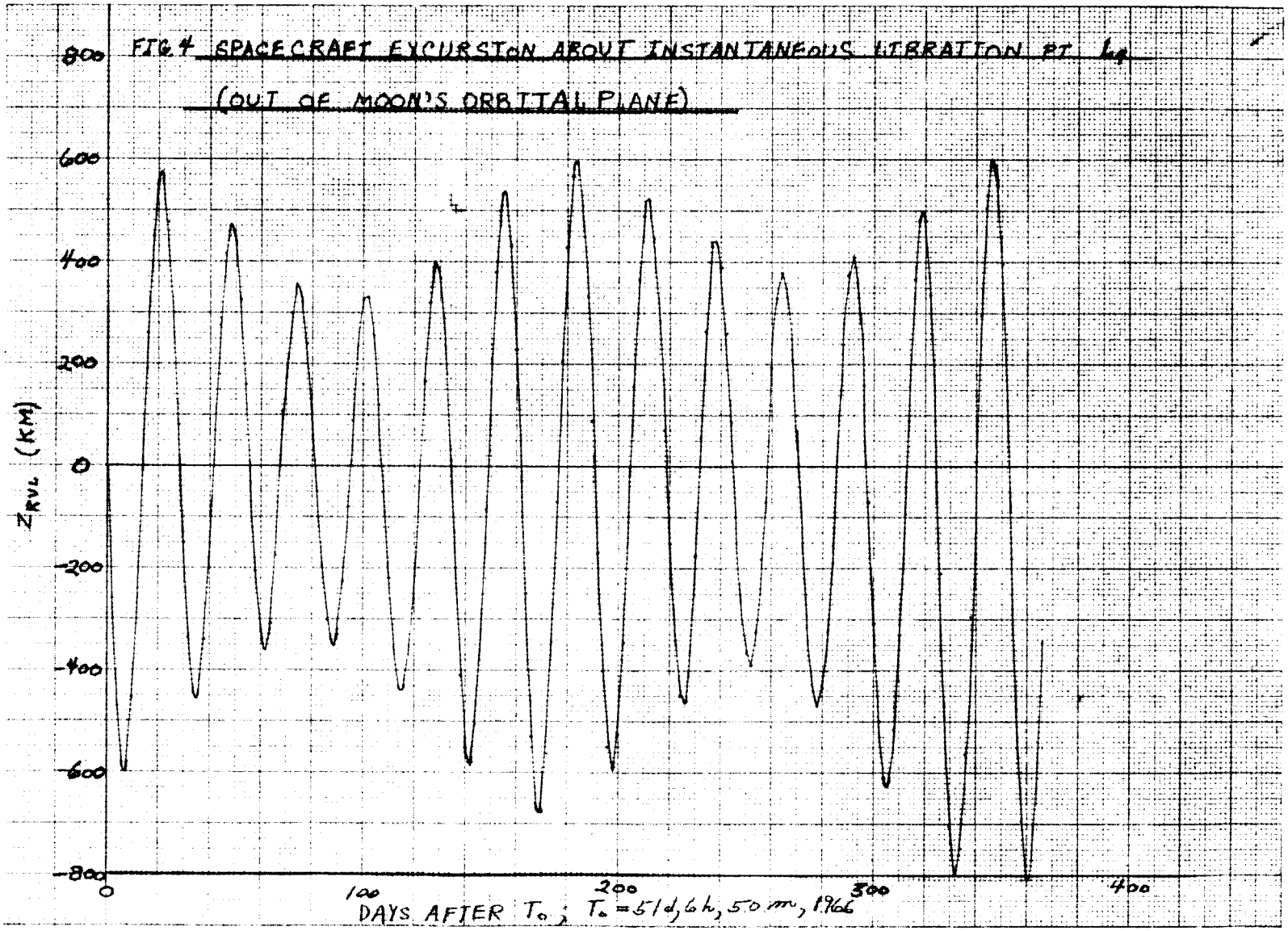
FIG 4 SPACECRAFT EXCURSION ABOUT INSTANTANEOUS LIBRATION PT L4
(OUT OF MOON'S ORBITAL PLANE)
800
600
400
200
0
-200
-400
-600
-800
$Z_{RVL}$ (KM)
0
100
200
300
400
DAYS AFTER $T_0$; $T_0$ = 51d, 6h, 50m, 1966

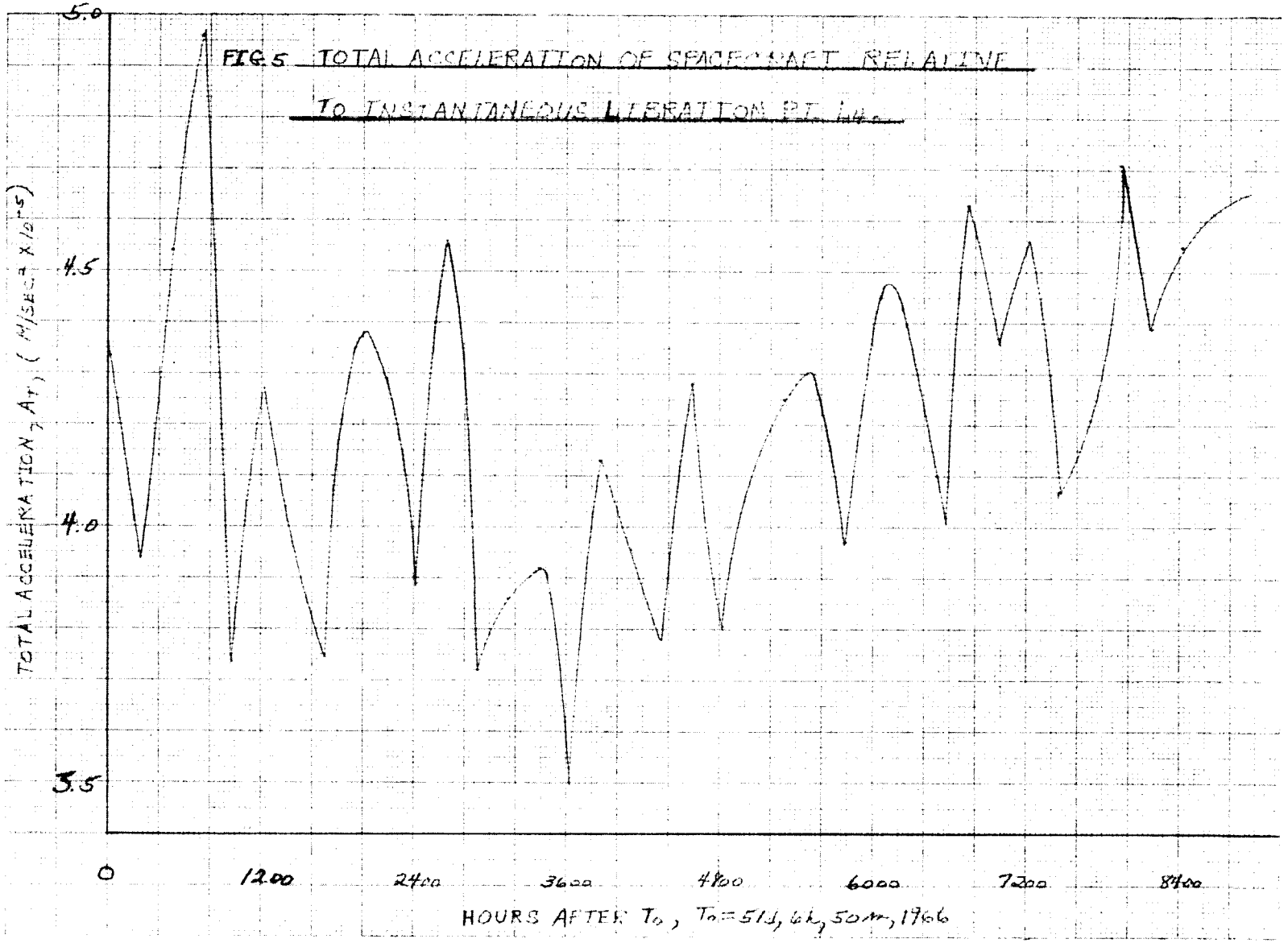
FIG. 5 TOTAL ACCELERATION OF SPACECRAFT RELATIVE
TO INSTANTANEOUS LIBERATION PT. L4
TOTAL ACCELERATION, $A_T$, ( $M/SEC^2 \times 10^{-5}$ )
5.0
4.5
4.0
3.5
0
1200
2400
3600
4800
6000
7200
8400
HOURS AFTER $T_0$, $T_0$ = 5h, 6h, 50m, 1966

# III. LUNAR ORBIT ESTIMATION

by George Kovatch

## SUMMARY

Chapter III of the Orbital and Lunar Flight Handbooks Extension (Ref. 1) presents a general mathematical treatise concerning the problem of orbit filtering, prediction and smoothing. The theory is presented in such a manner that it is applicable to problems of earth orbit, lunar orbit, or interplanetary trajectory estimation. Aspects of the theory provide error estimates of the vehicle's position and velocity, that is, the confidence with which the estimate can be made.

A very natural and useful extension to Chapter III of Ref. 1 is to formulate the actual equations necessary to solve a specific problem relevant to lunar flight. The problem discussed herein consists of determining the orbit of a vehicle in the vicinity of the moon by tracking the vehicle from the earth. In addition to estimating the orbit, this formulation includes the capability to determine the confidence of the estimate, that is, to determine confidence volumes in state space within which the vehicle's position and velocity should lie with a certain probability. The formulation assumes that the moon is the center of gravitational attraction. The relative position and orientation of the moon and earth are taken into account. The formulation utilizes a minimum variance filtering scheme. By merely changing the physical constants in the formulation, it is applicable to tracking a vehicle near Mars or near any other planet from the earth. A brief discourse on methods of accommodating onboard or other observational data in the formulation is also given.

## A. INTRODUCTION

In Ref. (1) a general mathematical development of methods for obtaining estimates of the state of orbiting vehicles is given. These include the problems of filtering, predicting and smoothing of measurement data where the system is disturbed by noisy and/or inaccurate data. The so-called Kalman-Schmidt minimum variance procedure is considered to be the best approach to handle this type of problem. Several reasons support this contention. The formulation seems most compatible with modern digital computers. The measurement data is used sequentially as it is obtained. One does not have to store up a certain amount of data before making an estimate. (Note the exception indicated in Section D of this Chapter on how to best start the recursive calculations.) A new estimate and an improved estimate can be made after each new piece of

data is obtained. Lower order matrix inversion is also an advantage in this approach. Finally, the procedure, by virtue of its matrix formulation, offers greater flexibility as it can accept observational data from many different sources. For example, data from different stations at different times as well as onboard or ground based data can be used.

The theory underlying the procedure is general enough to encompass problems with earth orbiting vehicles, lunar orbiting vehicles, or vehicles in orbit around any other planet with only minor modifications. It is also very useful for interplanetary missions.

In this discussion and development, emphasis is placed on estimating the trajectory of a vehicle orbiting the moon. It is assumed that all measurements are made at a tracking station on the earth. It is assumed further that the center of gravitational attraction is the moon, so that the two-body equations of motion may be used. This allows, as will be shown, an analytical development of the transition matrices not normally utilized. In the computations, the relative position of the earth and moon will be determined accurately; as will the location on the surface of the earth of the tracking station. An estimate of the errors made in making the orbit estimation will be obtained from the evaluation of the covariance matrix of errors.

The state vector of the vehicle consists of six elements; three position components and three velocity components. The time variation of this state vector is determined by the nonlinear equations of motion for the two-body system. These can be solved analytically, hence, the behavior of the perturbations can be specified analytically using transition matrix concepts Ref. (2). The state perturbation at any time $t_k$ is related to the state perturbation at time $t_j$ by the following

$$x(t_k) = \Phi(t_k, t_j)\, x(t_j) \tag{1}$$

The observer of the vehicle motion, who will be either on the earth, or in the vehicle itself, will not measure the state variables directly. He will, however, measure some function of the state variables--in general a nonlinear function. Linearizing these nonlinear functions will produce a measurement equation [with an additive noise vector $\delta(t_k)$]of the following form

$$\Delta y(t_k) = G(t_k)\, x(t_k) + \delta(t_k) \tag{2}$$

The true state perturbation vector can be represented as the sum of the best estimate made on the basis of measurements up to some time $t_j$ denoted by $\hat{x}(t_k \mid t_j)$ and the error in that estimate denoted by $\tilde{x}(t_k \mid t_j)$, hence

$$x(t_k) = \hat{x}(t_k \mid t_j) + \tilde{x}(t_k \mid t_j) \tag{3}$$

The idea behind the recursive procedure embodied in the minimum variance approach is conceptually simple. To illustrate this assume that the best estimate of the state perturbation is known at some time $t_n$ based on data up to and including the time $t_n$. If there were no other errors in the measurements, one would obtain the best estimate at time $t_{n+1}$ by simply multiplying the best estimate at $t_n$ by the appropriate transition matrix. However, with errors, this estimate is modified by adding some proportion of the difference in the actual measurement and the best estimate of the measurement. This is shown by Eq (61) of Ref. (1) as

$$\hat{x}(t_{n+1} \mid t_{n+1}) = \Phi \hat{x}(t_n \mid t_n) + K\left[\Delta y(t_{n+1}) - G\Phi \hat{x}(t_n \mid t_n)\right] \tag{4}$$

where the optimal weighing matrix K is given by Eq (57) of Ref. (1) as

$$K = \Phi P(t_n)\ \Phi^T G^T \left[G\Phi P(t_n)\ \Phi^T G^T + V\right]^{-1} \tag{5}$$

The covariance matrix of errors in estimation is given by Eq (60) of Ref. (1) by

$$P(t_{n+1}) = \Phi P(t_n)\ \Phi^T - KG\Phi P^T(t_n)\ \Phi^T \tag{6}$$

where

$$\Phi = \Phi(t_{n+1}, t_n)$$

$$G = G(t_{n+1})$$

When applying the minimum variance filter to the lunar vehicle estimation problem, it is possible to formulate the procedure in two ways. First a single reference trajectory can be used, and deviations from this reference are related between measurements via the state transition matrix and updated with measurements via Eq (4). The theory requires that the reference be within the neighborhood of the best estimate if the linearity assumption is not to be violated. The second method consists

of changing the reference each time a measurement is processed so as to cause it to agree with the best estimate at that time. Between estimates the deviations from this updated reference are related by the state transition matrix corresponding to this reference. Thus, although the initial estimate of the state that determines the reference may be considerably different from the final best estimate, as the processing continues the reference is corrected causing the linearity assumptions to be more closely obeyed. For this second formulation Eq (4) simplifies to

$$\hat{x}\,(t_{n+1}\,|\,t_{n+1}) + K\,\left[\Delta y\,(t_{n+1})\right] \qquad (4)$$

Both of the above methods for applying the filter can be used iteratively. That is, the data is repeatedly processed from initial to final time. Between each iteration the state at the final time is smoothed back to give an improved estimate at the initial time and then initiates the next iteration. Which of the two methods of application is best depends on the problem being solved, but one might suspect that for small measurement signal-to-noise ratios the first method might have advantages whereas with large signal-to-noise ratios the second method should have advantages.

To carry out the application to the estimation of the state of the lunar vehicle, it is only necessary to compute the observation matrix G, and the transition matrix $\Phi$. These computations are described next.

## LIST OF SYMBOLS

| | |
|---|---|
| A | Azimuth measured from tracking station to vehicle |
| a, b, c | Three of the orbital elements |
| E | Elevation measured from tracking station to vehicle |
| $G(t_k)$ | Observation matrix evaluated at time $t_k$ |
| K | Optimal weighting matrix |
| L | Constant, refers to number of standard deviations of random variable |

| | |
|---|---|
| $m$ | Mean of a random variable |
| $p$ | Probability density function |
| $P(t_{n+1})$ | Covariance matrix of error in estimation of state perturbation vector |
| $R$ | Range measured from tracking station to vehicle |
| $\dot{R}$ | Range rate measured from tracking station to vehicle |
| $t_k$ | Time at the kth instant |
| $V$ | Initial covariance matrix of disturbances |
| $x(t_k)$ | Perturbation in state vector at the time $t_k$ |
| $\hat{x}(t_k \mid t_j)$ | Best estimate of state perturbation vector at time $t_k$ based on data to time $t_j$ |
| $\tilde{x}(t_k \mid t_j)$ | Error in estimating state perturbation vector |
| $\Delta y(t_k)$ | Observation vector |
| $\delta(t_k)$ | Disturbance vector at time $t_k$ |
| $\sigma$ | Standard deviation of random variable |
| $\sigma^2$ | Variance of random variable |
| $\Phi(t_k, t_j)$ | Transition matrix between times $t_j$ and $t_k$ |

## B. OBSERVATION MATRIX

First a derivation of the observation matrix G shall be given. Figure 3 (Section J) shows a typical sketch of a tracking station coordinate system located on the surface of the earth. It is assumed that measurements of the range, range rate, elevation angle, and azimuth

angle of the vehicle with respect to the tracking station might be made as the vehicle orbits the moon. The nonlinear relations which describe these observation variables in terms of coordinates measured in the tracking system are given by

$$R = (X_T^2 + Y_T^2 + Z_T^2)^{1/2} \qquad \text{(range)} \qquad (7)$$

$$\dot{R} = \frac{X_T}{R}\dot{X}_T + \frac{Y_T}{R}\dot{Y}_T + \frac{Z_T}{R}\dot{Z}_T \qquad \text{(range rate)} \qquad (8)$$

$$E = \tan^{-1}(X_T/(Y_T^2 + Z_T^2)^{1/2}) \qquad \text{(elevation)} \qquad (9)$$

$$A = \tan^{-1}(Y_T/Z_T) \qquad \text{(azimuth)} \qquad (10)$$

Let the true values of these variables be represented as the sum of a nominal value and a perturbation value as follows

$$R = R_{nom} + r$$

$$\dot{R} = \dot{R}_{nom} + \dot{r}$$

$$E = E_{nom} + e$$

$$A = A_{nom} + a$$

$$X_T = X_{T_{nom}} + x_T$$

$$Y_T = Y_{T_{nom}} + y_T$$

$$Z_T = Z_{T_{nom}} + z_T$$

$$\dot{X}_T = \dot{X}_{T_{nom}} + \dot{x}_T$$

$$\dot{Y}_T = \dot{Y}_{T_{nom}} + \dot{y}_T$$

$$\dot{Z}_T = \dot{Z}_{T_{nom}} + \dot{z}_T$$

Introducing these into the nonlinear observation equations, Eq (7) through (10), and retaining up to linear terms of a Taylor series expansion gives the desired perturbational observation equation

$$\begin{bmatrix} r \\ \dot{r} \\ e \\ a \end{bmatrix} = \begin{bmatrix} (X_T/R) & (Y_T/R) \\ (\dot{X}_T - X_T \dot{R}/R)/R & (\dot{Y}_T - Y_T \dot{R}/R)/R \\ ((Y_T^2 + Z_T^2)^{1/2}/R^2) & (-X_T Y_T/R^2 (Y_T^2 + Z_T^2)^{1/2}) \\ 0 & (Z_T/(Y_T^2 + Z_T^2)) \end{bmatrix}$$

$$\begin{bmatrix} (Z_T/R) & 0 & 0 & 0 \\ (\dot{Z}_T - Z_T \dot{R}/R)/R & (X_T/R) & (Y_T/R) & (Z_T/R) \\ (-X_T Z_T/R^2 (Y_T^2 + Z_T^2)^{1/2}) & 0 & 0 & 0 \\ (-Y_T/(Y_T^2 + Z_T^2)) & 0 & 0 & 0 \end{bmatrix} \begin{bmatrix} x_T \\ y_T \\ z_T \\ \dot{x}_T \\ \dot{y}_T \\ \dot{z}_T \end{bmatrix} \quad (11)$$

Let H $(t_k)$ be the above matrix which multiplies the perturbational state vector to give

$$\left[r, \dot{r}, e, a\right]^T = H(t_k) \left[x_T, y_T, z_T, \dot{x}_T, \dot{y}_T, \dot{z}_T\right]^T$$

Hence, the perturbation observation equation (following the form of Eq (2), where $\delta(t_k)$ is added to represent noise components), is given by

$$\Delta y(t_k) = \left[r(t_k), \dot{r}(t_k), e(t_k), a(t_k)\right]^T + \delta(t_k) = H(t_k) \left[x_T, y_T, z_T, \dot{x}_T, \dot{y}_T, \dot{z}_T\right]^T + \delta(t_k) \quad (12)$$

However, this does not define the G matrix introduced in Eq (2) since the state vector being estimated is the state vector as viewed in the lunar inertial coordinate system. A transformation which carries the state vector as measured in the tracking station coordinate system into the lunar system must be introduced. This derivation is given in Section I-1. The relation between coordinates is given by Eq (45) as

$$\begin{bmatrix} x_T \\ y_T \\ z_T \\ \dot{x}_T \\ \dot{y}_T \\ \dot{z}_T \end{bmatrix} = J(t_k) \begin{bmatrix} x_{mI} \\ y_{mI} \\ z_{mI} \\ \dot{x}_{mI} \\ \dot{y}_{mI} \\ \dot{z}_{mI} \end{bmatrix} \tag{13}$$

With the transformation matrix $J(t_k)$ the observation matrix G is given by

$$G(t_k) = H(t_k)\, J(t_k) \tag{14}$$

This is the relation which is used in the recursive formulation embodied in Eqs (4) through (6).

## C. STATE TRANSITION MATRIX

One of the more complex problems, computationally at least, in the determination and estimation of orbits is that of obtaining the state transition matrix. In Eqs (11) through (15) of Ref. (1), (also see Ref. (2)), some relations which the transition matrix must satisfy are given. It is shown that the transition matrix may be computed by perturbing the initial state vector in all its components and computing the resulting behavior in order to determine the sensitivities. This approach is commonly employed in practice. However, it is also possible to obtain analytical expressions for the components of the transition matrix if analytical solutions of the equations of motion are known. For the two body formulation, these analytical solutions are indeed possible. In Refs. (3), (4), and (5) certain results are published on analytical forms for the components of the transition matrix. These results are written for an assumed set of orbital elements, so that a different set of expressions for the components of the transition matrix is obtained for elliptical orbits, nearly circular orbits, or parabolic orbits. This is done in order to avoid the difficulty caused by small eccentricities in the chosen set of orbital elements.

It was desired here to obtain a formulation which was general enough to apply to all types of orbits. By making use of the fact that a Keplerian orbit lies in a plane defined by

$$ax + by + c = r \tag{15}$$

and by using the constants a, b, and c as three of the orbital elements one can obtain such a universal formulation. The details of this formulation are given in Section I-2, and the expressions for the components of the transition matrix, $\Phi(t_i, t_0)$ are given in Table 4.

It is important to note at this stage that the transition matrix which is needed in the recursive form of the estimation procedure is $\Phi(t_{i+1}, t_i)$, that is, one needs the transition matrix between successive instants of time. This can be obtained analytically using additional properties of this particular transition matrix.

For example, the following relation holds for all transition matrices

$$\Phi(t_{i+1}, t_i) = \Phi(t_{i+1}, t_0)\, \Phi(t_0, t_i) = \Phi(t_{i+1}, t_0)\, \Phi^{-1}(t_i, t_0) \tag{16}$$

Now the inverse of the transition matrix can also be analytically expressed by a simple rearrangement of elements. Consider the partitioning of the matrix as follows

$$\Phi(t_i, t_0) = \left[\begin{array}{c|c} \Lambda_1(t_i, t_0) & \Lambda_2(t_i, t_0) \\ \hline \Lambda_3(t_i, t_0) & \Lambda_4(t_i, t_0) \end{array}\right] \tag{17}$$

It has been shown, see Refs. (3) and (4), for example, that the inverse matrix is given by

$$\Phi^{-1}(t_i, t_0) = \left[\begin{array}{c|c} \Lambda_4^T(t_i, t_0) & -\Lambda_2^T(t_i, t_0) \\ \hline -\Lambda_3^T(t_i, t_0) & \Lambda_1^T(t_i, t_0) \end{array}\right] \tag{18}$$

Hence, the desired form of the transition matrix, namely, between the successive instants of time $t_{i+1}$ and $t_i$, can be obtained analytically by multiplying the appropriate matrices, i.e., via Eqs (16), (17) and (18).

## D. STARTING THE ESTIMATION PROCEDURE

It is appropriate here to mention something about the best way to start the estimation process. It is theoretically possible to converge on the overall best estimate of the state regardless of how one obtains the initial value for the covariance matrix P. However, assuming that it is initially very large, i.e., assuming that one makes large errors initially, will result in a long convergence time. Hence, it seems desirable in the interest of computer time to start with a least squares

estimate. As a rule of thumb one should be sure to have more scalar equations than unknowns. This would determine the number of observations needed before starting the estimation.

For example, with six state variables and four observations one could start after two observation times. From Eqs (25) and (29b) of Ref. (1), the weighted least squares estimate and covariance error are

$$\hat{x}(t_2 | t_2) = \left[ M^T(t_2)\, V^{-1}\, M(t_2) \right]^{-1} M^T(t_2)\, V^{-1} \begin{bmatrix} \Delta y(t_1) \\ \Delta y(t_2) \end{bmatrix} \tag{19}$$

where

$$M(t_2) = \begin{bmatrix} G(t_1)\, \Phi(t_1, t_2) \\ \hline G(t_2) \end{bmatrix} \tag{20}$$

and

$$P(t_2) = \left[ M(t_2)\, V^{-1}\, M(t_2) \right]^{-1} \tag{21}$$

and

$$V = \left[\begin{array}{ccccc} \sigma_1^2(t_1) & & & & \\ & \sigma_2^2(t_1) & & & \\ & & \sigma_3^2(t_1) & & \\ & & & \sigma_4^2(t_1) & \\ \hline & & & & \sigma_1^2(t_2) \\ & & & & & \sigma_2^2(t_2) \\ & & & & & & \sigma_3^2(t_2) \\ & & & & & & & \sigma_4^2(t_2) \end{array}\right] \tag{22}$$

This estimate for the state Eq (19) would be used as the initial best estimate, and the optimal gain would be computed using the appropriate transition matrix and this P-matrix Eq (21). The recursive process would take over using Eqs (4), (5) and (6).

## E. CONFIDENCE HYPERELLIPSES AND THE COVARIANCE MATRIX P

The recursive formulation of the estimation process provides a means of determining an estimate of the "second order" statistics, namely, the variance-covariance matrix, commonly referred to as the covariance matrix, P (Ref. 6). This matrix is the expectation of the matrix formed by multiplying the error in estimating the state perturbation vector by its transpose. The diagonal terms of this matrix are the variances of the errors in each of the components of the perturbation vector. The off-diagonal terms represent the correlation between the various components. Since, this matrix is computed at each step in the computation process, one has a running check on the size of the errors. Of course, since this is a statistical process one never knows exactly what the error bounds are except with some probability assigned to the error bounds. For example, one might ask "what are the possible limits on a certain variable with a probability of 0.7?" To such a question a reasonable answer can be given. When asking a similar question about multivariable functions, the limits become, instead of some interval around a single variable, a volume in state space which contains all the variables with the assigned probability. The size of the region, of course, expands as one asks for a higher probability. In fact, as the probability approaches 1, the size of the region approaches the entire state space.

The covariance matrix provides a desirable means of obtaining information about the probable size of errors made in making the estimate.

For example, assume that one has only one variable to deal with at the moment. Further assume that this variable is normally distributed around a mean value, m, and with a standard deviation, $\sigma$. Now one can ask the question, what is the probability that the true value of the variable lies within the interval $m + k\sigma$ and $m - k\sigma$. This is expressed mathematically as

$$\Pr\left[m - k\sigma \leq X \leq m + k\sigma\right] = \frac{1}{\sqrt{2\pi\sigma^2}} \int_{m-k\sigma}^{m+k\sigma} \exp\left[-\frac{1}{2}\left(\frac{x - m}{\sigma}\right)^2\right] dx \tag{23}$$

There are numerous tables available to give this numerical information. For illustrative purposes a few of these values are given in Table 1.

TABLE 1

Sigma Probabilities

| k | Pr |
|---|---|
| 1 | 0.6827 |
| 2 | 0.9545 |
| 3 | 0.9973 |

This table says that the true value of the variable lies within $1\sigma$ of the mean value with a probability of 68.27%, that it lies within $2\sigma$ of the mean value with a probability of 95.45%, and that it lies within $3\sigma$ of the mean value with a probability of 99.73%. Note that for higher probabilities one obtains a larger interval containing the mean value.

Now consider the case of estimating the state vector with n components. The probability density function for the normally distributed state vector is given by

$$p(x) = \frac{1}{(2\pi)^{\frac{n}{2}} |P|^{\frac{1}{2}}} \exp\left[-\frac{1}{2}(x - \hat{x})^T P^{-1} (x - \hat{x})\right] \tag{24}$$

where P is the covariance matrix, and $|P|$ is the determinant of the covariance matrix.

One can diagonalize the covariance matrix by a similarity transformation of the form

$$y = S(x - \hat{x}) \tag{25}$$

This is equivalent to saying that the hypersurfaces of constant probability density in the x-space are hyperellipses and that by the similarity transformation into the y-space one is swinging the coordinate system around to line up with the principal axes of the ellipsoid. It is therefore desired to compute the probability that the state vector x is contained within an ellipsoid defined by

$$(x - \hat{x})^T P^{-1} (x - \hat{x}) = L^2 \tag{26}$$

where L is a constant.

The transformation to principal axes leads to the form

$$\sum_{i=1}^{n} \frac{y_i^2}{\sigma_i^2} = \sum_{i=1}^{n} z_i^2 = L^2 \tag{27}$$

where

$$z_i = \frac{y_i}{\sigma_i}$$

Eq (27) gives the equation for a hypersphere of n-dimensions. The probability of finding the z-vector inside this hypersphere is

$$Pr = \int\int \cdots \int_{Vol} \frac{1}{(2\pi)^{\frac{n}{2}}} \exp\left\{-\frac{1}{2}\left(\sum_{i=1}^{n} z_i^2\right)\right\} dz_1 \cdots dz_n \tag{28}$$

where the integration is carried out over the volume of the hypersphere.

This multiple integral can also be expressed as

$$Pr = \frac{1}{(2\pi)^{\frac{n}{2}}} \int_0^L \exp\left\{-\frac{1}{2} r^2\right\} f(r)\, dr \tag{29}$$

where f (r) dr is the n-dimensional spherically symmetric volume element.

A table of hyperellipse probabilities as a function of the dimension of the state vector, n, and of the constant, L, can be computed from this equation. The results for n = 1, ..., 7; and L = 1, ..., 4 are shown in Table 2.

TABLE 2

Hyperellipse Probabilities

| n \ L | 1 | 2 | 3 | 4 |
|---|---|---|---|---|
| 1 | 0.683 | 0.955 | 0.997 | 0.999 |
| 2 | 0.394 | 0.865 | 0.989 | 0.999 |

TABLE 2 (continued)

| n \ L | 1 | 2 | 3 | 4 |
|---|---|---|---|---|
| 3 | 0.200 | 0.739 | 0.971 | 0.999 |
| 4 | 0.090 | 0.594 | 0.939 | 0.997 |
| 5 | 0.037 | 0.450 | 0.891 | 0.993 |
| 6 | 0.014 | 0.323 | 0.826 | 0.986 |
| 7 | 0.005 | 0.220 | 0.747 | 0.975 |

Hence, it is seen that the probability that the six-dimensional state vector of position and velocity lies within a volume of radius 1 about the estimated mean value is only 1.4%; within a radius of 2 is 32.3%; within a radius of 3 is 82.6%; and within a radius of 4 is 98.6%. Note, that these probabilities for different radii are usually referred to as 1, 2, 3, or 4 sigma probabilities.

For an illustrative example of the above, consider a two dimensional state vector, with zero mean and a covariance matrix P, and inverse covariance matrix $P^{-1}$ given by

$$P = \begin{bmatrix} \sigma_1^2 & \sigma_{12} \\ \sigma_{12} & \sigma_2^2 \end{bmatrix}, \quad P^{-1} = \frac{1}{|P|} \begin{bmatrix} \sigma_2^2 & -\sigma_{12} \\ -\sigma_{12} & \sigma_1^2 \end{bmatrix} \tag{30}$$

where

$$|P| = \sigma_1^2 \sigma_2^2 - \sigma_{12}^2 . \tag{31}$$

From Eq (26) the ellipse of interest is given by

$$\sigma_2^2 x_1^2 - 2\sigma_{12} x_1 x_2 + \sigma_1^2 x_2^2 = L^2 \left( \sigma_1^2 \sigma_2^2 - \sigma_{12}^2 \right) \tag{31}$$

The ellipse has the general shape shown in the following sketch.

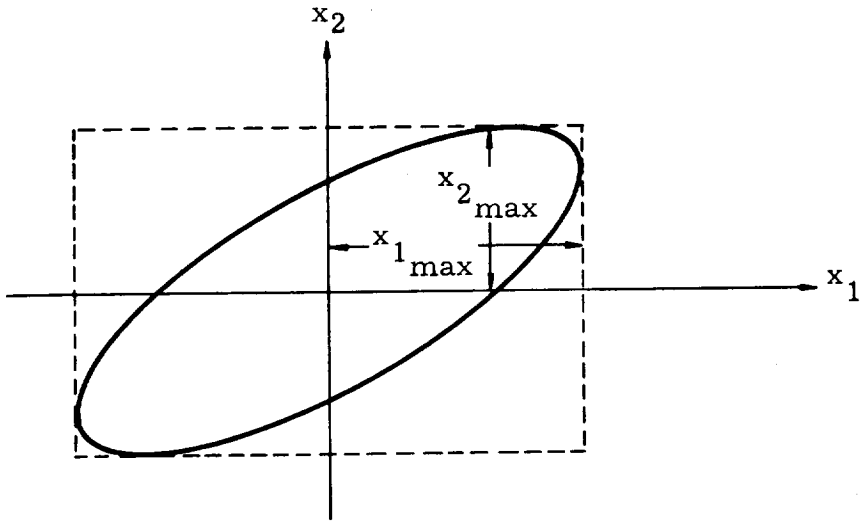


where

$$(x_1)_{max} = L\sigma_1$$

$$(x_2)_{max} = L\sigma_2$$

Hence, the probability that $x_1$ and $x_2$ lie simultaneously within the ellipse is read from Table 2 for a given value of L and for n = 2. However, the probability that $x_1$ lies between $-L\sigma_1$ and $+L\sigma_1$ regardless of the value of $x_2$ is given by the one-dimensional probabilities corresponding to the value of L. Likewise, the probability that $x_2$ lies between $-L\sigma_2$ and $+L\sigma_2$, regardless of the value of $x_1$, is given by the one dimensional probability corresponding to the value of L. Hence, the probability of both of these events occurring simultaneously is just the probability that $x_1$ and $x_2$ simultaneously lie in the rectangular region which encloses the ellipse. For L = 2, this is just $(0.955)^2 = 0.912$. This concept can be extended to higher dimensions as well, and one can form a table of Probabilities for "Hyperrectangles." This is given in Table 3.

TABLE 3

Hyperrectangle Probabilities

| n \ L | 1 | 2 | 3 | 4 |
|---|---|---|---|---|
| 1 | 0.683 | 0.955 | 0.997 | 0.999 |
| 2 | 0.466 | 0.912 | 0.994 | 0.999 |
| 3 | 0.319 | 0.871 | 0.991 | 0.999 |
| 4 | 0.218 | 0.832 | 0.988 | 0.999 |
| 5 | 0.149 | 0.794 | 0.985 | 0.999 |
| 6 | 0.102 | 0.759 | 0.982 | 0.999 |
| 7 | 0.070 | 0.724 | 0.979 | 0.999 |

Obviously, for any given values of L and n, the corresponding probability is higher for the hyperrectangle since it encloses the hyperellipse. Since the sides of the hyperrectangle are multiples of the standard deviation of the corresponding component it is sometimes useful and convenient to use the hyperrectangle probabilities rather than the hyperellipse probabilities.

## F. ONBOARD VERSUS EARTH BASED COMPUTATIONS

It is possible to obtain additional observational data from onboard the spacecraft and to use it in improving the estimation of the orbit. Some thoughts concerning this option are presented here to point out how it may be incorporated into the estimation scheme. Some work on this has been reported in Ref. (7). In this reference the authors studied the use of onboard observations as well as range and range-rate radar data. They included uncertainties such as bias errors, nonwhite noise in the radar measurements, radar station location errors, station clock errors, and error in the knowledge of the velocity of light. Their results showed that, in general, radar data was superior to onboard observations for estimating the trajectory. They also showed that significant improvement in the determination of radar station locations and of the velocity of light can be obtained by the optimal reduction of the radar tracking data.

To handle observations from different sources and at different times one only needs to have the computer programmed to take into account changes in the observation matrix. The observations will be some different set of data; hence, in the formulation all that changes is the

G-matrix. For example, assume that one gets input data from ground tracking station A at time $t_k$, from ground tracking station B, at time $t_{k+1}$, and from an onboard station C at time $t_{k+2}$. All these measurements can be denoted by

$$\Delta y_A (t_k) = G_A (t_k) \times (t_k) + \delta_A (t_k) \tag{32}$$

$$\Delta y_B (t_{k+1}) = G_B (t_{k+1}) \times (t_{k+1}) + \delta_B (t_{k+1}) \tag{33}$$

$$\Delta y_C (t_{k+2}) = G_C (t_{k+2}) \times (t_{k+2}) + \delta_C (t_{k+2}) \tag{34}$$

Hence, at the appropriate times, $t_k$, $t_{k+1}$, and $t_{k+2}$, for example, one would feed into the recursive equations the corresponding G-matrix, and the V-matrix which is dependent on the different noise vectors.

To handle the uncertainties from the various sources cited above one can increase the dimension of the state vector by making new components equal to various errors and unknowns in the equations. See Ref. (8) for further details of this procedure. For example, the first six components of the new state vector could be the three position and three velocity components, then the next components could be the unknowns in the equations of motion, and the next could be time correlated errors in the observations, etc. The basic recursive procedure would be applied as usual only with higher dimension transition matrixes to take into account the behavior of the additional variables. Hence, at the expense of increased complexity, and higher dimensional matrices, one obtains a running estimate of many of the unknowns in the problem. One can also evaluate the effect of these on the errors in estimating the position and velocity of the space vehicle.

## G. DIGITAL PROGRAM LOGIC

Figure 1 is a Program Flow Chart which outlines the various steps and options in performing the orbit estimation and prediction accuracy evaluation via a digital computer. The various subprograms are blocked out on the right hand side of the figure. The main program logic proceeds in a manner as depicted on the left of the figure. The functions in the blocks correspond to the descriptions given earlier.

One would initiate the computations by loading into the computer all constants, station locations, error variances, etc. Following this, one either computes an initial estimate and covariance matrix via the least squares fitting procedure or estimates the initial state vector and its corresponding covariance matrix.

All the observed data are read into the machine as they are obtained. The recursive process then loops through the various steps of the estimation process whenever new observation data are obtained.

An option to integrate numerically the equations of motion in order to obtain the trajectory of the orbit is included in the block named "non-station dependent calculations." Combining these results with the appropriate transformation of coordinates and the observation data will result in the computation of theoretically expected observations. This block is entitled "station dependent calculations."

The block labeled "state transition matrix" computes the transition matrix between two successive instants of time using the analytical formulation discussed in Sections C and I. The block labeled "G-matrix" contains the subprogram for the calculation of the G-matrix for any observation station and at any instant of time.

With all the necessary matrices evaluated for the ith instant of time, one goes into the subprogram which computes the optimal weighting matrix K, and the updated estimate of the state vector perturbation. Following this computation, the updated covariance matrix is computed. At any stage of the looping this can be used to give an estimate of the accuracy following the lines of the discussion given in Section E. Confidence regions can be constructed, and either hyperellipse or hyperrectangle probabilities computed. This updated P-matrix is used in the next loop of the computations to get the new K-matrix.

These updated estimations of the state vector perturbations can be combined in the "predicting and smoothing" block with the nominal value of the state vector to obtain the best estimate of the actual state vector at the particular instant.

Optional output can be achieved by suitably filling in the subprogram in the last block.

This program flow chart gives only the broadest outlines of the underlying steps in the recursive estimation process and some of the possible options. A more complete and detailed flow diagram would have to be constructed before actual programming for a digital computer is done.

## H. RESULTS AND CONCLUSIONS

In this report the underlying considerations and formulations for the estimation of the state vector of a space vehicle have been presented. Primary attention has been directed to the problem of predicting the state of a lunar orbiting vehicle where observations are

assumed to be taken from earth based tracking stations. The theory applies equally well to vehicles orbiting the earth, the moon, or any other planet. In fact, with straightforward modifications, the entire procedure could be readily adopted to estimate the trajectory of a circumlunar vehicle (or other long space voyage). The same basic equations, with appropriate changes in constants, coordinates, etc., apply to tracking and estimating the orbit of a vehicle orbiting the earth or the moon, and via the concept of "Virtual Mass," see Ref. (9), one can extend the procedure to the translunar section of the mission. The effort required to develop a digital program which is versatile enough to encompass the task of estimating the trajectory of a space vehicle on a complex mission such as the circumlunar one, would be well-worthwhile for future work.

It was pointed out in this report that one can, by extending the concept of the state vector and by increasing its dimension, estimate unknowns or various physical constants in the system of equations, such as the velocity of light, occultation time, etc.

Since the covariance matrix of the errors made in the estimation of the state vector is constantly updated, one obtains a means of determining confidence limits for the estimates. A certain hyperellipse or hyperrectangle can be readily constructed from this covariance matrix which bounds the estimate within a certain volume in state space for any given probability.

A discussion of the changes which must be made in order to accommodate both onboard data and tracking data from several locations is also given.

Finally, a program flow chart of the various steps and options involved in making the estimation and in determining the confidence in the estimate is given. The program logic is discussed briefly with suggestions given for the preparation of more detailed flow diagrams for actual programming.

## I. SUPPLEMENTARY DERIVATIONS

### 1. Transformation Between Tracking Station Coordinates and Lunar Coordinates

The transformation between the geodetic tracking coordinates $(X_T, Y_T, Z_T)$ on the earth (see Fig. 2) and the inertial coordinate system $(X_I, Y_I, Z_I)$ with origin at the center of the Earth which has its Z-axis pointed positive through the north pole, its X-axis to the vernal equinox, and its Y-axis completing the right handed triad is given by

$$\begin{bmatrix} X_I \\ Y_I \\ Z_I \end{bmatrix} = \begin{bmatrix} (c\theta c\lambda_T) & (-s\theta) & (-c\theta s\lambda_T) \\ (s\theta c\lambda_T) & (c\theta) & (-s\theta s\lambda_T) \\ (s\lambda_T) & (0) & (c\lambda_T) \end{bmatrix} \begin{bmatrix} X_T + R_0 \\ Y_T \\ Z_T \end{bmatrix} = [A] \begin{bmatrix} X_T \\ Y_T \\ Z_T \end{bmatrix} + A \begin{bmatrix} R_0 \\ 0 \\ 0 \end{bmatrix} \tag{35}$$

where $s \sim$ sine $\quad c \sim$ cosine

$R_0$ = radius of the Earth at the tracking station

$$\theta = \theta_T + \theta_{G_{ref}} + \Omega\,(t - t_{ref}) \tag{36}$$

$\theta_T$ = longitude of tracking station

$\lambda_T$ = latitude of tracking station

$\Omega$ = rotation of Earth about its axis

$t_{ref}$ = reference time or initial time

$\theta_{G_{ref}}$ = longitude of Greenwich at reference time with respect to vernal equinox

$$\theta_{G_{ref}} = 1.72218633 + 0.017202791478(N_{year}) + 0.5064083 \times 10^{-14}\,(N_{year})^2 + 0.017202791478\,(N_{day}) + 0.26251614\,(N_{hour}) \tag{37}$$

where time is counted from January 0, 1960, hence

$N_{year}$ = Year of Flight--1960

$N_{day}$ = Number of days from January 0 to day of flight

$N_{hour}$ = Number of hours from midnight to hour of flight

The inertial coordinate frame is rotated about $X_I$ by -23° 27' into the ecliptic plane (see Fig. 4); hence

$$\begin{bmatrix} X \\ Y \\ Z \end{bmatrix} = \begin{bmatrix} 1 & 0 & 0 \\ 0 & c(23°27') & -s(23°27') \\ 0 & s(23°27') & c(23°27') \end{bmatrix} \begin{bmatrix} X_I \\ Y_I \\ Z_I \end{bmatrix} = [B] \begin{bmatrix} X_I \\ Y_I \\ Z_I \end{bmatrix} \tag{38}$$

The next rotation is about the Z-axis by the amount of the right ascension of the moon's orbit, denoted $\Omega_M$, followed by a rotation about the new X-axis by the amount of the inclination of the lunar orbit to the ecliptic, denoted by $i_M$, which brings the coordinate system into coincidence with the lunar inertial frame, given by

$$\begin{bmatrix} X'_{MI} \\ Y'_{MI} \\ Z'_{MI} \end{bmatrix} = \begin{bmatrix} c\Omega_M & s\Omega_M & 0 \\ -ci_M s\Omega_M & ci_M c\Omega_M & si_M \\ si_M s\Omega_M & -si_M c\Omega_M & ci_M \end{bmatrix} \begin{bmatrix} X \\ Y \\ Z \end{bmatrix} = [C] \begin{bmatrix} X \\ Y \\ Z \end{bmatrix} \tag{39}$$

This will be the reference inertial direction for the lunar satellite motion.

The next transformation includes a rotation about the new $Z'_{MI}$-axis through the angle $\Lambda_M$ to the instantaneous position of the moon and then a translation of the origin to the center of the moon

$$\begin{bmatrix} X_M + r_{me} \\ Y_M \\ Z_M \end{bmatrix} = \begin{bmatrix} c\Lambda_M & s\Lambda_M & 0 \\ -s\Lambda_M & c\Lambda_M & 0 \\ 0 & 0 & 1 \end{bmatrix} \begin{bmatrix} X'_{MI} \\ Y'_{MI} \\ Z'_{MI} \end{bmatrix} = [D] \begin{bmatrix} X'_{MI} \\ Y'_{MI} \\ Z'_{MI} \end{bmatrix} \tag{40}$$

Then rotating back through $\Lambda_M$ about the $Z_M$ axis to the lunar inertial reference direction we obtain

$$\begin{bmatrix} X_{MI} \\ Y_{MI} \\ Z_{MI} \end{bmatrix} = \begin{bmatrix} C\Lambda_M & -S\Lambda_M & 0 \\ S\Lambda_M & C\Lambda_M & 0 \\ 0 & 0 & 1 \end{bmatrix} \begin{bmatrix} X_M \\ Y_M \\ Z_M \end{bmatrix} = [E] \begin{bmatrix} X_M \\ Y_M \\ Z_M \end{bmatrix} \tag{41}$$

Using the inverse transformations we obtain

$$\begin{bmatrix} X_T \\ Y_T \\ Z_T \end{bmatrix} = [S^T] \begin{bmatrix} r_{me} \\ 0 \\ 0 \end{bmatrix} + [F^T] \begin{bmatrix} X_{MI} \\ Y_{MI} \\ Z_{MI} \end{bmatrix} - \begin{bmatrix} R_0 \\ 0 \\ 0 \end{bmatrix} \tag{42}$$

Where S = DCBA, F = EDCBA. Therefore

$$\begin{bmatrix} \dot{X}_T \\ \dot{Y}_T \\ \dot{Z}_T \end{bmatrix} = [\dot{S}^T] \begin{bmatrix} r_{me} \\ 0 \\ 0 \end{bmatrix} + [S^T] \begin{bmatrix} \dot{r}_{me} \\ 0 \\ 0 \end{bmatrix} + [\dot{F}^T] \begin{bmatrix} X_{MI} \\ Y_{MI} \\ Z_{MI} \end{bmatrix} + [F^T] \begin{bmatrix} \dot{X}_{MI} \\ \dot{Y}_{MI} \\ \dot{Z}_{MI} \end{bmatrix} \tag{43}$$

So

$$\begin{bmatrix} X_T \\ Y_T \\ Z_T \\ \dot{X}_T \\ \dot{Y}_T \\ \dot{Z}_T \end{bmatrix} = \left[\begin{array}{c|c} & \\ F^T & 0 \\ & \\ \hline & \\ \dot{F}^T & F^T \\ & \end{array}\right] \begin{bmatrix} X_{MI} \\ Y_{MI} \\ Z_{MI} \\ \dot{X}_{MI} \\ \dot{Y}_{MI} \\ \dot{Z}_{MI} \end{bmatrix} + \left[\begin{array}{c|c} & \\ 0 & 0 \\ & \\ \hline & \\ \dot{S}^T & S^T \\ & \end{array}\right] \begin{bmatrix} r_{me} \\ 0 \\ 0 \\ \dot{r}_{me} \\ 0 \\ 0 \end{bmatrix} - \begin{bmatrix} R_0 \\ 0 \\ 0 \\ 0 \\ 0 \\ 0 \end{bmatrix} \tag{44}$$

and

$$\begin{bmatrix} x_T \\ y_T \\ z_T \\ \dot{x}_T \\ \dot{y}_T \\ \dot{z}_T \end{bmatrix} = \left[\begin{array}{c|c} F^T & 0 \\ \hline \dot{F}^T & F^T \end{array}\right] \begin{bmatrix} x_{MI} \\ y_{MI} \\ z_{MI} \\ \dot{x}_{MI} \\ \dot{y}_{MI} \\ \dot{z}_{MI} \end{bmatrix} = J(t_k) \begin{bmatrix} x_{MI} \\ y_{MI} \\ z_{MI} \\ \dot{x}_{MI} \\ \dot{y}_{MI} \\ \dot{z}_{MI} \end{bmatrix} \tag{45}$$

## 2. Analytical Formulation for the Transition Matrix

A right-handed lunar inertial coordinate system is given by the triad $X_M$, $Y_M$, $Z_M$. Consideration is next given to a coordinate system in the plane of the orbit of the lunar vehicle, denoted by $\bar{x}$, $\bar{y}$, and $\bar{z}$. Here, $\bar{z} = 0$. It is also noted that the coordinate system is set up initially so that $\bar{x}$ passes through perigee, and that $\bar{y}$ is at 90° with respect to the $\bar{x}$-axis. The coordinates initially satisfy the following conditions

$$\begin{aligned} &\bar{x}_0 > 0, \ \dot{\bar{x}}_0 = 0 \\ &\bar{y}_0 = 0, \ \dot{\bar{y}}_0 > 0 \\ &\bar{z}_0 = 0, \ \dot{\bar{z}}_0 = 0 \end{aligned} \tag{46}$$

In a Keplerian orbit the position coordinates satisfy

$$a\bar{x} + b\bar{y} + c = r = \sqrt{\bar{x}^2 + \bar{y}^2} \tag{47}$$

Figure 5 shows a typical orbit, where $\psi$ is the true anomaly. The $\bar{x}$ and $\bar{y}$ coordinates at the ith instant of time satisfy

$$\begin{aligned} \bar{x}_i &= r_i \cos \psi_i \\ \bar{y}_i &= r_i \sin \psi_i \end{aligned} \tag{48}$$

The elements of the transition matrix in the lunar coordinate system are just those of the Jacobian

$$\Phi(t_i, t_0) = \frac{\partial(x_M, y_M, z_M, \dot{x}_M, \dot{y}_M, \dot{z}_M)}{\partial(x_{M_0}, y_{M_0}, z_{M_0}, \dot{x}_{M_0}, \dot{y}_{M_0}, \dot{z}_{M_0})} = \begin{bmatrix} \frac{\partial x_M}{\partial x_{M_0}} & \frac{\partial x_M}{\partial y_{M_0}} & \cdots & \frac{\partial x_M}{\partial \dot{z}_{M_0}} \\ \frac{\partial y_M}{\partial x_{M_0}} & \frac{\partial y_M}{\partial y_{M_0}} & \cdots & \\ \vdots & & \ddots & \vdots \\ \frac{\partial \dot{z}_M}{\partial x_{M_0}} & \cdots & & \frac{\partial \dot{z}_M}{\partial \dot{z}_{M_0}} \end{bmatrix} \tag{49}$$

This matrix can be expressed as the product of three Jacobian matrices as follows

$$\frac{\partial(x_{MI}, y_{MI}, z_{MI}, \dot{x}_{MI}, \dot{y}_{MI}, \dot{z}_{MI})}{\partial(x_{MI_0}, y_{MI_0}, z_{MI_0}, \dot{x}_{MI_0}, \dot{y}_{MI_0}, \dot{z}_{MI_0})} = \frac{\partial(x_{MI}, y_{MI}, z_{MI}, \dot{x}_{MI}, \dot{y}_{MI}, \dot{z}_{MI})}{\partial(\bar{x}, \bar{y}, \bar{z}, \dot{\bar{x}}, \dot{\bar{y}}, \dot{\bar{z}})}$$

$$\cdot \frac{\partial(\bar{x}, \bar{y}, \bar{z}, \dot{\bar{x}}, \dot{\bar{y}}, \dot{\bar{z}})}{\partial(\bar{x}_0, \bar{y}_0, \bar{z}_0, \dot{\bar{x}}_0, \dot{\bar{y}}_0, \dot{\bar{z}}_0)} \cdot \frac{\partial(\bar{x}_0, \bar{y}_0, \bar{z}_0, \dot{\bar{x}}_0, \dot{\bar{y}}_0, \dot{\bar{z}}_0)}{\partial(x_{MI_0}, y_{MI_0}, z_{MI_0}, \dot{x}_{MI_0}, \dot{y}_{MI_0}, \dot{z}_{MI_0})} \tag{50}$$

This can be rewritten as

$$\Phi(t_i, t_0) = J_1 \cdot J_2 \cdot J_3 \tag{51}$$

Now of these, $J_1$ and $J_3$ can be readily evaluated since a simple transformation exists between the lunar inertial coordinate system and the orbit coordinate system as follows

$$\begin{bmatrix} X_{MI} \\ Y_{MI} \\ Z_{MI} \end{bmatrix} = \begin{bmatrix} (c\Omega\, c\omega - s\Omega\, ci\, s\omega) & (-c\Omega\, s\omega - s\Omega\, ci\, c\omega) & (s\Omega\, si) \\ (s\Omega\, c\omega + c\Omega\, ci\, s\omega) & (-s\Omega\, s\omega + c\Omega\, ci\, c\omega) & (-c\Omega\, si) \\ (si\, s\omega) & (si\, c\omega) & (ci) \end{bmatrix} \begin{bmatrix} \overline{X} \\ \overline{Y} \\ \overline{Z} \end{bmatrix} = [Q] \begin{bmatrix} \overline{X} \\ \overline{Y} \\ \overline{Z} \end{bmatrix} \qquad (52)$$

and

$$\begin{bmatrix} \overline{X} \\ \overline{Y} \\ \overline{Z} \end{bmatrix} = \begin{bmatrix} (c\Omega\, c\omega - s\Omega\, ci\, s\omega) & (s\Omega\, c\omega + c\Omega\, ci\, s\omega) & (si\, s\omega) \\ (-c\Omega\, s\omega - s\Omega\, ci\, c\omega) & (-s\Omega\, c\omega + c\Omega\, ci\, c\omega) & (si\, c\omega) \\ (s\Omega\, si) & (-c\Omega\, si) & (ci) \end{bmatrix} \begin{bmatrix} X_{MI} \\ Y_{MI} \\ Z_{MI} \end{bmatrix} = [Q^T] \begin{bmatrix} X_{MI} \\ Y_{MI} \\ Z_{MI} \end{bmatrix} \qquad (53)$$

where

$\Omega$ is the right ascension measured from the $X_{MI}$ direction, the ascending mode passing through the $X_{MI}$ - $Y_{MI}$ plane.

i is the inclination of the lunar orbit measured from the $X_{MI}$ - $Y_{MI}$ plane.

$\omega$ is the argument of pericenter measured from the $X_{MI}$ - $Y_{MI}$ plane to the pericenter point in the orbit plane.

Hence

$$J_1 = \begin{bmatrix} Q & O \\ O & Q \end{bmatrix}$$

$$J_3 = \begin{bmatrix} Q^T & 0 \\ 0 & Q^T \end{bmatrix}$$

It remains to specify the analytic form of the components of the matrix $J_2$. These have been derived, and they are presented and summarized in Table 4.

## J. REFERENCES


1. "Extension of Effort for Orbital and Lunar Flight Handbooks," Chapter III, Martin Company Report ER 13189-II, November 1963.

2. Batten, R. H., "Astronautical Guidance," McGraw-Hill Book Co., Chapter 9, New York, 1964.

3. Danby, J. M. A., "Integration of the Equations of Planetary Motion in Rectangular Coordinates," The Astronomical Journal, Vol. 67, No. 5, June 1962, pages 287-299.

4. Danby, J. M. A., "Matrix Methods in the Calculation and Analysis of Orbits," AIAA Journal, Vol. 2, No. 1, January 1964, pages 13-16.

5. Danby, J. M. A., "The Matrizant of Keplerian Motion," AIAA Journal, Vol. 2, No. 1, January 1964, pages 16-19.

6. Wagner, W. E., "Prediction Accuracy Program," Martin Company Report ER 13143, September 1963.

7. Smith, G. L. and Harper, E. V., "Midcourse Guidance Using Radar Tracking and On Board Observation Data," NASA TN D-2238, April 1964.

8. Smith, G. L., Schmidt, S. F. and McGee, L. A., "Application of Statistical Filter Theory to the Optimal Estimation of Position and Velocity On Board a Circumlunar Vehicle," NASA TR R-135, 1962.

9. "Feasibility Study of Two-Body Midcourse Guidance," Final Report for Contract NAS 1-2501, Martin Company Report ER 13138, September 1963.

TABLE 4

Summary of Partials

$$J_2(t_i,t_o)=\begin{bmatrix}
\frac{\partial \bar{X}_i}{\partial \bar{X}_o} & \frac{\partial \bar{X}_i}{\partial \bar{Y}_o} & \frac{\partial \bar{X}_i}{\partial \bar{Z}_o} & \frac{\partial \bar{X}_i}{\partial \dot{\bar{X}}_o} & \frac{\partial \bar{X}_i}{\partial \dot{\bar{Y}}_o} & \frac{\partial \bar{X}_i}{\partial \dot{\bar{Z}}_o} \\
\frac{\partial \bar{Y}_i}{\partial \bar{X}_o} & \frac{\partial \bar{Y}_i}{\partial \bar{Y}_o} & \frac{\partial \bar{Y}_i}{\partial \bar{Z}_o} & \frac{\partial \bar{Y}_i}{\partial \dot{\bar{X}}_o} & \frac{\partial \bar{Y}_i}{\partial \dot{\bar{Y}}_o} & \frac{\partial \bar{Y}_i}{\partial \dot{\bar{Z}}_o} \\
\frac{\partial \bar{Z}_i}{\partial \bar{X}_o} & \frac{\partial \bar{Z}_i}{\partial \bar{Y}_o} & \frac{\partial \bar{Z}_i}{\partial \bar{Z}_o} & \frac{\partial \bar{Z}_i}{\partial \dot{\bar{X}}_o} & \frac{\partial \bar{Z}_i}{\partial \dot{\bar{Y}}_o} & \frac{\partial \bar{Z}_i}{\partial \dot{\bar{Z}}_o} \\
\frac{\partial \dot{\bar{X}}_i}{\partial \bar{X}_o} & \frac{\partial \dot{\bar{X}}_i}{\partial \bar{Y}_o} & \frac{\partial \dot{\bar{X}}_i}{\partial \bar{Z}_o} & \frac{\partial \dot{\bar{X}}_i}{\partial \dot{\bar{X}}_o} & \frac{\partial \dot{\bar{X}}_i}{\partial \dot{\bar{Y}}_o} & \frac{\partial \dot{\bar{X}}_i}{\partial \dot{\bar{Z}}_o} \\
\frac{\partial \dot{\bar{Y}}_i}{\partial \bar{X}_o} & \frac{\partial \dot{\bar{Y}}_i}{\partial \bar{Y}_o} & \frac{\partial \dot{\bar{Y}}_i}{\partial \bar{Z}_o} & \frac{\partial \dot{\bar{Y}}_i}{\partial \dot{\bar{X}}_o} & \frac{\partial \dot{\bar{Y}}_i}{\partial \dot{\bar{Y}}_o} & \frac{\partial \dot{\bar{Y}}_i}{\partial \dot{\bar{Z}}_o} \\
\frac{\partial \dot{\bar{Z}}_i}{\partial \bar{X}_o} & \frac{\partial \dot{\bar{Z}}_i}{\partial \bar{Y}_o} & \frac{\partial \dot{\bar{Z}}_i}{\partial \bar{Z}_o} & \frac{\partial \dot{\bar{Z}}_i}{\partial \dot{\bar{X}}_o} & \frac{\partial \dot{\bar{Z}}_i}{\partial \dot{\bar{Y}}_o} & \frac{\partial \dot{\bar{Z}}_i}{\partial \dot{\bar{Z}}_o}
\end{bmatrix}$$

$$\frac{\partial \bar{X}_i}{\partial \bar{X}_o} = c\psi_i \frac{\partial r_i}{\partial \bar{X}_o} - \bar{Y}_i \frac{\partial \psi_i}{\partial \bar{X}_o}$$

$$\frac{\partial \bar{X}_i}{\partial \bar{Y}_o} = c\psi_i \frac{\partial r_i}{\partial \bar{Y}_o} - \bar{Y}_i \frac{\partial \psi_i}{\partial \bar{Y}_o}$$

$$\frac{\partial \bar{X}_i}{\partial \bar{Z}_o} = 0$$

$$\frac{\partial \bar{X}_i}{\partial \dot{\bar{X}}_o} = c\psi_i \frac{\partial r_i}{\partial \dot{\bar{X}}_o} - \bar{Y}_i \frac{\partial \psi_i}{\partial \dot{\bar{X}}_o}$$

$$\frac{\partial \bar{X}_i}{\partial \dot{\bar{Y}}_o} = c\psi_i \frac{\partial r_i}{\partial \dot{\bar{Y}}_o} - \bar{Y}_i \frac{\partial \psi_i}{\partial \dot{\bar{Y}}_o}$$

$$\frac{\partial \bar{X}_i}{\partial \dot{\bar{Z}}_o} = 0$$

$$\frac{\partial \bar{Y}_i}{\partial \bar{X}_o} = s\psi_i \frac{\partial r_i}{\partial \bar{X}_o} + \bar{X}_i \frac{\partial \psi_i}{\partial \bar{X}_o}$$

$$\frac{\partial \bar{Y}_i}{\partial \bar{Y}_o} = s\psi_i \frac{\partial r_i}{\partial \bar{Y}_o} + \bar{X}_i \frac{\partial \psi_i}{\partial \bar{Y}_o}$$

$$\frac{\partial \bar{Y}_i}{\partial \bar{Z}_o} = 0$$

$$\frac{\partial \bar{Y}_i}{\partial \dot{\bar{X}}_o} = s\psi_i \frac{\partial r_i}{\partial \dot{\bar{X}}_o} + \bar{X}_i \frac{\partial \psi_i}{\partial \dot{\bar{X}}_o}$$

$$\frac{\partial \bar{Y}_i}{\partial \dot{\bar{Y}}_o} = s\psi_i \frac{\partial r_i}{\partial \dot{\bar{Y}}_o} + \bar{X}_i \frac{\partial \psi_i}{\partial \dot{\bar{Y}}_o}$$

$$\frac{\partial \bar{Y}_i}{\partial \dot{\bar{Z}}_o} = 0$$

where

$s\psi_i = \sin(\psi_i)$

$c\psi_i = \cos(\psi_i)$

TABLE 4 (continued)

$$\frac{\partial \bar{Z}_i}{\partial \bar{X}_o} = 0 \qquad \frac{\partial \bar{Z}_i}{\partial \dot{X}_o} = 0$$

$$\frac{\partial \bar{Z}_i}{\partial \bar{Y}_o} = 0 \qquad \frac{\partial \bar{Z}_i}{\partial \dot{Y}_o} = 0$$

$$\frac{\partial \bar{Z}_i}{\partial \bar{Z}_o} = \frac{\bar{X}_i}{\bar{X}_o} \qquad \frac{\partial \bar{Z}_i}{\partial \dot{Z}_o} = \frac{\bar{Y}_i}{\dot{Y}_o}$$

$$\frac{\partial \dot{\bar{X}}_i}{\partial \bar{X}_o} = \left(\frac{\mu}{\bar{X}_c \dot{Y}_o}\right)\left[\frac{s\psi_i}{\bar{X}_o} - c\psi_i \frac{\partial \psi_i}{\partial \bar{X}_o}\right] \qquad \frac{\partial \dot{\bar{X}}_i}{\partial \dot{X}_o} = \left(\frac{\mu}{\bar{X}_o \dot{Y}_c}\right)\left[\frac{\bar{X}_o \dot{Y}_o}{\mu} - c\psi_i \frac{\partial \psi_i}{\partial \dot{X}_o}\right]$$

$$\frac{\partial \dot{\bar{X}}_i}{\partial \bar{Y}_o} = \left(\frac{\mu}{\bar{X}_o \dot{Y}_c}\right)\left[\frac{1}{\bar{X}_o} - c\psi_i \frac{\partial \psi_i}{\partial \bar{Y}_o}\right] \qquad \frac{\partial \dot{\bar{X}}_i}{\partial \dot{Y}_o} = \left(\frac{\mu}{\bar{X}_o \dot{Y}_o}\right)\left[\frac{s\psi_i}{\dot{Y}_o} - c\psi_i \frac{\partial \psi_i}{\partial \dot{Y}_o}\right]$$

$$\frac{\partial \dot{\bar{X}}_i}{\partial \bar{Z}_o} = 0 \qquad \frac{\partial \dot{\bar{X}}_i}{\partial \dot{Z}_o} = 0$$

$$\frac{\partial \dot{\bar{Y}}_i}{\partial \bar{X}_o} = \left(\frac{\mu}{\bar{X}_o \dot{Y}_o}\right)\left[\frac{a}{\bar{X}_o} - \frac{c\psi_i}{\bar{X}_o} + \frac{\dot{Y}_o^2}{\mu} - s\psi_i \frac{\partial \psi_i}{\partial \bar{X}_o}\right] \qquad \frac{\partial \dot{\bar{Y}}_i}{\partial \dot{X}_o} = -\frac{\mu}{\bar{X}_o \dot{Y}_o} s\psi_i \frac{\partial \psi_i}{\partial \dot{X}_o}$$

$$\frac{\partial \dot{\bar{Y}}_i}{\partial \bar{Y}_o} = -\frac{\mu}{\bar{X}_o \dot{Y}_o} s\psi_i \frac{\partial \psi_i}{\partial \bar{Y}_o} \qquad \frac{\partial \dot{\bar{Y}}_i}{\partial \dot{Y}_o} = \left(\frac{\mu}{\bar{X}_o \dot{Y}_o}\right)\left[\frac{a}{\dot{Y}_o} - \frac{c\psi_i}{\dot{Y}_o} + \frac{2\bar{X}_o \dot{Y}_o}{\mu} - s\psi_i \frac{\partial \psi_i}{\partial \dot{Y}_o}\right]$$

$$\frac{\partial \dot{\bar{Y}}_i}{\partial \bar{Z}_o} = 0 \qquad \frac{\partial \dot{\bar{Y}}_i}{\partial \dot{Z}_o} = 0$$

$$\frac{\partial \dot{\bar{Z}}_i}{\partial \bar{X}_o} = 0 \qquad \frac{\partial \dot{\bar{Z}}_i}{\partial \dot{X}_o} = 0$$

$$\frac{\partial \dot{\bar{Z}}_i}{\partial \bar{Y}_o} = 0 \qquad \frac{\partial \dot{\bar{Z}}_i}{\partial \dot{Y}_o} = 0$$

$$\frac{\partial \dot{\bar{Z}}_i}{\partial \bar{Z}_o} = \frac{\dot{X}_i}{\bar{X}_o} \qquad \frac{\partial \dot{\bar{Z}}_i}{\partial \dot{Z}_o} = \frac{\dot{Y}_i}{\dot{Y}_o}$$

TABLE 4 (continued)

$$\frac{\partial r_i}{\partial \bar{X}_0} = \frac{\frac{\dot{\bar{Y}}_0^2}{\mu}(2\bar{X}_0 - \bar{X}_i) - a\bar{Y}_i \frac{\partial \psi_i}{\partial \bar{X}_0}}{(1 - a(c\psi_i))}$$

$$\frac{\partial r_i}{\partial \bar{Y}_0} = \frac{\frac{\bar{Y}_i}{\bar{X}_0} - a\bar{Y}_i \frac{\partial \psi_i}{\partial \bar{Y}_0}}{(1 - a(c\psi_i))}$$

$$\frac{\partial r_i}{\partial \dot{\bar{X}}_0} = \frac{\frac{\bar{Y}_i \bar{X}_0 \dot{\bar{Y}}_0}{\mu} - a\bar{Y}_i \frac{\partial \psi_i}{\partial \dot{\bar{X}}_0}}{(1 - a(c\psi_i))}$$

$$\frac{\partial r_i}{\partial \dot{\bar{Y}}_0} = \frac{\frac{2}{\mu}\bar{X}_0 \dot{\bar{Y}}_0 (\bar{X}_0 - \bar{X}_i) - a\bar{Y}_i \frac{\partial \psi_i}{\partial \dot{\bar{Y}}_0}}{(1 - a(c\psi_i))}$$

$$\frac{\partial \psi_i}{\partial \bar{X}_0} = -\frac{\bar{X}_0 \dot{\bar{Y}}_0}{r_i^2}\left[\frac{3\tau_i}{\bar{X}_0} - \frac{\partial f}{\partial a}\frac{\dot{\bar{Y}}_0^2}{\mu}\right]$$

$$\frac{\partial \psi_i}{\partial \bar{Y}_0} = -\frac{\bar{X}_0 \dot{\bar{Y}}_0}{r_i^2}\left[\frac{\partial f}{\partial b}\frac{1}{\bar{X}_0} - \frac{1}{\dot{\bar{Y}}_0}\right]$$

$$\frac{\partial \psi_i}{\partial \dot{\bar{X}}_0} = -\frac{\bar{X}_0^2 \dot{\bar{Y}}_0^2}{\mu r_i^2}\frac{\partial f}{\partial b}$$

$$\frac{\partial \psi_i}{\partial \dot{\bar{Y}}_0} = -\frac{\bar{X}_0 \dot{\bar{Y}}_0}{r_i^2}\left[\frac{3\tau_i}{\dot{\bar{Y}}_0} - 2\frac{\partial f}{\partial a}\frac{\bar{X}_0 \dot{\bar{Y}}_0}{\mu}\right]$$

$$\frac{\partial f}{\partial a} = \frac{\bar{X}_0^3 \dot{\bar{Y}}_0^3}{\mu^2}\left[\frac{s\psi_i\left\{(3P^3 + 5PQ^2)(c\psi_i/2)^2 + (5P^2Q + 3Q^3)(s\psi_i/2)^2\right\}}{4P^2Q^2\left(P(c\psi_i/2)^2 + Q(s\psi_i/2)^2\right)^2} + \frac{3}{2}\frac{(Q^2 - P^2)}{(PQ)^{5/2}}\tan^{-1}\left\{\left(\frac{Q}{P}\right)^{1/2}\tan\psi_i/2\right\}\right]$$

where $P = 1 - a$, $Q = 1 + a$

$$\frac{\partial f}{\partial b} = \frac{\bar{X}_0^3 \dot{\bar{Y}}_0^3}{\mu^2}\left[\frac{2 - 2c\psi_i - a(s\psi_i)^2}{P^2(1 - a(c\psi_i))^2}\right]$$

# ILLUSTRATIONS

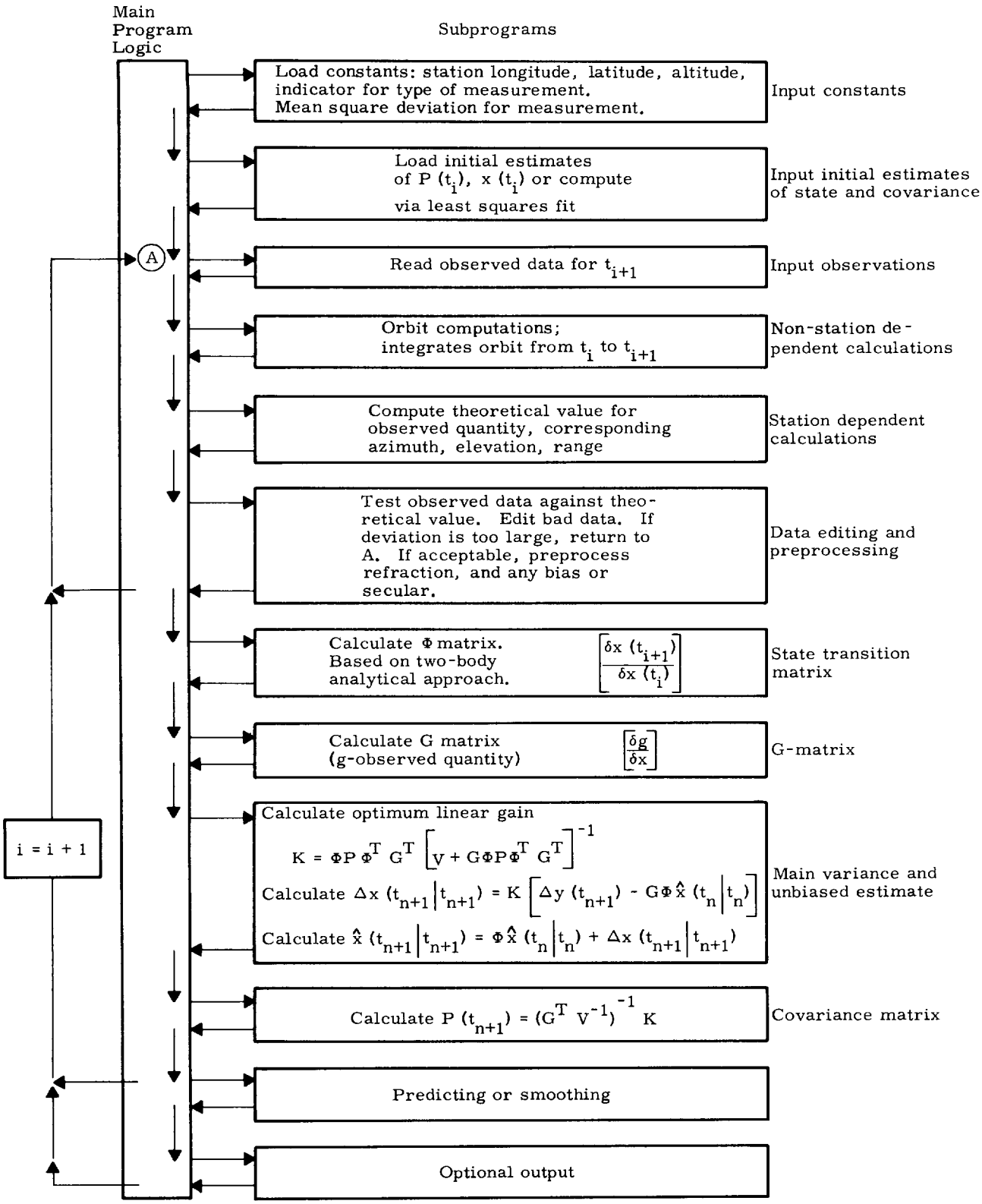


Fig. 1. Program Flow Chart

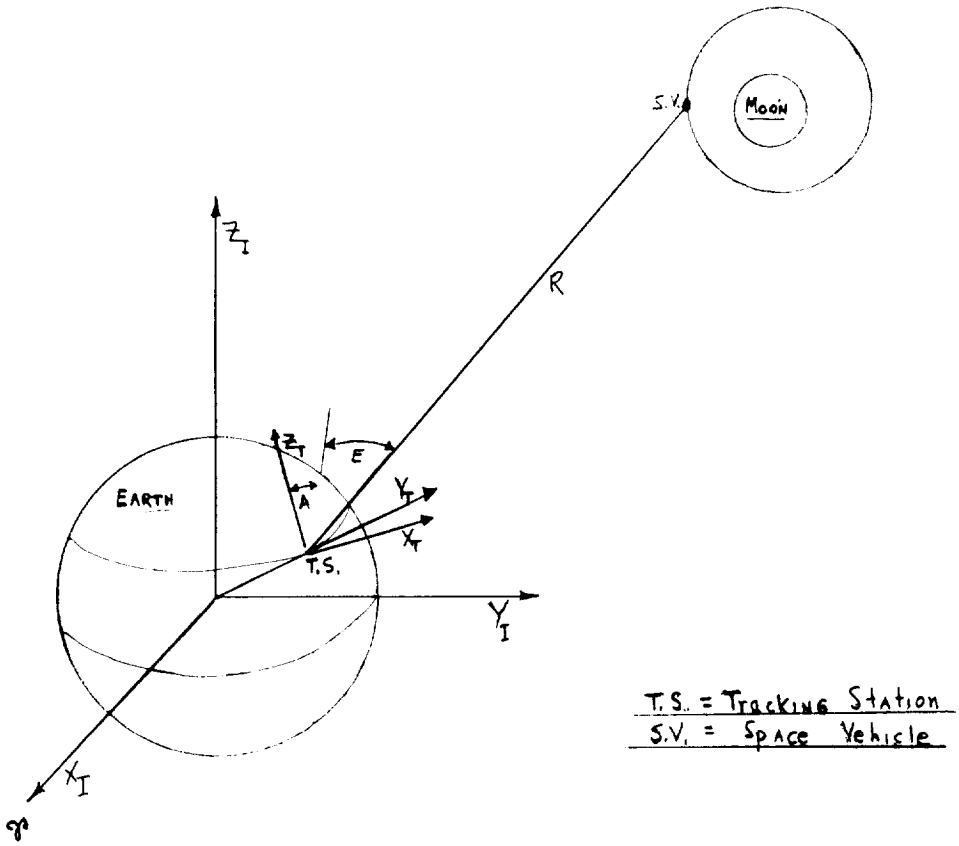


Fig. 2. Coordinate System of Tracking Station Located on Earth

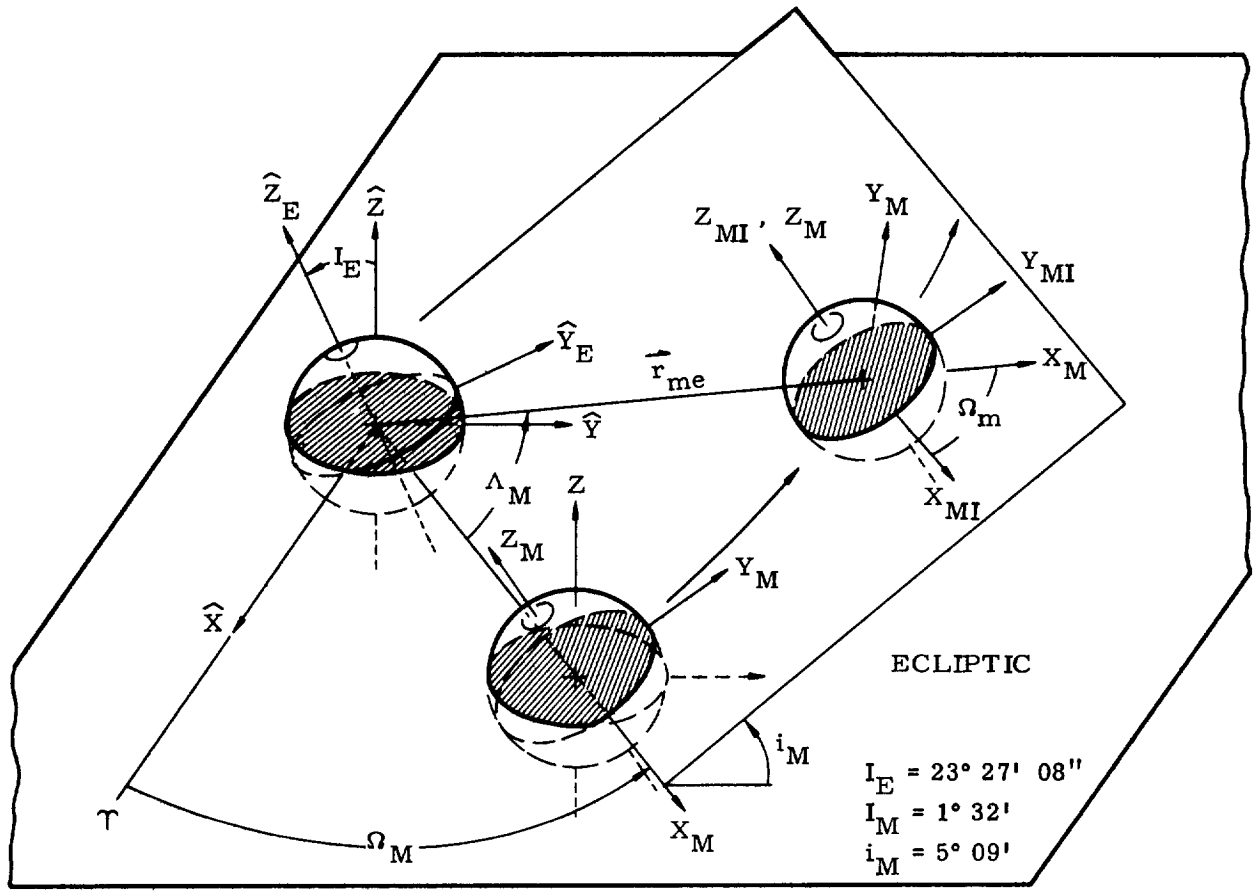


Fig. 3. Orientation of Principal Planes

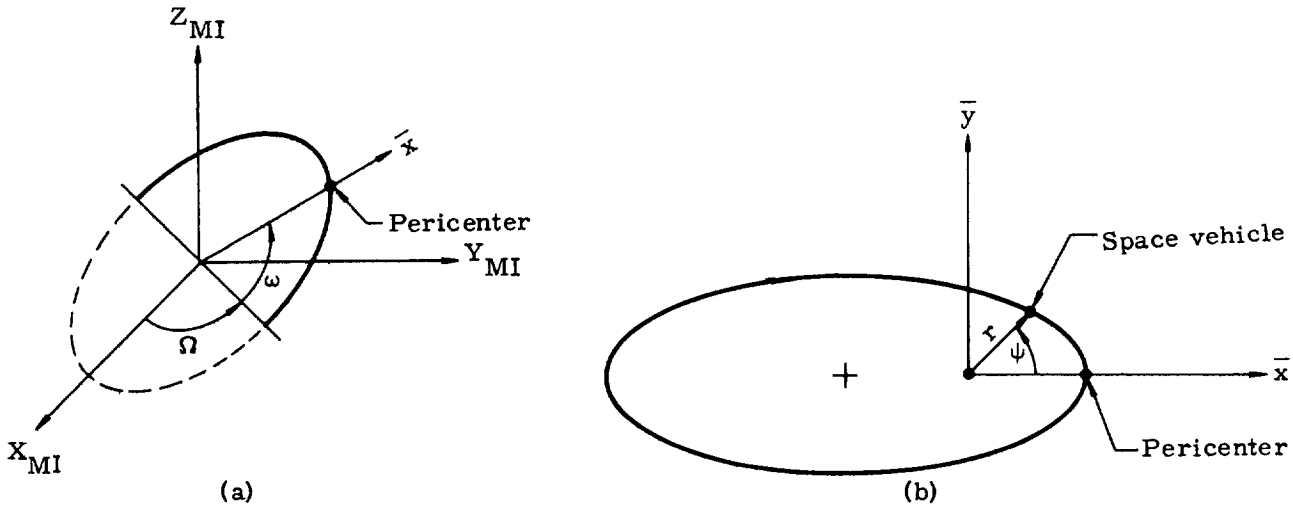


Fig. 4. Coordinate System

# IV. LUNAR ORBITER THEORY

by J. G. Gegner

## A. INTRODUCTION

In Ref. 1 a rather simplified approach to the determination of the orbital elements as a function of time is discussed. The assumption of a linear disturbing function led to very convenient and inexpensive method of predicting orbital stability for earth satellites in the form of the program, SOLUN.

The mathematical model that is used for SOLUN is readily adaptable to lunar orbits and a new model, which can be used for earth orbits as well as for lunar orbits, is disscussed. The newer model has been incorporated into a program, SOME (Ref. 2), and some comparative data is presented for an earth and a lunar orbit.

Long-period secular effects due to lunar asphericity on the three orientation elements of a lunar satellite are presented in the mathematical model and orbital stability, which can be determined very easily from the analytical terms in the perturbations, is discussed in its appropriate section.

Some working graphs are also provided to further update the Handbook information.

### DEFINITIONS

| | |
|---|---|
| a | Semimajor axis |
| e | Eccentricity |
| ECL | Ecliptic |
| EEP | Earth's equatorial plane |
| EOP | Earth's orbital plane (≡ MOP) |
| i | Inclination |
| $MCP_{\mathbb{C}}$ | Mean center point of moon |
| MEP | Moon's equatorial plane |
| MOP | Moon's orbital plane |
| n | Satellite's mean angular rate |
| q | Periapsis radius |
| r | Radial distance |
| $R_E$ | Reference body radius |

| | |
|---|---|
| R, S, W | Components of force acting on satellite |
| SOP | Satellite orbital plane |
| $\omega_{\oplus}$ | Spin rate of earth |
| t | Universal time of day |
| T | Time from injection |
| $\Gamma_D$ | Position of disturbing body in its orbit relative to SOP's ascending node |
| $\omega$ | Argument of periapsis |
| $\theta$ | True anomaly |
| $\Omega$ | Angular position of SOP ascending node in disturbing body plane from arbitrary reference |
| $\Omega_0$ | Position of lunar SOP's ascending node to MCP☾ |
| $\Omega_1$ | Angular position of MCP☾ + z |
| $\Omega_s$ | Ascending node of satellite relative to Aries along reference body equator |

Ephemeris Symbols

| | |
|---|---|
| $i_{☾}$ | Inclination of MOP to ECL |
| ☾ | Moon's mean anomaly + $\Gamma'$ |
| $\Gamma'$ | Moon's mean argument of perigee + ☊ |
| ☊ | Geocentric ecliptic position of MOP ascending node |
| I | Inclination of MEP to ECL |
| $i_{\oplus}$ | Inclination of MOP to EEP |
| $\Omega_{☾}$ | Right ascension of MOP's ascending node |
| $\omega_{☾}$ | Position of MOP's ecliptic ascending node relative to EEP along MOP |
| $\epsilon$ | Obliquity |
| L | Sun's mean anomaly + $\Gamma$ |
| $\Gamma$ | Sun's mean argument of perigee |
| l, b | Lunar librations in longitude, latitude |
| $\mu$ | Gravitational constant |

Subscripts

| | |
|---|---|
| ☾ | Moon |
| S | Satellite (relative to reference body equator) |
| ⊙ | Sun |
| ⊕ | Earth |
| D | Disturbing body |

## B. SECULAR PERTURBATIONS

For convenience and completeness, portions of Refs. 1 and 3 are repeated here.

First, choose a right-handed triaxial system whose z-axis is coincident with the angular momentum vector of the orbit of the disturbing body. Let the x-axis have an arbitrary direction at some time, let the orbit be defined by its osculating elements (a, e, i, $\omega$, $\Omega$, $\theta$) relative to the x-y plane, and let R, S, and W represent the radial, tangential, and normal forces acting on the satellite (see Fig. 1).

The rate of change of each of the first five elements is then:

$$
\begin{aligned}
\frac{d}{dt}\, a &= \frac{2\, e \sin\theta}{n\sqrt{1-e^2}}\, R + \frac{2\, a\sqrt{1-e^2}}{r_s\, n}\, S \\
\frac{d}{dt}\, e &= \frac{\sqrt{1-e^2}\,\sin\theta}{n \cdot a}\, R + \frac{\sqrt{1-e^2}}{n \cdot e}\left[\frac{(1-e^2)}{r_s} - \frac{r_s}{a^2}\right] \cdot S \\
\frac{d}{dt}\, i &= \frac{r_s \cos(\theta+\omega)}{na^2\sqrt{1-e^2}} \cdot W \\
\frac{d}{dt}\, \Omega &= \frac{r_s \sin(\theta+\omega)}{na^2\sqrt{1-e^2}\,\sin i}\, W \\
\frac{d}{dt}\, \omega &= -\frac{\sqrt{1-e^2}}{nae}\left[R\cos\theta - \frac{2+e\cos\theta}{1+e\cos\theta} \cdot \sin\theta \cdot S\right] - \cos i\, \frac{d}{dt}\, \Omega \\
R,\ S,\ W &= F_i\,(\mu_D,\ \bar{r}_D,\ \bar{r}_S)
\end{aligned}
\qquad (1)
$$

After expanding R, S, and W by truncating the disturbing function at the linear term and integrating each of the elements over a finite displacement of the disturbing body and once over the orbital period of the satellite while assuming the remaining elements to be constant, the average rate of change during the disturbing body displacement is for each element:

$$\Delta a = 0$$

$$\Delta e = A_{11} \cos 2\omega \cos i + A_{12} \sin 2\omega \sin^2 i + A_{13} \sin 2\omega (1 + \cos^2 i)$$

$$\Delta i = A_{21} \sin i (1 - e^2 (1 - 5 \cos^2 \omega)) + A_{22} \sin 2\omega \sin 2 i$$

$$\Delta \Omega = A_{31} \sin 2\omega + A_{32} \cos i \left[ (1 - e^2) \cos^2 \omega + (1 + 4e^2) \sin^2 \omega \right] \quad (2)$$

$$\Delta \omega = \left[ A_{41} \sin 2\omega - \Delta \Omega \right] \cos i + A_{42} \left[ 2 + (1 - 5 \cos^2 \omega) \sin^2 i - 3 \cos^2 i \right] + A_{43} \left[ (1 - 5 \cos^2 \omega)(1 + \cos^2 i) + 3 \cos^2 i \right]$$

$$\Delta q = -a \Delta e$$

where

$$A_{11} = -15 \cdot H \cdot e \cdot f (\Gamma_D)$$

$$A_{12} = 15 \cdot H \cdot e \cdot \Delta \Gamma_D$$

$$A_{13} = 7.5 \cdot H \cdot e \cdot g (\Gamma_D)$$

$$A_{21} = -3 \cdot H \cdot f (\Gamma_D)/(1 - e^2)$$

$$A_{22} = -7.5 \cdot H \cdot e^2 (\Delta \Gamma_D - \tfrac{1}{2} g (\Gamma_D))/(1 - e^2)$$

$$A_{31} = -7.5 \cdot H \cdot e^2 \cdot f (\Gamma_D)/(1 - e^2)$$

$$A_{32} = -6 H (\Delta \Gamma_D - \tfrac{1}{2} g (\Gamma_D))/(1 - e^2)$$

$$A_{41} = 15 \cdot H \cdot f(\Gamma_D)$$

$$A_{42} = -6H \cdot \Delta\Gamma_D$$

$$A_{43} = -3H \cdot g(\Gamma_D)$$

$$f(\Gamma_D) = \cos 2\,\Gamma_D - \cos 2\,(\Gamma_D + \Delta\Gamma_D)$$

$$g(\Gamma_D) = \sin 2\,(\Gamma_D + \Delta\Gamma_D) - \sin 2\,\Gamma_D$$

$$H = \frac{\mu_D \sqrt{1 - e^2}}{8 \cdot n\ \dot{\Gamma}_D \cdot a_D^3}$$

$\Delta\Gamma_D$ = finite angular displacement of disturbing body

During "integration" then, the only variables not held constant are $\Gamma_D$ and $\theta$.

Hence, in order to determine a history of the orbital elements over a long period of time, it is required only to cyclically compute the change in the elements and step them by that change. But before the "integration" of the elements can be made, the elements must be transformed from an appropriate reference plane (earth or lunar equator) to the plane of the disturbing body. The reference directions for transformations are Aries and the ascending node of the moon's equatorial plane at epoch for earth and lunar satellites, respectively (see Figs. 2 and 3). The equations which avail themselves for transformation are

$$\cos i = \cos i_D \cos i_S \pm \sin i_D \sin i_S \cos \Omega_T$$

$$\sin i = \sqrt{1 - \cos^2 i}$$

$$\cos \Omega_1 = \mp (\cos i_S - \cos i_D \cos i)/\sin i_D \sin i$$

$$\sin \Omega_1 = \sin i_S \sin \Omega_T / \sin i$$

$$\cos \omega_1 = (\cos i_D - \cos i_S \cos i)/\sin i_S \sin i$$

$$\sin \omega_1 = \sin i_D \sin \Omega_T / \sin i$$

$$\omega = \pm (\omega_S - \omega)$$

where, when transformation occurs

| FROM/TO | EEP/ECL | EEP/MOP | MEP/ECL | MEP/MOP |
|---|---|---|---|---|
| $\Omega_T$ = | $\Omega_s$ | $\Omega_s - \Omega_{\mathbb{C}}$ | $\Omega_0 + \Omega_1 - 1$ | $\Omega_0 + \Omega_1 - 1$ |
| | | | $\Omega_s - 180 - \Omega$ | $\Omega_s - 180 - \Omega$ |
| $\Omega_1$ = | $\Omega$ | $\Omega + \omega_{\mathbb{C}}$ | $\Omega - \Omega - 180$ | $\Omega$ |
| SIGN | UPPER | | LOWER | |

| FROM/TO | ECL/EEP | MOP/EEP | ECL/MEP | MOP/MEP |
|---|---|---|---|---|
| $\Omega_T$ = | $\Omega$ | $\Omega + \omega_{\mathbb{C}}$ | $\Omega - \Omega - 180$ | $\Omega$ |
| $\Omega_1$ = | $\Omega_s$ | $\Omega_s - \Omega_{\mathbb{C}}$ | $\Omega_0 + \Omega_1 - 1$ | $\Omega_0 + \Omega_1 - 1$ |
| SIGN | LOWER | | UPPER | |
| $i_D$ | $\epsilon$ | $i_\oplus$ | I | $I + i_{\mathbb{C}}$ |

The disturbing body position relative to the reference in the disturbing body plane is then $\Gamma_D$ where

$\Gamma_D$ = $\theta_\odot - \Omega$ for solar perturbations

= $\theta_{\mathbb{C}} + \Gamma' - \Omega$ for earth/lunar perturbations

$\theta_\odot = \theta_T (L - \Gamma)$, $\theta_{\mathbb{C}} = \theta_T (\mathbb{C} - \Gamma')$

$\theta_T$ = a function which transforms mean to true anomaly.

L, $\Gamma$, $\mathbb{C}$, $\Gamma'$ are the almanac representations for the sun's and moon's mean longitudes of position and perigee, respectively.

In the case of lunar satellites, the earth-moon distance is neglected in computing solar perturbations; hence, the moon relative to the sun appears to be in the earth's position.

Thus only five osculating elements of the orbit are required to determine stability of the orbit; here, stability implies a safe upper and lower limit on perigee radius. SOME (Ref. 2) provides six options of inputting the position and velocity at epoch.

For lunar satellites, physical and optical librations are determined from the equations within Ref. 4, as well as the elements of the sun and moon. Greenwich hour angle (right ascension of Greenwich) is then computed from

$$GHA = L + 180 + \omega_{\oplus} t$$

The secular perturbations due to asphericity of the reference body are determined from the following:

(1) Secular

$$\Delta\omega_s = B \cdot (2 - 2.5 \sin^2 i_s)$$

$$\Delta\Omega_s = -B \cdot \cos i_s$$

(2) Long-period secular (lunar orbits only) (Ref. 5)

$$\Delta\omega_s = -C (1 - 2.5 \sin^2 i_s) \cos 2\Omega_0$$

$$\Delta\Omega_0 = C \cos i_s \cos 2\Omega_0$$

$$\Delta i_s = C \sin i_s \sin 2\Omega_0$$

$$\Delta a = \Delta e = 0$$

where

$$B = 540 \cdot J \left( \frac{R_E/a}{1 - e^2} \right)^2 \frac{\text{degree}}{\text{orbit period}}$$

$$C/B = K/J$$

$$J_{\leftmoon} = 0.2125 \times 10^{-3}$$

$$K_{\leftmoon} = 0.0188 \times 10^{-3}$$

$$J_{\oplus} = 1.0823 \times 10^{-3}$$

In the case of lunar orbits, a correction is made for the ecliptic precession of the moon's equatorial plane by transforming the satellite orbital plane to the ecliptic, precessing the moon's equatorial plane, and then transforming the satellite orbit plane to the moon's equatorial plane.

## C. RESULTS

The equations of Section B were incorporated into a program, SOME (Ref. 2) and a few comparative runs were made to establish the effects of the linear theory. The elements for these orbits are presented in Table I.

Figure 4 presents a comparison between SOME and the Launch Window Program (based on mathematics of Ref. 6) for three EGO orbits (Ref. 7). The slight oscillations in the SOME results are due to the long-period lunar effects. In the Launch Window Program, these periodic effects are eliminated by integrating the lunar effects over the moon's orbital period. SOME is a refinement of SOLUN (see Ref. 1) and it yields much better results as can be seen by comparing Fig. 4 with Fig. II-7 of Ref. 1.

Figures 5 and 6 depict a good comparison between SOME and the program, ITEM (Ref. 8). The difference in impact times is approximately five orbital revolutions. The lunar comparison yields better results than the EGO comparisons due to lower eccentricity. The inclinations are graphically coincident. As analytically concluded in Ref. 5, the lunar polar orbit is unstable.

For 7094 computation, a year's orbit consumes approximately 9 sec for an integration interval of one day. Overall, the linear theory offers a convenient, inexpensive means for computing satellite elements. As implied in Ref. 1, however, one must question the linear theory for eccentricities greater than 0.9.

## D. ORBITAL STABILITY

It is often desired, in the case of many satellite mission requirements, to know what injection conditions must be had to ensure a "healthy" lifetime (orbital stability dependent upon periapsis history) without becoming involved in an expensive parametric study.

A close look at Eqs 2 of Section B shows that the most dominant term, the trend-setting term, for the elements is the linear or $\Delta\Gamma_D$ term. A modified form of this term for the periapsis and the argument of periapsis function from Section B, Eqs 2, is:

$$\omega - \omega_0 = \Delta\omega = -K\left[ (2 + 5\cos^2\omega)\sin^2 i - 1\right] T,$$

$$K = \frac{3}{4}\left(\frac{\mu}{a^3}\right)_D \frac{\sqrt{1-e^2}}{n}$$

$$q - q_0 = \Delta q = - K_1 \left[\sin 2\omega \sin^2 i\right] T, \quad K_1 = \frac{5}{2} K \cdot ae$$

In the case of a three-body problem, stability is ensured if $0 < i < 180$, and furthermore if $\omega$ is in the second or the fourth quadrant. If i is close to its limits, i.e., $i \approx 0°$ or $180°$, $\omega$ should initially be equal to 135° or 315°. If $\omega$ lies close to the quadrant boundaries, it is desired to have $\Delta\omega$ possess a positive slope when at the lower boundaries (90° and 270°) and a negative slope when at the upper boundaries (180° and 360°).

These constraints can be satisfied from the test condition at injection that

$$\frac{d\Delta\omega}{dT} \lessgtr 0, \text{ where } \lessgtr \text{ implies greater than or less than.}$$

Then $\sin i \lessgtr (2 + 5 \cos^2 \omega)^{-1/2}$, which yields

| | |
|---|---|
| $\omega = 90°$ or $270°$ | $0 < i < 45°$<br>$135° < i < 180°$ |
| $\omega = 180°$ or $360°$ | $22° < i < 158°$ |

In the case of a four body problem, such as an earth or a lunar satellite, the general trend is determined from the sums of the two general-trend terms. In this case, the relative influences of the $(\mu/a^3)_D$ term must be studied. For example, this latter term is approximately equal to:

| Sun | Earth | Moon |
|---|---|---|
| $3.97 \times 10^{-14}$ | $7 \times 10^{-12}$ | $8.6 \times 10^{-14}$ |

Thus for an earth orbit, the disturbing bodies will contribute almost equivalent effects, and the general trend must be observed in the light of the sum of both effects, using the foregoing equations.

For a lunar orbit, the earth is the more influential force, and since the sun's effects can be neglected, the problem reduces to the three-body problem analyses above.

There are, however, four points one should bear in mind when performing the foregoing analyses

(1) That $\omega$ and i are measured relative to the disturbing body plane and, hence,

(2) $\omega$ and i are reflected through the position of periapsis and position of ascending node in the orbit's reference body.

(3) That the analysis should be performed on the initial set of elements.

(4) Should be relied upon only for stability to some time T that is not very large; for at some large T the trend may reverse itself. A computer run will establish the stability to a much better degree at this time as well as validate the initial analytical approach.

For orbits which are close to the reference body, i.e., e is very small, the asphericity effects must be considered in $\Delta\omega$. Again from section B,

$$\Delta\omega = - K_2 \left[ 2.5 \sin^2 i_s - 2 \right] T, \quad K_2 = \frac{540\ J}{\tau} \left( \frac{R_E/a}{1 - e^2} \right)^2$$

For stability then, if $\omega$ is close to the quadrant boundaries, it is desired to constrain $i_s$ as follows:

| | |
|---|---|
| $\omega = 90°$ or $270°$ | $0 < i_s < 63.5°$ |
| | $116.5 < i_s < 180°$ |
| $\omega = 180°$ or $360°$ | $63.5 < i_s < 116.5$ |

In the case of an earth satellite, even at high eccentricities, the oblateness effect is at times equivalent in magnitude to the extraterrestrial perturbations; for a lunar satellite, the asphericity and the earth perturbations are of the same order; hence, effects of asphericity must be observed in light of the extraterrestrial perturbations.

## E. LUNAR SATELLITE DATA

Figures 7, 8 and 9 provide relationships between the osculating elements, a and e, and the injection conditions, $V_P$ $H_P$, $V_A$ and $H_A$ whenever launch occurs from the lunar surface. (Data supplied by NASA-MSFC, Huntsville.)

## F. REFERENCES


1. Extension Effort for Orbital and Lunar Flight Handbooks, ER 13189-II, Martin Company, Space Systems Division, Baltimore, November 1963.

2. Summary and Utilization Report for SOME (ZB-044) ER 13668, Martin Company, Space Systems Division, Baltimore, November 1963.

3. Moe, M.. "Solar-Lunar Perturbations of the Orbit of an Earth Satellite," Space Technology Laboratories, STL-TR-60-0000-00871, 29 September 1959, Reprinted ARS Journal, May 1960.

4. Explanatory Supplement to the Astronomical Ephemeris . . . . ., Joint Authors, Her Majesty's Stationery Office, London, 1961.

5. Lorell, J., "Lifetimes of Lunar Satellites," Space Programs Summary No. 37-15, Volume IV, Jet Propulsion Laboratories, 30 June 1962.

6. Musen, P., "A Discussion of Halphen's Method . . . . . .Bodies, Part 1," NASA TR-176, 1963.

7. Montgomery, H. E., Paddack, S. J., "S-49, EGO Launch Window and Orbit," NASA (GSFC) X-640-63-119, 1 July 1963.

8. Shaffer, F., et al, "Interplanetary Trajectory Encke Method (ITEM) Program Manual," NASA (GSFC) X-640-63-71, 1 May 1963.

TABLE I

Initial Conditions for Orbits

| Definition | EGO | Lunar |
|---|---|---|
| Eccentricity | 0.893 | 0.501 |
| Semimajor axis (km) | 62067. | 3685. |
| Inclination | 30.78 | 89.44 |
| Azimuth | 66.36 | 0.56 |
| Periapsis altitude (km) | 269.1 | 100 |
| Argument of periapsis | -45.6 | 0. |
| Latitude | -20.28 | 0. |
| Longitude | 111.90 (E) | 6.10 |
| Injection epoch--date<br>--hour (U.T.) | 4/14/64<br>5, 12, 16 | 1/06/64<br>0. |
| Period (hr) | 42.75 | 5.58 |

ILLUSTRATIONS

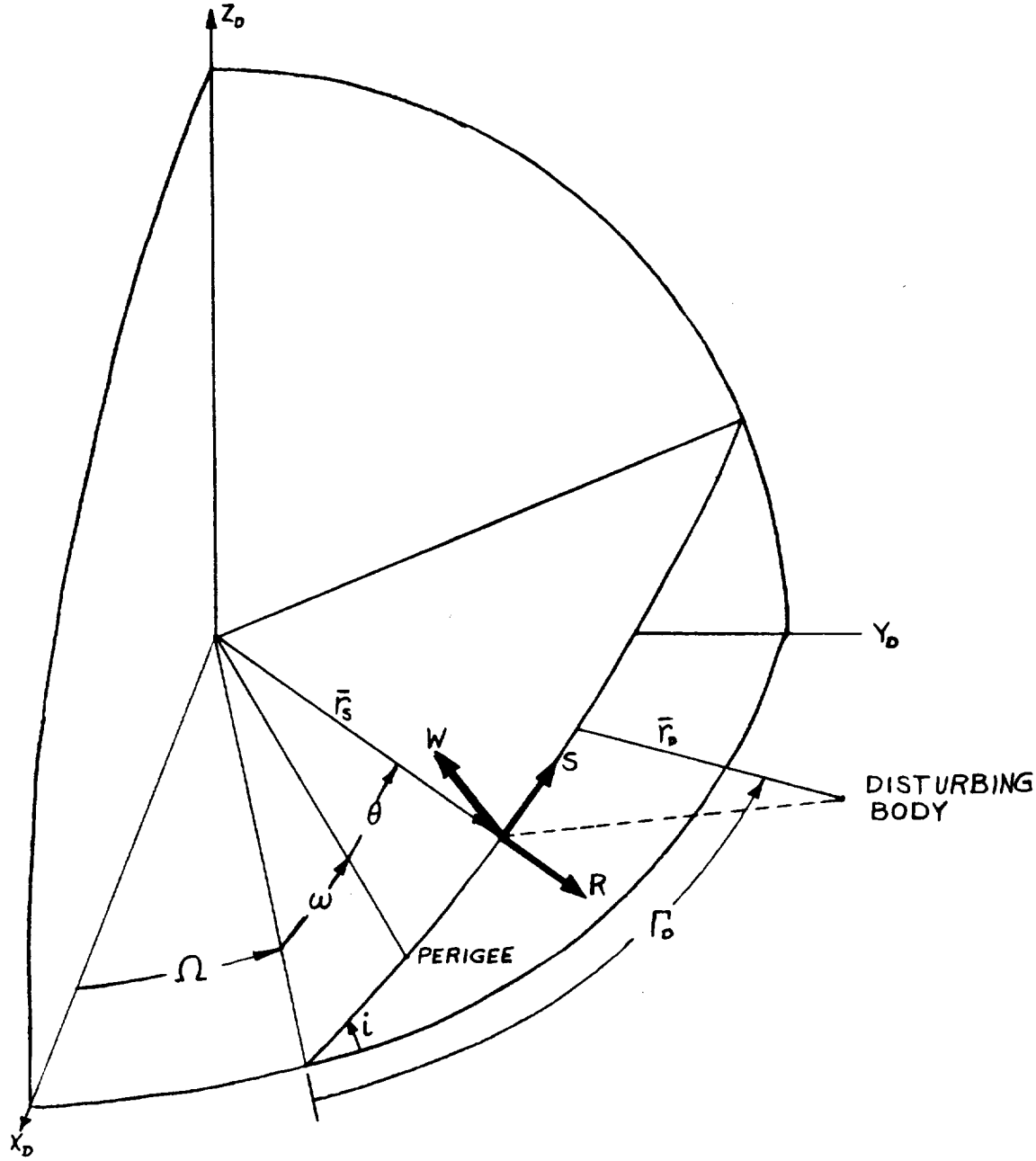


Fig. 1. Coordinate System

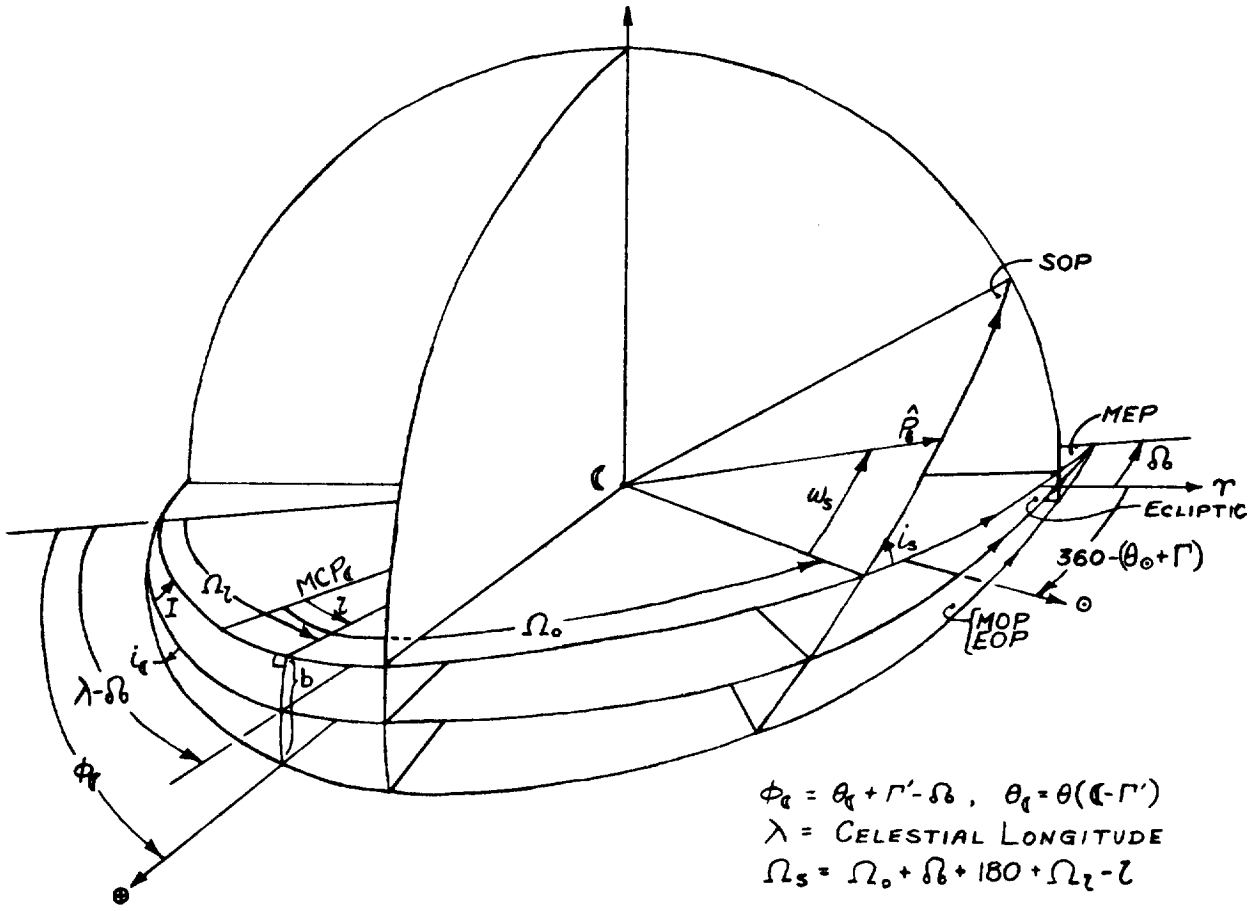


Fig. 2. Lunar Orbit Geometry

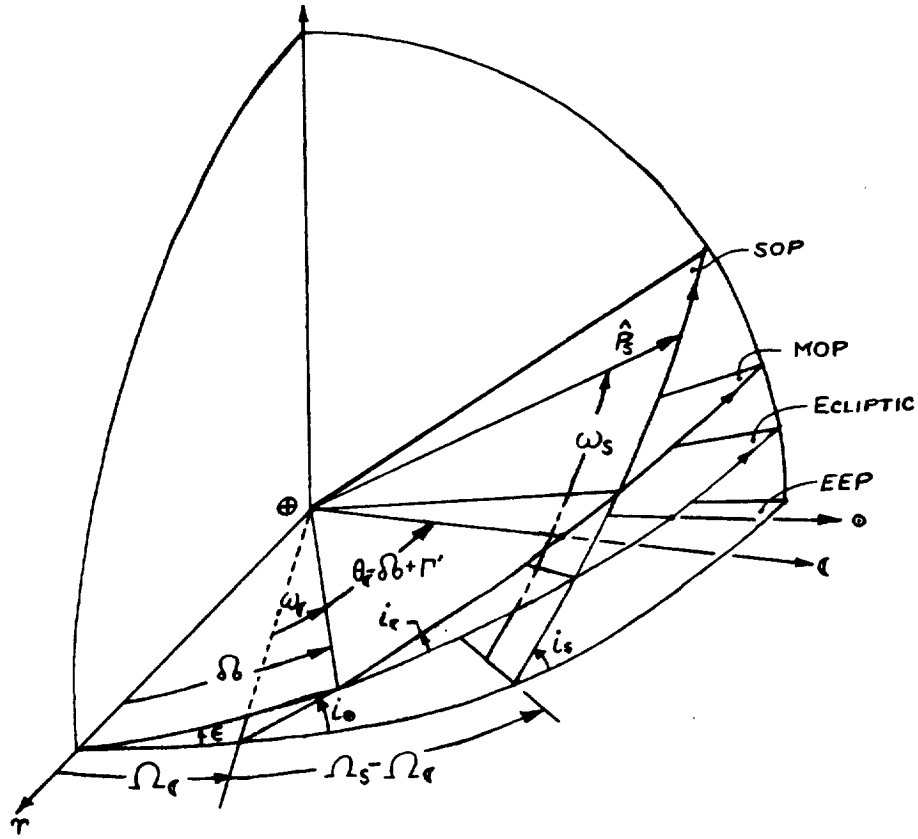


Fig. 3. Earth Orbit Geometry

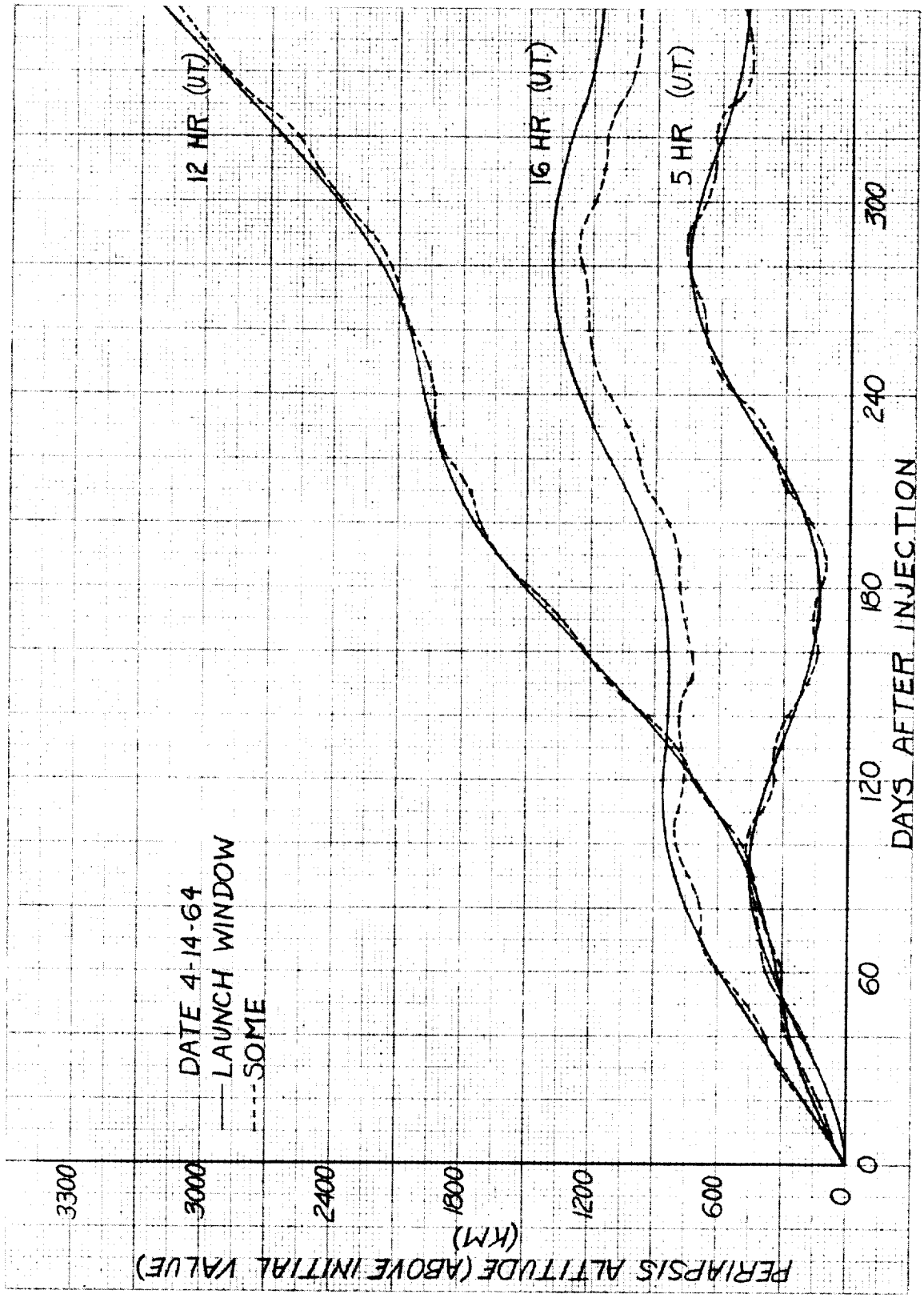


Fig. 4. Periapsis Comparison-EGO Orbits

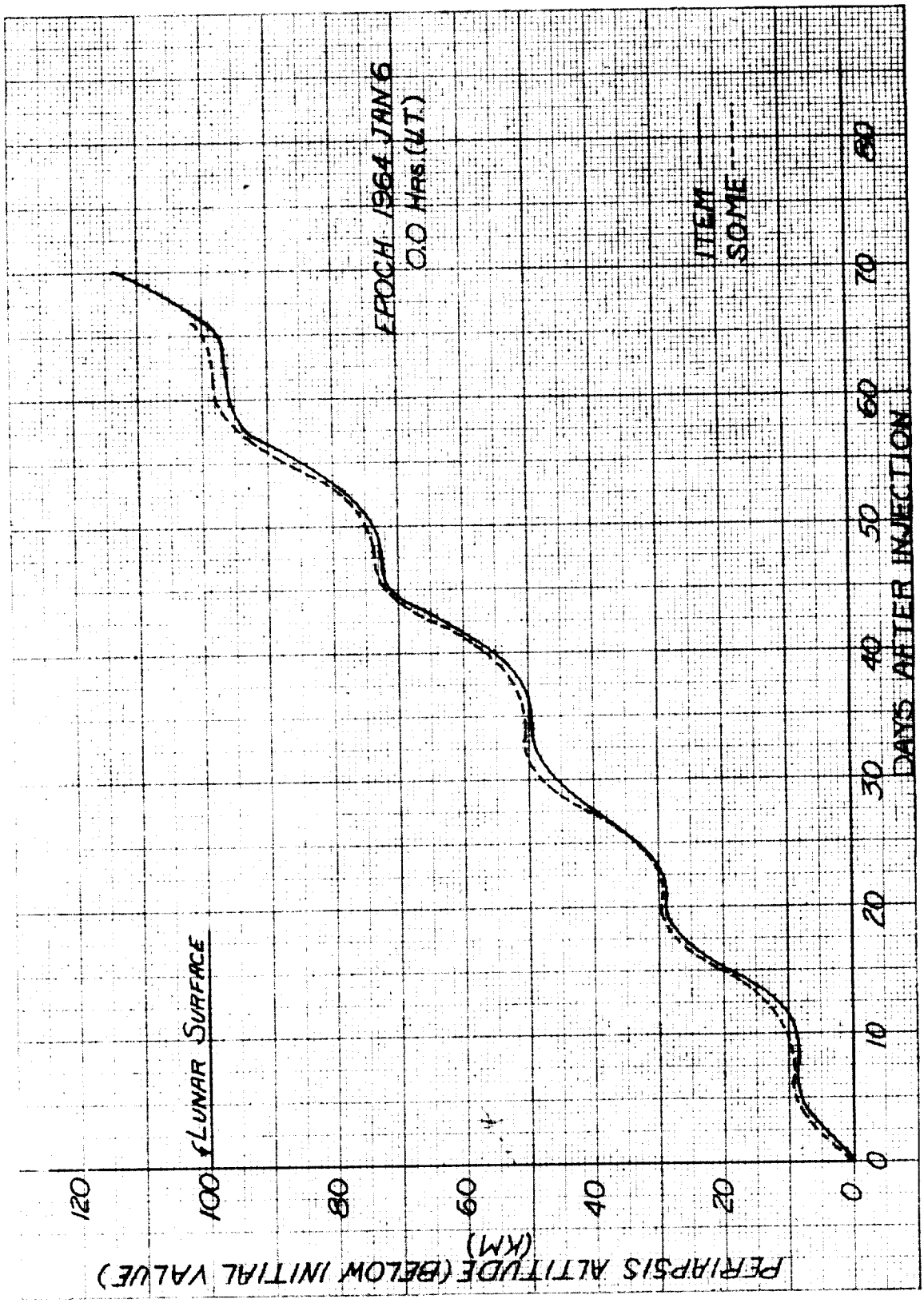


Fig. 5. Periapsis Comparison Lunar Orbit

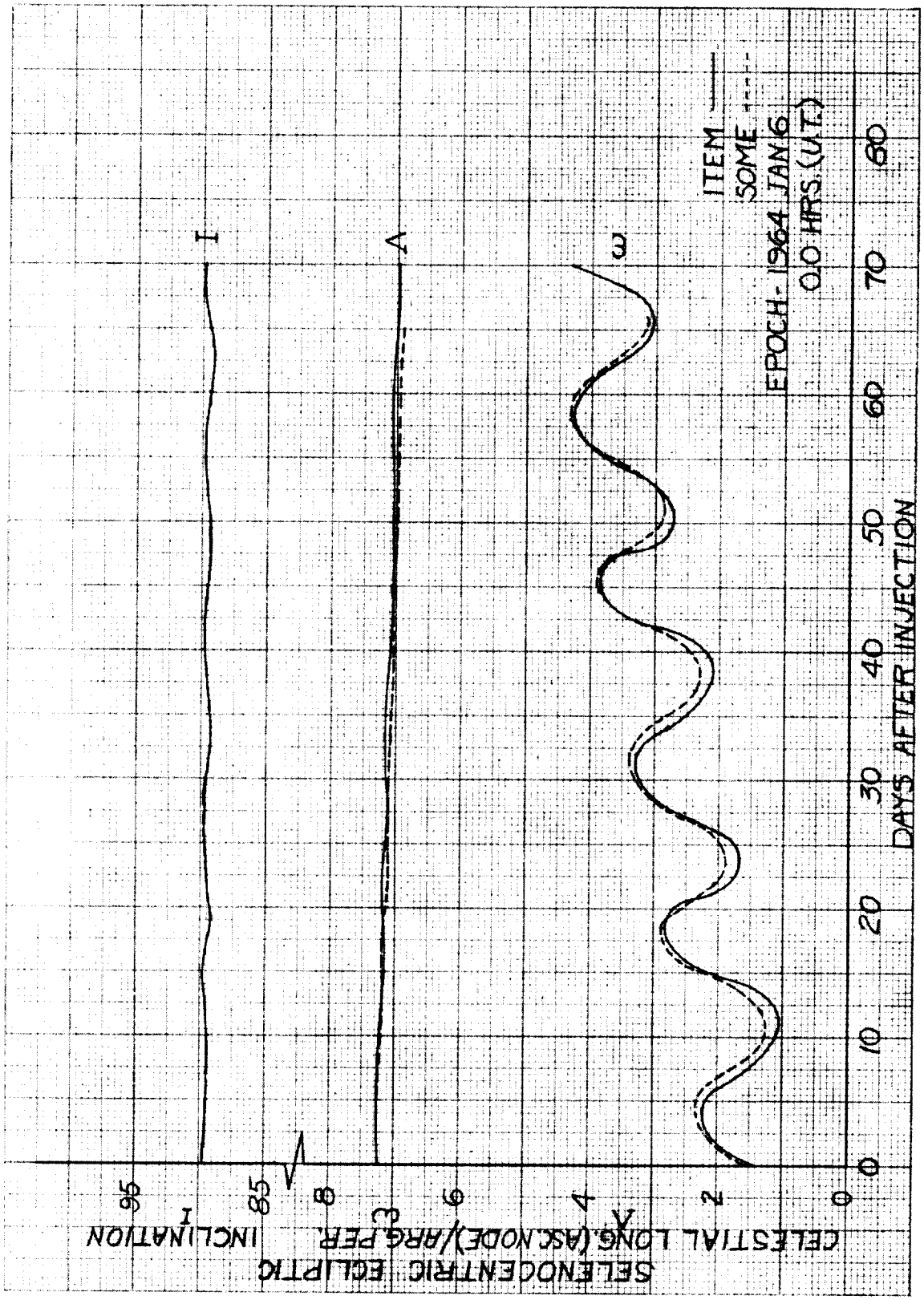


Fig. 6. Orientation Comparison Lunar Orbit

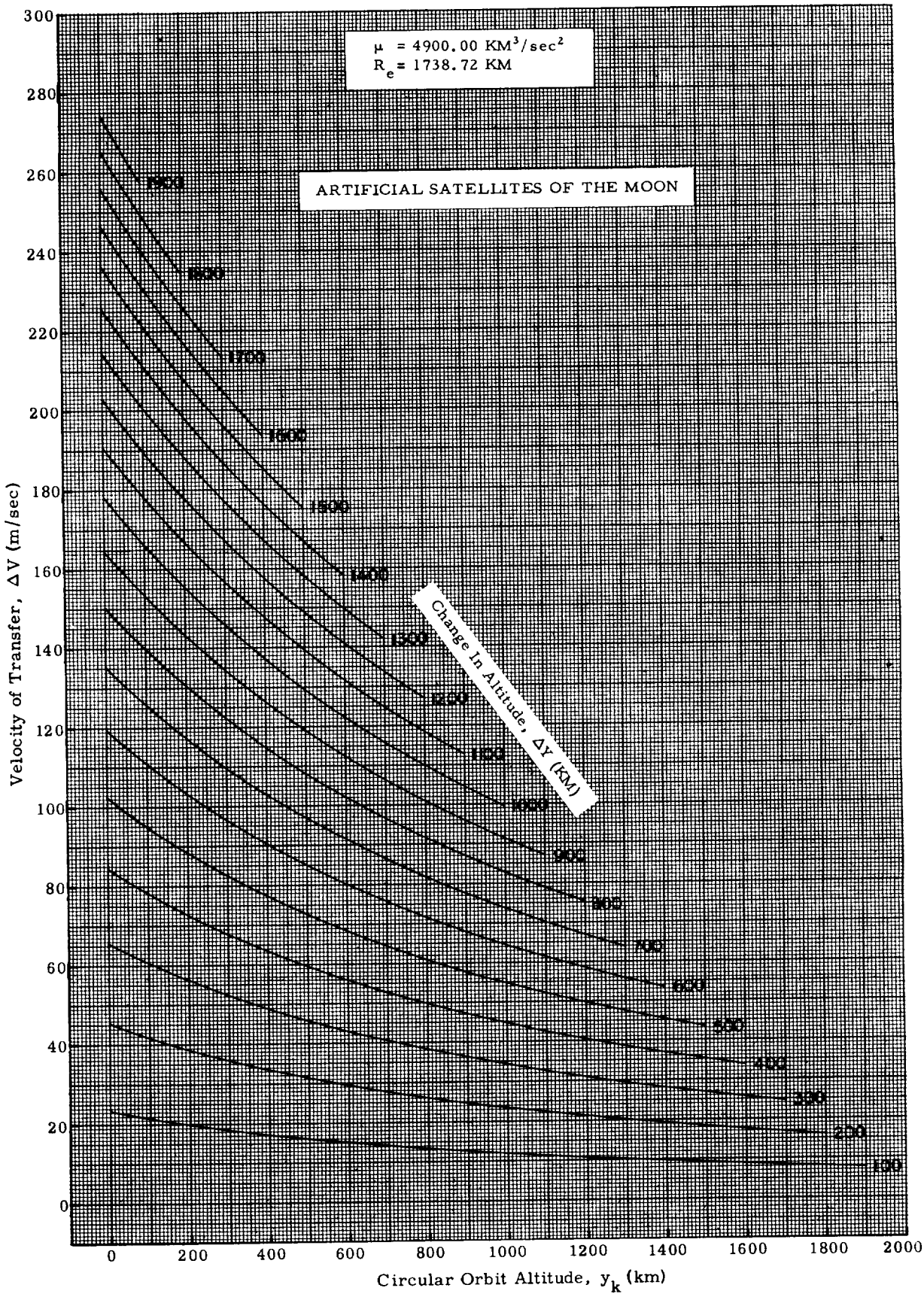


Fig. 7. Velocity Required for Transfer from a Circular to an Eccentric Orbit Versus Circular Orbit Altitude with Change in Altitude (ΔY) as a Parameter

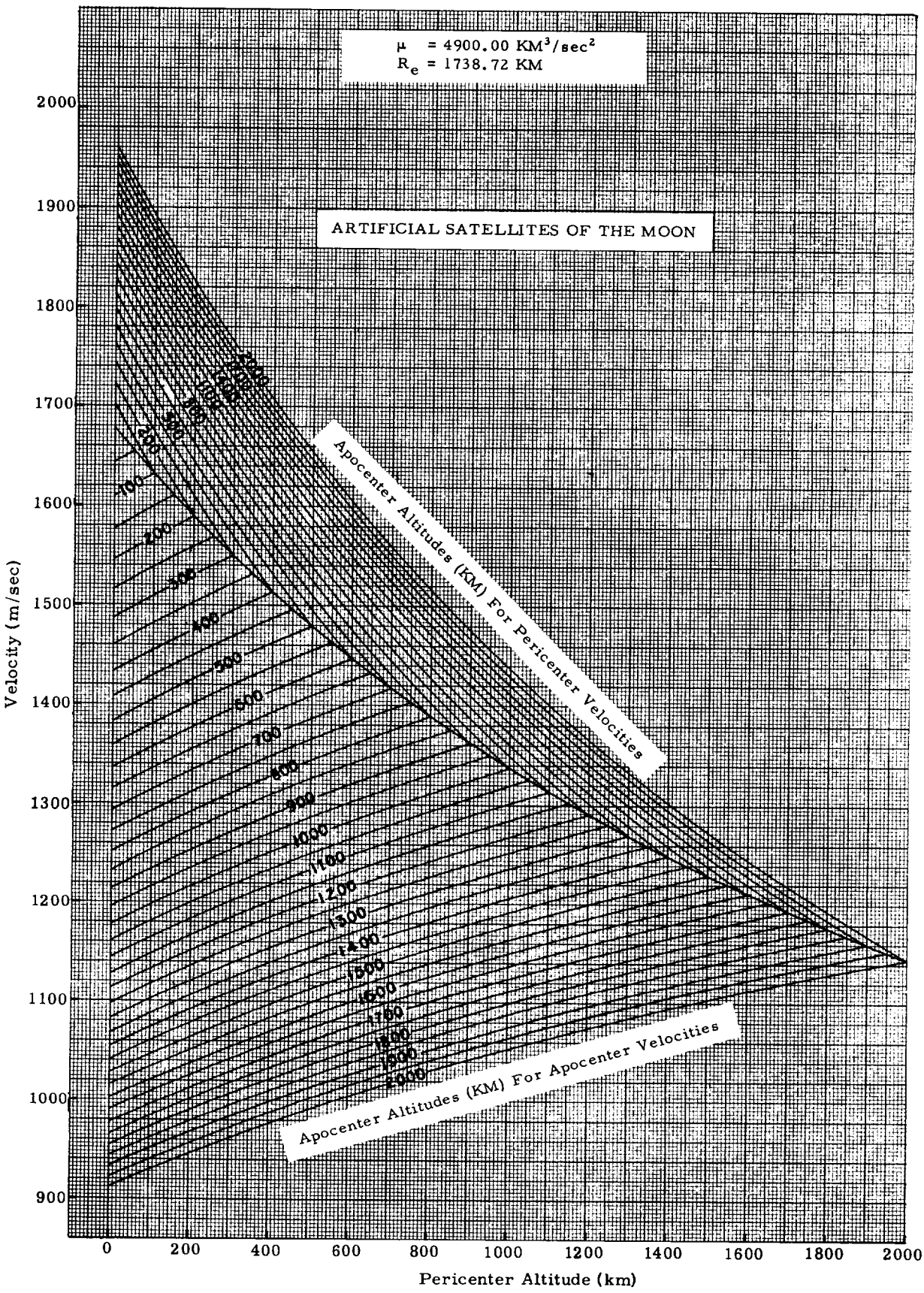


Fig. 8. Velocity (M/sec) Versus Pericenter Altitude (KM) with Apocenter Altitude (KM) for Pericenter Velocities and Apocenter Altitude (KM) for Apocenter Velocities as Parameters

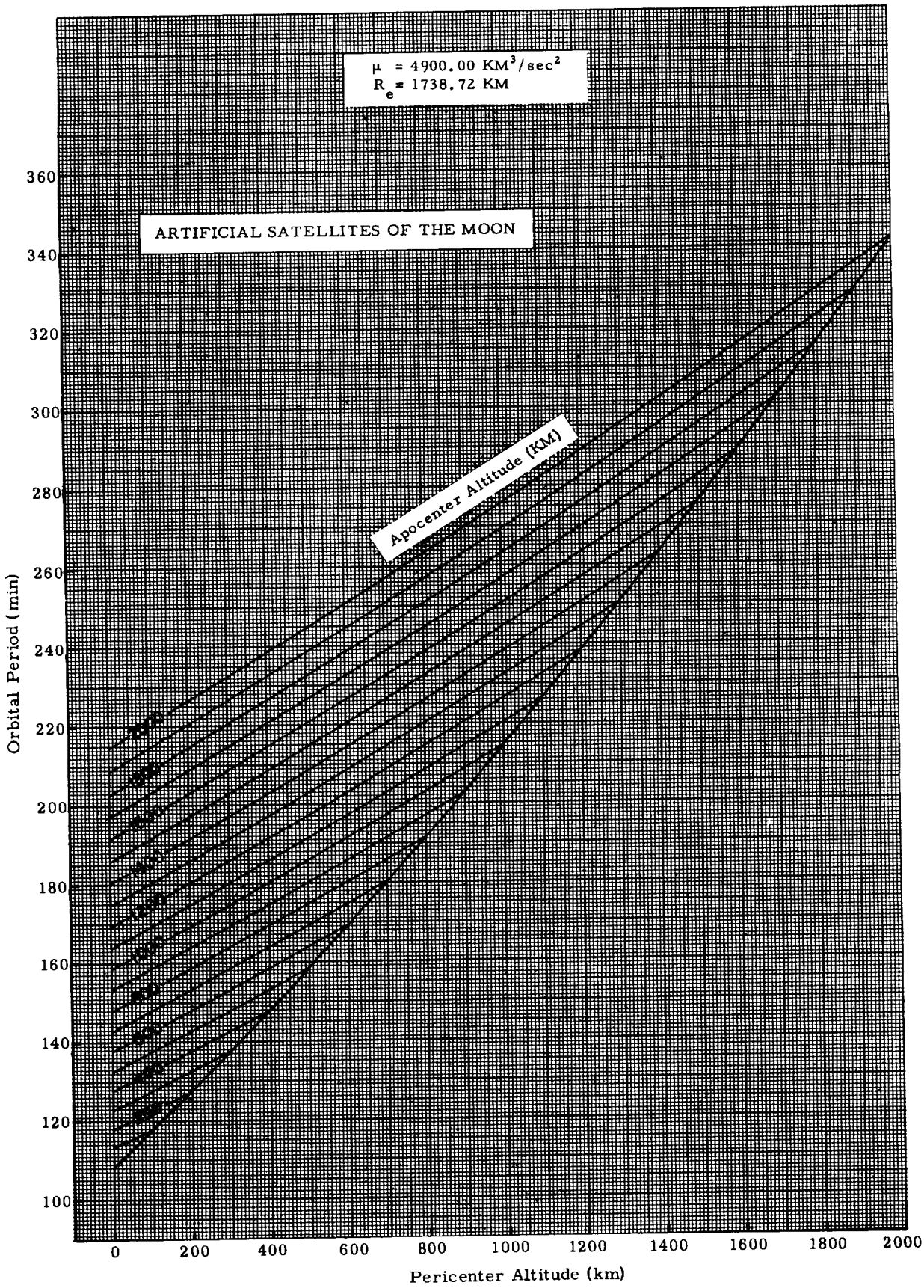


Fig. 9. Orbital Period (min) Versus Pericenter Altitude (KM) with Apocenter Altitude (KM) as a Parameter

# V. ORBITAL OPERATIONS
# (PREPARED FOR USE AS AN ADDENDUM TO LUNAR FLIGHT HANDBOOK)

The subject contract (NAS 8-5031) requests that a chapter entitled "Orbital Operations" be prepared for use as an addendum to the Lunar Flight Handbook. The main subject matter of this chapter deals exclusively with the initiation of translunar and transearth flights from parking orbits around the parent body. Emphasis is placed upon orbital and inject-on-time departure windows, with a detailed discussion on various departure techniques and their applicability to different missions. The new chapter is presented now as a complete entity without further explanation.

# ADDENDUM I

## ORBITAL OPERATIONS

Prepared by
F. A. Santora and R. G. Salinger

| | | Page |
|---|---|---|
| A. | Earth Orbit Operations | 2 |
| B. | Lunar Orbit Operations | 13 |
| C. | Mission Implications | 25 |

# ORBITAL OPERATIONS

It is inevitable that man will undertake more encompassing, more intricate and more demanding missions as experience, confidence and the passing of time will dictate. It is with this forethought that the present chapter is written and also with the hope that it will serve as an aid in firming future mission concepts.

The term "orbital operations" is generally thought of as those tasks and activities conducted in orbit as a natural or required sequence necessary to fulfilling the mission. Such operations include rendezvous, docking, refueling, repair, crew rotation, checkout, countdown and major propulsion phases.

In order to achieve such an operational capability, spatial support facilities are required and may consist of manned stations equipped with checkout computers, instrumentation and necessary repair equipment. In addition, astrotugs, spare parts, and navigation, tracking and communication links would be provided by a support station. Furthermore, the operations complex will be completed by specially designed support "shuttle" vehicles which can be employed as "lifelines" from the "ground" to the mission vehicle and/or the manned support station.

Thus, one can see that the degree of complexity and sophistication related to orbital operations can become quite high and that an analysis or treatment of all factors and ramifications associated with various missions would become very involved. Therefore, the subject chapter concentrates only on the major flight mechanics aspects which are prime factors in relegating and establishing operational procedures for lunar missions. As will be seen subsequently, these main aspects revolve around the determination of departure windows that reflect the imposition of various mission constraints.

There are at least ten different launch or departure windows that are associated with orbital operations; they are categorized below from Ref. 1. Some are impractical, such as the "direct" translunar injection window, No. 2 (Section C-2 of Chapter V), and others, such as the translunar launch window, No. 3 (Section B of Chapter V), are an important phase of a lunar mission. However, the most relevant windows that will afford the greatest appreciation of orbital operations are concerned with the departure from a parking orbit about the parent body, Nos. 4 and 9.

Earth-to-Earth-Orbit Launch Window (No. 1). This window is defined as the time available for initiating the launch of a given vehicle from a site on the Earth's surface in such a manner that its resultant boost maneuvers will put it into an Earth orbit of a given altitude, inclination, and orientation with respect to inertial space, etc. This time interval is further constrained by the vehicle's payload, velocity capability, and range safety considerations.

Direct Injection Translunar Launch Window (No. 2). This window is defined as the time available for initiating the launch of a vehicle from a site on the Earth's surface in such a manner that, after a series of burning phases (staging operations), an acceptable (i. e., satisfying specified end conditions in selenocentric space) translunar trajectory results. In this mode of operation translunar injection conditions are attained at burnout of last stage; accordingly, at no time in the boost trajectory is the vehicle in orbit.

Translunar Launch Window (No. 3). This window is defined as the time available for initiating the launch of a vehicle from a site on the Earth's surface into a translunar trajectory using the following series of maneuvers:

(1) The vehicle goes into a parking orbit about the Earth.

(2) The vehicle coasts in parking orbit to a point at which initiation of a translunar trajectory is possible.

(3) Injection into the translunar trajectory is made.

In general, this launch window is less restrictive than the direct injection translunar launch window mentioned above, the primary limitation being range safety considerations. In this case the parking orbit phase permits a great relaxation of the rather stringent geometrical constraints associated with the direct injection launch window.

Translunar Orbital Departure Window (No. 4). This window is defined as the time available for initiating the launch of a vehicle from an Earth orbit with the vehicle having the velocity capabilities to make the plane changes required to achieve a translunar trajectory. Implicit in the definition of this window is the assumption that injection always takes place at the optimum point in orbit.

Translunar Inject-on-Time Window (No. 5). This window is defined as the time period in each orbit of the mission vehicle during which the vehicle has the velocity capability to make the required flight path angle changes to depart from Earth orbit into a translunar trajectory. It differs from the translunar orbital launch window in that injection does not have to take place at the optimum point in orbit.

Moon-to-Lunar Orbit Launch Window (No. 6). This window is defined as the time available for

initiating the launch of the vehicle from a site on the moon's surface in such a way that its resultant boost maneuvers will put it into a lunar orbit of a given altitude, inclination, orientation with respect to inertial space, etc. This time period is constrained by vehicle payload and velocity capabilities.

Direct Injection Transearth Launch Window (No. 7). This window is defined as the time available for initiating the launch of a vehicle from a site on the moon's surface in such a way that, after a series of burning phases (staging operations), an acceptable (i.e., satisfying specified end conditions in geocentric space) transearth trajectory results. In this mode of operation, transearth injection conditions are attained at burnout of the last stage. Accordingly, at no time in the boost trajectory is the vehicle in orbit.

Transearth Launch Window (No. 8). This window is defined as the time available for initiating the launch of a vehicle from a site on the moon's surface into a transearth trajectory using the following series of maneuvers:

(1) The vehicle enters a parking orbit about the moon.

(2) The vehicle coasts in parking orbit to a point at which initiation of a transearth trajectory is possible.

(3) Injection into the transearth trajectory occurs.

In general, this launch window is less restrictive than the direct injection transearth launch window.

Transearth Orbital Departure Window (No. 9). This window is defined as the time available for initiating the launch of a vehicle from a lunar orbit with vehicle having the velocity capabilities to make the plane changes required to achieve a transearth trajectory. Implicit in the definition of this window is the assumption that injection always takes place at the optimum point in orbit.

Transearth Inject-on-Time Window (No. 10). This window is defined as the time period in each lunar orbit of the mission vehicle during which the vehicle has the velocity capability to make the required flight path angle changes to depart from lunar orbit into a transearth trajectory. It differs from the transearth orbital launch window in that injection does not have to take place at the optimum point in orbit.

Section C of Chapter V touches on this very same approach but is very limited in scope and treatment. In fact, Section C only qualitatively discusses operations in an earth orbit and presents a meager amount of numerical data. No specific treatment is given to orbital operations from the moon; however, Chapter IX catalogs a large quantity of departure requirements.

Lunar missions and their planning have become of prominent interest with the advent of the Ranger, Surveyor and Apollo projects. Future manned missions, such as lunar logistics, lunar exploration and lunar surveillance, now envision extended stay times in parking orbits both at earth and at the moon. The use of such parking orbits depends on the mode of operation for conducting the missions. For example, rendezvous and assembly may be required prior to departing for the moon; then, upon arrival at the moon, supplies and personnel may have to be transferred to the lunar surface. The questions arise: In normal operations, what is the available time to complete work tasks? What is the wait time before the next opportune go time if tasks cannot be completed on time, etc.? Naturally, the questions also arise as to what the consequences if the time in parking orbit must be prolonged in the event of an unplanned delay or malfunction. Can the mission be successfully carried through and at what cost?

It is important to note that a "missed" injection can be unintentional or completely deliberate. In the former case, it may be impossible to inject at the proper moment because of system malfunctions, incomplete checkouts, etc., and the spacecraft must wait until the next opportune go time. Deliberate postponement of injection may be dictated by the mission itself. For example, consider a logistics vehicle that arrived from earth and entered a lunar orbit. While in this orbit, the shuttling" of supplies to the lunar surface may take longer than anticipated, thereby delaying the transearth injection. As another example, assume that the following mission specification exists: "Rendezvous with earth orbiting space station upon return from the moon." It now becomes obvious that injection must be delayed until it is possible to establish a transearth trajectory which arrives coplanar with the space-station's orbit at earth.

Thus, the problem at hand is to determine mission departure windows and their requirements. Orbital departure windows connote the available length of time that missions can be originated from a parking orbit with a given propulsion allowance. For lunar missions, departure window studies can be divided into two areas: those related to earth departures and those associated with lunar departures.

In all of the above cases, it becomes mandatory to determine the flexibility of the spacecraft to adjust or compensate for these delays. Thus, departure windows and their frequencies must be established which take into account the gravitational and geometrical constraints but which are of such a generalized nature that they represent various types of missions.

## A. EARTH ORBIT OPERATIONS

In the initiation of a lunar mission, the spacecraft must acquire a specific position and velocity vector at the time of translunar injection. After injection, the vehicle is in ballistic flight until arrival at the moon at which time propulsive maneuvers are executed to acquire a specified landing site or lunar orbit. The flight can also be completely ballistic (except for midcourse corrections) in which case the specification is either a flyby or a lunar impact mission.

Prior to attaining the correct injection conditions, the spacecraft will most likely be in a parking orbit around the earth. The establishment of such a parking orbit allows a greater mission flexibility by providing:

(1) Injection capability any time of the month, twice a day (for missions initiated from the earth's surface).

(2) Injection capability for many orbit passes (for missions initiated from an earth orbit).

(3) Time for final onboard and ground checkouts before translunar injection is initiated.

(4) The same ascent and injection flight profile (nominally) for any mission.

Whether the mission is delayed by design or by circumstance, mission flexibility can be enhanced if provisions are incorporated to allow for such contingencies (Ref. 2).

## 1. Geometrical Considerations (Earth Departure)

Consider first a nominal trajectory that satisfies a specified lunar mission (i.e., a specific lunar miss-distance or landing point, a desired lunar approach direction, a given flight time, etc.).

Prior to establishing the translunar trajectory, the spacecraft is located in an earth parking orbit plane as shown in the following sketch which has been prepared to aid in the visualization of the trajectory parameters associated with lunar missions.

The earth parking orbit plane (POP) is inclined to the moon's orbital plane (MOP) by an angle $i_{VTL}$. The MOP is a plane of symmetry and is chosen as a reference plane because it generalizes trajectory data and lends itself readily to the clarification of the problem. At the time of the nominal injection ($t_0$), the spacecraft is positioned an angular distance, $\psi_0$, from the ascending node of the parking orbit and has a flight path angle of $\gamma_0$ and an injection velocity of $\vec{V}_0$. Immediately after inspection, the translunar flight plane has the same inclination to the MOP as did the POP, namely, $i_{VTL}$. The following sketch also indicates the position of the moon at $t_0$. Note the included angle $\phi^*$ between the parking orbit nodal line and the vector position of the moon ($\vec{R}_{\oplus\mathbb{C}}$). This angle will be referred to as the moon lead angle throughout the discussion; it plays a significant role in launch window determination. At time $t_p$, the vehicle arrives at the moon (i.e., at pericynthion) with certain approach geometry. The sketch depicts the moon's location at this time, together with the approach orientation. More specifically, the vehicle approaches the moon in a flight plane inclined to the MOP by an angle $i_m$. The flight plane itself is oriented by the

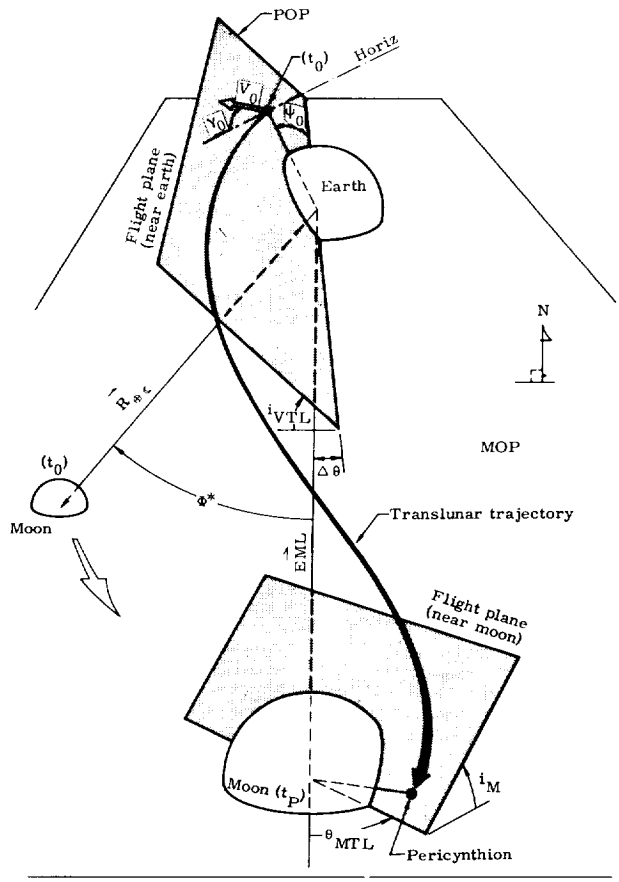


Translunar Trajectory Geometry

angle $\theta_{MTL}$, which is measured from the earth-moon line ($\overrightarrow{EML}$) to the descending node of the arrival trajectory (or measured eastward from the moon-earth line ($\overrightarrow{MEL}$) to the ascending node of the arrival trajectory). An interesting phenomenon of lunar trajectories employing this model is the fact that the included angle $\Delta\theta$ between the POP nodal line and the $\overrightarrow{EML}$ is small in magnitude--approximately 1° for a wide spectrum of missions. The importance of this point will be borne out presently.

Thus far, the pertinent geometry of a nominal lunar mission has been presented (also see Chapter VI). For further details, reference can be made to actual data from the trajectory catalogue given in Chapter IX. These data represent the "approach" class of trajectories (as defined in Chapter IV), which is entirely general in nature since the "circumlunar" class (Chapter VI) is a special approach case. The data presented are the translunar injection velocity ($V_0$), the required braking impulse ($\Delta V$) to establish a lunar parking orbit,* the flight time ($t_p$) from injection

*Braking maneuver takes place at pericynthion, thereby establishing a circular orbit.

to pericynthion and ($\psi_0$) the translunar injection position as a function of the translunar inclination ($i_{VTL}$). $\theta_{MTL}$ is the field parameter in these figures and sets of data are derived for various lunar approach inclinations ($i_m$).

Before proceeding, it is well to mention the fact that launches from an earth parking orbit inclined approximately 30° to the equator will restrict the translunar inclination thusly: $-60° \leq i_{VTL} \leq 60°$. From the trajectory catalogue of Chapter IX it can be seen that practical flight times for this $i_{VTL}$ range lie between 50 and 100 hr, otherwise velocity requirements may become too large for the former and trajectory sensitivities too high for the latter. Furthermore, $\theta_{MTL}$, the lunar orbit orientation, will range from 60° to 150° depending on $i_{VTL}$. A $+i_{VTL}$ is an "inject north" case as depicted in the sketch above whereas $-i_{VTL}$ is designated as an "inject south" and departs from earth on a southerly course relative to the MOP. A more precise and complete definition is given in Chapter VI.

Thus far, the "static" trajectory picture has been given, and it now becomes necessary to examine the dynamic situation wherein the geometric relationships between the vehicle's parking orbit plane, the moon's orbital plane (MOP), the moon's position, and the earth's equatorial plane (EEP) are continually changing. Since these relationships are based on the laws of gravitation which cannot be altered, all orbital operations must be subjected to and adapted to these laws.

The three planes of interest, together with the angles which define their orientation, are displayed in the next sketch, which shows an earth centered system. The reference direction is the mean vernal equinox located in the EEP. The right ascension of the MOP is given by the angle $\Omega_{\mathbb{C}}$ and its inclination to the celestial equator by $i_{MOP}$. The former varies by 26° over an 18.6-year period, while the latter varies slowly between 18.3° and 28.7° over the same period. Figure 1 shows a "time history" of both these parameters from the years 1964 to 1981.

The moon itself is located at a central angle, $\beta_{\mathbb{C}}$, and is moving at a rate of $\omega_{\mathbb{C}\oplus}$ in its orbit, thereby completing one revolution in approximately 28 days.

The parking orbit plane of the spacecraft (POP) has a right ascension of $\Omega_\Delta$ and is inclined to the equatorial plane by the angle $i_{eq}$. For injection into a nominal trajectory, the spacecraft will be located at $\psi_0$; it will possess a velocity $V_0$, and it will have the proper lead angle $\Phi^* + \Delta\theta$.

Because of the oblateness of the earth, the parking orbit node is not fixed, but has a regression rate, $\dot{\Omega}_\Delta$.

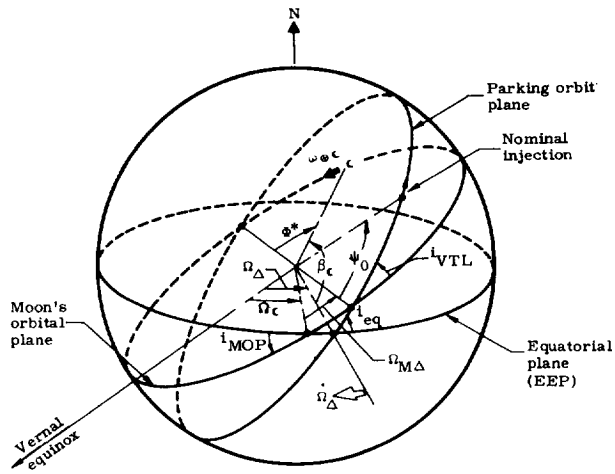


Problem Geometry

Since the fundamental plane of interest in this study is the MOP, it will be necessary to determine the motion of the parking orbit node in this plane resulting from $\dot{\Omega}_\Delta$. It is convenient to define a new angle, $\Omega_{M\Delta}$, as the right ascension of the parking orbit relative to the right ascension of the lunar orbit (above sketch). Due to the inclination of the MOP ($i_{MOP}$) and the difference in right ascensions ($\Omega_\Delta - \Omega_{\mathbb{C}}$), it is important to note that the rate of change of $\Omega_{M\Delta}$ will not be constant.

It is of interest to note that $i_{eq}$ and $h_0$ can be selected such that $\Omega_\Delta$ rotates through 360° during an integral number of lunar months. The result of this selection is that the geometrical relationships between the three planes of interest at the end of this time are identical to those at the nominal injection time (assuming the changes in $i_{MOP}$ and $\Omega_{MOP}$ are zero). As an example, with a constant $i_{eq}$ of 30°, a parking orbit altitude of 487 km would be required for repeated geometry after two months.

Data presented in the following sections are obtained from a "patched-conic" digital program (VOICE) as described in Chapter IV. The earth-moon model employed in this program is that of a spherical moon revolving in a circular orbit around a spherical earth. Other pertinent assumptions and ground rules are as follows.

(1) Since the variation in $i_{MOP}$ is relatively slow when compared to the time for any practical orbital launch mission, this angle is considered a constant, once a launch date is specified.

(2) The inclination of the POP (to the equator) is specified as a constant 30° and "direct" (posigrade) in nature. This represents typical launches from Cape Kennedy. $\Omega_\Delta$ varies at a rate of approximately -6.5°/day for the particular parking orbit chosen. (Only first order secular changes are accounted for.)

(3) The altitude of the parking orbit is taken as a constant (circular orbit); $h_0$ = 588 km above a spherical earth.

(4) The effects of atmospheric drag on the spacecraft are neglected.

(5) The period of interest is from 1969 to 1978. These years were chosen since they correspond to maximum, average, and minimum values of $i_{MOP}$.

(6) All required orbital maneuvers (except midcourse corrections) are conducted while in the earth parking orbit. Major maneuvers along the translunar trajectory are prohibited.

(7) Only circular, retrograde lunar orbits are established at the time of pericynthion. Their altitude is 185.2 km.

(8) The inclination, $i_m$, of the lunar orbits is restricted $-20° \leq i_m \leq 20°$ since, at present, it is anticipated that lunar bases will be located near the lunar equatorial plane.

With the above items in mind, and returning again to the physical situation (see above sketch), it can be seen that because of the POP regression rate ($\dot{\Omega}_\Delta$), $i_{VTL}$ varies with time, even though $i_{eq}$ is constant. At a specific date, $i_{VTL}$ is given by

$$i_{VTL} = \cos^{-1}\left[\cos i_{MOP} \cos i_{eq} + \sin i_{MOP} \sin i_{eq} \cos (\Omega_\Delta - \Omega_{\mathbb{C}})\right] \quad (1)$$

and the right ascension of the parking orbit relative to the MOP is then found by

$$\Omega_{M\Delta} = \cos^{-1}\left[\frac{\cos i_{MOP} \cos i_{VTL} - \cos i_{eq}}{\sin i_{MOP} \sin i_{VTL}}\right] \quad (2)$$

It can be shown by the above equations that for a constant $i_{eq}$ of 30°, the minimum and maximum values for the period of interest are: $i_{VTL_{min}}$ = 1.5 deg, $i_{VTL_{max}}$ = 58.5 deg.

Figure 2 presents a typical variation of $i_{VTL}$ and $\Omega_{M\Delta}$ for a two-month span for 1978. Observe that both $i_{VTL_{min}}$ and $i_{VTL_{max}}$ are experienced during this span and also note the nonlinear behavior of $\Omega_{M\Delta}$.

## 2. Translunar Orbital Departure Windows

### a. Without parking orbit maneuvers

Consider now the case where a nominal trajectory is selected having given values of $\Omega_{M\Delta}$, $i_{VTL}$ and $\phi^*$. Assume for the moment that the required $\psi_0$ is 0° and that the spacecraft is located at the proper injection point. The following sketch illustrates this situation by showing the lunar position and the nodal line N ($t_0$) of the POP at the injection time $t_0$. If the injection is missed, it is obvious that the vehicle must complete approximately one orbit revolution before another possible efficient injection can take place. Assuming that injection takes place at a later time, $t_1$, the node and lunar position will have changed during that time interval. The new lunar position is $\beta'_{\mathbb{C}}$ and the new nodal position is $N_{(t_1)}$. Consequently, there is a new lead angle $\phi^{*'}$ at $t_1$.

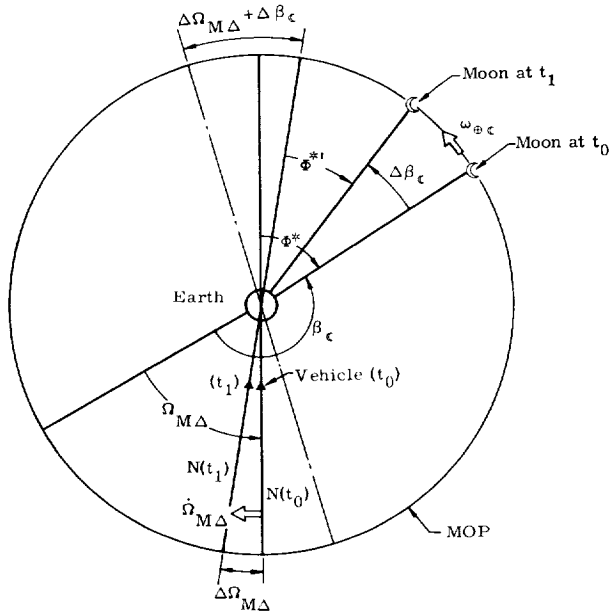


Nodal Shift Geometry

By referring back to the catalogue in Chapter IX, and assuming some nominal flight time, $t_p$(nom), a $\phi^*$ can be determined, together with a $\theta_{MTL}$ for a given $i_{VTL}$. Now, if $\phi^*$ changes because of a delayed injection, a new flight time can be calculated ($t'_p = \phi^{*'} \cdot \omega_{\mathbb{C}\oplus}$). With the further assumption that $i_{VTL}$ does not change, a new injection position $\psi'_0$ and injection velocity $V'_0$ can be found for the corresponding $\theta'_{MTL}$. Thus, the most obvious method to complete the mission in the event of a delayed injection is to change the injection position, together with the velocity magnitude. This method does not require any maneuvers in the parking orbit to successfully fulfill the mission. One limiting factor in utilizing this technique is the allowable (or practical) flight times. Another limiting factor is the inability to regulate the arrival orientation, $\theta_{MTL}$--although $i_m$ can be controlled quite adequately.

Figures 3 and 4 show the injection velocity requirement ($\Delta V_0$), and the lunar orbit retro impulse requirement ($\Delta V$), respectively, as a function of elapsed time during the departure window.

A departure window is defined as "that interval of time wherein a possible injection may take place without exceeding the vehicle's propulsion capabilities."

Figure 3 is a summary chart depicting the departure window envelope wherein the minimum window is 22.5 hr and the maximum window is 37.5 hr. Essentially, this means that the spacecraft has a minimum and maximum injection frequency of 14 and 23. Injection frequency is defined as "the departure window (hr) divided by the spacecraft's period in the parking orbit." Note that the figure does not show injection velocity explicitly, but rather the increment required above satellite speed. Figure 4 indicates the window effects on velocity braking requirements on arrival at the moon. For the above flight time restriction, a spacecraft must have a total velocity potential (above earth circular speed) of 4.6 km/sec to realize the minimum and maximum windows. Decreasing this potential reduces the windows accordingly.

Thus far, a "departure window" and an "injection frequency" have been defined. Another important consideration is the "departure frequency" which is defined as "the number of departure windows occuring in a certain span of time."

Figure 5 presents the moon lead angle for a time span of two months (≈1344 hr). Whenever the lead angle is between 28° and 55° or 208° and 235°, a possible departure window exists. These acceptable increments of $\Phi^*$ are a consequence of the flight time restriction. Note that, for this period of time, the departure frequency is 7 with injection "cycling" from north to south and that both minimum and maximum windows are encountered.

Although the data included in Figs. 3 and 4 represent the year 1978 and only the descending node, they nevertheless are highly indicative of any year and any $\Omega_{M\Delta}$, as will become obvious in the following sections.

In obtaining a window by this method (without parking orbit maneuvers), the following facts can be summarized:

(1) Practical flight time considerations limit the window size.

(2) In maintaining a specific $i_m$, the resulting $\theta_M$ will vary, depending on the window departure time.

(3) Flight time varies throughout the window.

(4) When the injection direction is reversed, $\theta_{MTL}$ must change by 180° or the windows will drastically be reduced or disappear.

These facts immediately pose a number of questions which make the method unacceptable under certain circumstances.

(1) What can be done if it becomes imperative to have a larger window size due to various orbital operations or contingencies?

(2) What can be done to obtain a window when an explicit $i_m - \theta_{MTL}$ relation is required, such as in a time-critical rescue mission?

(3) What can be done to acquire windows if nearly constant flight times become a mission specification, e.g., because of limited life support capability?

(4) What window sizes can be obtained if a combination of the above is required?

In order to answer these questions, an additional degree of flexibility is allowed whereby maneuvers in the earth parking orbit are permitted.

b. With parking orbit maneuvers

$i_m$-$\theta_{MTL}$ constraints. Consider first the case where a specific $i_m$-$\theta_{MTL}$ combination is desired at all times, i.e., regardless of the injection direction (inject north or south). In other words, $i_m$ and $\theta_{MTL}$ are mission constraints during any departure window.

Figure 31, for example, of Chapter IX shows that flight time varies as a function of $i_{VTL}$ for a constant $i_m - \theta_{MTL}$ relation. As a result of this variation, the required moon lead angle also changes in such a way that flight time increases as $i_{VTL}$ becomes progressively southern. The increase in flight time is acceptable in this case (up to practical limits) since the only mission stipulations are the lunar orbit constraints. It is not meant to imply that all southerly injections are of longer flight time, quite the contrary; the opposite situation can exist depending on the selection of $\theta_{MTL}$. However, this is not directly seen in Fig. 31. But it was noted in Chapter IX that by either the addition or subtraction of 180 deg from $\theta_{MTL}$ a "mirror image" can be obtained. The method of "images" is discussed in detail in Chapter IX and implies that only the lunar approach direction (from north or south of the MOP) is reversed. Thus, the more practical flight times ($40 < t_p < 120$ hr) occur for $\theta_{MTL}$'s somewhat greater than 90° and again greater than 270° for a given $i_m$.

For the $i_m$ selected here ($10° \leq i_m \leq 20°$), a corresponding $\theta_{MTL}$ range of 90° to 120° is chosen. For these values of $\theta_{MTL}$, the $\Delta V$ required to brake into a lunar orbit can vary from 760 to 1300 m/sec. The corresponding injection velocity increment, $\Delta V_0$, can be 3.04 to 3.16 km/sec. Therefore, when the translunar inclination ($i_{VTL}$) is known, the propulsion requirement to meet the mission can be found:

$$\Delta V_{req} = \Delta V + \Delta V_0 + \Delta V_m + \Delta V_g \qquad (3)$$

where $\Delta V_m$ is the increment required for any earth parking orbit maneuvers and $\Delta V_g$ is that required for the midcourse corrections.

In short, if an injection is delayed and if a given $i_m$ and $\theta_{MTL}$ relation is to be held constant, the moon lead angle must be equal to the required $\Phi^*$ for the actual departure $i_{VTL}$.

A delayed injection is defined as one which involves a single corrective maneuver some time after the nominal GO time. This time may occur after one parking orbit revolution or after several hundred, but no maneuvers will have been performed prior to this time. Once the nominal trajectory has been specified as to the $\theta_{MTL}$ and $i_m$ relationship, a position of the moon (time of the month) and year must be specified to define the initial geometrical relationships. Since the inclination of the MOP relative to the EEP varies over a 18.6-year cycle, the choice of year will determine the possible inclination of the POP relative to the MOP. The choice of a lunar position determines $\Omega_{S\mathbb{C}}$ required for the initial injection and a particular year determines $\Omega_{S\oplus}$ and the nominal $i_{VTL}$.

The requirement for a maneuver stems from the following facts. Referring to previous sketch, the nodal line of the POP relative to the MOP is rotated through an angle $\Delta\Omega_{M\Delta}$ because of the delay. At the same time, $\beta_{\mathbb{C}}$ has changed to $\beta_{\mathbb{C}} + \Delta\beta_{\mathbb{C}}$ and $i_{VTL}$ of the POP has also varied to $i'_{VTL}$. For the moment however, assume that $i_{VTL}$ did not change, thereby still requiring $\Phi^* + \Delta\theta$ to meet the lunar orbit constraints. But $\Phi^*$ has decreased by an amount $(\Delta\Omega_{M\Delta} + \Delta\beta_{\mathbb{C}})$ and thus it is obvious that the nodal line N' must be rotated by the same amount $(\alpha)$ in order to

$$\alpha = \Delta\Omega_{M\Delta} + \Delta\beta_{\mathbb{C}} \tag{4}$$

again achieve a moon lead angle equal to $\Phi + \Delta\theta$. This can be accomplished only by means of a side thrust maneuver executed somewhere in the present parking orbit, as illustrated in the following sketch.

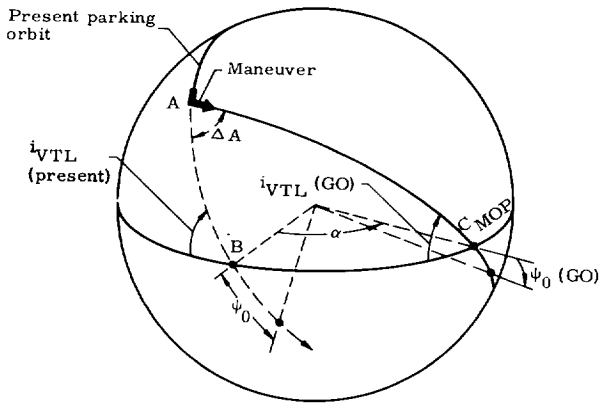


$\alpha = \Delta\Omega_{M\Delta} + \Delta\beta_{\mathbb{C}}$

Arc length ~ $\widehat{AB}$

Arc length ~ $\widehat{AC}$

Departure Maneuver Geometry

The required change in azimuth ($\Delta A$) for the maneuver can be found by spherical trigonometry:

$$\Delta A = \cos^{-1}\left[\cos i_{VTL_{present}} \cos i_{VTL_{GO}} + \sin i_{VTL_{present}} \sin i_{VTL_{GO}} \cos\alpha\right] \tag{5}$$

where the present $i_{VTL}$, before the maneuver is $i_{VTL_{present}}$, and the actual departure $i_{VTL}$, after the maneuver is $i_{VTL_{GO}}$:

$$i_{VTL_{GO}} = \tan^{-1}(\tan i_{VTL_{present}} \cos\alpha) \tag{6}$$

Thus, knowing $\alpha$ and $i_{VTL_{present}}$, an $i_{VTL_{GO}}$ can be found which minimizes $\Delta A$.

As mentioned above, for a particular $\theta_{MTL}$ - $i_m$ relation, the moon lead angle $\Phi^*$ is a function of the actual translunar inclination $i_{VTL}$. Since the $i_{VTL_{present}}$ which minimizes $\Delta A$ will not be equal to the nominal $i_{VTL}$ upon which $\alpha$ is based, the lead angles corresponding to the two cases will not be equal. This change in lead angle, $\Delta\Phi$, will increase or decrease $\alpha$ and the actual shift in nodal position becomes $\alpha^*$ where:

$$\alpha^* = \alpha + \Delta\Phi \tag{7}$$

The actual GO $i_{VTL}$ is found by an iterative process as follows:

(1) Let the initial value of $\alpha^*$ equal $\alpha$.

(2) Determine $i_{VTL}(1)$ from Eq (6).

(3) Calculate $\Delta\Phi(1)$ from:

$$\Delta\Phi(1) = \Phi(i_{VTL}(1)) - \Phi(i_{VTL}(nom))$$

(4) Let $\alpha^* = \alpha + \Delta\Phi(1)$.

(5) Determine values for $i_{VTL}(2), \ldots,$ $i_{VTL}(n)$ by repeating the iteration process until $i_{VTL}(n) - i_{VTL}(n-1)$ reaches some specified limit (say, 0.01°).

$\Delta A$ resulting from $i_{VTL}(n)$ will then be a minimum for the actual shift $\alpha^*$.

As a result of the maneuver, the injection time does not occur at an integral multiple of the nodal periods after the nominal time. This is caused by two effects; first, if the maneuver is such that $i_{VTL_{GO}}$ differs from $i_{VTL}$ nominal, the injection position $\psi_0$ will vary. Second, the trajectory of the vehicle after the maneuver will be different from the trajectory of the vehicle if no maneuver were performed. This

situation is also illustrated in the sketch above. The difference in paths from the maneuver point is given by

$$\Delta S = (\psi_0 - \psi_0\,(\text{nom})) + (\widehat{AC} - \widehat{AB}) \qquad (8)$$

Since the arc lengths are parts of great circles at the same altitude, and if the small change in nodal period due to a change in inclination is neglected, then the difference in time is given by:

$$\Delta t = n_\beta \, \Delta S \qquad (9)$$

where $n_\beta$ is the mean motion of the vehicle in the earth parking orbit. The injection time is therefore equal to:

$$T = n\tau_\beta + \Delta t \qquad (10)$$

where n = Number of nodal periods after nominal injection time and $\tau_\beta$ = nodal period of the vehicle in earth parking orbit. Equation (5) assumed that $t_1$ was known; however, due to the maneuver, $t_1 = T + t_0$, which now includes the correction, $\Delta t$; the actual $\Delta\beta_{\mathbb{C}} = \omega_{\mathbb{C}\oplus} T$. Since $\Delta\beta_{\mathbb{C}}$ affects the maneuver and therefore the injection time, the actual injection time is also found by an iterative process as outlined below:

(1) Calculate an initial value of $\Delta\beta_{\mathbb{C}} = \omega_{\mathbb{C}\oplus}(n\tau_\beta)$.

(2) Calculate the azimuth change and difference in paths due to the maneuver.

(3) Calculate $\Delta t$ from Eq (9).

(4) Recalculate an initial value of $\Delta\beta_{\mathbb{C}} = \omega_{\mathbb{C}\oplus}(n\tau_\beta + \Delta t)$.

(5) Repeat iteration until the difference between successive values of $\Delta t$ approaches zero.

This iteration results not only in the proper injection time, but yields a maneuver which reflects the time spent in parking orbit after the maneuver to injection.

If the velocity before and after the maneuver is the same (circular orbit velocity), then the velocity impulse required for the maneuver is

$$\Delta V_m = 2\, V_c \sin(\Delta A/2) \qquad (11)$$

where $V_c$ is the circular orbit velocity.

Since orbital departure windows are a function of the geometrical relations between the MOP, the EEP and the POP, a detailed study of all possible situations would involve an enormous amount of time and manpower. The work would be further complicated if all the methods of obtaining departure windows were applied to each situation. Because of this, representative years and positions of the moon are chosen for discussion to indicate the major trends during the period from 1969 to 1980. By chosing the following three years, the influence of $i_{MOP}$ on the problem is found:

| | $i_{MOP}$ (deg) |
|---|---|
| (1) April 1969 | 28.6 |
| (2) April 1974 | 23.3 |
| (3) July 1978 | 18.3 |

Since $i_{MOP}$ is periodic, with an 18.6-year period, these data, together with the results obtained from them, are applicable to all corresponding years.

Fixing the position of the moon at arrival (time of the month) during a certain year requires a certain value of the right ascension ($\Omega_\Delta$) of the POP. This is important since, as can be seen from Fig. 2, the right ascension and its rate of change will strongly affect the duration of the departure windows. In order to determine the effects of $\Omega_\Delta$ on the departure windows, four positions of the moon were chosen which covered the possible range of $\Omega_\Delta$ (0° to 360°). These positions, which correspond to the time at which the vehicle reaches pericynthion, are:

(1) Ascending Node (AN).

(2) Descending Node (DN).

(3) Maximum Northerly Declination (MND).

(4) Maximum Southerly Declination (MSD).

The initial orientation elements for these conditions are given in Table 1.

TABLE 1

Initial Departure Geometry for Numerical Analyses

| Moon Position | $\Omega_\Delta$ (deg) | $\Omega_{M\Delta}$ (deg) | $i_{VTL_{(nom)}}$ (deg) |
|---|---|---|---|
| April 1969 | | | |
| AN | 180.00 | 180.00 | 58.60 |
| DN | 0.00 | 0.00 | 1.4 |
| MND | 340.80 | 270.00 | 9.46 |
| MSD | 19.20 | 90.00 | 9.46 |
| April 1974 | | | |
| AN | 166.98 | 180.00 | 53.30 |
| DN | 346.98 | 0.00 | 6.70 |
| MND | 305.25 | 270.00 | 19.45 |
| MSD | 28.75 | 90.00 | 19.45 |
| July 1978 | | | |
| AN | 180.00 | 180.00 | 48.30 |
| DN | 0.00 | 0.00 | 11.70 |
| MND | 305.00 | 270.00 | 24.18 |
| MSD | 55.00 | 90.00 | 24.18 |

Figures 6 and 7 present the variation (with elapsed time) of the maneuver requirements, $\Delta V_m$, for the year 1978. The base time (t = 0) is the nominal GO date. It should be noted that the curves presented in these figures are not continuous, but represent injection points which are separated by approximately one nodal period (~1.6 hr).

In these figures, observe the oscillating peak $\Delta V_m$. This oscillation is dependent on the $i_{VTL}$ of the POP where high $i_{VTL}$'s require a larger $\Delta V_m$ for a required nodal shift. The variation in time interval between minimum $\Delta V_m$ values is caused by the variable rate of change of $\Omega_{M\Delta}$. Note further that the minimum $\Delta V_m$'s are not zero. This is due to the incorrect orbital phasing of the spacecraft even though the proper $i_{VTL}$ lead angle has been satisfied.

Orbital departure windows are dependent on the magnitude of the velocity impulse available for the corrective maneuver. Therefore, whenever numerical values of departure windows are given, they must be accompanied by a maximum $\Delta V_m$ capability. For purposes of illustration two velocity levels are assumed, 0.5 km/sec and 1.0 km/sec, and the minimum and maximum departure windows (over a 2-month period) for these cases are presented in Table 2 for $i_m$ = 20° and $\theta_M$ = 90°.

TABLE 2

Delayed Departure Windows

| | $\Delta V_m$ = 0.5 km/sec | | $\Delta V_m$ = 1.0 km/sec | |
|---|---|---|---|---|
| | Window Max ΔT (hr) | Window Min ΔT (hr) | Window Max ΔT (hr) | Window Min ΔT (hr) |
| April 1969 | | | | |
| AN | 50 | 12 | 204 | 26 |
| DN | 56 | 10 | 232 | 30 |
| MND | 128 | 13 | 248 | 32 |
| MSD | 132 | 12 | 176 | 30 |
| April 1974 | | | | |
| AN | 40 | 12 | 92 | 28 |
| DN | 40 | 13 | 84 | 28 |
| MND | 40 | 10 | 100 | 28 |
| MSD | 40 | 12 | 85 | 28 |
| July 1978 | | | | |
| AN | 32 | 15 | 64 | 26 |
| DN | 31 | 14 | 65 | 25 |
| MND | 32 | 12 | 64 | 28 |
| MSD | 32 | 14 | 66 | 28 |

An important fact demonstrated by the above table is that, for a fixed $\Delta V_m$ level, the minimum departure window for all cases (for the 2-month period) is essentially constant, with average values of 12.5 hr for $\Delta V_m$ = 0.5 km/sec and 28 hr for $\Delta V_m$ = 1.0 km/sec. These departure windows yield minimum injection frequencies of 8 injections for $\Delta V_m$ = 0.5 km/sec and 18 injections for $\Delta V_m$ = 1.0 km/sec. The maximum departure windows are seen to be a function of the year (i.e., $i_{MOP}$) and (in the case of 1969) are also a function of the position of the moon.

The variation in the maximum departure windows for 1969 is due to the fact that $i_{MOP}$ assumes its maximum value of 28.7° during this year. Thus, for a range of $\Omega_\Delta$, $i_{VTL}$ will approach its minimum of 1.4°; thus, the change in azimuth will be small. The maximum injection frequencies are approximately 120° for 1969, 56° for 1974 and 40° for 1978.

For all cases, there are practical periods during the 2-month time span of the parking orbit in which departures are possible. These periods are in the neighborhood of the points of minimum $\Delta V_m$ required, and the time between these points is an indication of the waiting time between successive departure windows. The maximum and minimum times are listed below in Table 3.

TABLE 3

Wait Time Between Minimum $\Delta V_m$ Points

| | Max Time (hr) | Min Time (hr) |
|---|---|---|
| April 1969 | | |
| AN | 330 | 110 |
| DN | 338 | 124 |
| MND | 334 | 66 |
| MSD | 334 | 82 |
| April 1974 | | |
| AN | 312 | 152 |
| DN | 328 | 144 |
| MND | 314 | 152 |
| MSD | 314 | 152 |
| July 1978 | | |
| AN | 302 | 172 |
| DN | 312 | 156 |
| MND | 306 | 156 |
| MSD | 302 | 166 |

After the maneuver, the spacecraft's orbital plane has a different value of $i_{VTL}$ from that prior to the maneuver. The new value is the actual or GO $i_{VTL}$ of the translunar trajectory and therefore is the governing trajectory parameter needed to ascertain flight time, $\Delta V_0$ and $\Delta V$ for the particular situation. Figure 8 shows the corresponding $i_{VTL}$ associated with $\Delta V_m$ (Figs. 6 and 7) and departure time for the year 1978. If $i_{VTL}$ is known, then $\Delta V_0$ and $\Delta V$ can be easily found.

The nominal trajectory (t - 0) depicted in Figs. 6 and 7 and in the above tables are direct-north injections; however, after a sufficient time lapse, $\alpha^*$ becomes greater than 90°, and it is then possible to inject directly to the south. The negative values of $i_{VTL}$ in Fig. 8 reflect this inject-south condition. If one is restricted to either a north or south injection only, the departure windows may be reduced in size in some situations.

Once the actual translunar $i_{VTL}$ has been found, the actual mission flight time can also be determined (see Fig. 9). This actual flight time is then compared to any desired limits which can be reflected upon the window. This approach enables the mission planner to find the effect of such flight limitations on the departure window frequency and size. For example in Fig. 6, it is most important to note that any inject-south condition exceeds a flight-time of 120 hr. Thus, instead of having 7 departure windows for the 2-month period, only 4 would be realized.

In some missions, it may be acceptable to approach the moon either from the north or south, as long as $i_m$ is maintained constant. If the lunar orbit constraints are allowed to be modified in this fashion, then the theory of images mentioned previously can be applied to help remedy the above situation. If this switching of $\theta_{MTL}$ is allowable, the max and min departure windows and injection frequencies remain unchanged, but now seven injection periods are again possible. As a natural consequence, wait times between departure windows can be reduced from approximately 500 hr to 250 hr.

The influence of the lunar orbit constraints on the departure windows and injection frequencies are found by varying $\theta_{MTL}$ and $i_m$ for the case of the moon at its descending node during 1978. A summary of the findings is given in Table 4.

TABLE 4

Departure Windows for Various Lunar Orbit Constraints

| | Max Departure Window (hr) | Max Wait Time | Min Departure Window (hr) | Min Wait Time |
|---|---|---|---|---|
| | $\theta_{MTL}$ = 120 deg; $i_m$ = 10 deg | | | |
| $\Delta V_m$ = 0.5 km/sec | 31 | 342 | 10 | 150 |
| $\Delta V_m$ = 1.0 km/sec | 68 | 342 | 26 | 150 |
| | $\theta_{MTL}$ = 120 deg; $i_m$ = 20 deg | | | |
| $\Delta V_m$ = 0.5 km/sec | 32 | 284 | 13 | 166 |
| $\Delta V_m$ = 1.0 km/sec | 65 | 284 | 30 | 166 |
| | $\theta_{MTL}$ = 90 deg; $i_m$ = 10 deg | | | |
| $\Delta V_m$ = 0.5 km/sec | 32 | 494 | 12 | 114 |
| $\Delta V_m$ = 1.0 km/sec | 64 | 494 | 29 | 114 |

It is seen that the maximum and minimum departure windows and thereby the injection frequencies vary little for the various $\theta_{MTL}$ - $i_m$ combinations. However, for $\theta_{MTL}$ = 90 deg and $i_m$ = 10 deg, only 6 launch periods exist instead of the normal 7, due to the extremely long flight times caused by direct south injections. Again, the number of launch periods can be increased to 7 by changing the approach to the moon in the same manner as mentioned above.

It has been found that departure window sizes are little affected by the difference in earth-moon distance, but the wait time between possible windows near lunar perigee decreases due to the higher $\omega_{\oplus\mathbb{C}}$. When the moon is near apogee, the opposite will be true, since $\omega_{\oplus\mathbb{C}}$ is lower than the average $\omega_{\oplus\mathbb{C}}$ used in generating the above data. The maximum decrement or increment in window size due to a variable earth-moon distance is 20 hr ($\Delta V_m$ = 1.0 km/sec) and the minimum is 10 hr ($\Delta V_m$ = 0.5 km/sec).

NOTE:

As mentioned before, all of the nominal (t = 0) trajectories are "inject north" cases. However, the tables and figures presented thus far are also applicable to nominal "inject south" cases as well through the following manipulations. For inject south cases, reverse the node or declination (e.g., AN → DN or MSD → MND, etc.), reverse the sign of $i_{VTL}$ (Fig. 8), and add 180 deg to the related $\theta_{MTL}$ orbit constraint ($i_m$ remains unchanged).

$i_m$ - $t_p$ constraints. Consider next the case where a mission specification states that the translunar flight time must be kept at a constant value. Referring to Fig. 6 of Chapter IX, for example, it is noted that for a constant flight time and constant $i_m$, $\theta_{MTL}$ will change as a function of the translunar inclination $i_{VTL}$. Therefore, the primary objective of the corrective maneuver is to adjust the POP node (in the MOP) to maintain a constant $\Phi^*$.

Essentially, by choosing a constant translunar flight time the moon lead angle becomes independent of $i_{VTL}$; however, this method requires a different relationship between the injection velocity $\Delta V_0$, the injection position $\psi_0$ and the translunar inclination $i_{VTL}$, from that for a constant $\theta_{MTL}$. The $\Delta V_m$ requirements in this method are independent of the flight time during any particular year or position of the moon; however, the variation in $\theta_{MTL}$ does depend on the flight time. For $i_m$ fixed at 20°, this variation is:

| Flight Time | $\theta_{MTL}$ Variation | |
|---|---|---|
| 50 hr | $125° \leq \theta_M \leq 180°$ | for $-60° \leq i_{VTL} \leq 60°$ |
| | $305° \leq \theta_M \leq 360°$ | |
| 90 hr | $75° \leq \theta_M \leq 150°$ | for $-60° \leq i_{VTL} \leq 60°$ |
| | $255° \leq \theta_M \leq 330°$ | |

Since $\Delta V_m$ is independent of the desired flight time, only the year 1978 and four positions of the moon are investigated.

Typical velocity corrections ($\Delta V_m$) required for these conditions are presented in Figs. 10 and 11 for two lunar positions, and the resulting maximum and minimum departure windows are listed below in Table 5.

TABLE 5

Constant Flight Time

July 1978

| | $\Delta V_m$ = 0.5 km/sec | | $\Delta V_m$ = 1.0 km/sec | |
|---|---|---|---|---|
| | Maximum Window $\Delta T$ (hr) | Minimum Window $\Delta T$ (hr) | Maximum Window $\Delta T$ (hr) | Minimum Window $\Delta T$ (hr) |
| AN | 33 | 14 | 64 | 29 |
| DN | 32 | 15 | 65 | 28 |
| MND | 32 | 13 | 64 | 28 |
| MSD | 31 | 15 | 64 | 29 |

When comparing Table 5 to the corresponding data in the previous section for lunar orbit constraints, it is seen that there is no difference in the window sizes; they are now independent of lunar position, and that the departure frequency for two months is the same, i.e., 7.

However, the maximum and minimum wait times do change when Table 6 is compared with the corresponding information above. The wait times between points of minimum $\Delta V_m$ for the case of constant flight time are as follows. Note the near constancy of the wait times with lunar position.

TABLE 6

Wait Times

| | Maximum Time (hr) | Minimum Time (hr) |
|---|---|---|
| AN | 248 | 174 |
| DN | 248 | 178 |
| MND | 250 | 173 |
| MSD | 248 | 170 |

Essentially, the maximum wait time is reduced by approximately 50 hr and the minimum wait time is increased by approximately 10 hr.

$i_m - \theta_{MTL} - t_p$ constraints. Another case worthy of examination is the mission specification wherein it is stated that both a constant $i_m - \theta_M$ relation and constant flight time must be maintained. In order to accomplish this, it is immediately obvious from Fig. 6, Chapter IX, for example, that $i_{VTL}$ must remain constant. This also implies that a constant lead angle is required.

If the correction maneuver is performed with the translunar trajectory inclination ($i_{VTL}$) kept equal to the initial inclination ($i_{VTL}$ (nom)), constant flight time and fixed lunar orbit trajectories can be obtained. Since the maneuver only corrects for the shift in nodal position $\alpha^*$, this method results in maintaining the nominal injection conditions. The change in azimuth ($\Delta A$) becomes for this case:

$$\Delta A = \cos^{-1} \cos i_{VTL} \cos i_{VTL}\,(\text{nom}) + \sin i_{VTL} \sin i_{VTL}\,(\text{nom}) \cos \alpha^*$$

It is now impossible to minimize $\Delta A$, since all the parameters $i_{VTL}$, $i_{VTL}$ (nom), and $\alpha^*$ are held constant. However, no iteration procedure is required in this method because there is no change in lead angle (a result of $i_{VTL}$ being invariant). A disadvantage of this method is that after a significant length of time, the difference between the present $i_{VTL}$ and nominal $i_{VTL}$ becomes large and consequently the required azimuth change also becomes large. A typical variation $\Delta V_m$ for 1978 and for $\theta_M = 90°$; $i_M = 20°$ is shown in Figs. 12 and 13 for two positions of the moon.

For this method, at most, three practical departure periods exist during the two-month span of the parking orbit. For the inject south cases noted in these figures $\theta_{MTL}$ must be interpreted as $\theta_{MTL} + 180°$ so that $i_{VTL} = -i_{VTL}$ (nom). This is due to the fact that $i_{VTL}$ (nom) only holds for north injections if $\theta_{MTL}$ is fixed at an initial value.

For purposes of demonstration, the departure frequency is assumed to be 2 (t = 0 and at t ≈ 2 months). The departure window sizes for two representative $\Delta V_m$ magnitudes are listed in Table 7.

TABLE 7

Delayed Windows

1978

| | $\Delta V_m$ = 0.5 km/sec | | $\Delta V_m$ = 1.0 km/sec | |
|---|---|---|---|---|
| | ΔT (max) (hr) | ΔT (min) (hr) | ΔT (max) (hr) | ΔT (min) (hr) |
| AN | 15 | 14 | 30 | 28 |
| DN | 31 | 31 | 64 | 64 |
| MND | 22.5 | 14 | 44 | 42 |
| MSD | 22 | 12 | 46 | 44 |

c. Sequential injections

It is well to mention at this point an alternative but less efficient method for generating departure windows. A "sequential" window is defined as one which involves a succession of correction maneuvers--or a continuous updating of the departure geometry whether the actual injection takes place or not. Thus, the $\Delta V_m$ corrections are cumulative, and the window is considerably reduced from the "delayed" windows presented in the previous sections. However, the sizes of the sequential windows, regardless of mission constraints, agree quite closely with the first delay window ($i_m - \theta_{MTL}$ constraints) for $t \geq 0$ for the corresponding lunar positions.

3. Translunar Inject-on-Time Windows

In each successive orbital pass during a possible departure window, there is a specific point at which injection can nominally take place. For this study, this point is associated with a nominal injection flight path angle ($\gamma_0$) of zero degrees. Actually, the instant of time at which this point is encountered can be enlarged by controlling the injection velocity vector to different directions before and after arrival at the nominal point. In other words, there exists a secondary departure window for each orbital pass, hereafter termed the "inject-on-time" window. Since the inject-on-time window is of shorter duration, several assumptions can be made, which simplify its determination considerably, but which can be shown to have a very small effect on the actual physical situation. These assumptions are:

(1) The parking orbit and the translunar trajectory lie in the same plane.

(2) The plane of the parking orbit does not change due to nodal regression during the launch window.

(3) The time to traverse the nominal and the off-nominal translunar trajectories is the same.

(4) The maneuver is impulsive (zero burning time).

Now it is possible to inject earlier at a negative flight path angle and later at a positive flight angle with an accompanying velocity loss. This is illustrated in the next sketch. The velocity loss is due to the requirement of deflecting the parking orbit velocity vector to a desired $\gamma_0$ and increasing the velocity magnitude to $V_0$ when using "impulsive" corrections.

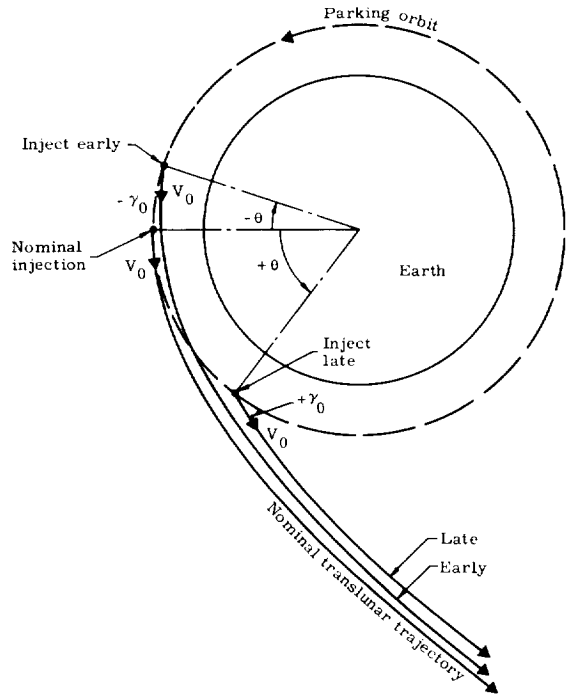


Inject-on-Time Window

If the nominal altitude and circular parking orbit velocity are kept the same, then the energy will remain the same, and only the flight path angle $\gamma_0$ will change with the central angle $\theta$. The problem thus reduces to determining $\theta$ as a function of $\gamma_0$ and relating these two parameters to the injection velocity and time.

The positive and negative limits of $\gamma$ about the nominal $\gamma_0 = 0$ are subject to certain constraints as follows:

(1) Negative $\gamma$ constraint: minimum perigee altitude to avoid re-entry.

(2) Negative and positive $\gamma$ constraints: maximum practical $\Delta V$ limitation to go from circular parking orbit velocity to translunar injection velocity.

For typical lunar trajectories, it appears that $\gamma$ can be easily varied from -10 deg to +10° and still satisfy the constraints of minimum perigee altitude and $\Delta V$.

For a parabolic earth escape trajectory, $\theta = 2\gamma$; therefore, the central angle launch window is approximately 40°. For a parking orbit altitude of 588 km, the period is approximately 1.6 hr, and thus the duration of the inject-on-time window is approximately 10.7 min.

The $\Delta V$ required to leave an earth parking orbit and enter a translunar trajectory is a function of the mission being flown (i.e., $\theta_{MTL}$ and $i_m$ relation at pericynthion) and inclination of the translunar trajectory to the MOP. However, it has been found that the velocity impulse

$$\Delta(\Delta V) = \Delta V_i - \Delta V_0$$

where $\Delta V_0$ is the mission requirement for $\gamma_0 = 0$ and for a particular $i_{VTL}$ is essentially independent of mission and inclination with a maximum error of 10 m/sec for any combination. The variation of $\Delta(\Delta V)$ with time and flight path angle is shown in Fig. 14. Zero time corresponds to the nominal injection point. $\Delta V$ for injection is then found by simply adding $\Delta V_0$ and $\Delta(\Delta V)$.

The effects of finite burning are also indicated in Fig. 14 for thrust-to-weight ratios (T/W) of 1.0 and 0.5. The results reflect a nonvariable mass vehicle (constant T/W) during burning and demonstrate how the optimum $\gamma_0$ shifts from zero degrees (impulsive case) to positive values. However, the most important effect is the increase in $\Delta(\Delta V)$. For an average T/W ratio of 1.0, $\Delta(\Delta V)$ increases by 0.1 km/sec; for $T/W_{avg} = 0.5$, $\Delta(\Delta V)$ increases by 0.7 km/sec over an "impulsive" injection.

## B. LUNAR ORBIT OPERATIONS

On arrival at the moon, the spacecraft will brake into a lunar parking orbit. From this orbit, the preplanned tasks will be accomplished and preparations for the return flight will be made. Again, lunar operational procedures will be significantly influenced (Ref. 3) by allowable lunar stay times, departure window sizes and departure techniques.

### 1. Geometrical Considerations

As a first step in defining the departure window problem, consider that the spacecraft is in a circular orbit around the moon. The vehicle may have been placed into this lunar orbit either at the terminal phase of a translunar trajectory, or after ascending from the lunar surface possibly at the conclusion of a lunar landing and exploratory operation.

The orientation of the orbit is illustrated in the next sketch, which shows the lunar circular orbit, called the "parking orbit." The reference plane is the moon's orbital plane (MOP) and the reference direction is the earth-moon line ($\overrightarrow{EML}$). At a given instant, the parking orbit has an inclination of $i_m$ ($0° \leq i_m \leq 90°$) relative to the MOP, and the descending node of the parking orbit is located at an angular distance of $\theta_{MTE}$ measured positively from the $\overrightarrow{EML}$ eastward to the descending node of the parking orbit--or eastward from the moon-earth line ($\overrightarrow{MEL}$) to the ascending node of the parking orbit. This angle ($\theta_{MTE}$) has been more commonly referred to as the "longitude angle" of the parking orbit. "North" is defined as the direction of the angular monentum vector of the moon's orbital motion around the earth. The parking orbit depicted in the sketch is retrograde (i.e., moving from "east to west" relative to the lunar surface). The position of the spacecraft in this orbit at the same instant is given by $\beta_M$ and is measured positively toward the north from the descending node. Thus, the orientation of the parking orbit relative to the MOP is given by $i_m$, $\theta_{MTE}$ and the vehicle's position in orbit by $\beta_M$. As the spacecraft progresses in orbit, it will eventually reach a point where injection can be initiated in such a way that the desired return to earth is realized. The complete specification of injection conditions after the spacecraft has been accelerated is given by $\theta_{MTE}$, $i_M$, $\beta_{M0} = \beta_M$ (at injection), $V_{\mathbb{C}0}$ (transearth injection velocity), $h_{PL}$ (injection altitude) and $\gamma_{\mathbb{C}0}$ (elevation of velocity vector).

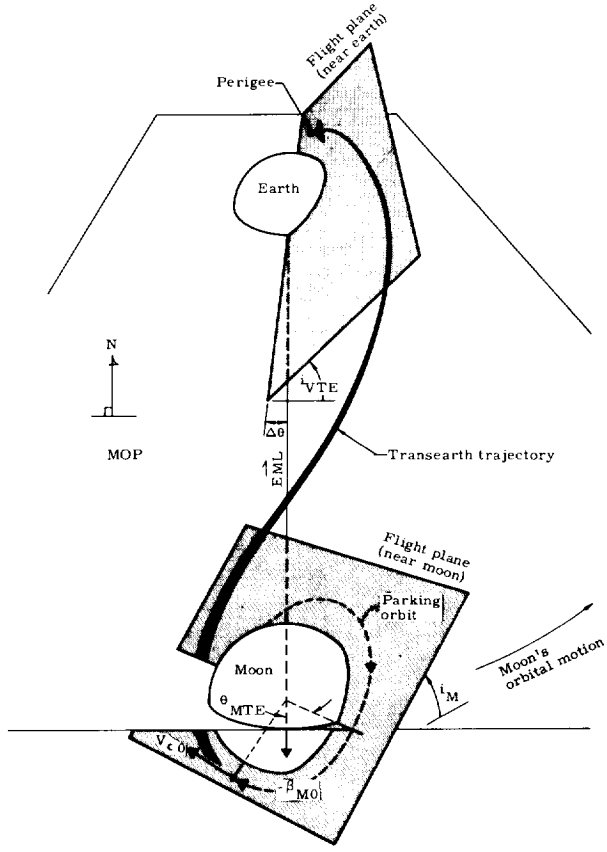


Transearth Trajectory Geometry

If, however, a transearth injection does not take place, the possibility of a future injection depends on the future orientation of the moon and of the lunar parking orbit. In order to define the dynamic situation, the following sketch has been prepared. Consider a celestial sphere centered

at the earth. The moon's orbital plane (MOP) is inclined to the celestial equator by the angle $i_{MOP}$. The moon itself (at a specific time) is located at a central angle $\beta_{\mathbb{C}}$ measured from the ascending node of the moon's orbit. At the same time, the lunar parking orbit has the aforementioned orientation ($i_m$, $\theta_{MTE}$). If injection were to take place at this time, the resultant transearth trajectory plane would have its line of nodes displaced from the $\overrightarrow{EML}$ (at injection) by an angular distance $\Delta\theta$.

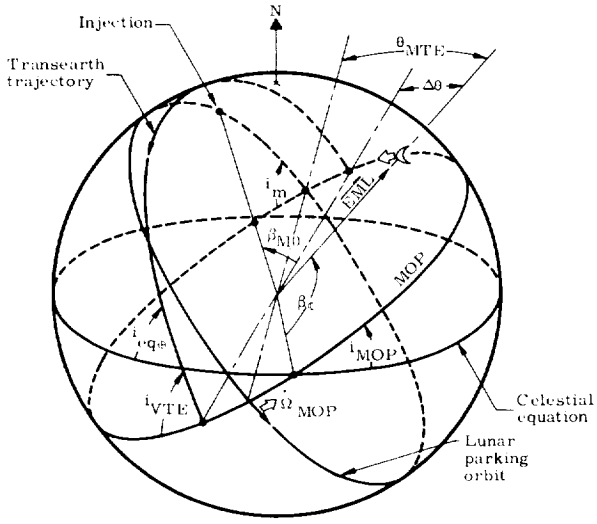


Problem Geometry

When the vehicle nears earth, the inclination of its trajectory plane relative to the MOP is $i_{VTE}$. But because of the inclination $i_{MOP}$ and the lunar position ($\beta_{\mathbb{C}}$) at injection, the trajectory plane has a different inclination relative to the equatorial plane--namely, $i_{eq\oplus}$. It is this parameter ($i_{eq\oplus}$) that is a major constraint on the return flight, since the best use of tracking facilities depends on it. Furthermore, specific landing sites for direct re-entries may require certain "inclined" approaches, and, more apparent, establishment of proper inclinations for earth orbit rendezvous purposes will depend on $i_{eq\oplus}$.

Now, if the transearth injection is delayed, the moon continues to move at a nonlinear rate in its elliptical orbit (eccentricity $\approx 0.0549$) about the earth.

Thus, $\theta_{MTE}$, which is referenced to the $\overrightarrow{EML}$, and $\beta_{\mathbb{C}}$, which defines the position of the moon, will vary in a nonlinear fashion. Simultaneously, the nodal line of the lunar parking orbit regresses at a nonlinear rate, $\dot{\Omega}_{MOP}$, relative to the MOP. This can be better visualized by referring to the next sketch which shows the orientation of the true lunar equatorial plane, the lunar parking orbit plane (POP), and the moon's orbital plane (MOP).

The lunar parking orbit regresses in the direction shown for a retrograde orbit at a constant average rate, $\dot{\Omega}_{eq\mathbb{C}}$, relative to the lunar equatorial plane (assuming first order secular changes only). However, since the MOP is inclined approximately 6.71° ($i_{eqM}$) to the lunar equator, the nodal regression of the lunar parking orbit is nonlinear relative to the MOP. The first order secular change in the inclination of the parking orbit relative to the lunar equatorial plane, $i_{eq\mathbb{C}}$, is 0, but the inclination $i_m$ relative to the MOP varies nonlinearly due to $i_{eqM}$. Thus, if the injection takes place at a later time, the elements $i_m$, $\theta_{MTE}$, and $\beta_{\mathbb{C}}$ must be updated. It naturally follows that the return earth trajectory inclinations, $i_{VTE}$, relative to the MOP, and $i_{eq\oplus}$, relative to the earth equator also vary.

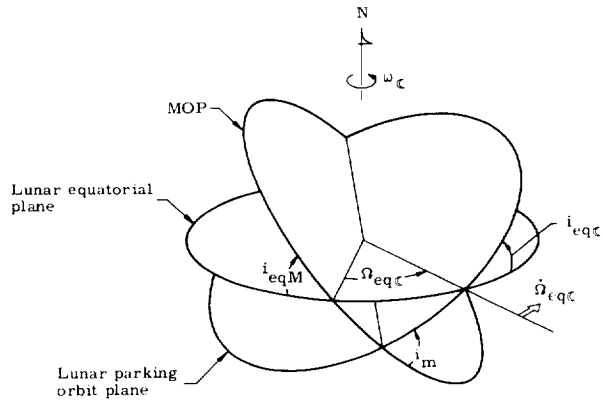


Principal Reference Planes

The subsequent data that are presented are based on the following list of ground rules and assumptions.

## 2. Ground Rules

The exactness of any analysis depends on the stated ground rules and assumptions. Having defined the problem at hand in the above discussion, it now becomes necessary to list the suppositions with which the analysis was conducted.

(1) The first ground rule specifies that both the lunar parking orbit and the earth return parking orbit are assumed circular, with the lunar altitude ($h_{PL}$) at 185.2 km and the earth altitude ($h_{PE}$) at 588 km. This latter altitude is also equal to the earth return perigee altitude or the altitude of the earth orbiting space station when considered.

(2) It is assumed that the period of the lunar parking orbit ($\tau_{\mathbb{C}}$) is constant which implies that the rate of change of the position of the spacecraft in its orbit ($\dot{\beta}_M$) is also constant.

(3) The transearth injection takes place in the same direction as the spacecraft's motion in its lunar orbit, and, thus, no turns are made during the transearth injection phase. In this discussion, only retrograde lunar orbits are considered.

(4) The eccentricity of the moon's elliptical orbit about the earth is assumed constant (e = 0.0549). Furthermore, it is assumed that the moon's mean orbital elements as presented in Ref. 4 can be used to adequately describe the moon's motion.

(5) All maneuvers (injection or otherwise) are purely "impulsive" changes.

(6) Once the spacecraft is injected onto the transearth trajectory, inclination changes are prohibited ($\Delta i_{VTE} = 0$) unless a rendezvous with an earth space station is desired. This ground rule assumes that the transearth trajectory satisfies all mission specifications except, possibly, that of "timing" the reentry point at earth. In the following analysis, "timing" maneuvers along the transearth trajectory are also prohibited.

(7) Every transearth trajectory is to satisfy a single specified $i_{eq\oplus}$. At present, it is felt that a value of $i_{eq\oplus} = 30°$ is of most interest. This value is representative of tracking projection for the next decade for flights over the ETR and WTR. In addition, an $i_{eq\oplus}$ of 30° would complement the earth parking orbit used for the above translunar departure window analysis. An $i_{eq}$ of 30° will also be used as the inclination of an earth orbiting space station for the rendezvous mission. All returns are posigrade.

(8) Finally, it is assumed that a "patched-conic" trajectory approach which utilizes a spherical earth and a spherical moon yields transearth trajectory data of sufficient accuracy.

In the generation of departure windows with specified constraints, it becomes necessary to determine the "true" position of the moon from the mean-orbital elements, i.e., $\overline{EML}$ and $|\overline{EML}|$. In addition, the orientation of the MOP relative to the earth's equator and the orientation of the lunar equator relative to the MOP must be known. Before proceeding to the derivation of these parameters plus other pertinent geometry, a sketch is presented below for clarification and convenience.

This sketch presents the overall problem geometry by giving the orientation of the moon's orbital plane, the earth equatorial plane, the ecliptic plane, the lunar equatorial plane and the lunar parking orbit plane in a moon-centered reference. In addition, the referenced directions used are the mean vernal equinox ($\Upsilon_\oplus$), and $\Upsilon_\mathbb{C}$; the common intersection of the lunar equator, ecliptic and MOP, or more precisely, the intersection of the lunar descending node and the ascending node of the lunar equator in the ecliptic plane.

Also included are the parameters: I = 1.5639° $\gamma$ = 5.1454°, $i_{MOP}$, $\mathbb{C}-\Omega_\mathbb{C}$, $\overline{EML}$, and $\beta_\mathbb{C}$.

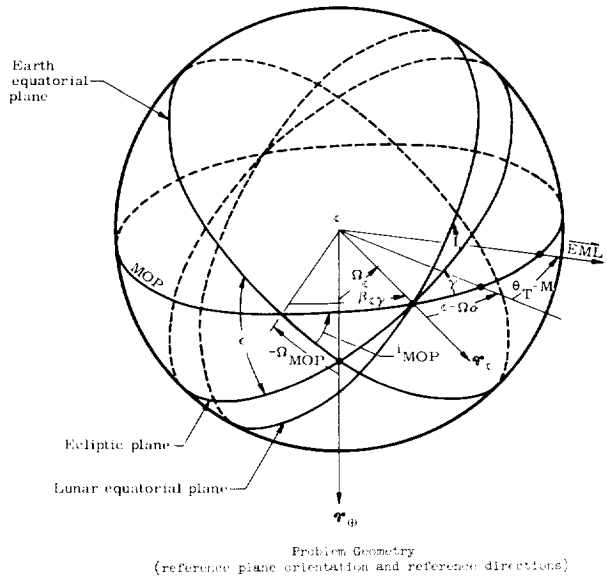


Problem Geometry
(reference plane orientation and reference directions)

With reference to the above sketch, a few of the more important parameters can be found.

First, the angle $\beta_{\mathbb{C}\Upsilon}$ in the moon's orbital plane measured from the ascending node of the lunar orbit on the earth's equatorial plane to $\Upsilon_\mathbb{C}$, is determined from spherical trigonometry

$$\beta_{\mathbb{C}\Upsilon} = \tan^{-1}\left[\frac{\sin\Omega_\mathbb{C}}{\cos\gamma\cos\Omega_\mathbb{C} - \sin\gamma\cot\epsilon}\right] \qquad (12)$$

where $\gamma$ is the almost constant (5.1454°) inclination of the moon's orbital plane relative to the ecliptic and $\epsilon$ is the obliquity ($\epsilon \approx 23.4445°$). With $\beta_{\mathbb{C}\Upsilon}$ known, two additional mean elements can be defined:

$\beta'_\mathbb{C} = \mathbb{C} - \Omega_\mathbb{C} + \beta_{\mathbb{C}\Upsilon}$ = mean longitude of the moon measured in the moon's orbital plane from the ascending node of the lunar orbit on the earth's equator.

$\omega_{\mathbb{C}\oplus} = \omega_{\mathbb{C}\odot} + \beta_{\mathbb{C}\Upsilon} + 180°$ = argument of perigee of the lunar orbit relative to the earth's equator.

The true longitude of the moon is now given by:

$$\beta_\mathbb{C} = \theta_T + \omega_{\mathbb{C}\oplus} \qquad (13)$$

where $\theta_T$ is the true anomaly as derived from the mean orbital elements (Ref. 4).

The inclination, $i_{MOP}$, and right ascension of the lunar orbit ascending node, $\Omega_{MOP}$, relative to the earth's equatorial plane can also be found with spherical trigonometry:

$$i_{MOP} = \cos^{-1}\left\{\cos\epsilon\cos\gamma + \sin\epsilon\sin\gamma\cos\Omega_\mathbb{C}\right\} \qquad (14)$$

$$\Omega_{MOP} = \cos^{-1}\left\{\frac{\cos\gamma - \cos i_{MOP}\cos\epsilon}{\sin i_{MOP}\sin\epsilon}\right\}$$

It has been mentioned previously that the initial orientation of the lunar parking orbit is given by $i_m$, its inclination relative to the moon's orbital plane and by $\theta_{MTE}$, the longitude of its descending node relative to the earth-moon line. However, the orientation of the parking orbit relative to the lunar equatorial plane is also desired. The following angles are defined.

$A = \beta_{\mathbb{C}} - \beta_{\mathbb{C}\Upsilon}$ = true longitude of the moon measured in the moon's orbital plane from $\Upsilon_{\mathbb{C}}$.

$B = A + \theta_{MTE}$ = true longitude of the descending node of the lunar parking orbit measured along the moon's orbital plane from $\Upsilon_{\mathbb{C}}$.

The inclination of the lunar parking orbit plane relative to the lunar equatorial plane can now be found:

$$i_{eq\mathbb{C}} = \cos^{-1}\left\{\cos i_m \cos(I+\gamma) + \sin i_m \sin(I+\gamma)\cos B\right\}. \tag{15}$$

Next, the longitude of the descending node of the lunar parking orbit measured in the lunar equatorial plane from $\Upsilon_{\mathbb{C}}$ is

$$\Lambda_{eq\mathbb{C}} = \cos^{-1}\left\{\frac{\cos(I+\gamma)\cos i_{eq\mathbb{C}} - \cos i_m}{\sin(I+\gamma)\sin i_{eq\mathbb{C}}}\right\} \tag{16}$$

If an injection into a transearth trajectory does not take place at the time of orientation of the lunar parking orbit is known, the orientation must then be computed for the time of the next possible injection. A combination of two motions must be taken into account during this time span. These are the motion of the earth-moon line in the moon's orbital plane (optical librations) and the nodal regression of the lunar parking orbit. The first order secular change in the inclination $i_{eq\mathbb{C}}$ is 0 and, thus, a constant $i_{eq\mathbb{C}}$ is established once the initial orientation of the lunar parking orbit is specified. At some time (t) after the initial time ($t_0$), the longitude relative to the lunar equatorial plane becomes $\Lambda'_{eq\mathbb{C}}$, and the moon's true longitude at a time later than $t_0$ becomes $A'$. The inclination of the parking orbit, $i_m$, at a later time t is then:

$$i_m = \cos^{-1}\left\{\cos(I+\gamma)\cos i_{eq\mathbb{C}} - \sin(I+\gamma)\sin i_{eq\mathbb{C}}\cos\Lambda'_{eq\mathbb{C}}\right\}$$

The true longitude of the descending node of the lunar parking orbit at time t is

$$B' = \cos^{-1}\left\{\frac{\cos i_{eq\mathbb{C}} - \cos(I+\gamma)\cos i'_m}{\sin(I+\gamma)\sin i'_m}\right\} \tag{17}$$

Finally, the longitude of the descending node of the lunar parking orbit relative to the earth-moon line at the later time t is determined as:

$$\theta_{MTE} = B' - A'.$$

It is now desirable to obtain the orientation of the return earth trajectory relative to earth equatorial plane.

The longitude of the descending node of the earth return trajectory at perigee relative to the ascending node of the lunar orbit is:

$$\Omega_{\Delta\mathbb{C}} = \Delta\theta \text{ (see 1st sketch)} + \beta_{\mathbb{C}} + 180^\circ$$

The inclination relative to the earth equatorial plane is then found to be

$$i_{eq\oplus} = \cos^{-1}\left\{\cos i_{VTE}\cos i_{MOP} + \sin i_{\oplus R}\sin i_{MOP}\cos\Omega_{\Delta\mathbb{C}}\right\}$$

It can be seen that the difference between $i_{VTE}$ and $i_{eq\oplus}$ depends on the year ($i_{MOP}$) and on the time of month ($\beta_{\mathbb{C}}$). The right ascension of the ascending node of the near-earth trajectory is given by:

$$\Omega_{\Delta\oplus} = \Omega_{MOP} + \Omega$$

where $\Omega$ is computed from

$$\Omega = \cos^{-1}\left\{\frac{\cos i_{eq\oplus}\cos i_{MOP} + \cos i_{VTE}}{\sin i_{eq\oplus}\sin i_{MOP}}\right\}.$$

3. Transearth Orbital Departure Windows

There are four missions which are of greatest concern in this discussion; they are defined by the constraints imposed on the moon-to-earth trajectory. These constraints are

(1) A constant inclination of the earth return trajectory relative to the earth equatorial plane ($i_{eq\oplus}$).

(2) A constant flight time from lunar injection to earth return perigee ($t_f$).

(3) An orientation of the earth return trajectory such that a rendezvous is possible with another spacecraft already in an earth parking orbit.

The missions are then defined as:

| Mission | Constraints |
|---|---|
| I | (1) |
| II | (1) and (3) |
| III | (1) and (2) |
| IV | (1), (2) and (3) |

Mission I ($i_{eq\oplus}$ = constant) can also be interpreted as a return to earth with a direct atmospheric re-entry without recourse to an intermediate earth parking orbit. This same interpretation can be applied to Mission III ($i_{eq\oplus}$ = constant; $t_f$ = constant) as well. Missions II and IV require an earth parking orbit in order to satisfy constraint (3). It has been found from previous studies (Ref. 2) that constraint (1) ($i_{eq\oplus}$ = constant) can be satisfied by adjusting the injection position, $\beta_M$. That is, the spacecraft remains in its lunar parking orbit until it reaches the proper $\beta_M$, at which time injection into the transearth trajectory takes place. The particular $\beta_M$ will depend on the desired return inclination ($i_{eq\oplus}$), on the position of the moon ($\beta_{\mathbb{C}}$) (or time of the month), and on the inclination of the moon's orbital plane relative to the earth equatorial plane ($i_{MOP}$ or year). No side-thrust maneuver in the lunar parking orbit is required to satisfy constraint (1). However, for the other two constraints, orbital side-thrust maneuvers are required. For example, in order to satisfy constraint (2), which involves a constant transearth flight time ($t_f$), the longitude of the lunar parking orbit node at injection, $\theta_{MTE}$, must be adjusted by a side-thrust maneuver. Furthermore, upon arrival at earth, the orientation of the earth return orbit may not be coplanar with a rendezvous orbit of another earth orbiting vehicle. Thus, a side-thrust maneuver is similarly required in the earth parking orbit to satisfy constraint (3) and make a rendezvous possible.

Therefore, a general mission sequence of events can now be outlined for clarity (see Table 8).

An attempt is made to provide sufficient data that is representative of an entire missions spectrum. This is a difficult task since myriad possible conditions present themselves for analyses and therefore a judicious selection is order.

First, in order to indicate the effects of the varying inclination of the moon's orbital plane relative to the earth's equatorial plane, $i_{MOP}$, two particular dates, April 1969 and July 1978, were selected. During this first date (1969), $i_{MOP}$ has a maximum value of 28.6° while it has a minimum value of 18.3° during the second date (1978). The dependence of the departure windows on the inclination of the lunar parking orbit relative to the lunar equatorial plane, $i_{eq\mathbb{C}}$, was determined be selecting the initial position of the moon in its orbit, $\beta_{\mathbb{C}}$.

The initial orientation of the lunar parking orbit relative to the moon's orbital plane was specified by its inclination $i_m$, and its longitude, $\theta_{MTE}$. The values used in this study for $i_m$ were 20° and 10°, and for $\theta_{MTE}$ 120° and 90°. These orientations are the same as those imposed on the lunar parking orbit in Section A. The inclinations, $i_{eq\mathbb{C}}$, which were dependent upon $i_m$, $\theta_{MTE}$, $\beta_{\mathbb{C}}$, and $i_{MOP}$, were found to be as shown in Table 9.

TABLE 9

| Year | $\beta_{\mathbb{C}}$ | $\theta_{MTE}$ | $i_m$ | $i_{eq\mathbb{C}}$ |
|---|---|---|---|---|
| April 1969 | 0° (AN) | 120° | 20° | 17.51° |
| July 1978 | 0° (AN) | 120° | 20° | 24.07° |
| July 1978 | 90° (MND) | 120° | 20° | 26.06° |
| July 1978 | 180° (DN) | 120° | 20° | 17.65° |
| July 1978 | 270° (MSD) | 120° | 20° | 14.56° |
| July 1978 | 0° (AN) | 120° | 10° | 14.58° |
| July 1978 | 0° (AN) | 90° | 20° | 21.09° |

TABLE 8

Sequence of Events

| Maneuver Impulse Nomenclature | Missions | | | |
|---|---|---|---|---|
| | I | II | III | IV |
| $\Delta V_{m\mathbb{C}}$ | | | 1. Adjust longitude ($\theta_{MTE}$) of lunar parking orbit node with a side-thrust maneuver. | 1. Adjust longitude ($\theta_{MTE}$) of lunar parking orbit node with a side-thrust maneuver. |
| $\Delta V$ | 1. Inject into transearth trajectory after attaining correct position ($\beta_M$) in the lunar parking orbit. | 1. Inject into transearth trajectory after attaining correct position ($\beta_M$) in the lunar parking orbit. | 2. Inject into transearth trajectory after attaining correct position ($\beta_M$) in the lunar parking orbit. | 2. Inject into transearth trajectory after attaining correct position ($\beta_M$) in the lunar parking orbit. |
| $\Delta V_E$ | *2. Brake into an earth parking orbit upon arrival at earth with a retro-thrust maneuver. | 2. Brake into an earth parking orbit upon arrival at earth with a retro-thrust maneuver. | *3. Brake into an earth parking orbit upon arrival at earth with a retro-thrust maneuver. | 3. Brake into an earth parking orbit upon arrival at earth with a retro-thrust maneuver. |
| $\Delta V_{m\oplus}$ | | 3. Adjust longitude of earth parking orbit node with a side-thrust maneuver for rendezvous compatibility with an earth orbiting space station. | | 4. Adjust longitude of earth parking orbit node with a side-thrust maneuver for rendezvous compatibility with an earth orbiting space station. |

*Option: Directly re-enter earth's atmosphere without an intermediate earth parking orbit.

The quantities of interest which are obtained as a result of a time history of energy requirements for the transearth mission are: departure window size, departure window frequency, injection frequency, and wait time, as defined previously in Section A. However, the interval of interest for establishing the departure window frequency is the time for $\theta_{MTE}$ to rotate through 360° -- approximately 30 days. It is well to note again that regardless of mission a single specified $i_{eq\oplus}$ of ±30° is satisfied. All returns are posigrade and the (±) sign only indicates the return hemisphere of the transearth trajectory: (+) northern hemisphere, (-) southern hemisphere.

The data discussed below are for the situation in which only direct-north translunar injections from earth are allowed (Chapter VI) and are the only cases considered herein. It is felt that the resultant windows are representative both in duration and number for the translunar inject-south cases as well.

a. Without parking orbit maneuvers

Missions I and II represent that class of missions where the return flight time is not a constraint and therefore maneuvers in the parking orbit are not required.

$i_{eq\oplus}$ constraint. This constraint specifies that the spacecraft perform a transearth injection which results in arriving at earth with a trajectory inclination of ±30° (constraint 1) relative to the earth's equator. The transearth flight time, as mentioned above, is arbitrary and in addition there is no earth rendezvous requirement. Upon arrival at earth, the spacecraft may make a direct atmospheric re-entry, or may establish an earth parking orbit. Figure 15 depicts typical transearth departure windows for July 1978, beginning when the moon is at its ascending node (t = 0). This figure shows the transearth injection impulse requirement, ΔV, as a function of elapsed time after the nominal arrival at the moon.

The solid lines denote returning from the north ($i_{eq\oplus}$ = 30°); the broken curve represents an earth arrival from the south ($i_{eq\oplus}$ = -30°).

The pronounced solid points on each curve mark the return flight times ($t_f$). Departure windows are determined thusly: let there be a range of practical transearth flight times as mentioned in Section A. Also assume a propulsion capability, ΔV (horizontal line). The departure windows are then determined by the intersection of the horizontal line (ΔV) and/or practical flight time limits.

After arrival at the moon, the spacecraft generally will remain in its lunar parking orbit until the first departure window is entered. This time interval is referred to specifically as the "first wait time" or "stay time." The time interval between successive departure windows is termed only as "wait time." As can be observed in Fig. 15, window sizes can possibly be increased and wait times reduced if both returns ($\pm i_{eq\oplus}$) are utilized.

Also from Fig. 15, it is seen that two departure windows exist for a 1-month time span. Since there is a large overlap between both northerly and southerly returns, the number of windows remain the same when both returns are permitted. However, there is an accompanied increase in window size.

Transearth flight times between 40 and 120 hr are indicated in the figure in 10-hr increments. In order to gain an insight into the magnitude of numbers associated with departure windows for Mission I, a velocity capability (ΔV) of 1.0 km/sec is considered reasonable. Furthermore, transearth flight times ($t_f$) between 50 and 100 hr are considered practical. Two different restrictions for determining the departure windows now become apparent.

(1) Flight time restrictions only

$$50 \leq t_f \leq 100 \text{ hr}$$

(2) Flight time and ΔV restrictions

$$\Delta V \leq 1.0 \text{ km/sec}, \quad 50 \leq t_f \leq 100 \text{ hr}$$

The results for the above conditions are presented in subsequent tables as a function of year and time of the month (i.e., the position of the moon at the nominal moon arrival). The following codes are used to signify the allowable earth return direction:

$+i_{eq}$: only returns to the northern earth hemisphere ($i_{eq\oplus}$ = +30°) are allowed

$-i_{eq}$: only returns to the southern earth hemisphere ($i_{eq\oplus}$ = -30°) are allowed

$\pm i_{eq}$: returns to either the northern earth hemisphere ($i_{eq\oplus}$ = +30°) or the southern earth hemisphere ($i_{eq\oplus}$ = -30°) are allowed.

Table 10 presents the results for the above specified conditions. For the flight time restriction ($50 \leq t_f \leq 100$ hr), there is little variance in the magnitude of the departure windows from 1969 to 1978. The actual magnitude varies from 54 hr to 144 hr depending on what earth return directions are allowed. With the ΔV restriction ($\Delta V \leq 1.0$ km/sec) included, the window sizes are reduced by 5 to 30 hr. In all cases, allowing a return to be from either direction ($\pm i_{eq\oplus}$) the windows are wider by approximately 12 to 76 hr for the restriction $50 \leq t_f \leq 100$ hr with the greatest change being realized in 1978. With both restrictions ($t_f$ and ΔV) the same trends are exhibited.

The injection frequencies (i.e., the number of possible injections during a departure window) can be immediately found from the previous results and are presented in Table 11.

TABLE 10

Mission I
Lunar Departure Windows

| First Departure Window (hr) | | | | | | | | | | | | | | | |
|---|---|---|---|---|---|---|---|---|---|---|---|---|---|---|---|
| Year | 1969 | | | 1978 | | | 1978 | | | 1978 | | | 1978 | | |
| Position of moon (Ba) | AN | | | AN | | | MND | | | DN | | | MSD | | |
| | $+i_{eq}$ | $-i_{eq}$ | $\pm i_{eq}$ | $+i_{eq}$ | $-i_{eq}$ | $\pm i_{eq}$ | $+i_{eq}$ | $-i_{eq}$ | $\pm i_{eq}$ | $+i_{eq}$ | $-i_{eq}$ | $\pm i_{eq}$ | $+i_{eq}$ | $-i_{eq}$ | $\pm i_{eq}$ |
| $50 \leq t_f \leq 100$ hr | 88 | 64 | 100 | 100 | 70 | 132 | 100 | 78 | 134 | 106 | 80 | 138 | 96 | 66 | 130 |
| $50 \leq t_f \leq 100$ hr $\Delta V < 1.0$ km/sec | 68 | 46 | 82 | 80 | 36 | 98 | 72 | 62 | 118 | 86 | 68 | 126 | 84 | 56 | 120 |
| Second Departure Window (hr) | | | | | | | | | | | | | | | |
| | $+i_{eq}$ | $-i_{eq}$ | $\pm i_{eq}$ | $+i_{eq}$ | $-i_{eq}$ | $\pm i_{eq}$ | $+i_{eq}$ | $-i_{eq}$ | $\pm i_{eq}$ | $+i_{eq}$ | $-i_{eq}$ | $\pm i_{eq}$ | $+i_{eq}$ | $-i_{eq}$ | $\pm i_{eq}$ |
| $50 \leq t_f \leq 100$ hr | 60 | 68 | 84 | 62 | 78 | 108 | 90 | 104 | 144 | 86 | 136 | 162 | 54 | 90 | 118 |
| $50 \leq t_f \leq 100$ hr $\Delta V \leq 1.0$ km/sec | 52 | 64 | 80 | 56 | 66 | 102 | 76 | 78 | 130 | 70 | 108 | 146 | 46 | 72 | 110 |

TABLE 11

Mission I

| Injection Frequency for First Departure Window | | | | | | | | | | | | | | | |
|---|---|---|---|---|---|---|---|---|---|---|---|---|---|---|---|
| Year | 1969 | | | 1978 | | | 1978 | | | 1978 | | | 1978 | | |
| Position of moon | AN | | | AN | | | MND | | | DN | | | MSD | | |
| | $+i_{eq}$ | $-i_{eq}$ | $\pm i_{eq}$ | $+i_{eq}$ | $-i_{eq}$ | $\pm i_{eq}$ | $+i_{eq}$ | $-i_{eq}$ | $\pm i_{eq}$ | $+i_{eq}$ | $-i_{eq}$ | $\pm i_{eq}$ | $+i_{eq}$ | $-i_{eq}$ | $\pm i_{eq}$ |
| $50 \leq t_f \leq 100$ hr | 42 | 30 | 72 | 48 | 33 | 81 | 47 | 37 | 84 | 50 | 38 | 88 | 46 | 31 | 77 |
| $50 \leq t_f \leq 100$ hr $\Delta V \leq 1.0$ km/sec | 32 | 22 | 54 | 38 | 17 | 55 | 34 | 29 | 63 | 41 | 32 | 73 | 40 | 27 | 67 |
| Injection Frequency for Second Departure Window | | | | | | | | | | | | | | | |
| | $+i_{eq}$ | $-i_{eq}$ | $\pm i_{eq}$ | $+i_{eq}$ | $-i_{eq}$ | $\pm i_{eq}$ | $+i_{eq}$ | $-i_{eq}$ | $\pm i_{eq}$ | $+i_{eq}$ | $-i_{eq}$ | $\pm i_{eq}$ | $+i_{eq}$ | $-i_{eq}$ | $\pm i_{eq}$ |
| $50 \leq t_f \leq 100$ hr | 29 | 32 | 61 | 30 | 37 | 67 | 43 | 49 | 92 | 41 | 65 | 106 | 26 | 43 | 69 |
| $50 \leq t_f \leq 100$ hr $\Delta V \leq 1.0$ km/sec | 25 | 30 | 55 | 27 | 31 | 58 | 36 | 37 | 73 | 33 | 51 | 84 | 22 | 34 | 56 |

TABLE 12

Mission I
Wait Times (hr)

| First Wait Time | | | | | | | | | | | | | | | |
|---|---|---|---|---|---|---|---|---|---|---|---|---|---|---|---|
| Year | 1969 | | | 1978 | | | 1978 | | | 1978 | | | 1978 | | |
| Position of moon | AN | | | AN | | | MND | | | DN | | | MSD | | |
| | $+i_{eq}$ | $-i_{eq}$ | $\pm i_{eq}$ | $+i_{eq}$ | $-i_{eq}$ | $\pm i_{eq}$ | $+i_{eq}$ | $-i_{eq}$ | $\pm i_{eq}$ | $+i_{eq}$ | $-i_{eq}$ | $\pm i_{eq}$ | $+i_{eq}$ | $-i_{eq}$ | $\pm i_{eq}$ |
| $50 \leq t_f \leq 100$ hr | 100 | 136 | 100 | 78 | 140 | 78 | 72 | 128 | 72 | 38 | 96 | 38 | 48 | 112 | 48 |
| $50 \leq t_f \leq 100$ hr $\Delta V \leq 1.0$ km/sec | 100 | 136 | 100 | 78 | 140 | 78 | 72 | 128 | 72 | 38 | 96 | 38 | 48 | 112 | 48 |
| Wait Time Between Windows | | | | | | | | | | | | | | | |
| | $+i_{eq}$ | $-i_{eq}$ | $\pm i_{eq}$ | $+i_{eq}$ | $-i_{eq}$ | $\pm i_{eq}$ | $+i_{eq}$ | $-i_{eq}$ | $\pm i_{eq}$ | $+i_{eq}$ | $-i_{eq}$ | $\pm i_{eq}$ | $+i_{eq}$ | $-i_{eq}$ | $\pm i_{eq}$ |
| $50 \leq t_f \leq 100$ hr | 310 | 234 | 234 | 280 | 244 | 244 | 276 | 188 | 188 | 304 | 196 | 196 | 352 | 254 | 254 |
| $50 \leq t_f \leq 100$ hr $\Delta V \leq 1.0$ km/sec | 332 | 250 | 250 | 300 | 262 | 262 | 304 | 204 | 204 | 324 | 208 | 208 | 364 | 268 | 268 |

Note that the injection frequencies follow the same trend as the departure window sizes since the number of possible injections varies directly with window size. Also note from Fig. 15, that because northerly and southerly return windows do overlap, it is possible to have two transearth injection points on the same orbital pass if either return ($\pm i_{eq}$) is acceptable. In this circumstance, injection frequencies are the sum of the two separate injection frequencies ($+i_{eq}$, $-i_{eq}$). For returning from one direction only ($+i_{eq}$ or $-i_{eq}$), the number of possible injections can range from 17 to 65, and for returns from either direction ($\pm i_{eq}$), possible injections can range from 54 to 106.

Another important variable is the wait time. A listing of the wait times is given in Table 12.

The first wait times for both $t_f$ and $\Delta V$ restrictions are the same since the transearth flight time is the determining factor for the first departure window. There is a variance in the first wait times which is a function of year and nominal position of the moon. This is due to the fact that even though the energy requirements for transearth injection are the same, the time at which they occur is dependent on the geometrical configuration of the principal planes and on the position of the moon.

First wait times in 1978 can vary from 38 to 78 hr and wait times between successive windows may vary between 180 and 370 hr.

Thus far, only an $i_m = 20°$ and $\theta_{MTE} = 120°$ has been considered. Comparison situations for initial orientations of $i_m = 20°$ and $\theta_{MTE} = 90°$ and of $i_m = 10°$ and $\theta_{MTE} = 120°$ yielded the results shown in Table 13 for July 1978, when the moon is at its ascending node.

Comparing this table with Table 10, it is noted that the change in the departure windows due to a change in $\theta_{MTE}$ is from 2 to 20 hr for both single return directions ($+i_{eq}$ or $-i_{eq}$) and for any direction ($\pm i_{eq}$). Thus, a change in $\theta_{MTE}$ in the range considered is not very influential in altering window sizes. The above statement is also true for a change in $i_m$.

For an initial $\theta_{MTE} = 90°$, and for northerly returns to earth, there is a small first wait time (12 hr) since the node of the lunar parking orbit is such that satisfactory transearth trajectories can take place sooner than for initial $\theta_{MTE}$ greater than 90°. This can be seen in Table 13 which also lists wait times for the above comparison conditions. Note that the wait times between windows are quite comparable to those presented in Table 12.

$i_{eq\oplus}$ and earth rendezvous constraints. Mission II is a direct extension of Mission I and specifies that the spacecraft, upon arriving at earth with an $i_{eq\oplus}$ of ±30°, enters into an earth parking orbit, then performs a side-thrust maneuver for rendezvous purposes. This maneuver makes the return parking orbit plane coplanar with a space station orbital plane. For this particular case it is assumed that the returning spacecraft initiated

TABLE 13

Mission I
April 1978--Moon at AN

| | First Departure Window (hr) | | | | First Wait Time (hr) | | | |
|---|---|---|---|---|---|---|---|---|
| | $i_m = 20°$, $\theta_{MTE} = 90°$ | | | $i_m = 10°$, $\theta_{MTE} = 120°$ | | | $i_m = 10°$, $\theta_{MTE} = 120°$ | |
| | $+i_{eq}$ | $-i_{eq}$ | $\pm i_{eq}$ | $+i_{eq}$ | $-i_{eq}$ | $\pm i_{eq}$ | $+i_{eq}$ | $-i_{eq}$ | $\pm i_{eq}$ | $+i_{eq}$ | $-i_{eq}$ | $\pm i_{eq}$ |
| $50 \leq t_f \leq 100$ hr | 104 | 66 | 130 | 90 | 50 | 145* | 12 | 76 | 12 | 60 | 178 | 60 |
| $50 \leq t_f \leq 100$ hr, $\Delta V \leq 1.0$ km/sec | 82 | 56 | 120 | 80 | 38 | 118* | 12 | 76 | 12 | 60 | 178 | 60 |
| | Second Departure Window (hr) | | | | | | Wait Time Between Windows (hr) | | | | | |
| | $+i_{eq}$ | $-i_{eq}$ | $\pm i_{eq}$ | $+i_{eq}$ | $-i_{eq}$ | $\pm i_{eq}$ | $+i_{eq}$ | $-i_{eq}$ | $\pm i_{eq}$ | $+i_{eq}$ | $-i_{eq}$ | $\pm i_{eq}$ |
| $50 \leq t_f \leq 100$ hr | 52 | 80 | 106 | 50 | 80 | 130* | 330 | 250 | 250 | 362 | 208 | 208 |
| $50 \leq t_f \leq 100$ hr, $\Delta V \leq 1.0$ km/sec | 48 | 68 | 102 | 46 | 66 | 112* | 352 | 260 | 260 | 390 | 220 | 220 |

*For an initial orientation of $i_m = 10°$ and $\theta_{MTE} = 120°$, the departure windows for northerly and southerly earth returns do not overlap. For the first departure windows there is an additional wait time of 10 hr (included in quoted number) between the north and south returns and for the second departure windows there is an additional wait time of 14 hr (included in quoted number) between the north and south returns.

its lunar mission from the earth orbiting space station. Figure 16 presents departure windows for this case by showing the total velocity requirement ($\Delta V + \Delta V_E + \Delta F_{m\oplus}$) versus elapsed time from date of moon arrival. The maneuver impulse required to enter an earth parking orbit is $\Delta V_E$, and $\Delta V_{m\oplus}$ is the side-thrust maneuver impulse required for rendezvous purposes.

Again, in this figure, the solid lines denote a northerly return ($+i_{eq\oplus}$) and the broken lines a southerly return ($-i_{eq\oplus}$). However, for this mission there are two representative curves for a given elapsed time. The two curves for any $i_{eq\oplus}$ are for two translunar flight times ($t_p$) which affect the right ascension of the space station parking orbit at the time of arrival at earth. The two translunar flight times ($t_p$) selected are 50 hr and 100 hr which are considered as practical outbound durations. If the moon-to-earth trajectory flight time is $t_f$, then the right ascension at the time of return is:

$$\Omega_{s\oplus} = \Omega_{s\oplus 0} + \frac{d\Omega_{s\oplus}}{dt}(t_p + t_f + t_s) \qquad (28)$$

where

$\Omega_{s\oplus 0}$ = right ascension of earth parking orbit at the time of translunar injection

$\frac{d\Omega_{s\oplus}}{dt}$ = constant average nodal regression rate

$t_s$ = stay time in the lunar parking orbit

The right ascension of the earth return parking orbit at the time of return earth perigee is $\Omega_{\Delta\oplus}$, and thus a nodal shift of $\Omega_{\Delta\oplus} - \Omega_{s\oplus}$ must be accomplished. The required azimuth change is:

$$\Delta A_\oplus = \cos^{-1}\left\{\cos^2 i_{eq\oplus} + \sin^2 i_{eq\oplus}\cos(\Omega_{\Delta\oplus} - \Omega_{s\oplus})\right\} \qquad (29)$$

In Fig. 16, the pronounced solid points on each curve again mark the return flight times ($t_f$) in 10-hr increments. For the windows given below this practical flight range is again 50 to 100 hr.

If a $\Delta V$ (propulsion capability) $\leq$ 5.0 km/sec is assumed and allowing both northerly and southerly earth returns, there exists at least one departure window during a 1-mo time interval. Table 14 gives a summary of mission II. It is quite evident that in addition to a decrease in departure window frequency from mission I, a large reduction in window size is also realized.

From Table 14 it is observed that the windows a are strongly dependent on both year and time of month and in some cases also dependent on translunar flight time ($t_p$). The related injection frequency is also shown.

Table 15 presents departure windows for an $i_m = 20°$, $\theta_{MTE} = 90°$ and $i_m = 10°$, $\theta_{MTE} = 120°$.

TABLE 14

Mission II
Departure Windows (hr)

$\Delta V \leq 5$ km/sec
Translunar flight time between 50 and 100 hr
Transearth flight time between 50 and 90 hr
$i_m = 20°$; $\theta_{MTE} = 120°$

| Year | April 1969 | | July 1978 | | July 1978 | | July 1978 | | July 1978 | |
|---|---|---|---|---|---|---|---|---|---|---|
| Initial position of moon | AN | | AN | | MND | | DN | | MSD | |
| | $t_p = 50$ | $t_p = 100$ | $t_p = 50$ | $t_p = 100$ | $t_p = 50$ | $t_p = 100$ | $t_p = 50$ | $t_p = 100$ | $t_p = 50$ | $t_p = 100$ |
| $i_{eq\oplus} = -30°$ | 62 | 60 | 32 | 8 | 32 | 36 | 8 | 0 | 0 | 0 |
| $i_{eq\oplus} = +30°$ | 0 | 0 | 0 | 0 | 0 | 0 | 16 | 30 | 70 | 68 |
| Injection Frequency--Mission II | | | | | | | | | | |
| | $t_p = 50$ | $t_p = 100$ | $t_p = 50$ | $t_p = 100$ | $t_p = 50$ | $t_p = 100$ | $t_p = 50$ | $t_p = 100$ | $t_p = 50$ | $t_p = 100$ |
| $i_{eq\oplus} = -30°$ | 30 | 29 | 15 | 4 | 15 | 17 | 4 | 0 | 0 | 0 |
| $i_{eq\oplus} = +30°$ | 0 | 0 | 0 | 0 | 0 | 0 | 8 | 14 | 33 | 32 |

TABLE 15

Mission II

Departure Windows and Injection Frequency

$\Delta V \leq 5$ km/sec

| Year | July 1978 | | July 1978 | |
|---|---|---|---|---|
| Initial position of moon | AN | | AN | |
| $i_m$, $\theta_{MTE}$ | 20° ; 90° | | 10° ; 120° | |
| | $t_p$ = 50 | $t_p$ = 100 | $t_p$ = 50 | $t_p$ = 100 |
| $i_{eq\oplus}$ = -30° | 52 | 68 | 42 | 22 |
| $i_{eq\oplus}$ = +30° | 0 | 0 | 0 | 26 |
| Injection frequency | 25 | 32 | 20 | 10 |
| | 0 | 0 | 0 | 12 |

As can be seen, the resultant departure windows are sensitive to $i_m$ and $\theta_{MTE}$ variations and can actually be enlarged with a proper selection.

Since there is usually only one departure window per month, the first wait time becomes most important. A summary listing of wait times is given in Table 16 and comparing this table with Tables 12 and 13 shows that the first wait time has increased significantly--on the order of 100 to 400 hr because of the rendezvous requirement (constraint 3).

b. With parking orbit maneuvers

Missions III and IV represent that class of missions where the transearth flight time is a specified constraint. Therefore, side-thrust maneuvers will be required in the lunar parking orbit to adjust $\theta_{MTE}$.

$i_{eq\oplus}$ - $t_f$ constraints. This mission specifies that the spacecraft perform a transearth injection which results in arriving at earth in a prespecified flight time (constraint 2) and with a trajectory inclination of ±30° ($i_{eq\oplus}$, constraint 1). At arrival, the spacecraft may make a direct atmospheric re-entry, or may establish an earth parking orbit.

Figure 17 shows graphically typical departure windows for this case by giving the transearth injection requirement ($\Delta V$ km/sec) and the maneuver requirement ($\Delta V_m$ km/sec) to adjust the parking orbit node as a function of elapsed time (hr) after the nominal arrival at the moon.

The solid lines denote returning posigrade from the north ($i_{eq\oplus}$ = +30°) while the dashed lines represent a posigrade southerly return ($i_{eq\oplus}$ = -30°). Each figure depicts a window for a constant transearth flight time ($t_f$). Two extreme values of $t_f$ are used as criteria in establishing the windows, namely, $t_f$ = 50 hr and $t_f$ = 90 hr. The departure windows are determined by the intersection of the $\Delta V$ (propulsion capability) line and ($\Delta V + \Delta V_{m\mathbb{C}}$) curves. Referring to the above reference figure, there are two departure windows for both northerly and southerly earth returns during the one month

TABLE 16

Mission II

First Wait Times (hr)

| Year | 1969 | 1978 | 1978 | 1978 | 1978 | 1978 | 1978 |
|---|---|---|---|---|---|---|---|
| Moon position | AN | AN | MND | DN | MSD | AN | AN |
| $i_m$ (deg) | 20 | 20 | 20 | 20 | 20 | 20 | 10 |
| $\theta_{MTR}$ (deg) | 120 | 120 | 120 | 120 | 120 | 90 | 120 |
| Wait time | | | | | | | |
| $t_p$ = 50 hr | 452 | 444 | 440 | 128 | 78 | 420 | 436 |
| $t_p$ = 100 hr | 444 | 444 | 426 | 112 | 54 | 392 | 436 |

time span. Assuming a $\Delta V$ capability of 1.5 km/sec, Table 17 lists window sizes for an initial lunar parking orbit orientation of $i_m = 20°$ and $\theta_{MTE} = 120°$.

TABLE 17

Mission III

Departure Windows (hr)
$\Delta V = 1.5$ km/sec

| Year | 1969 | | | 1978 | | | 1978 | | |
|---|---|---|---|---|---|---|---|---|---|
| Lunar Position | AN | | | AN | | | MND | | |
| | $+i_{eq}$ | $-i_{eq}$ | $\pm i_{eq}$ | $+i_{eq}$ | $-i_{eq}$ | $\pm i_{eq}$ | $+i_{eq}$ | $-i_{eq}$ | $\pm i_{eq}$ |
| 1st window | | | | | | | | | |
| $t_f = 50$ hr | 88 | 100 | 112 | 92 | 114 | 150 | 110 | 122 | 150 |
| $t_f = 90$ hr | 242 | 276 | 284 | 256 | 584* | U** | -- | -- | -- |
| 2nd window | | | | | | | | | |
| $t_f = 50$ hr | 120 | 110 | 130 | 144 | 132 | 172 | 134 | 134 | 166 |
| $t_f = 90$ hr | 196 | 214 | 248 | 592 | 584* | U** | -- | -- | -- |

*The first and second departure windows overlap to give a total window as quoted.

**Unlimited windows--capable of returning to earth at any time.

The preceding table emphasizes the effect of transearth flight time on window size. Essentially, for longer flight times ($t_f$), the $\Delta V$ to perform a transearth injection diminishes and therefore additional $\Delta V$ can be allocated for maneuvering purposes. Note also in the table that the year and time of month do not influence the window sizes to any significant degree.

As pointed out above, since the longer flight times provide wider windows, it is to be expected that the wait times involved will be shortened. Table 18 verifies this statement and shows that the wait times also are, to a high degree, independent of year or time of the month.

Although independent of year and time of month, they are however, sensitive to both the initial $i_m$ and $\theta_{MTE}$. Essentially, lower values of $i_m$ shift the available windows toward the nominal arrival time as do longer flight times. Lower values of $i_m$ do not shift the windows but rather lower $\Delta V + \Delta V_{m\mathbb{C}}$ requirements which also effectively increase window size. The latter point is due to the fact that the required azimuth change (to change nodal position) is much more efficiently obtained with lower values of $i_m$.

$i_{eq\oplus}$ - $t_f$ and earth rendezvous constraints.

As was the case for Mission II, Mission IV is

TABLE 18

Mission III

Wait Time (hr)
$\Delta V = 1.5$ km/sec

| Year | 1969 | | | 1978 | | | 1978 | | |
|---|---|---|---|---|---|---|---|---|---|
| Lunar Position | AN | | | AN | | | MND | | |
| | $+i_{eq}$ | $-i_{eq}$ | $\pm i_{eq}$ | $+i_{eq}$ | $-i_{eq}$ | $\pm i_{eq}$ | $+i_{eq}$ | $-i_{eq}$ | $\pm i_{eq}$ |
| 1st wait time | | | | | | | | | |
| $t_f = 50$ hr | 140 | 152 | 140 | 116 | 152 | 116 | 122 | 150 | 122 |
| $t_f = 90$ hr | 0 | 8 | 0 | 0 | 0 | 0 | -- | -- | -- |
| Wait time between windows | | | | | | | | | |
| $t_f = 50$ hr | 244 | 210 | 210 | 260 | 194 | 194 | 230 | 158 | 158 |
| $t_f = 90$ hr | 138 | 52 | 52 | 118 | 0 | 0 | -- | -- | -- |

now an extension of Mission III in the sense that, after arrival at earth, the spacecraft performs a side thrust maneuver to establish a coplanar orbit with an earth orbiting station.

The total velocity required to eject from a lunar parking orbit and return to an earth parking orbit is presented as a function of elapsed time for a typical situation in Fig. 18. This total velocity is the sum ($\Delta V + \Delta V_{m\mathbb{C}} + \Delta V_E + \Delta V_{m\oplus}$) and is dominated by $\Delta V_{m\oplus}$, the impulse to perform the earth parking orbit maneuver.

As before, the solid and broken curves on this figure represent northerly ($+i_{eq}$) and southerly ($-i_{eq}$) returns, respectively. Departure windows and wait times are determined by the $\Delta V$ capability intersections. Observe from Fig. 18 that there are three potential windows during a month. The cycling of the windows for a translunar inject-north case is: northerly returns ($+i_{eq}$), southerly ($-i_{eq}$) and again, northerly.

This cycling is reversed when the translunar injection is southerly.

Table 19 has been prepared from the referenced figures assuming a $\Delta V$ of 5.0 km/sec. This table gives the departure windows (in hours) and the corresponding injection frequency (enclosed in parentheses). As was the case for Mission III, longer transearth flight times ($t_f$) can increase the windows significantly. However, contrary to the Mission III results, reducing $\theta_{MTE}$ or $i_m$ does not increase the window sizes nor reduce the wait times because the impulse ($\Delta V_E + \Delta V_{m\oplus}$) completely dominates the width of the windows.

The related first wait times are shown in Table 20. With the rendezvous requirement, the first wait time is on the order of 200 hr.

c. Departure window sensitivities

It is advantageous to qualitatively summarize what effect certain parameters have on transearth

TABLE 19

Mission IV

Departure Windows and Injection Frequencies

| Year, Lunar Position, $i_m$, $\theta_{MTE}$ | 1st Window Northerly Return ($+i_{eq}$) | | 2nd Window Southerly Return ($-i_{eq}$) | | 3rd Window Northerly Return ($\pm i_{eq}$) | |
|---|---|---|---|---|---|---|
| | $t_p$ = 50 hr | $t_p$ = 100 hr | $t_p$ = 50 hr | $t_p$ = 100 hr | $t_p$ = 50 hr | $t_p$ = 100 hr |
| **$t_f$ = 50 hr** | | | | | | |
| April 1969, AN, 20°, 120° | 6 (3) | 8 (4) | 24 (11) | 26 (12) | 36 (17) | 50 (24) |
| July 1978, AN, 20°, 120° | 12 (6) | 14 (7) | 16 (8) | 16 (8) | 28 (13) | 36 (17) |
| July 1978, MND, 20°, 120° | 10 (5) | 14 (7) | 16 (8) | 12 (6) | 0 (0) | 0 (0) |
| **$t_f$ = 90 hr** | | | | | | |
| April 1969, AN, 20°, 120° | 9 (4) | 12 (6) | 48 (23) | 68 (32) | 50 (24) | 40 (19) |
| July 1978, AN, 20°, 120° | 18 (8) | 20 (9) | 50 (24) | 52 (25) | 36 (17) | 36 (17) |
| July 1978, AN, 20°, 90° | 14 (7) | 16 (8) | 48 (23) | 56 (27) | 34 (16) | 26 (12) |
| July 1978, AN, 10°, 120° | 28 (13) | 32 (15) | 56 (27) | 56 (27) | 54 (26) | 50 (24) |

TABLE 20

Mission IV

$\Delta V \leq 5.0$ km/sec

1st Wait Time (hr)

| Year | Lunar Position | $i_m$ (deg) | $\theta_{MTE}$ (deg) | $t_f$ | $t_p = 50$ | $t_p = 100$ |
|---|---|---|---|---|---|---|
| 1969 | AN | 20 | 120 | 50 | 248 | 236 |
| 1978 | AN | 20 | 120 | 50 | 226 | 212 |
| 1978 | MND | 20 | 120 | 50 | 222 | 208 |
| 1969 | AN | 20 | 120 | 90 | 240 | 228 |
| 1978 | AN | 20 | 120 | 90 | 210 | 196 |
| 1978 | AN | 20 | 90 | 90 | 212 | 196 |
| 1978 | AN | 10 | 120 | 90 | 208 | 188 |

departure window sizes and wait times. The table below gives a brief description of window sensitivity due to year, lunar position, lunar parking orbit orientation and flight times. The window variations are described as being minor, moderate or major in nature, assessed from the data presented above.

Aside from the above, window sizes and delay times can also be affected by the governing constraints of $i_{eq\oplus}$, $t_f$, $h_{PL}$ and $h_{PE}$. It has been found that a tolerance of ±0.5° on the earth return inclination ($i_{eq\oplus}$) has negligible effect on window sizes and wait times. It is felt that the data presented herein is representative of tolerances of ±1° to ±3° or in other words $i_{eq\oplus} = \pm 27°$ to ±33°.

A flight time tolerance of ±0.5 hr on the transearth flight time ($t_f$) is also quite acceptable. In fact, it can be confidently stated that this tolerance could be extended to ±1.5 hr without seriously detracting from the study results.

Variations in the lunar parking orbit altitude ($h_{PL}$) and earth perigee altitude ($h_{PE}$) have not been specifically investigated. However, from the related experience in Chapters VI and IX and in Chapter I of Ref. 1, it can be said with assurance that variations of ±100 km in $h_{PE}$ and ±10 km in $h_{PL}$ will not alter the data to any significant degree.

4. Transearth Inject-on-Time Windows

An approach identical to that in Section A3. is taken to determine a lunar inject-on-time window. Figure 19 presents a window for a transearth flight time of 70 hours (eccentricity ≈ 1.422).

For the situation depicted in this figure, the minimum $\gamma_{\mathbb{C}}$ was found to be -19.3° which corresponded to a time of -11.1 min. If the maximum velocity impulse [$\Delta(\Delta V)$] available is 0.1 km/sec, then this secondary departure window at a lunar altitude of 185.2 km yields a window size of 17 min. As was shown in Ref. 1 of Chapter I, the $\Delta(\Delta V)$ requirements will increase because of finite burning and the optimum $\gamma_{\mathbb{C}}$ will shift from 0° to some positive value.

## C. MISSION IMPLICATIONS

The foregoing sections have discussed in detail the various methods which can be employed to generate orbital departure windows from a lunar or earth parking orbit. Also included are numerical results for departure window sizes, injection frequencies, and waiting times for these methods

Transearth Departure Window Sensitivities

| | Mission I | | | Mission II | | | Mission III | | | Mission IV | | |
|---|---|---|---|---|---|---|---|---|---|---|---|---|
| | Window | 1st Wait Time | Wait Time | Window | 1st Wait Time | Wait Time | Window | 1st Wait Time | Wait Time | Window | 1st Wait Time | Wait Time |
| Year | Minor | Moderate | Minor | Moderate | Minor | Moderate | Minor | Minor | Minor | Minor | Minor | Major |
| Lunar position | Minor | Moderate | Minor | Moderate | Major | Major | Minor | Minor | Minor | Moderate | Minor | Moderate |
| $i_m$ | Minor | Minor | Minor | Minor | Minor | Moderate | Major | Major | Major | Minor | Minor | Minor |
| $\theta_{MTE}$ | Minor | Major | Minor | Minor | Minor | Minor | Minor | Major | Major | Minor | Minor | Minor |
| $t_f$ | -- | -- | -- | -- | -- | -- | Major | Major | Major | Minor | Minor | Moderate |
| $t_p$ | -- | -- | -- | Minor | Minor | Minor | -- | -- | -- | Minor | Minor | Minor |

which reflect various imposed constraints. It is the intent of this section to give an insight to the philosophy that is presently associated with lunar missions and their related windows. This can be best accomplished by depicting sample missions and the circumstances that may be present during their execution.

## 1. Mission Methodology

First, the spacecraft may originally leave the earth's vicinity either from an "independent" parking orbit or from a "dependent" parking orbit. The former implies a convenient orbit established at the end of boost and the latter refers to a parking orbit of an earth orbiting space station. It may be necessary to transfer additional personnel and supplies and also assemble necessary "space structure" in the independent orbit prior to embarking on the translunar trip. Likewise, supplies and personnel may have to be "shuttled" to the space station if the station is being used as a "jumping off" point. In either case, there may be extensive waiting in the earth parking orbit before the lunar mission is initiated. Once all the tasks are complete and the spacecraft makes an entrance into an earth-to-moon departure window, the spacecraft then injects into a translunar trajectory that arrives at the moon with a specific orientation. However, the translunar injection could be temporarily cancelled because of system malfunctions, insufficient checkout, a need for reverification of system status, ground equipment breakdown or perhaps by uncompleted orbital tasks.

The "delayed" injection technique, in which only one orbit adjustment maneuver takes place prior to injection, will most likely be used when the delay time is predictable. For example, if it is known that a certain repair will take at least a certain number of orbital passes, there is no reason to conduct any maneuver during this time interval.

For the "sequential" maneuver technique, the probable cause will stem from "last minute" delays; that is, even though the parking orbit has been properly adjusted, another unforeseen problem arises prior to injection which necessitates a further delay. Assuming that this problem is remedied, the parking orbit is readjusted only again to have the injection postponed because of additional trouble.

Adjustment maneuvers in the parking orbit can be eliminated if the adjustment is allowed to take place along the translunar trajectory instead. (Ref. 5). However, this technique is considered highly demanding because of the difficulty in determining the maneuver, and because of the additional tracking and midcourse correction requirements. Thus, for the next decade, adjustments made in the earth parking orbit are considered most practical.

After transit through cislunar space, the spacecraft will arrive at the moon and will establish a parking orbit with a retrograde-maneuver. It is important to realize that there are two arrival envelopes that satisfy flight time and periselenium considerations. These envelopes are determined by the locii of the possible descending node positions as illustrated in the following sketch.

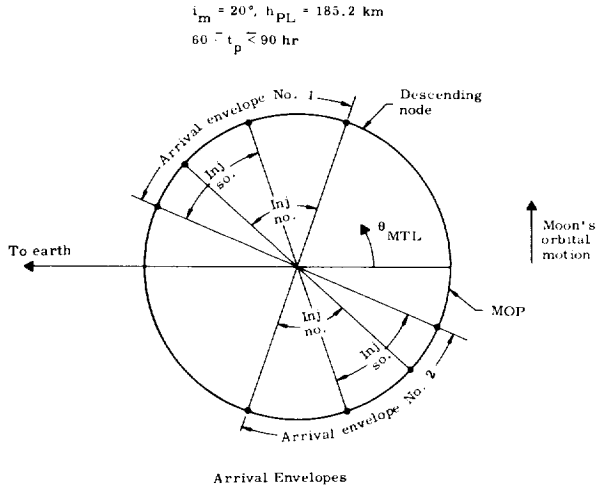


Arrival Envelopes

As noted, the envelopes satisfy the mission constraints of: $i_m = 20°$, $60 \leq t_p \leq 90$ hr and $h_{PL} = 185.2$ km. $\theta_{MTL}$ denotes the longitude angle, measured in the MOP, of the descending node of the arrival trajectory.

When $\theta_{MTL}$ is less than 180°, it can be seen that the orbital traces will "cover" lunar sites located above the MOP for the lunar hemisphere facing the earth and sites below the MOP for the opposite hemisphere. When $\theta_{MTL}$ is greater than 180°, the converse is true. Also observe from the above sketch how each arrival envelope is divided into sections which represent the translunar injection direction.

After the vehicle establishes a lunar parking orbit, the next phase of the mission commences. This phase may be a photographic or surveillance operation or perhaps supplies and personnel are "shuttled" to and from a lunar base. Or, possibly, a separate vehicle module is used to descend to the lunar surface for surface exploration and upon completion of its mission rejoins the orbiting module. All of these possible mission phases utilize a lunar parking orbit which is regressing with time because of the moon's triaxiality. In addition, the parking orbit orientation is changing rapidly because of the moon's travel around the earth. As soon as the lunar mission phase is completed and the spacecraft enters a moon-to-earth departure window, the transearth injection maneuver is executed.

The transearth departure window is also characterized by two departure envelopes as shown by the next sketch where $\theta_{MTE}$ now represents the departure trajectory longitude angle. Now $\theta_{MTE} \approx \theta_{MTL} + \omega_{\mathbb{C}} t_s$, and, thus, the spacecraft must remain in its parking orbit a certain interval of time ($t_s$) until one of the departure envelopes is entered.

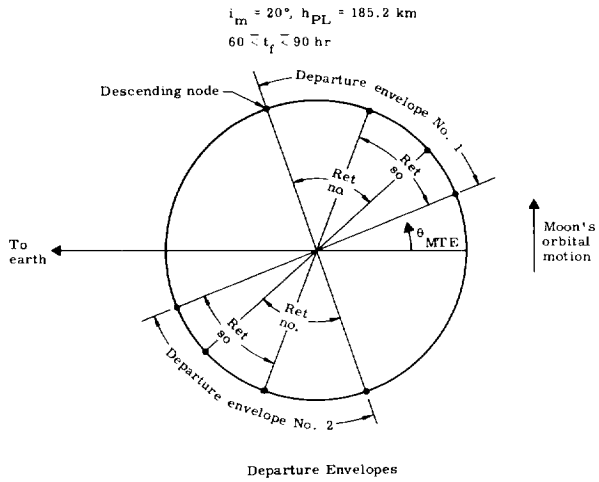


Departure Envelopes

The transearth trajectory will have stringent requirements depending on the operational concept. For example, by timing the arrival at earth, the spacecraft may directly re-enter the earth's atmosphere and be recovered at a landing site. An alternative that eliminates the timing consideration is to enter an earth parking orbit and allow the earth to rotate underneath it until a proper orientation is attained that allows shuttle service from the earth's surface. It may be required to rendezvous with the earth orbiting space station for resupply and to initiate another logistics mission from this station. In any event, the inclination and flight time of the transearth trajectory is most important and must be considered the prime criteria for defining the transearth injection requirements. However, the translunar injection requirements are dependent on the wait time in lunar orbit that is required to complete the lunar tasks and also to allow for contingencies. This wait time is referred to as the first wait time and also has frequently been termed the lunar stay time when there is a specific mission in mind. Therefore, it is very logical to have a moon-to-earth departure window located immediately after this stay time to minimize life-support requirements and space-exposure time. However, depending on the complexity of the mission, it may be desirable to provide ample life support capability until the next launch window, e.g., in the event a malfunction exceedingly delays the transearth injection.

First, it will be specified, as part of a sample operational concept, that maneuvers other than the transearth injection maneuver (Missions I and II) are not permitted in the lunar parking orbit. With this restriction, transearth flight time is not readily controllable and is a function of the time since entering the departure window. The placement of the departure window itself and consequently the duration of the lunar stay time are realized by planning the lunar mission for a given time during the month and/or by controlling the parking orbit longitude ($\theta_{MTE}$) at the nominal lunar arrival. Generally there are two departure windows per month for this case and returns to earth can be from the southerly or northerly direction (relative to earth's equator).

Although a transearth window may exist for a considerable length of time, it must be realized that there are some practical problems associated with this case. For example, if a direct atmospheric re-entry is to be made, there is the necessary timing requirement that allows recovery to take place on a given land mass. Since the transearth flight time is not controllable at the time of transearth injection, two choices present themselves. First, although within a departure window, the transearth injection may be delayed until the timing requirement is met or, second, the transearth injection may be performed with a subsequent timing maneuver along the transearth trajectory prior to reaching earth. With either choice, or even a combination of choices, only portions of the windows will actually be available. The full window could be realized only if the spacecraft returns to an independent parking orbit (no timing or rendezvous restrictions).

If the spacecraft must return and rendezvous with the orbiting space station, with which it had originated the lunar mission, there generally will be one transearth departure window per month. The first wait time (or stay time) associated with this requirement is usually of a much longer duration than without the rendezvous requirement. The date of translunar departure is the controlling variable to effectively regulate the stay time. Normally, the entire window is available for earth departures, but, in the event of an extremely long unscheduled delay, there is usually a very long wait time (as long as a month) until entrance into the next departure window. The spacecraft may have to revert, in this circumstance, to returning to earth into an independent parking orbit which can be supplied by earth shuttle until rendezvous with the space station can be effected.

Next, assume an operational concept that allows maneuvers to take place in the lunar parking orbit. This mission flexibility now enables the spacecraft to control its transearth flight time as well as its return inclination. If there are no rendezvous requirements (Mission III) at earth, there are again two transearth departure windows per month that allow both northerly and southerly returns to earth. Since flight time can be controlled, the entire transearth departure window is usually available. However, the exact use of the window depends on the required transearth flight time, which may be continually changing. Thus, it cannot be expected to have a specific value of flight time that is held constant throughout the window. Instead, the return time will be variable according to the geometry of the earth and transearth trajectory plane and therefore the windows may actually be larger than those presented for one constant return flight time.

The width of the windows for this case is controlled by lunar parking orbit inclination ($i_m$) and the transearth flight time, especially when the required flight time can be preplanned to have higher values consistently throughout the window. The placement of the windows is governed by the above mentioned factors plus the initial lunar parking orbit orientation, $\theta_{MTE}$.

When a rendezvous requirement is present, there are usually three windows in a month's

span, but the return direction is not arbitrary. Control of the initial wait time (stay time) is not readily accomplished, and the window sizes are nearly invariant regardless of initial conditions.

## 2. Mission Planning Charts

The data presented in Sections A and B are incorporated into a composite set of mission planning charts. Although these charts do not provide an exact means for mission analyses, they nevertheless do give an accurate insight to the missions under consideration. A description and use of each chart is given below:

Chart No. 1. Figure 20 is designated as Chart No. 1. In this chart, one can find the required $i_m$* to establish a given stay time ($\Delta T$) for a given lunar base latitude. The stay time is the interval of time required for the base to rotate (rate = $\omega_{\mathbb{C}}$) from its initial intersection with the lunar parking orbit plane to its second intersection (for the duration of $\phi_B \leq i_m$). This stay time represents the required time needed to conduct resupply and rendezvous operations associated with a specific selenographic coordinates. Also from Chart No. 1., the maximum turning angle, $\xi$, required for rendezvous purposes for ascents made to and from the site can be found.

Chart No. 2. For a given base latitude $\phi_B$, and $i_m$, this chart (Fig. 21) is entered knowing the corresponding base longitude, $\lambda_B$ and yields the required longitude angle (at arrival) $\theta_{MTL}$, of the descending node of the parking orbit that satisfies the required stay time, $\Delta T$. The translunar injection direction is also estimated from this chart.

Chart No. 3. Chart No. 3 (Fig. 22) presents the minimum and maximum translunar orbital departure window ($\Delta T_{\oplus}$) that can be realized for a given propulsion capability ($\Delta V_{m_{\oplus}}$). Data is presented for any year and time of month. The constraints that are implied in this chart are $i_m$-$\theta_{MTL}$ or $i_m - t_p$ (see Section A) constraints; which require correction maneuvers in the earth parking orbit. These particular constraint combinations are chosen since it is felt that they represent the most logical approach in mission planning.

Chart No. 4. For the above constraints ($i_m$, $\theta_{MTL}$), this chart (Fig. 23) determines the translunar flight time ($t_p$) the translunar injection impulse ($\Delta V_0$), and the braking impulse at the moon ($\Delta V$) for the given launch date and injection direction. Thus it now becomes possible to determine if a flight to a given lunar base is feasible and, if so, when it is feasible.

*It is assumed that $i_m \approx i_{eq_{\mathbb{C}}}$.

Chart No. 5. In general, after arrival at the moon, there will be a waiting time before a transearth departure window is entered. From Chart 5 (Fig. 24), this initial wait time (or stay time, $\Delta T_i$) may be found when the arrival date and arrival geometry is known. The data is based on the transearth departure window technique that requires no correction maneuvers in the lunar parking orbit. It is believed that this technique is highly acceptable when earth orbit rendezvous is not a mission requirement. The energy requirements for this technique are presented in Chart No. 6.

Chart No. 6. In addition to the energy requirements, this chart (Fig. 25) presents the size of the initial transearth departure window ($\Delta T_{TE}$) and the transearth flight time ($t_f$). This chart is based on the initial arrival geometry of $i_m$, $\theta_{MTL}$, moon declination and year. The transearth direction is not considered a mission constraint, and returns from either the north or south are considered acceptable.

Chart No. 7. This chart (Fig. 26) allows the determination of wait times between transearth windows ($\Delta T_1$) for the constraints: $50 \leq t_s \leq 100$ hr and $\Delta \leq 1$ km/sec. It may be necessary to know these wait times if the initial stay time and departure window is less than the desired stay time.

Chart No. 8. This chart (Fig. 27) is most important when logistics missions, with continuous round trips, are considered. Chart No. 8 enables one to determine the next arrival date at the moon for a given stay time at the moon. Also the necessary stay times for earth orbit rendezvous purposes are noted and for this case the $\Delta V$ requirement for transearth injection and orbit "circularization" at earth is 4.8 km/sec. It is assumed, for the earth rendezvous case, that maneuvers in the lunar parking orbit are permitted. Therefore Charts Nos. 5, 6 and 7 are not applicable for this case.

With this chart, an indefinite number of consecutive round trips can be analyzed.

a. Typical mission

One of the most probable missions that will be conducted in the future is the lunar logistics mission. Therefore, this mission is chosen as an example to illustrate the use of the planning charts. The objective of this mission is to continuously resupply a lunar base. It is assumed that the logistics spacecraft only operates to and from parking orbits around the earth and moon. Basically there are two modes of operation; first, the spacecraft, when in an earth parking orbit, is resupplied by a "shuttle" service from earth. It then departs and establishes a lunar parking orbit, wherein supplies and personnel are "shuttled" to the lunar surface. After returning to earth, another earth parking orbit is established and the cycle then repeats. A second mode of operation is identical to the first with

the exception that, after arrival at earth, a rendezvous must be made with an earth orbiting facilities station that is in orbit indefinitely.

Following is a list of mission specifications:

(1) Lunar site latitude: $\phi_B = -11°$ (selenographic).

(2) Lunar site longitude: $\lambda_B = -21°$ (selenographic).

(3) Lunar stay time to complete tasks: $\Delta T = 3$ days.

(4) Initial earth departure date: 1978.

(5) Initial arrival day or declination: descending node - DN.

(6) Propulsion capability at earth: $\Delta V_{m\oplus} = 0.3$ km/sec.

(7) Propulsion capability at moon: $\Delta V_{\mathbb{C}} = 1$ km/sec.

(8) Initial translunar injection direction: south.

1. Mission Mode 1 (without earth rendezvous)

From Chart No. 1: By entering this chart at the base latitude and required stay time, and assuming that $i_{eq\mathbb{C}} \approx i_m$, the $i_m$ required for a 3 day stay time is found to be 11.5°. The maximum accompanied plane change ($\xi$) requirement is 0.6°.

From Chart No. 2. The ratio of $\phi_B/i_m$ is $\frac{-11°}{11.5°} = -0.955$. For a base longitude of -21°, the required $\theta_{MTL} = 260°$ for a first choice south injection direction. Note that this chart gives a choice of injection direction. Where the two choices overlap, the first choice should always be used. Although only one of the two choices may be indicated, this choice (usually the 2nd choice) may prove unacceptable from the flight time and $\Delta V$ point of view as ascertained from Chart No. 4.

From Chart No. 3. For an earth propulsion capability ($\Delta V_{m\oplus}$) of 0.3 km/sec and the year 1978, the minimum and maximum orbital departure windows are 8 and 18 hours respectively. Thus the minimum number of possible GO times (injection frequency) is: 8 hr/1.6 hr (period) = 5.

From Chart No. 4. Entering this chart at the descending node position for an inject-south condition (see mission specification) and proceeding to the specified year, the required $i_m$ can be "spotted" according to the choice determined from Chart No. 2. For the present case, the flight time ($t_p$) to achieve an $i_m$ of 11.5° and a $\theta_{MTL}$ of 260° is 81 hr. The injection velocity requirement at earth $\Delta V_0$ is 3.052 km/sec and the braking impulse ($\Delta V$) needed to establish a circular lunar parking with an 185.2 km altitude is 830 m/sec.

From Chart No. 5. With an arrival date of DN, 1978, an $i_m$ of 11.5° and a $\theta_{MTL}$ of 260°; it is seen that the initial stay time $\Delta T_1$ before entering a transearth departure window is 0 hr; or in other words the spacecraft arrives in a portion of the arrival envelope that overlaps the departure envelope.

From Chart No. 6. For a propulsion capability ($\Delta V_{\mathbb{C}}$) of 1.0 km/sec and the above mission conditions, the transearth departure window sizes ($\Delta T_{\mathbb{C}}$) can be found. As pointed out in Section C-1, two choices of earth return direction are available and these choices are so indicated in Chart No. 6. The resulting two departure windows are:

(1) Return north, $t_f \approx 40$ hr, $\Delta T_{\mathbb{C}} = 96$ hr $\approx$ 4 days.

(2) Return south, $50 < t_f < 100$ hr, $\Delta T_{\mathbb{C}} =$ 11 hr $\approx 0.5$ day.

Since the mission specifies a 3 day stay time, the return north case is selected. Deleting this stay time from the window infers that the remaining time of 1 day is the available window after all tasks are completed. It is assumed at this point, that a 1-day window is acceptable.

From Chart No. 7. In the event that either the return direction or the available window is not acceptable, the spacecraft must remain in the lunar parking orbit until the next opportune window. The wait time between windows, in this circumstance, would be 172 hr.

From Chart No. 8. It is assumed that the total stay time in a lunar parking orbit is 4 days or 96 hr. From Chart No. 8, the next nominal lunar arrival day is 1.25 day past the AN position. From the above data, the total round trip flight time is now determined from earth departure to earth arrival:

$$\left.\begin{aligned} t_p &= 81 \text{ hr} \\ t_s &= 96 \text{ hr} \\ t_f &= 40 \text{ hr} \end{aligned}\right\} 5.6 \text{ days}$$

$$\Sigma t = 217 \text{ hr or } 9.1 \text{ days}$$

$$t_s = \Delta T_1 + \Delta T_2 + \Delta T_{\mathbb{C}}$$

The elapsed time from the first arrival date (DN) to the second arrival date (AN + 1.25 days) is 14.85 days. Assuming, as a first estimate, that the second translunar flight time will be 3 days; the time spent in an earth parking orbit, prior to the second translunar injection, is approximately 14.85 days - 3 days - 5.6 days = 6.2 days. Therefore, the time to transfer crews, personnel, supplies and

fuel is 6.20 days. The translunar injection direction will be the same as the transearth return direction; north in this case. If, however, this is an insufficient earth stay time, then the spacecraft must await the next translunar injection window. The wait time between windows will vary approximately from 145 hr to 195 hr and is estimated by the following empirical relationship

$$\text{wait time (hr)} = 170 + 25 \sin \nu$$
$$\nu = \left(\frac{\text{day of mo} \times \pi}{13.6}\right)$$

For this case, the wait time is 1.77 hr or 7.4 days, or the next arrival date will be 7.4 + 1.25 day = 8.65 days of the lunar month. Therefore the total earth stay time prior to departure is 6.2 days + 8.6 days = 14.85 days and now the translunar injection direction will be reversed, i.e., south.

For the present example, it is assumed that an earth stay time of 6.2 days is sufficient and the injection direction is north. With the above information, it is now possible to begin the mission cycle again by entering Chart No. 2 if the same lunar base is to be supplied.

Sample lines on the charts are not shown for the second consecutive round-trip that will be continued below.

Referring to Chart No. 2, it is noted that only an inject south case will satisfy the mission specifications of lunar site coordinates. Therefore, even though the earth stay time of 6.2 days is adequate, the translunar departure window must be bypassed as inferred above until the date* of 8.65 days. As previously pointed out, the translunar injection direction is now south and the earth stay time is 14.85 days.

Entering Chart No. 4 with an inject S case, a date of 8.65 days (1978) and an $i_m$ requirement of 11.5° (1st choice), a flight time ($t_p$) of 93.5 hr is realized for a lunar orbit orientation ($\theta_{MTL}$) of 260°. The related $\Delta V_0$ and $\Delta V$ are 3.045 km/sec and 800 m/sec, respectively.

From Chart No. 5, the wait time before entering the transearth departure window is zero hours.

Chart No. 6 reveals that the a maximum window is realized if a northerly transearth return direction is selected

(1) Return north, $t_f \approx 40$ hr, $\Delta T_{\mathbb{C}}$ = 110 hr ~ 4.6 days.

(2) Return south, $t_f \approx 75$ hr, $\Delta T_{\mathbb{C}}$ = 40 hr ~ 1.7 days.

*Days after beginning of lunar month.

This allows a total lunar stay time of 4.6 days of which 3 days is allotted to orbital tasks and 1.6 days is the available return window.

The process can be continued indefinitely by making use of Chart No. 8 at this point. However, the present example is terminated at this time with a brief synopsis of the mission.

The total elapsed time for two consecutive round trip missions is derived as follows:

| | | |
|---|---|---|
| 1st round trip | Translunar flight time | ~ 81 hr |
| | Lunar stay time | ~ 96 hr |
| | Transearth flight time | ~ 40 hr |
| 2nd round trip | Earth stay time | ~ 304 hr |
| | Translunar flight time | ~ 94 hr |
| | Lunar star time | ~ 110 hr |
| | Transearth flight time | ~ 40 hr |
| | | 765 hr ≈ 32 days |

Thus, two round trips can be conducted within a time span of 31.4 days. Further, the time interval that the base must sustain itself is 19 days.

2. Mission Mode 2 (with earth rendezvous)

The missions specifications used in the exemplification of Mode 1 are also dictated for the illustration of Mode 2.

The steps and relevant data for Mode 1 are applicable to Mode 2 up to the point of determining the lunar stay time. For this mode, Chart No. 8 is entered immediately after exiting Chart No. 5. Proceeding to the first earth orbit rendezvous requirement, it is observed that a stay time of 230 hr instead of 96 hr is required to satisfy this requirement. The second translunar injection will be in the same direction as the initial injection, namely south. This implies that the first transearth return direction is also from the south. The next lunar arrival date is 6.5 days of the lunar month which occurs near the MND. The elapsed time between the sequential lunar arrivals is 20.1 days.

Return to Chart No. 4; the flight time for the second lunar arrival is 104 hr for $\theta_{MTL}$ = 260°. This flight time can be reduced to 82 hr if a $\theta_{MTL}$ of 280° is selected. However, upon arrival at the moon, initiation of orbital operations is delayed until the lunar site rotates into the parking orbit plane. This delay is $\frac{280° - 260°}{13.2°/\text{day}}$ = 1.5 days. Following the delay, orbital tasks are carried on for a period of 3 days. Thus a total lunar stay time of 4.5 days is required to complete tasks. However, from Chart No. 8 for an initial arrival date of 6.5 days, the first earth orbit rendezvous window requires an additional wait period of 122 hr or 5.1 days.

The mission can now be summarized:

| | | |
|---|---|---|
| 1st round trip | Translunar flight time | = 81 hr |
| | Lunar stay time | = 230 hr |
| | Transearth flight time | = 70 hr |
| 2nd round trip | Earth stay time | = 100 hr |
| | Translunar flight time | = 82 hr |
| | Lunar stay time | = 230 hr |
| | Transearth flight time | = 70 hr |
| | | 863 hr<br>36 days |

The base must sustain itself for 15.5 days.

For the above earth rendezvous mode, maneuvers are allowed in the lunar parking orbit (see Section B3.b) and therefore the transearth flight time can be controlled ($t_f$ = 70 hr in the above example). In addition, in order to have continuous mission capability, a total propulsion requirement, $\Sigma \Delta V$, of 4.8 km/sec is required. This includes the retropulse for establishing the lunar orbit ($\Delta V$), the maneuvers in the lunar orbit ($\Delta V_{m\mathbb{C}}$) and the retropulse to re-enter an 'earth' parking orbit ($\Delta V_E$); where the magnitude of $\Delta V_E$ is 3.15 km/sec.

It can be seen from the above examples, that both modes are competitive if maneuvers are allowed in the lunar parking orbit. Furthermore, the competitiveness increases as the required lunar stay increases. The critical factor appears to be the earth-stay times between trips. The earth stay time has been reduced from 12.7 days (without rendezvous) to 4.2 days (with rendezvous). If 4.2 days is not acceptable, then the spacecraft must await the next window which means a delay of approximately 7 days.


Ref. 1. Ling-Temco-Vought, Inc. "Final Report, Advanced Orbital Launch Operations, Report No. 00.368, Vol. II Space Mechanics" 4 May 1964, Dallas, Texas.

Ref. 2. "Extension of Effort for Orbital and Lunar Flight Handbooks," Vol. II, Martin Company, Space Systems Division, Baltimore, Maryland, ER 13189-II, 1963.

Ref. 3. "Extension of Effort for Lunar Flight Handbook," Vol. III, Martin Company, Baltimore Division, Maryland, ER 13550-III.

Ref. 4. "Explanatory Supplement to the Astronomical Ephemeris and the American Ephemeris and Nautical Almanac," Her Majesty's Stationery Office, London, 1961.

Ref. 5. Wells, W. R., "The Influence of Precession of Earth Rendezvous Orbits on Lunar Mission Requirements," NASA TN D-1512, November 1962.

# ILLUSTRATIONS

## LIST OF ILLUSTRATIONS


| Figure | Title | Page |
|---|---|---|
| 1 | Inclination of Moon' s Orbital Plane and Right Ascension of Lunar Orbit | 37 |
| 2 | Inclination and Right Ascension of Parking Orbit Relative to MOP | 38 |
| 3 | Injection Velocity Requirement for Departure Window (without orbital maneuvers) | 39 |
| 4 | Lunar Orbit Velocity Requirement for Departure Window (without orbital maneuvers) | 40 |
| 5 | Departure Windows Without Orbital Maneuvers (1978) | 41 |
| 6 | Energy Requirements for Departure Windows | 42 |
| 7 | Energy Requirements for Departure Windows | 43 |
| 8 | Actual Translunar Inclination Versus Elapsed Time | 44 |
| 9 | Flight Time Versus Translunar Inclination Approach Class Trajectories | 45 |
| 10 | Energy Requirements for Departure Windows | 46 |
| 11 | Energy Requirements for Departure Windows | 47 |
| 12 | Energy Requirements for Departure Windows | 48 |
| 13 | Energy Requirements for Departure Windows | 49 |
| 14 | Velocity Requirements for Inject-on-Time Window as Affected by Thrust-to-Weight Ratio | 50 |
| 15 | Energy Requirements for Transearth Departure Windows | 51 |
| 16 | Energy Requirements for Transearth Departure Windows | 52 |
| 17 | Energy Requirements for Transearth Departure Windows | 53 |

LIST OF ILLUSTRATIONS (continued)


| Figure | Title | Page |
|---|---|---|
| 18 | Energy Requirements for Transearth Departure Windows | 54 |
| 19 | Velocity Requirements for Inject-on-Time Window | 55 |
| 20 | Surface Stay Time as Dictated by Rendezvous Requirements in Parking Orbit | 56 |
| 21 | Required Longitude Angle of Descending Node of Lunar Parking Orbit | 57 |
| 22 | Translunar Orbital Departure Windows | 58 |
| 23 | Translunar Flight Time and Velocity Requirements | 59 |
| 24 | Initial Wait Time for Transearth Departure Window Entrance | 60 |
| 25 | Initial Transearth Departure Window | 61 |
| 26 | Wait Time Between Transearth Orbital Departure Windows | 62 |
| 27 | Updating of Translunar Launch Date | 63 |

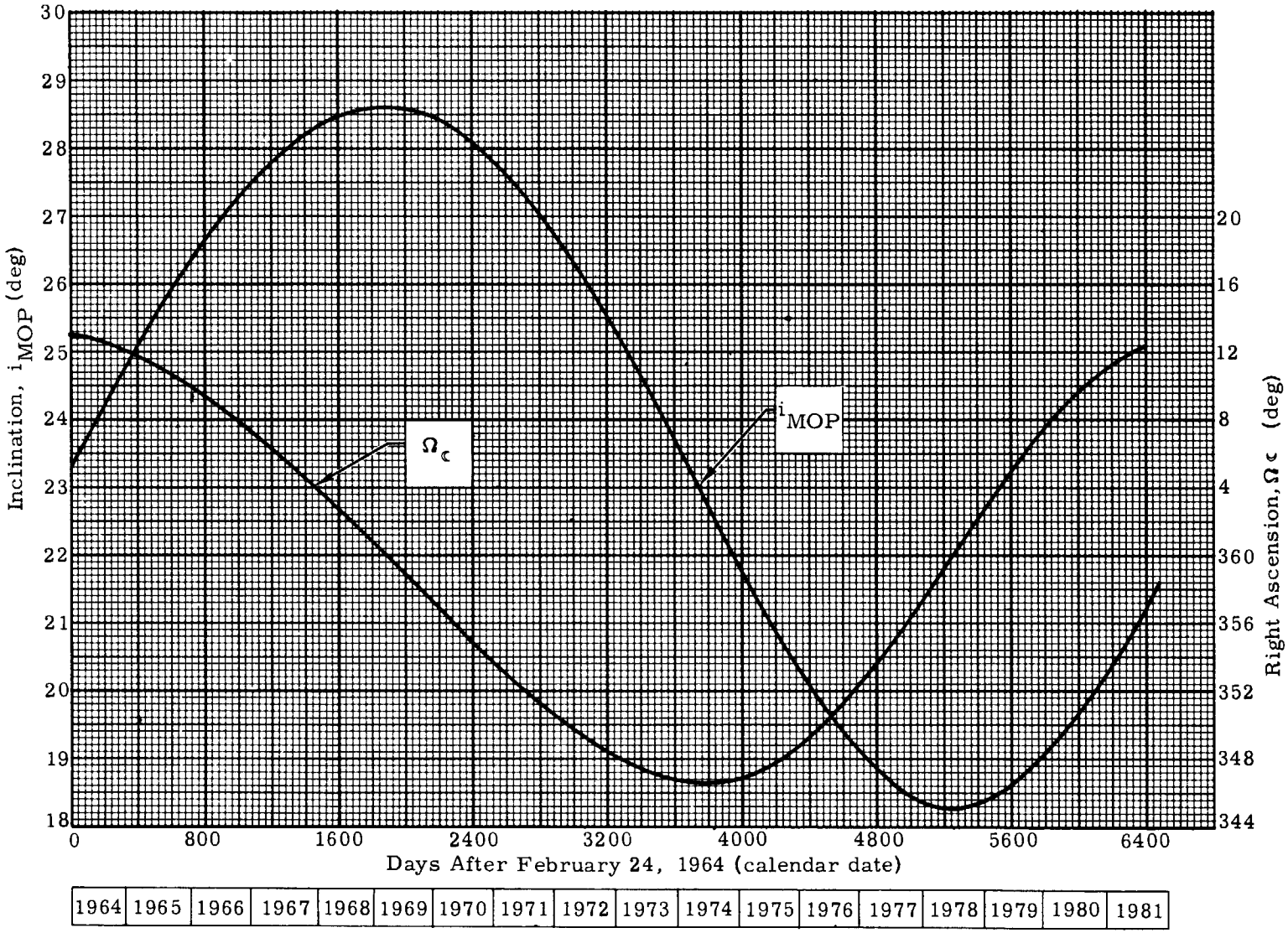


Fig. 1. Inclination of Moon's Orbital Plane and Right Ascension of Lunar Orbit

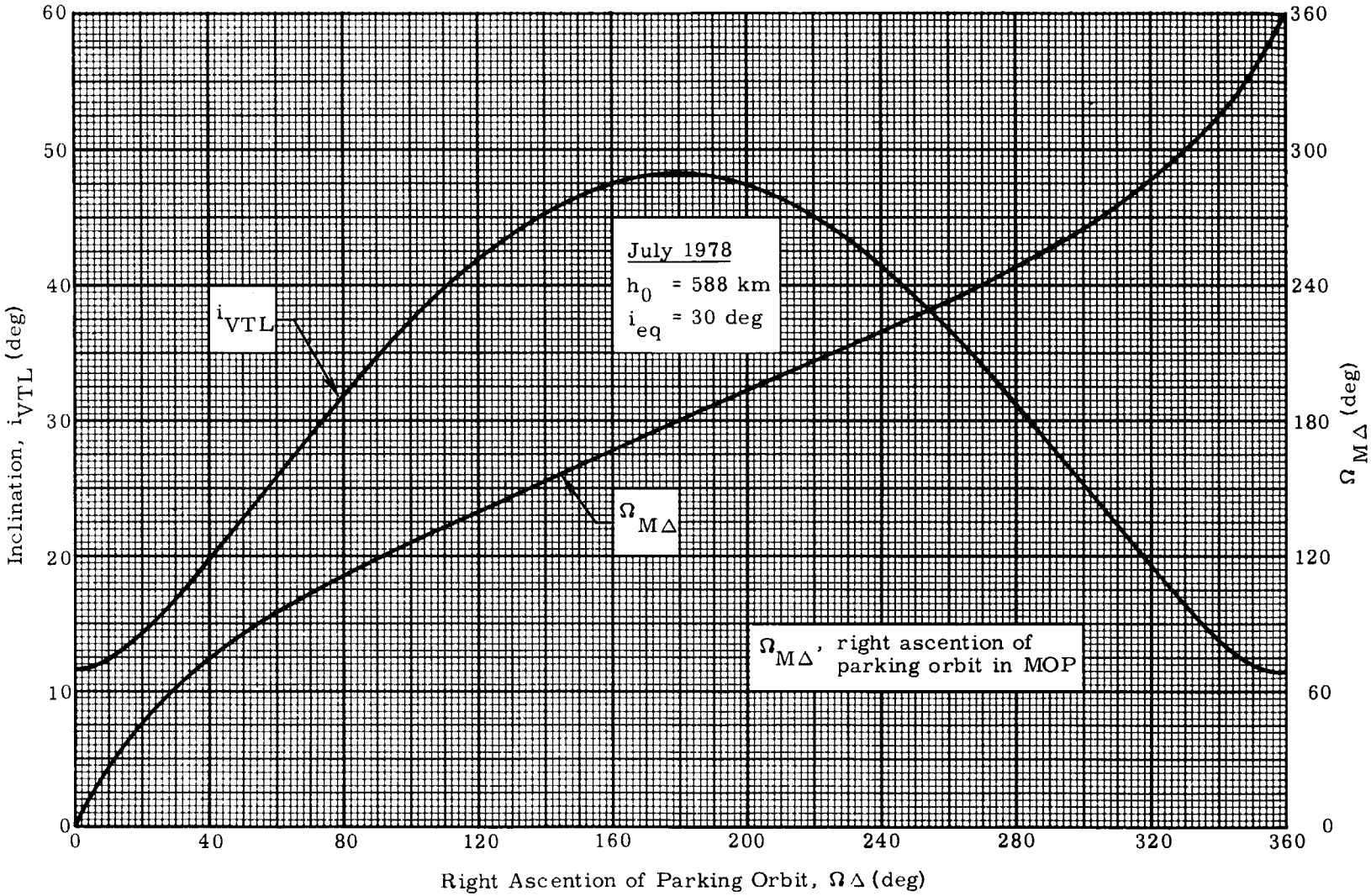


Fig. 2. Inclination and Right Ascension of Parking Orbit Relative to MOP

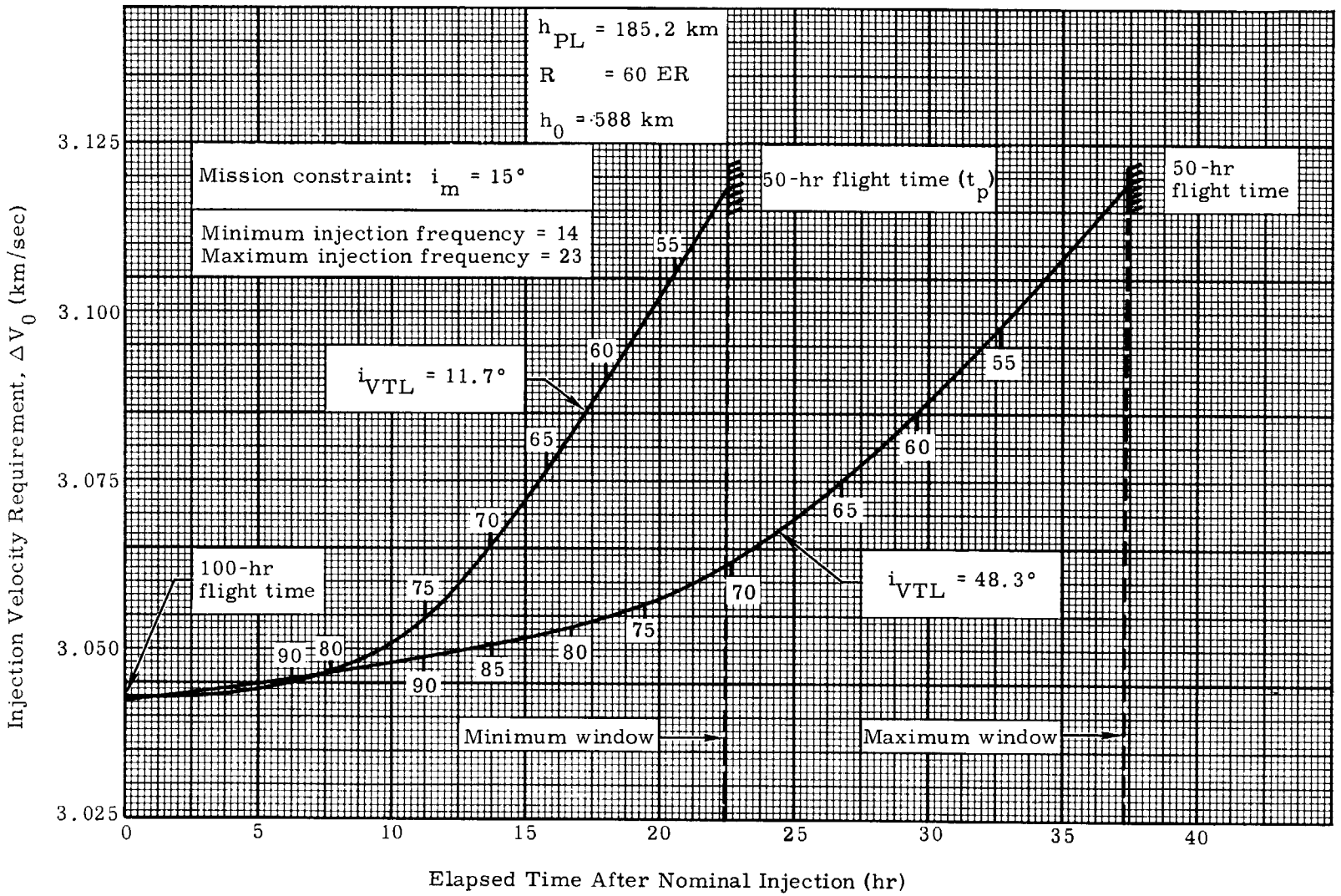


Fig. 3. Injection Velocity Requirement for Departure Window (without orbital maneuvers)

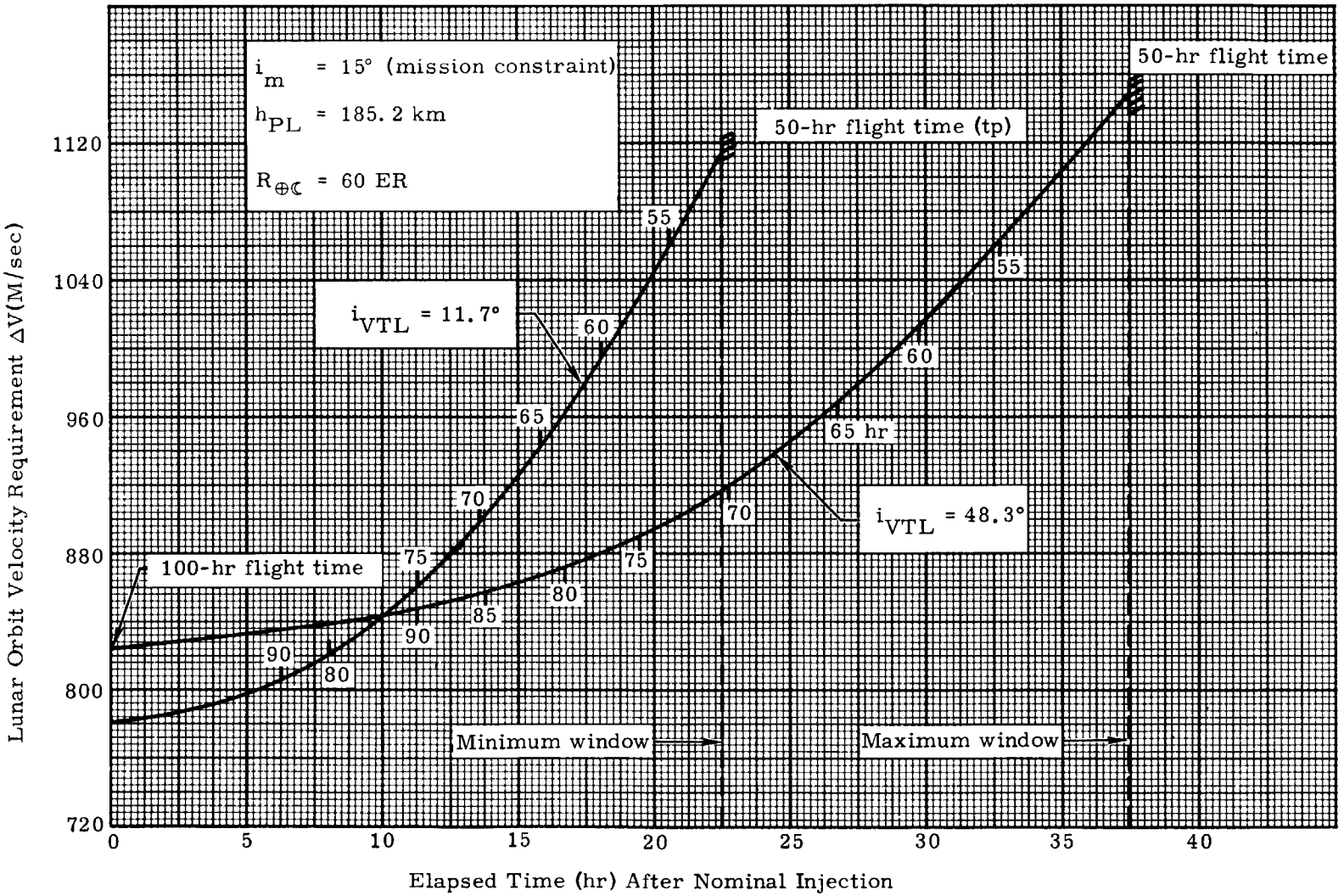


Fig. 4. Lunar Orbit Velocity Requirement for Departure Window (without orbital maneuvers)

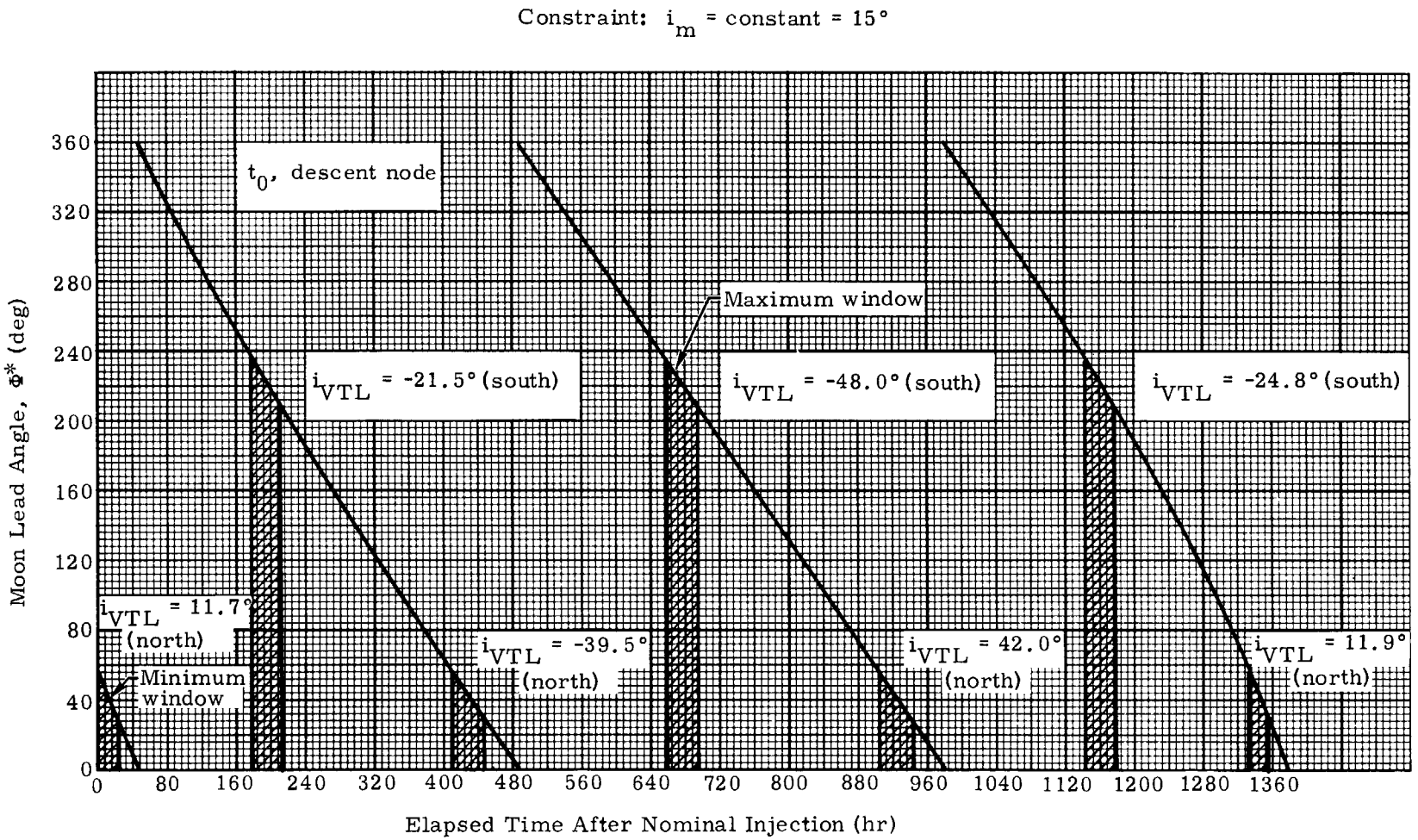


Fig. 5. Departure Windows Without Orbital Maneuvers (1978)

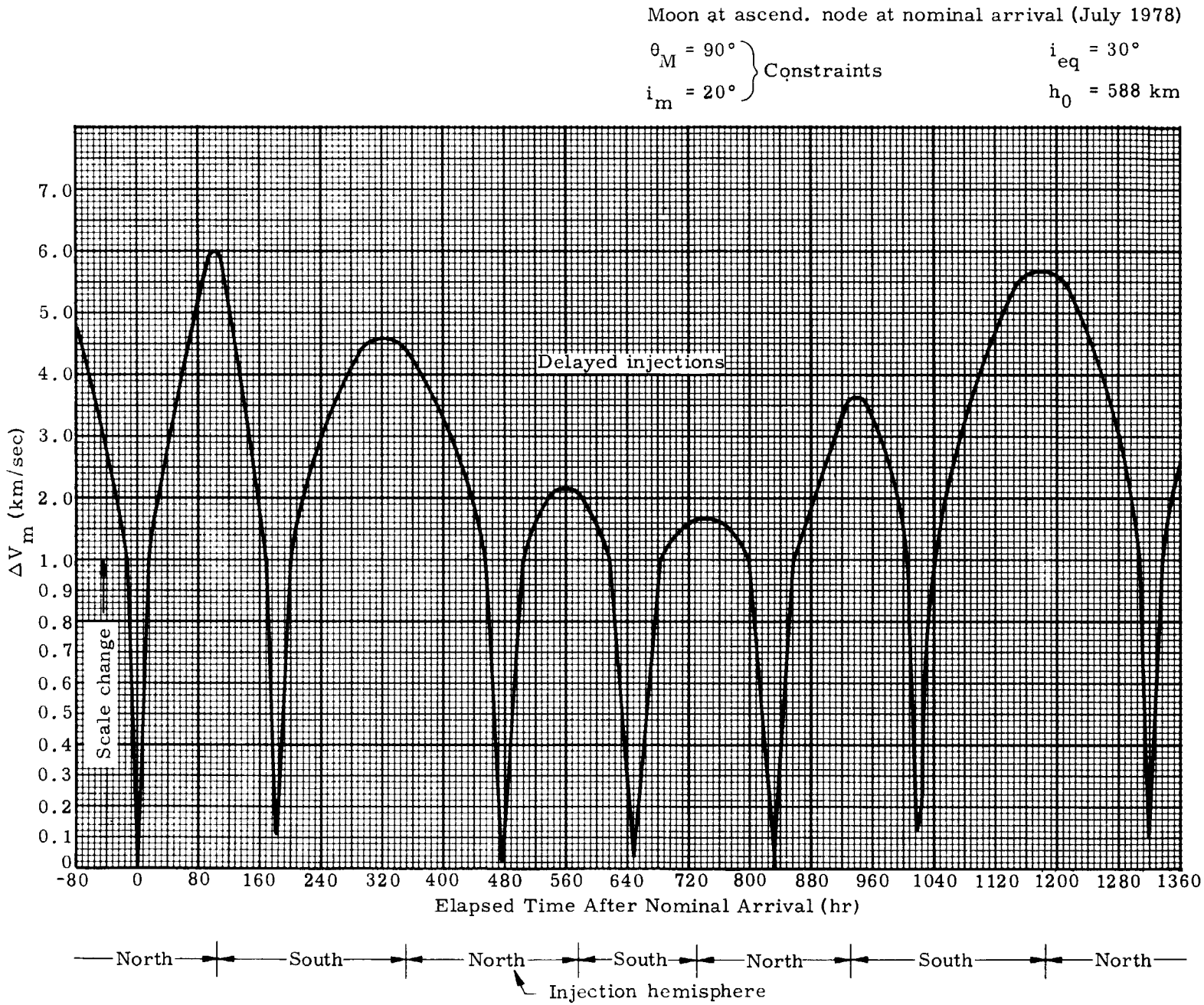


**Fig. 6.** Energy Requirements for Departure Windows

Moon at descend. node at nominal arrival (July 1978)

$\theta_M = 90°$, $i_m = 20°$ } Constraints $i_{eq} = 30°$, $h_0 = 588$ km

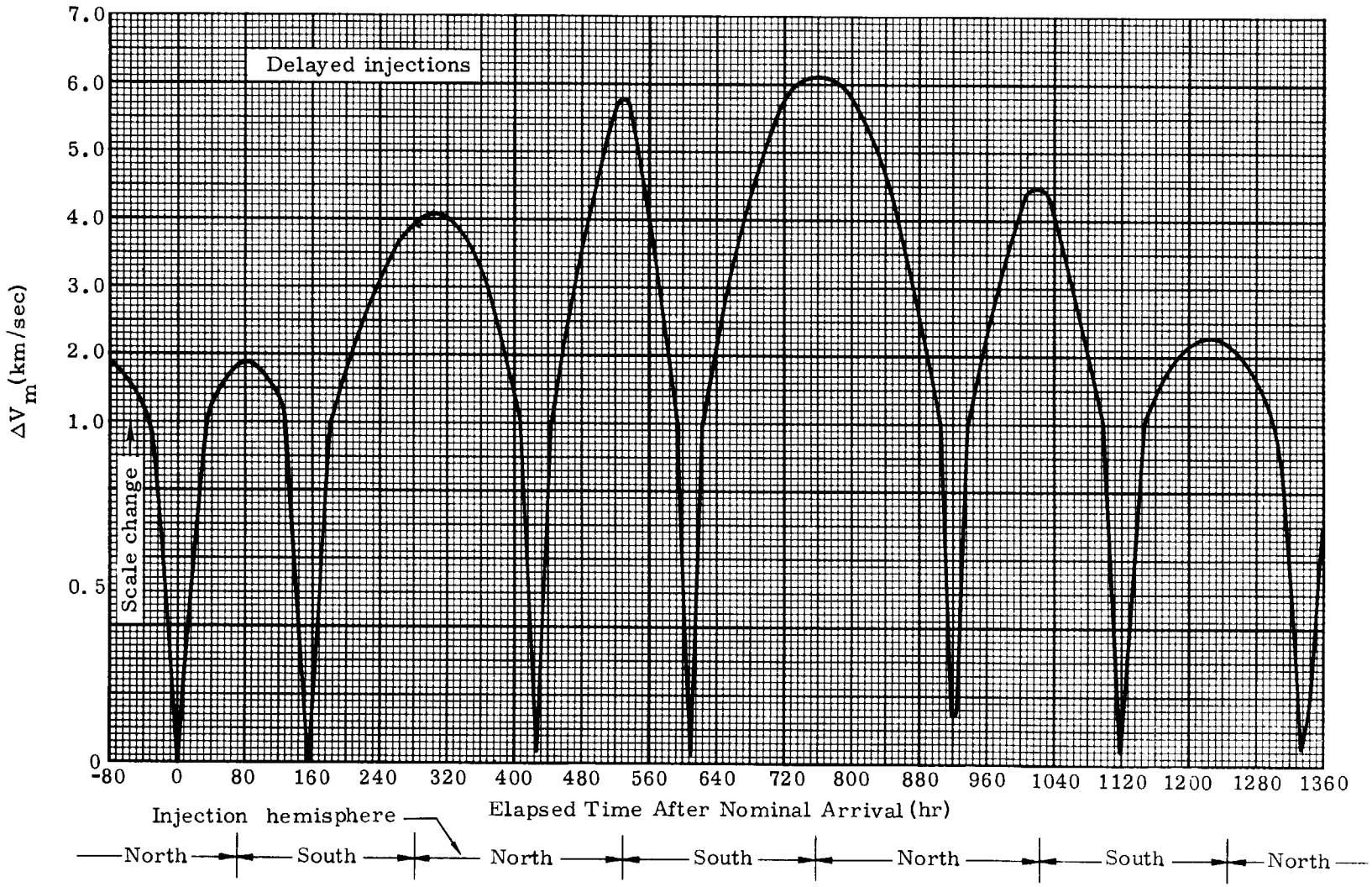


Fig. 7. Energy Requirements For Departure Windows

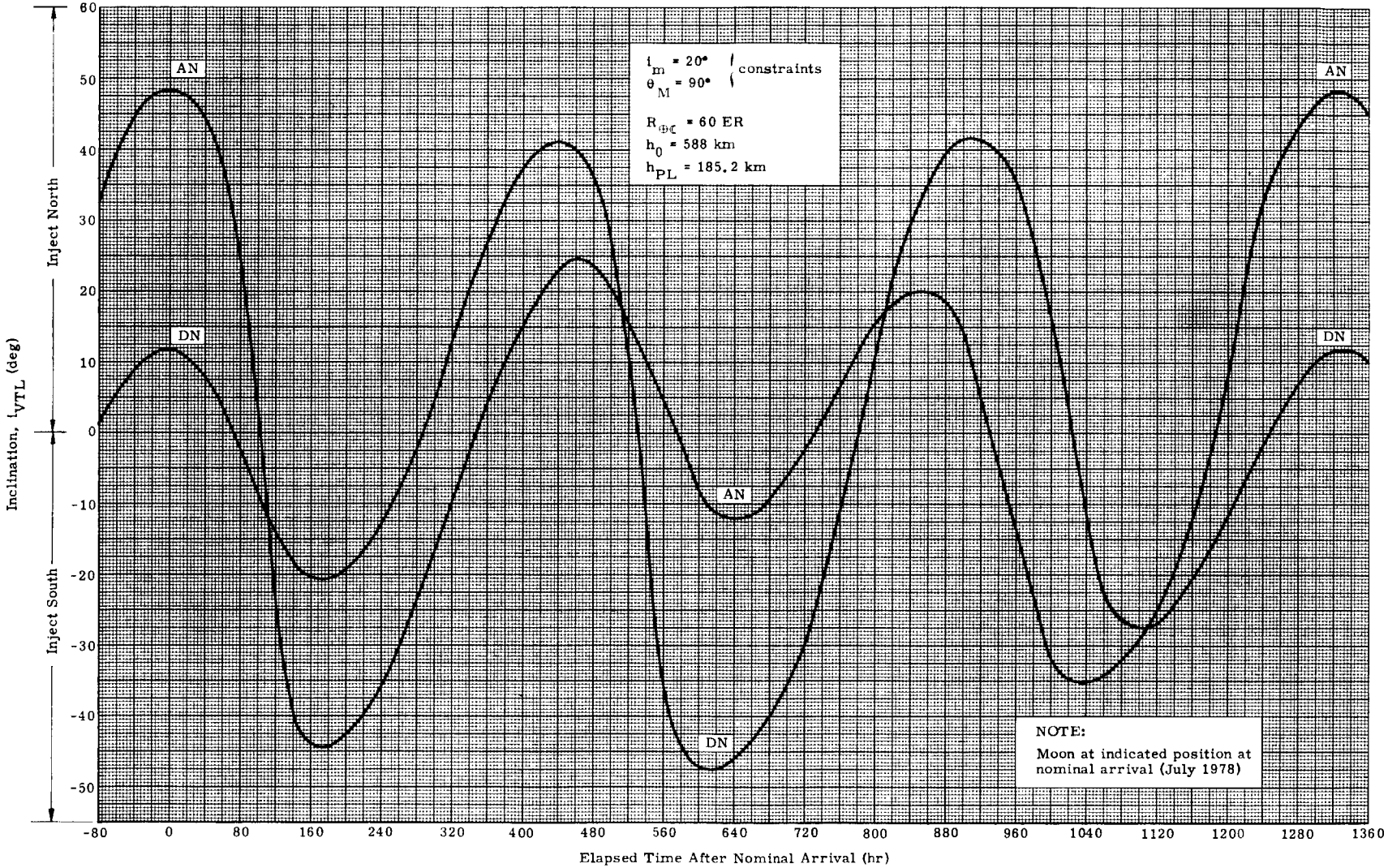


Fig. 8. Actual Translunar Inclination Versus Elapsed Time

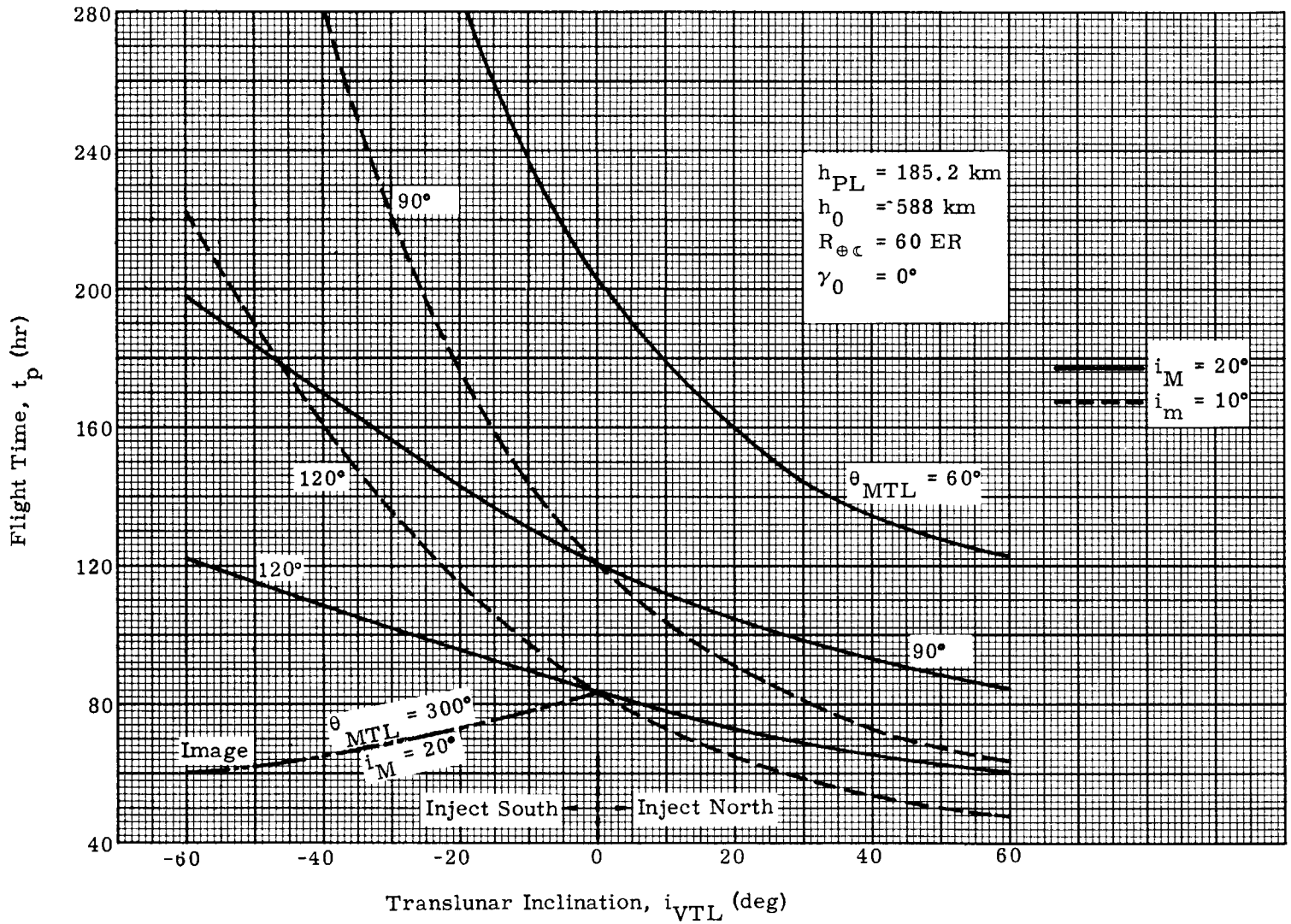


Fig. 9. Flight Time Versus Translunar Inclination Approach Class Trajectories

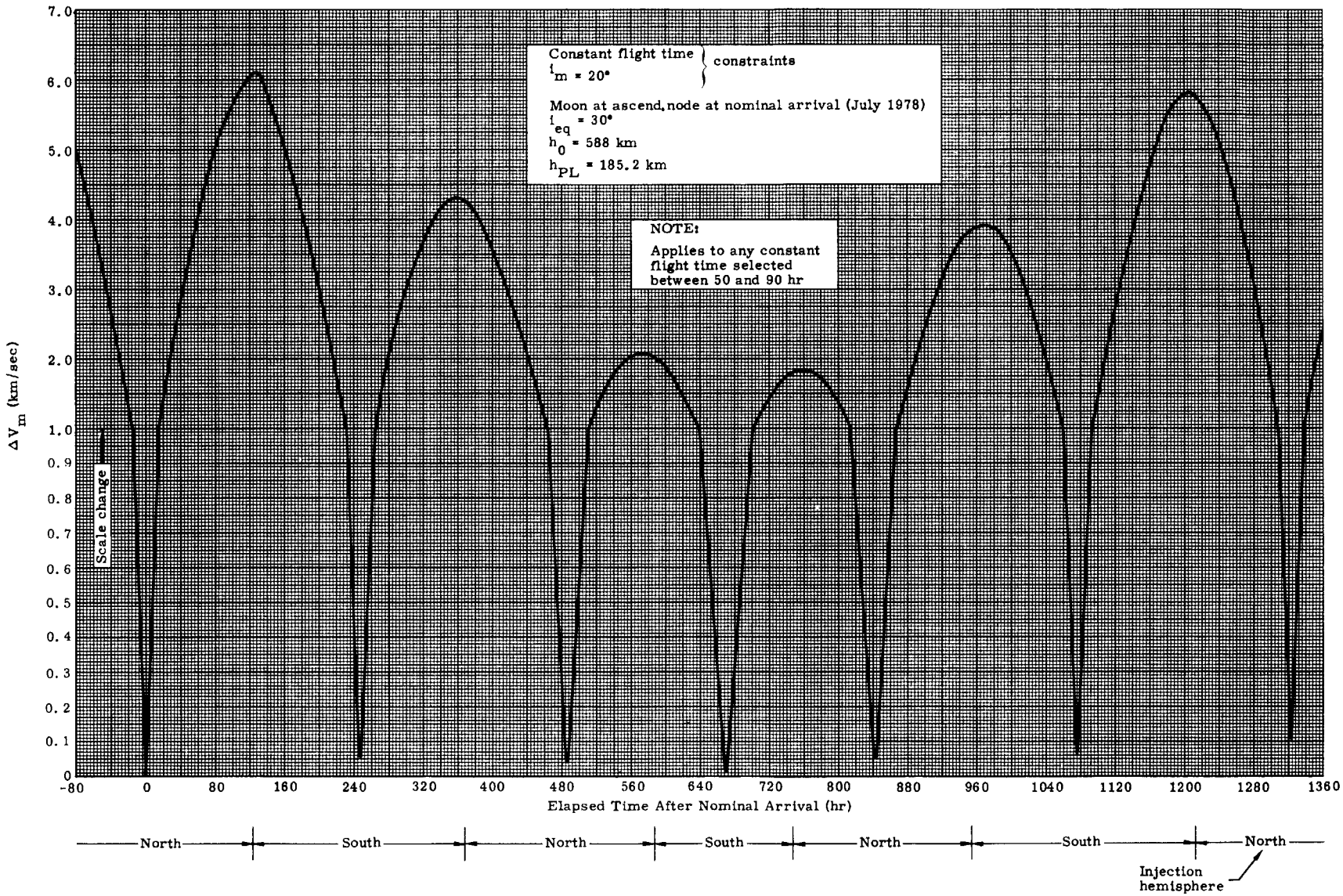


Fig. 10. Energy Requirements for Departure Windows

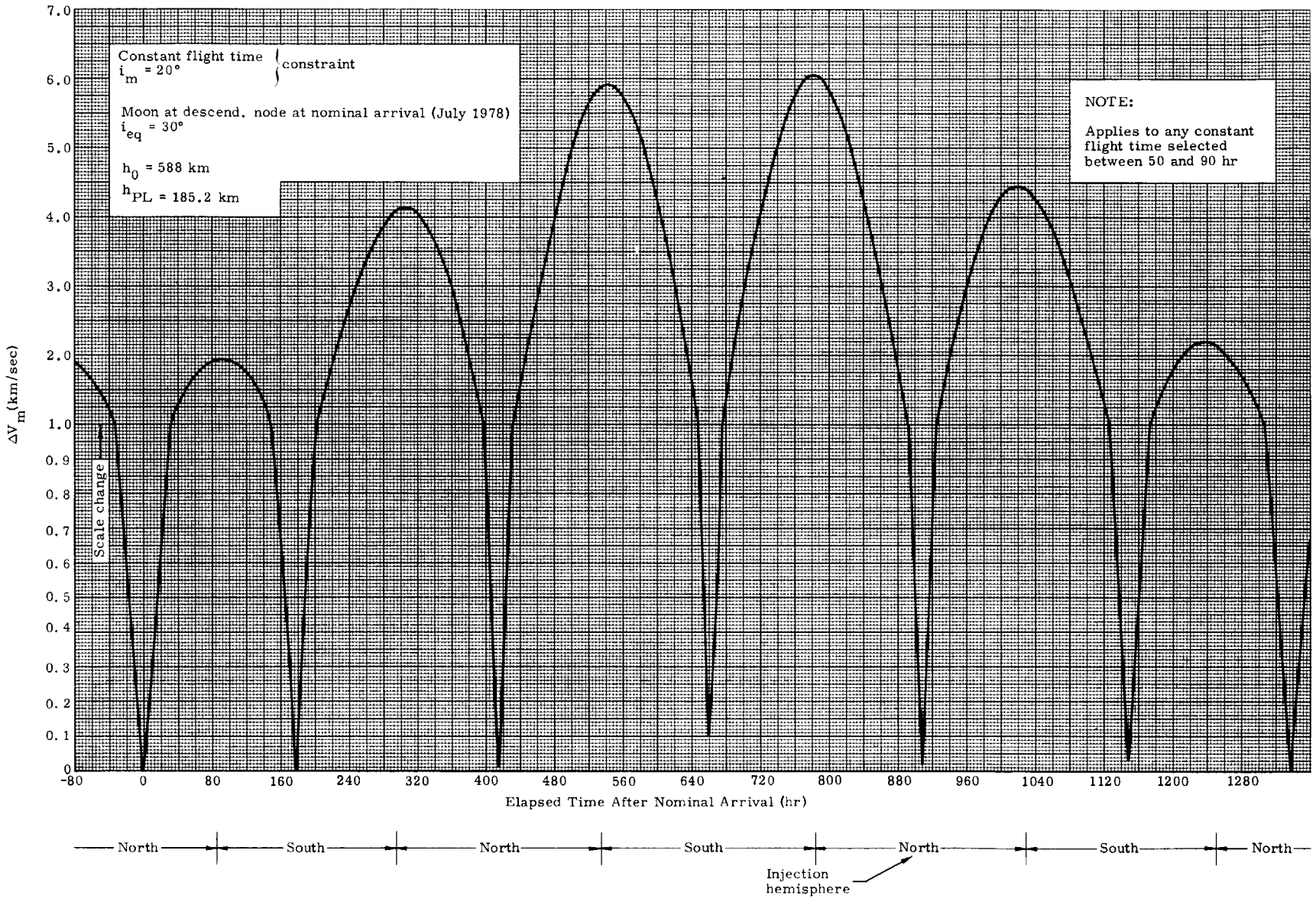


Fig. 11. Energy Requirements for Departure Windows

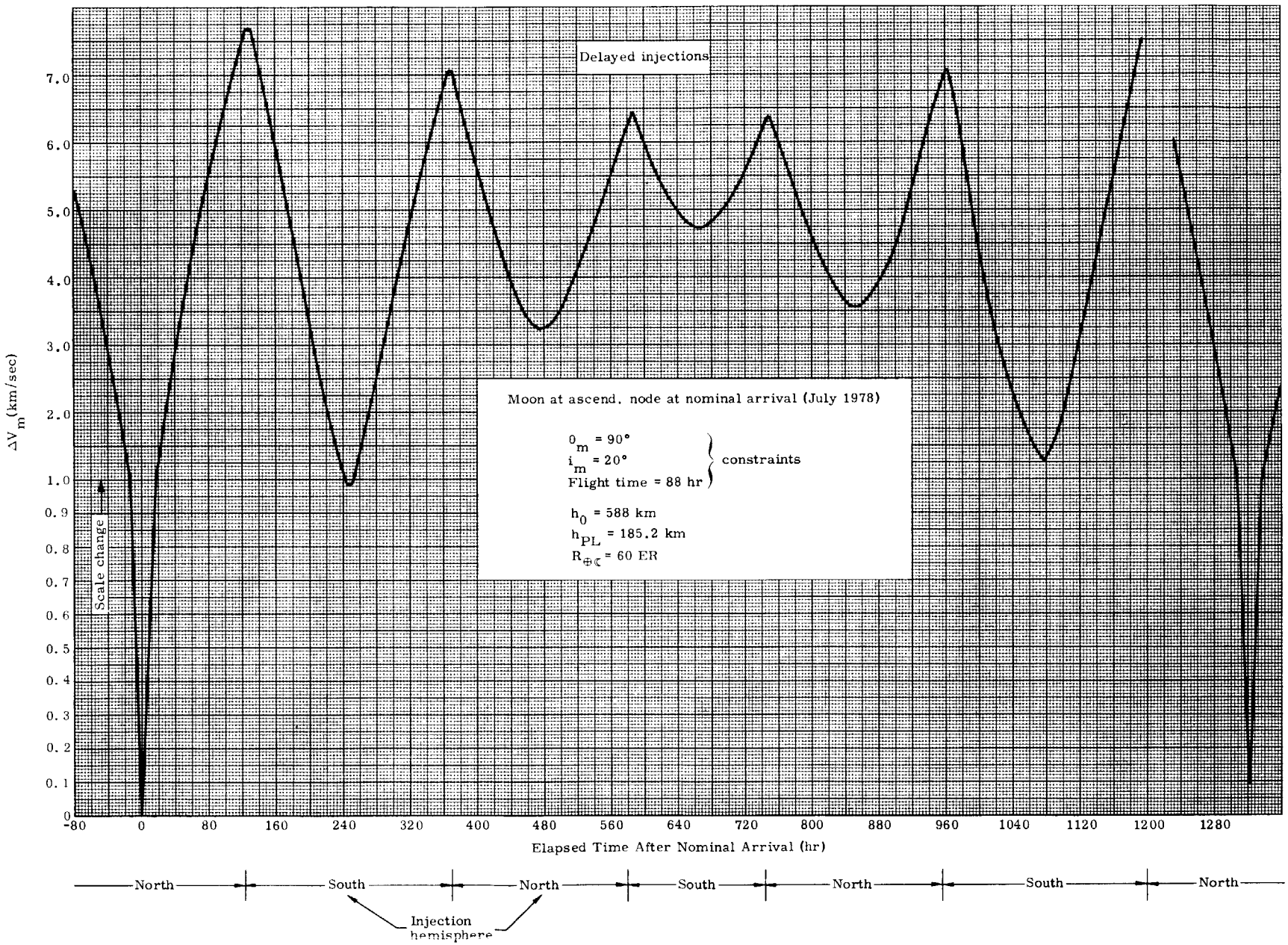


Fig. 12. Energy Requirements for Departure Windows

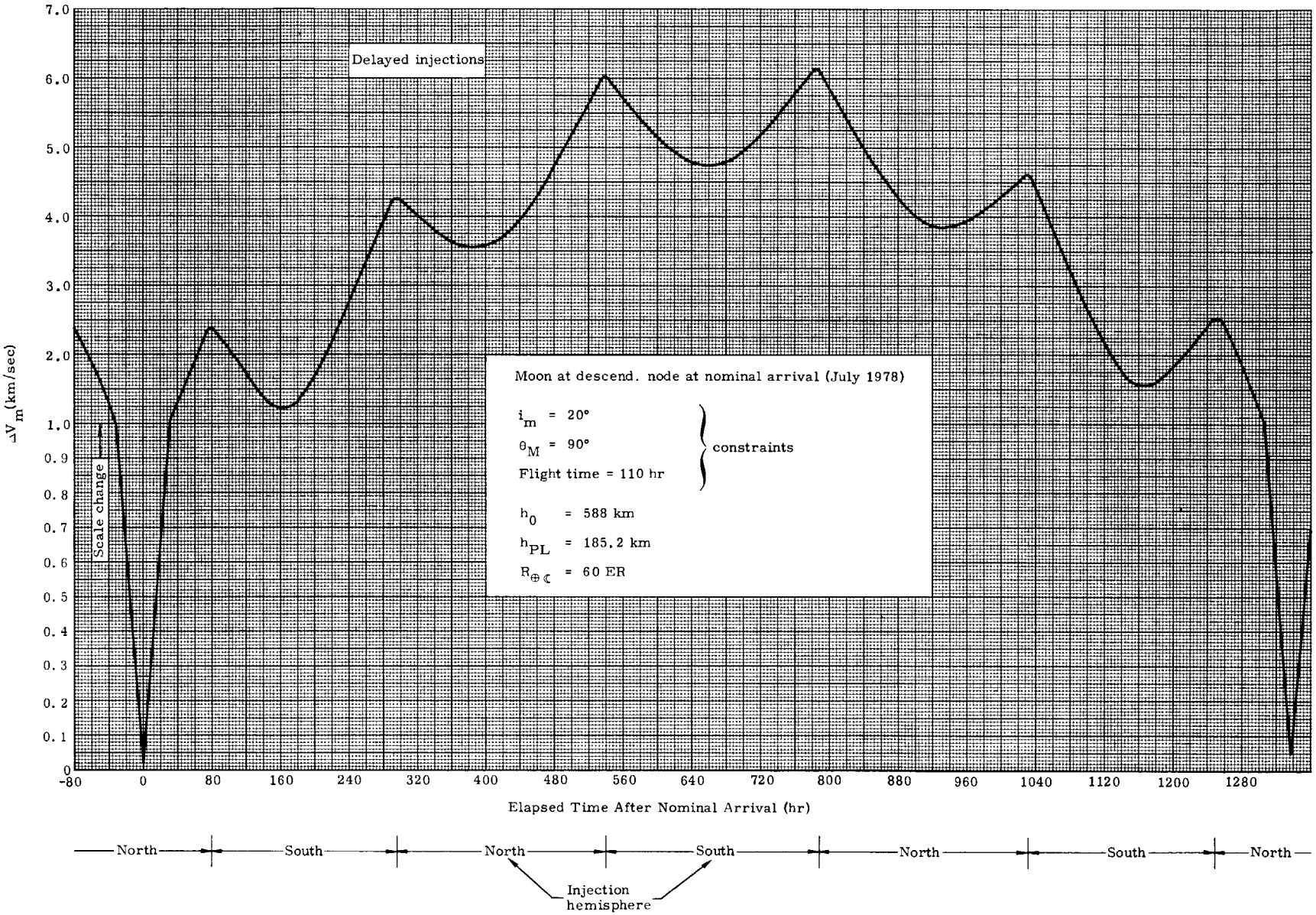


Fig. 13. Energy Requirements for Departure Windows

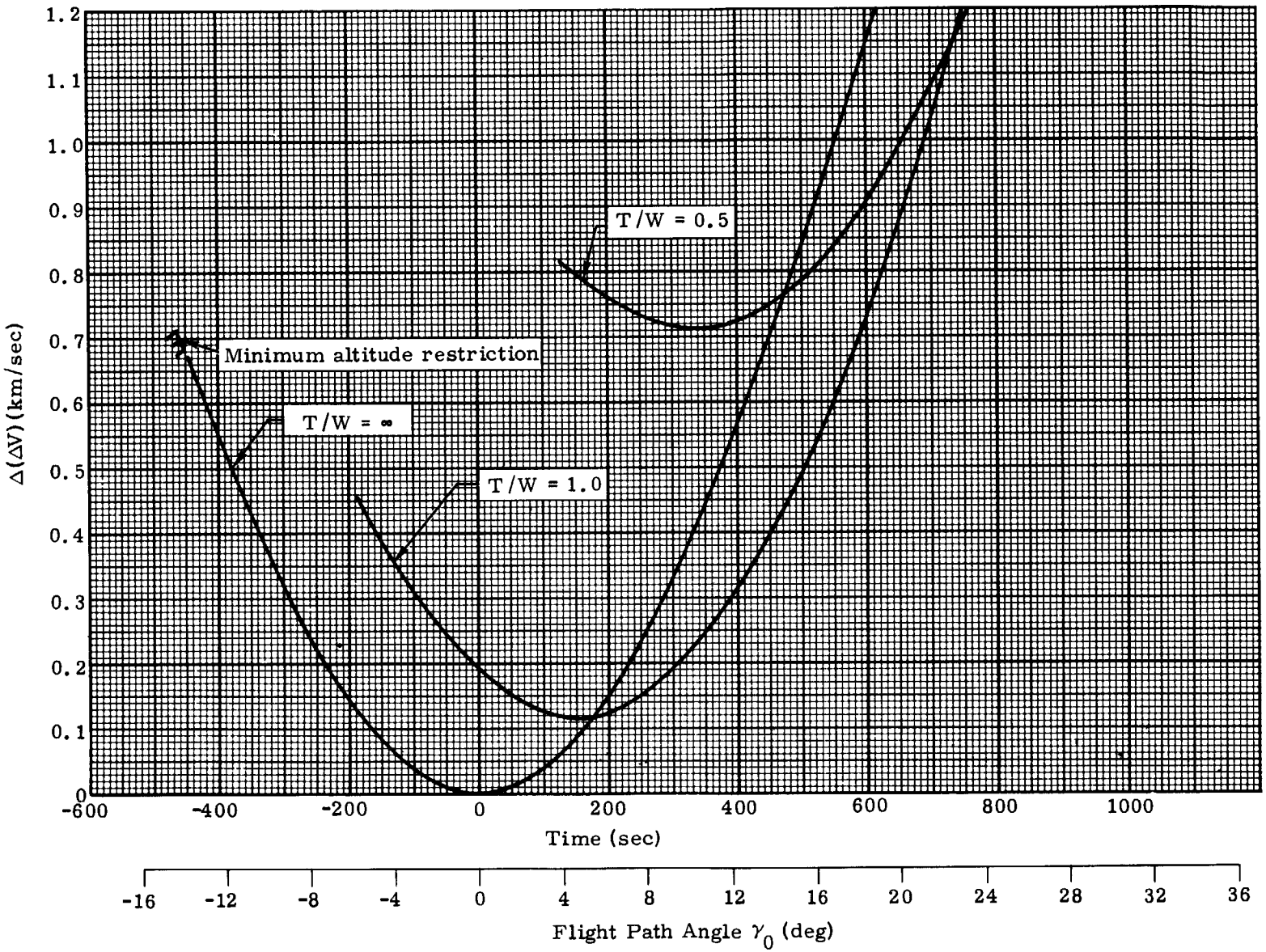


Fig. 14. Velocity Requirements for Inject-on-Time Window as Affected by Thrust-to-Weight Ratio

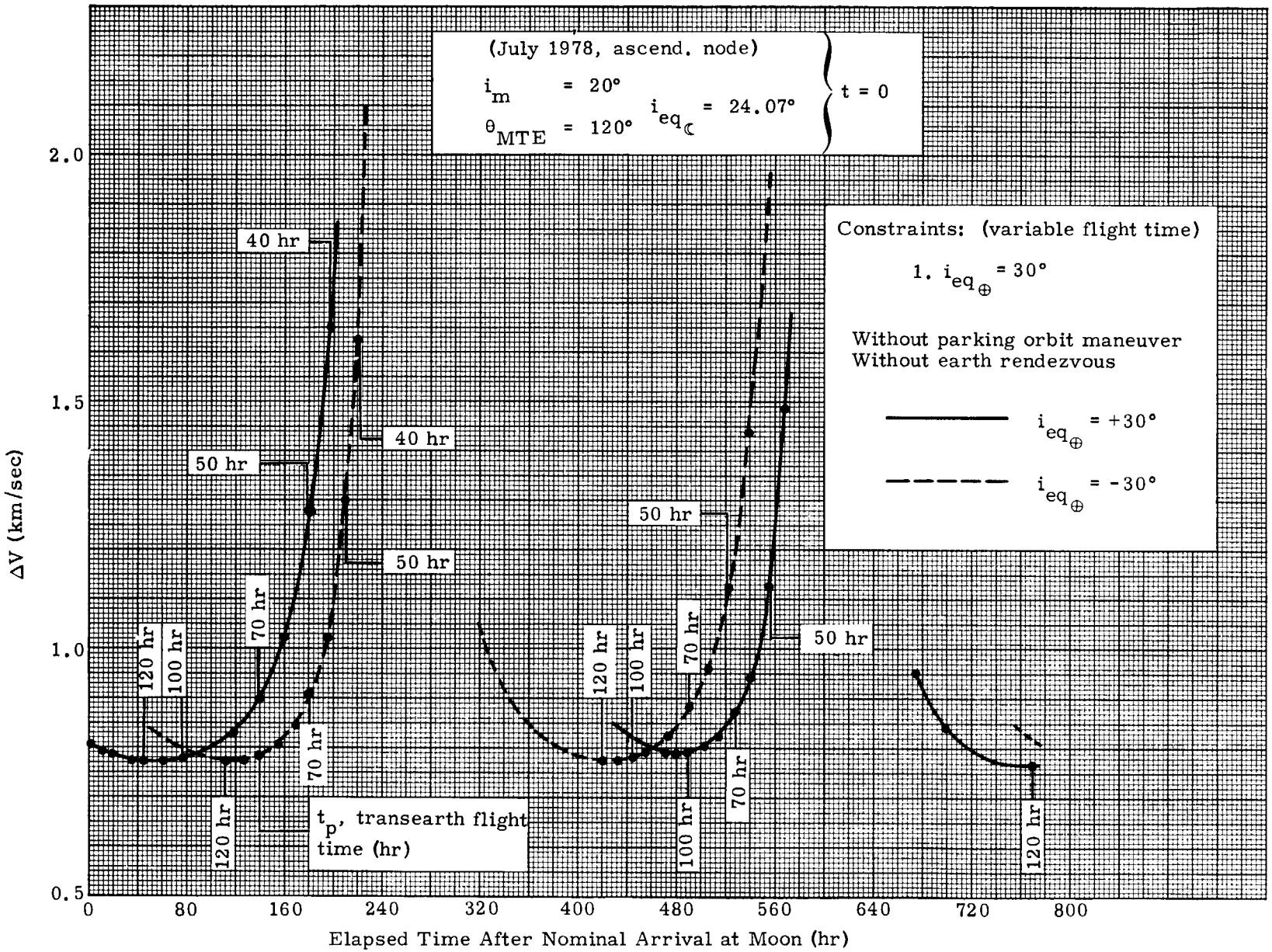


Fig. 15. Energy Requirements for Transearth Departure Windows

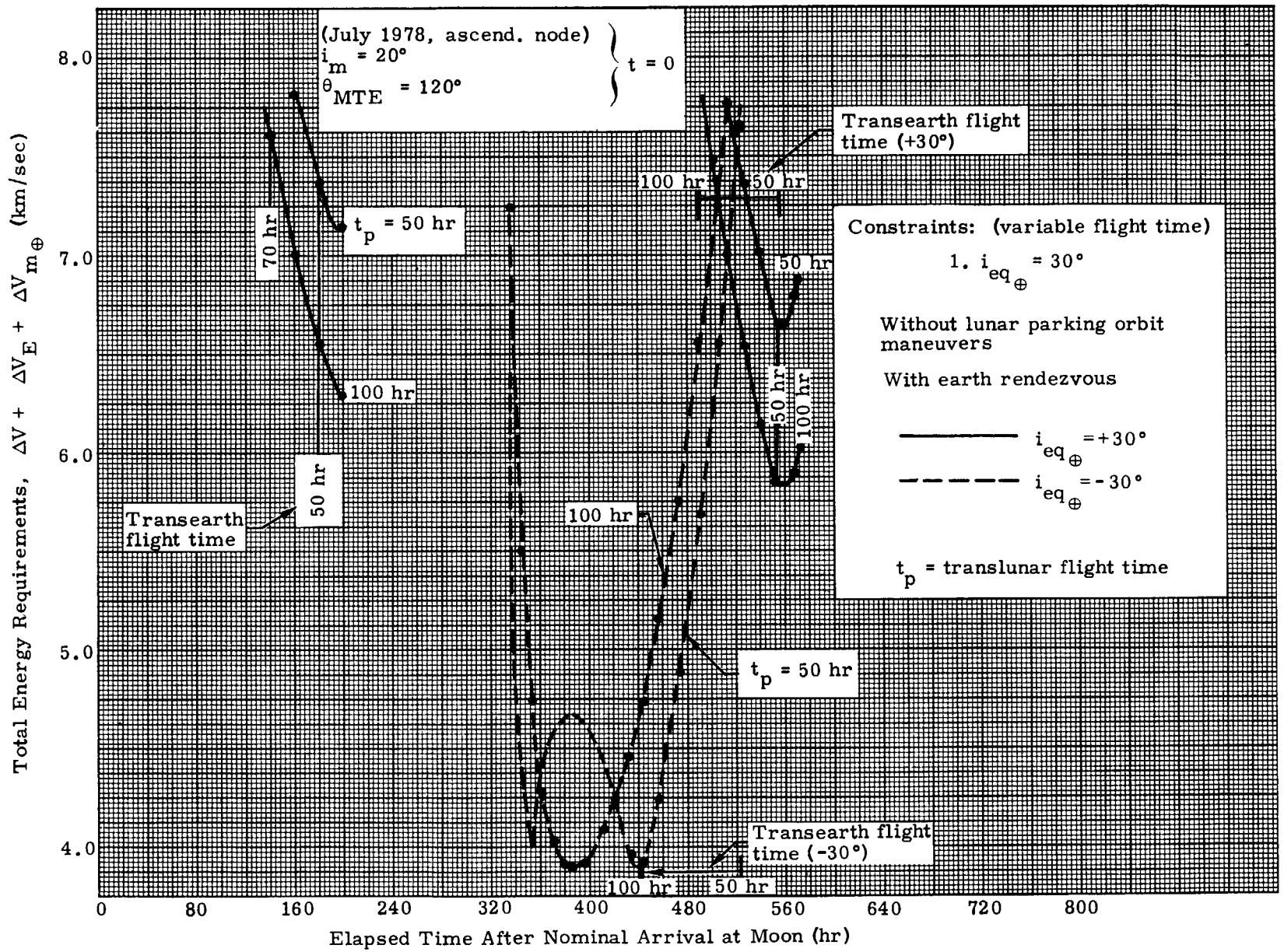


Fig. 16. Energy Requirements for Transearth Departure Windows

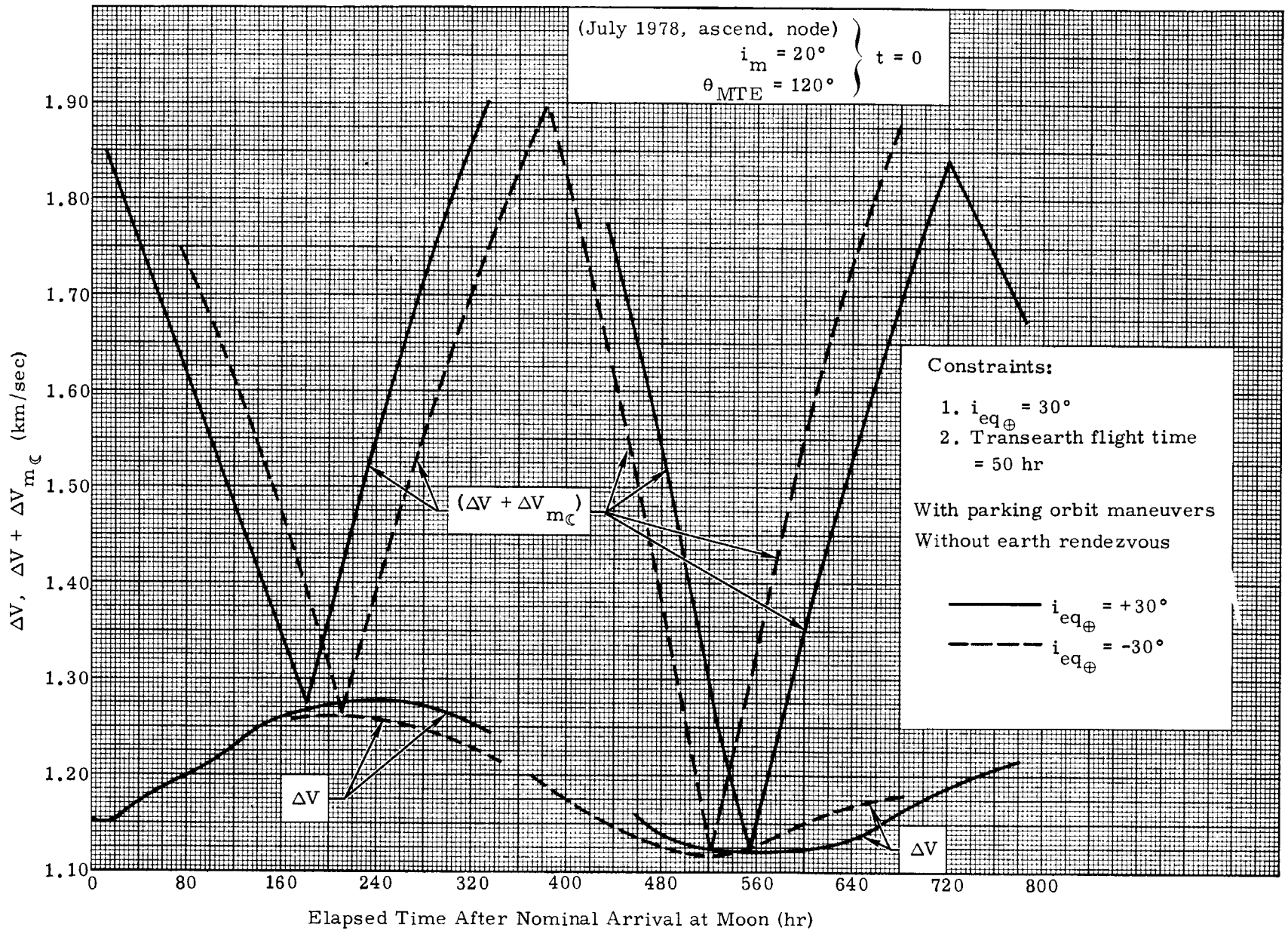


Fig. 17. Energy Requirements for Transearth Departure Windows

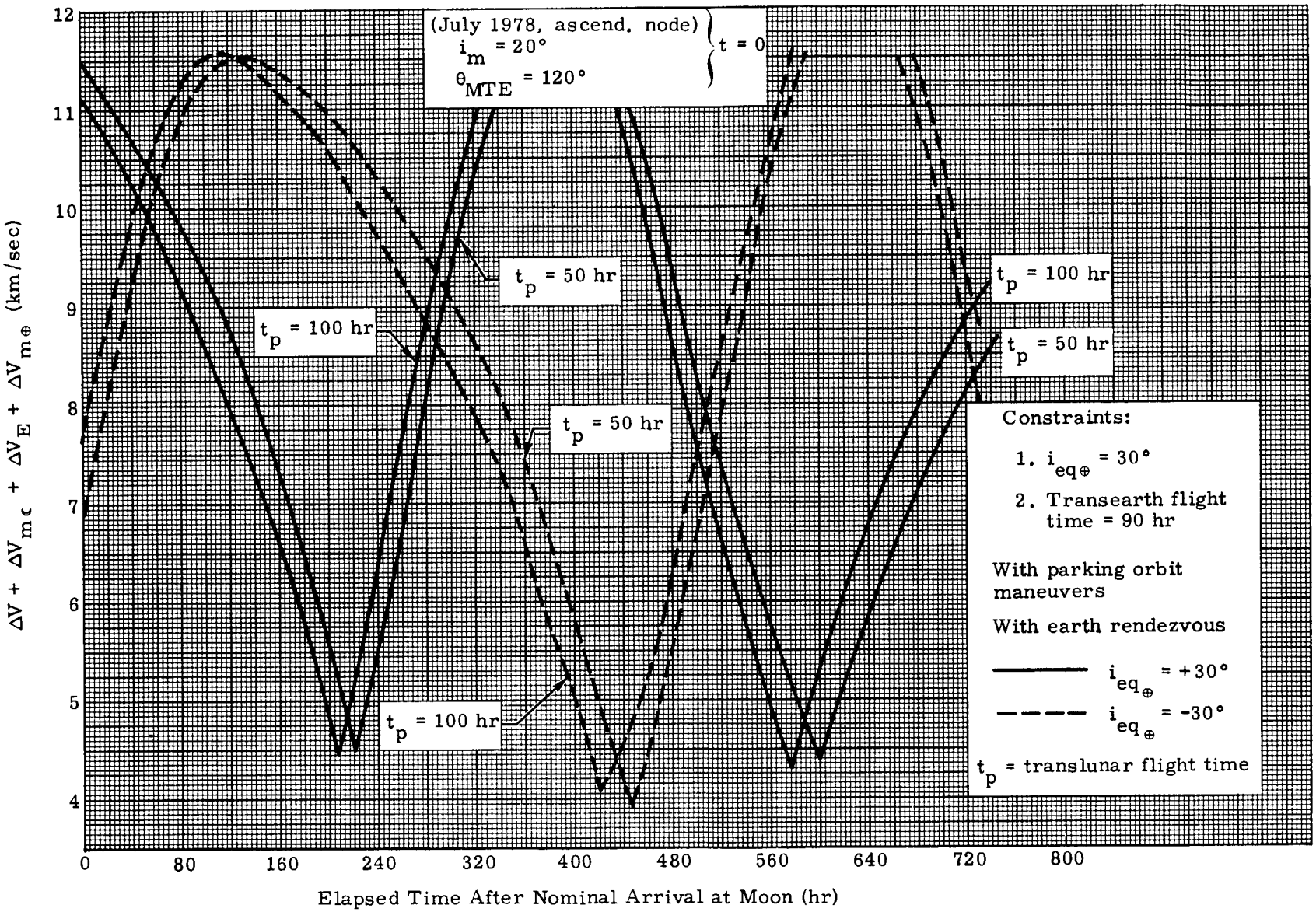


Fig. 18. Energy Requirements for Transearth Departure Windows

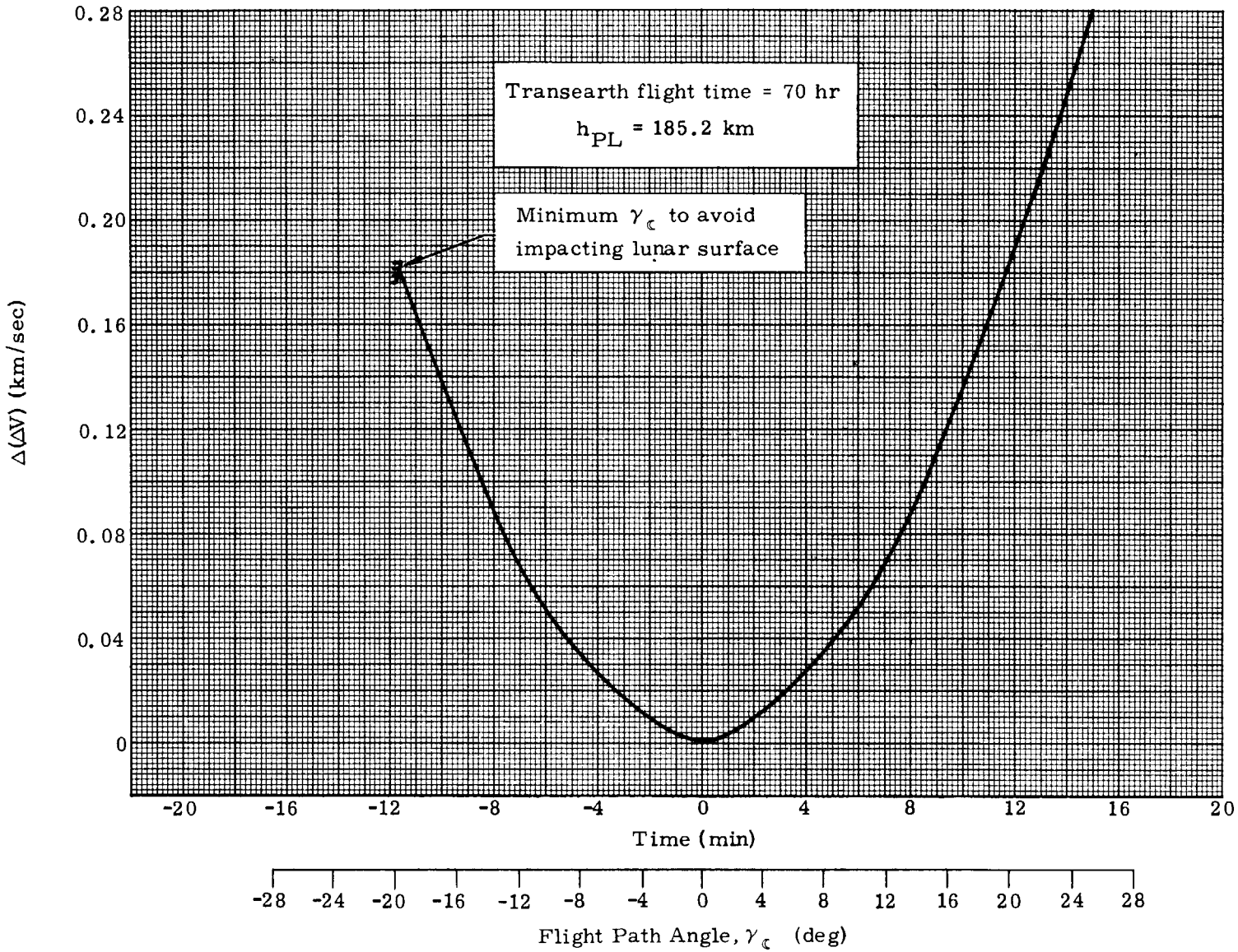


Fig. 19. Velocity Requirements for Inject-on-Time Window

CHART 1

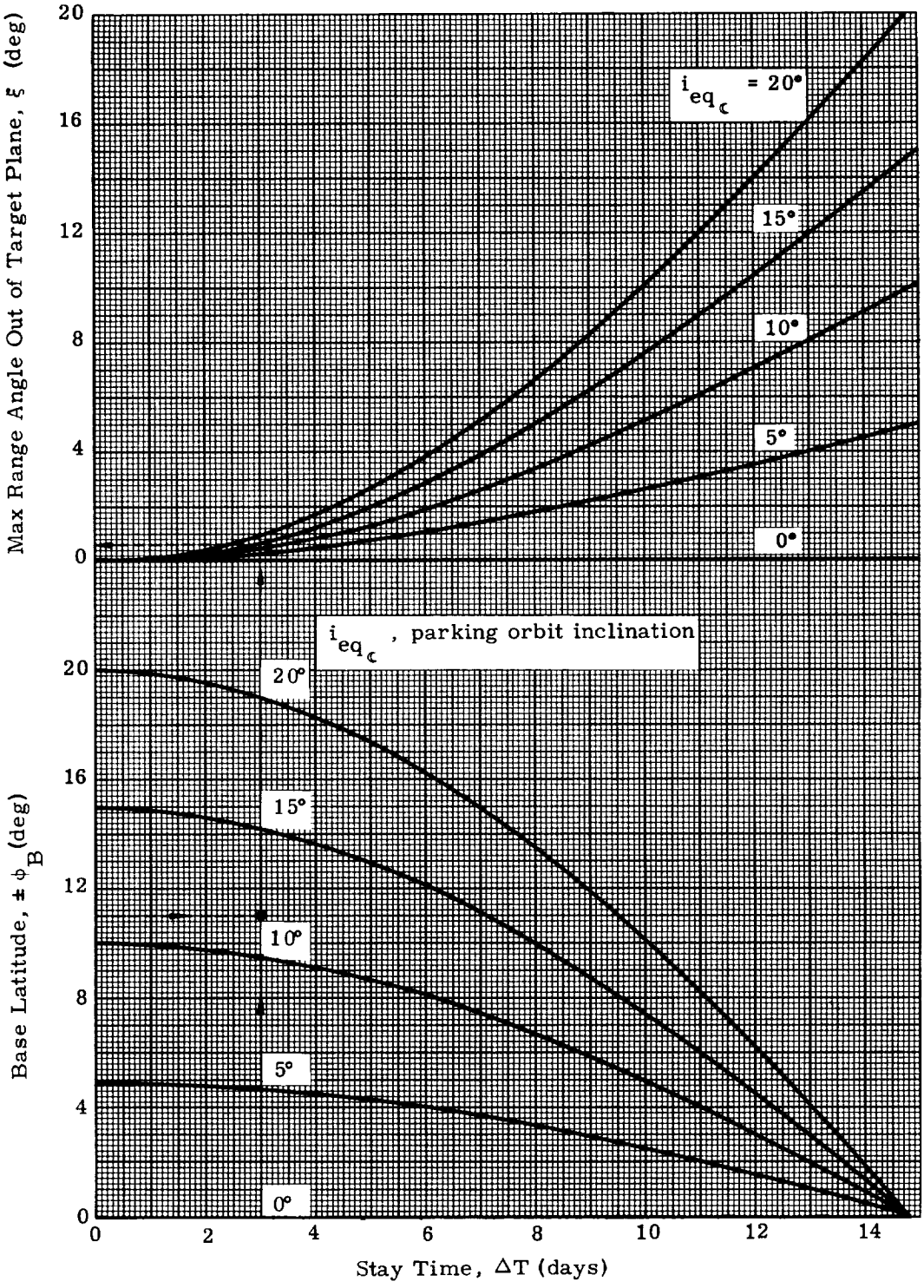


Fig. 20. Surface Stay Time as Dictated by Rendezvous Requirements in Parking Orbit

CHART 2

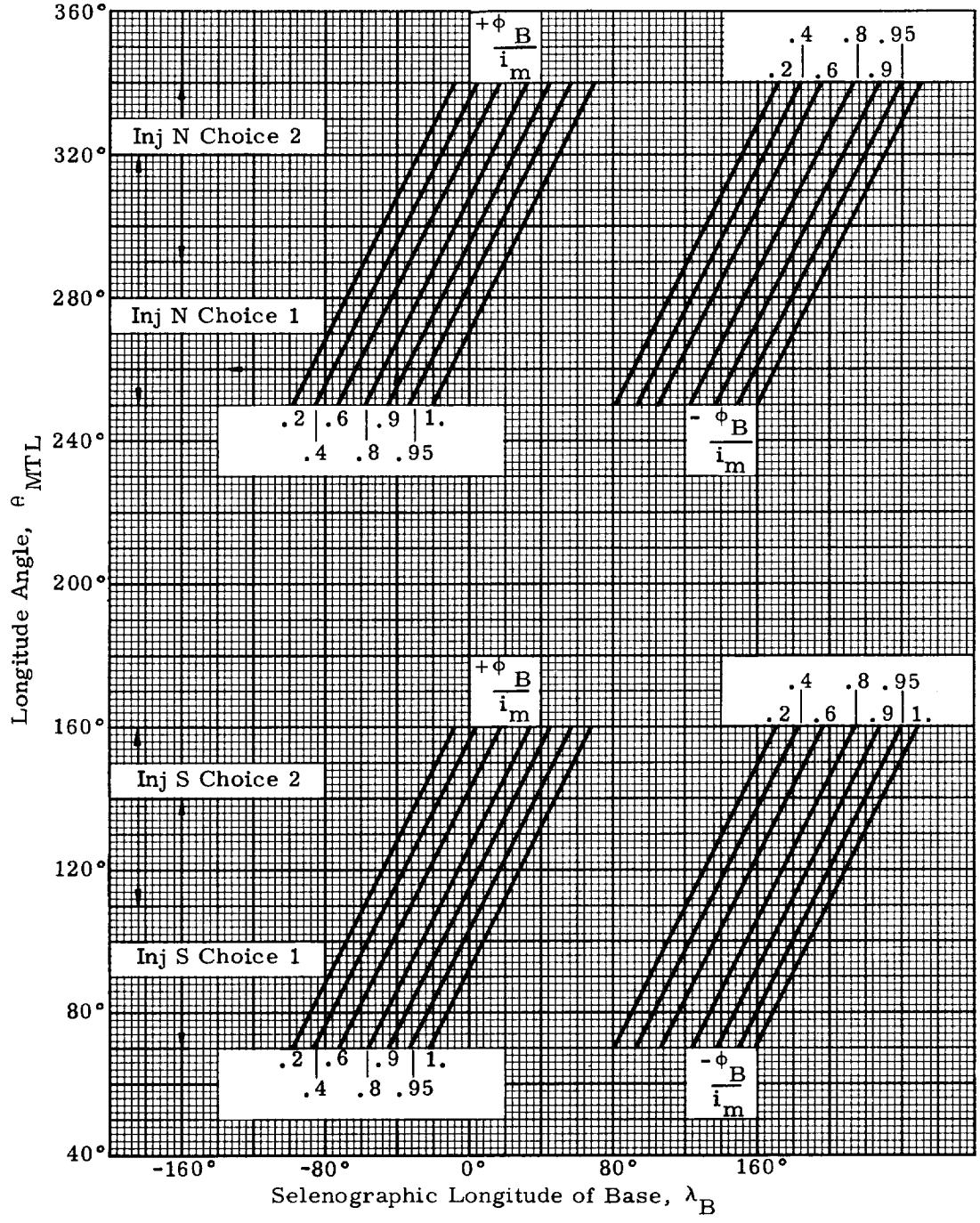


Fig. 21. Required Longitude Angle of Descending Node of Lunar Parking Orbit

CHART 3

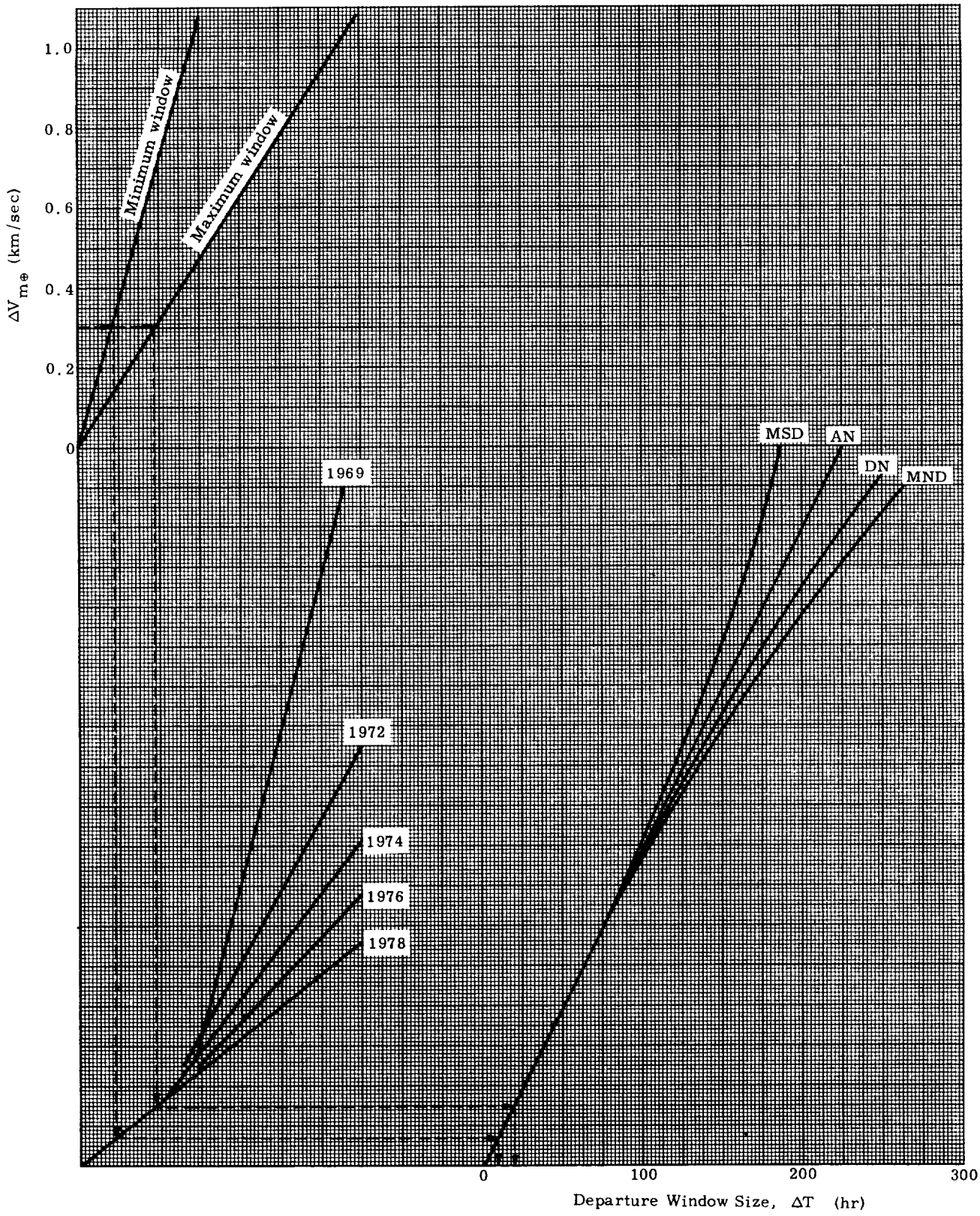


Fig. 22. Translunar Orbital Departure Windows

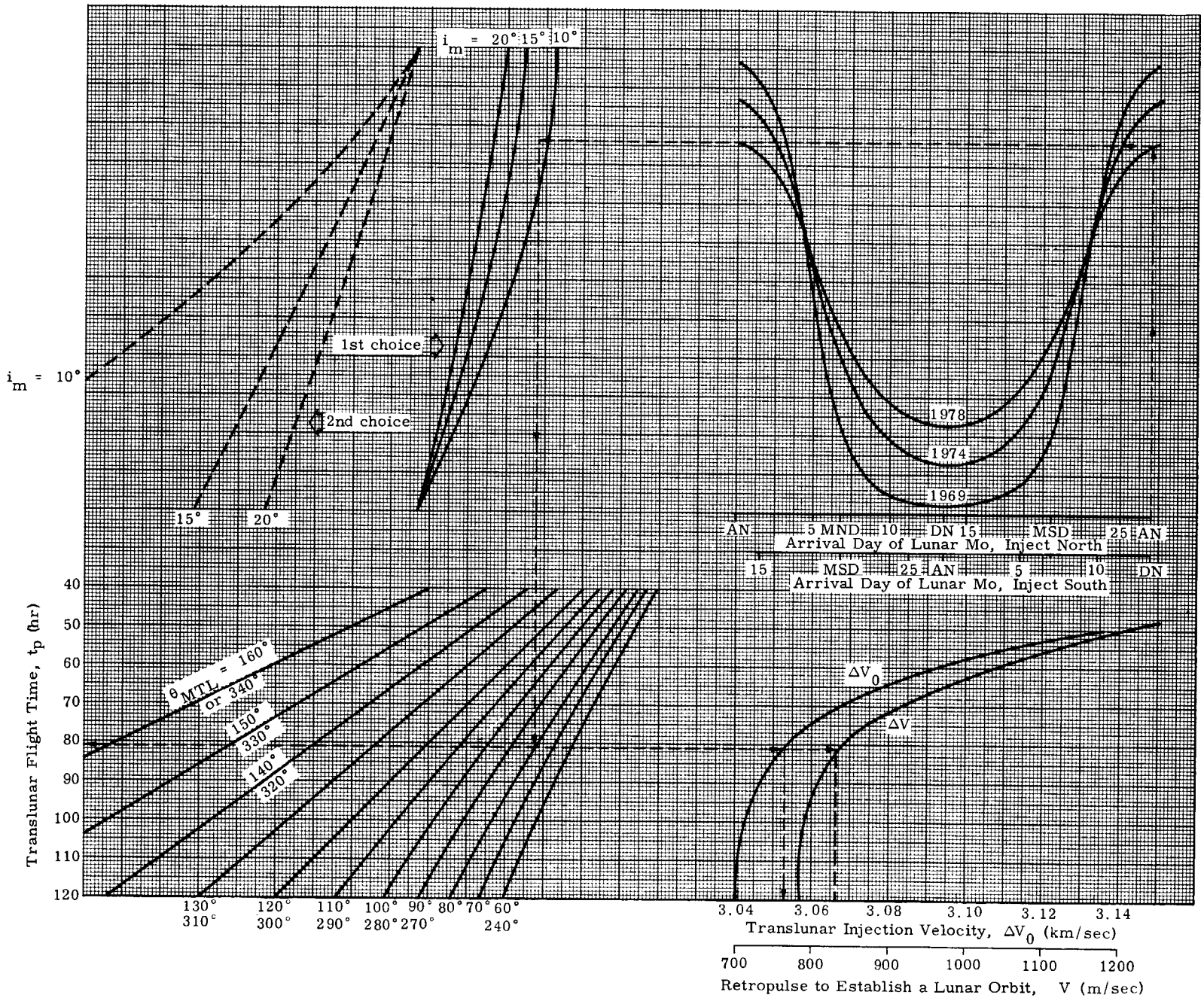


Fig. 23. Translunar Flight Time and Velocity Requirements

CHART 5

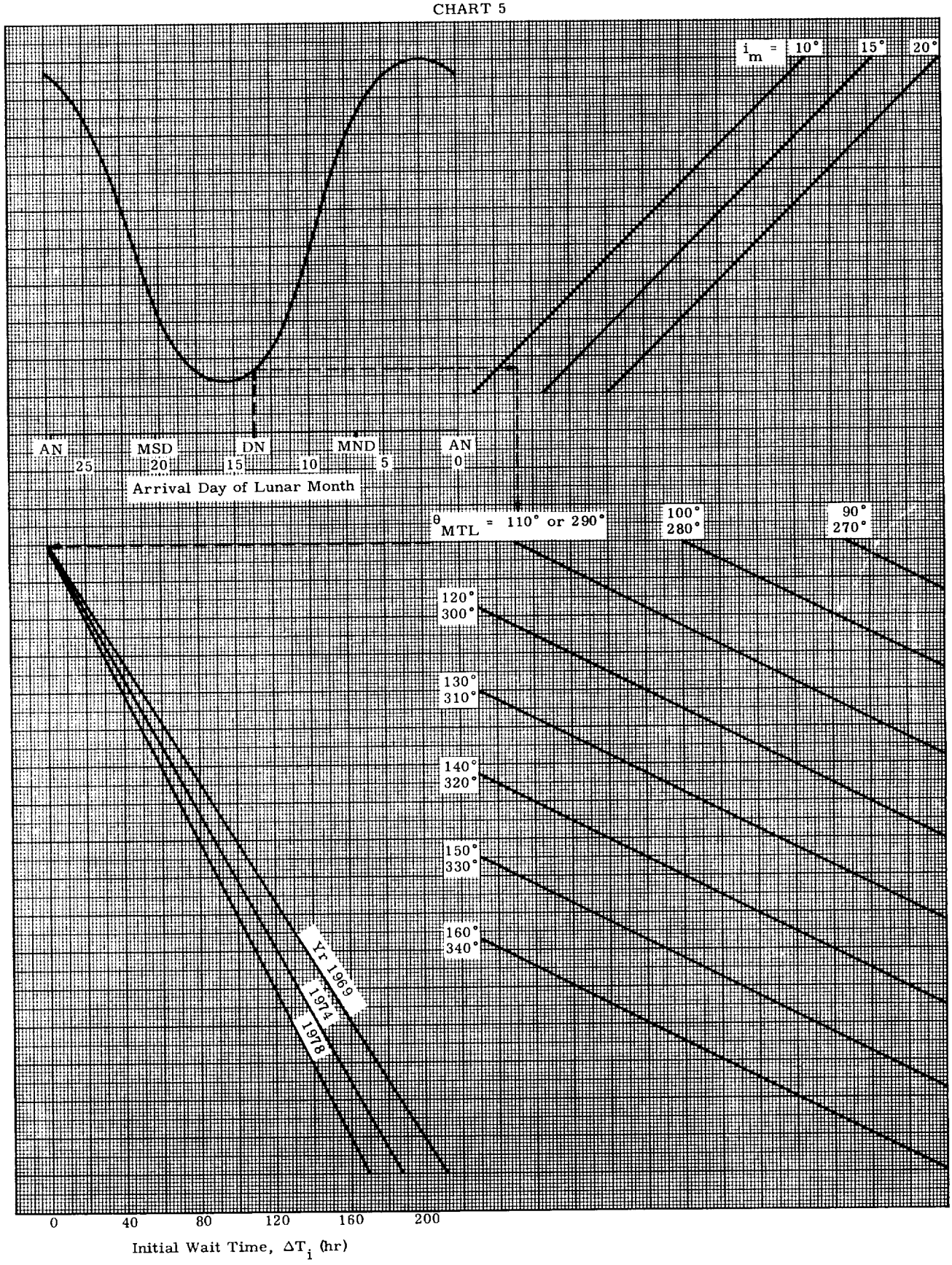


Fig. 24. Initial Wait Time for Transearth Departure Window Entrance

CHART 6

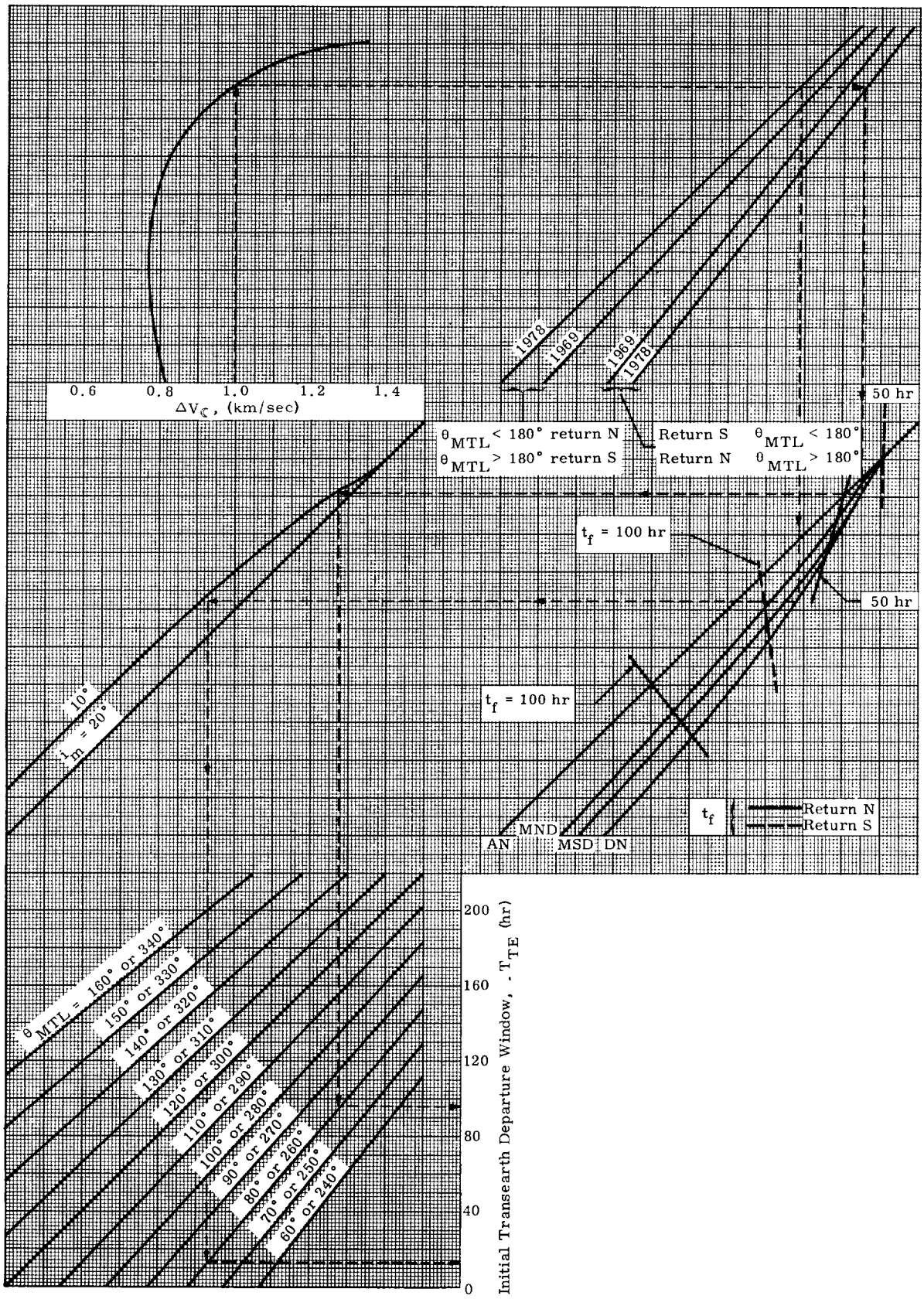


Fig. 25. Initial Transearth Departure Window

CHART 7

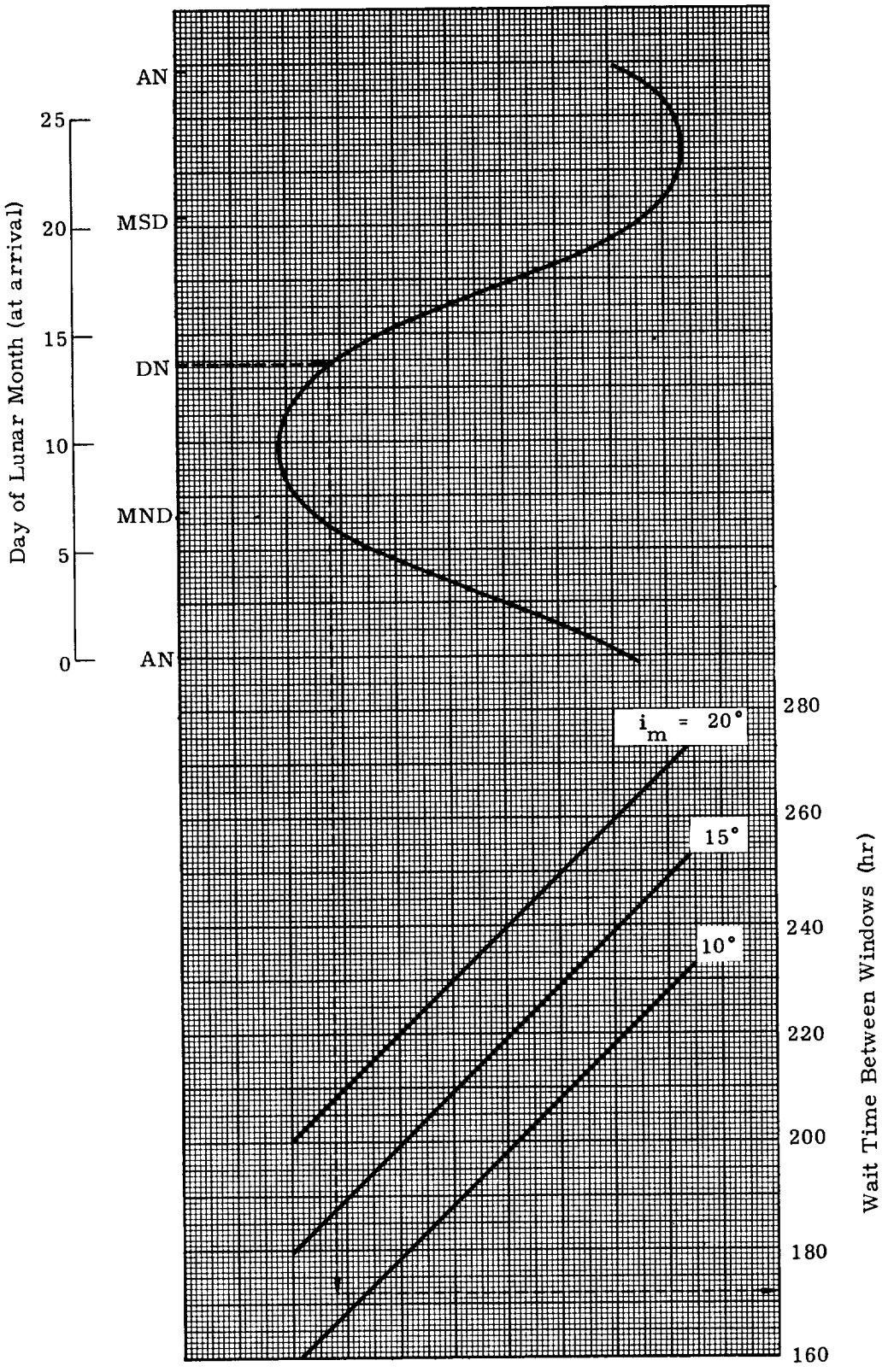


Fig. 26. Wait Time Between Transearth Orbital Departure Windows

CHART 8

NOTE:

$t_s$ = 400 hr is an elapsed time of one lunar month from initial arrival to second arrival.

$t_s$, stay time at moon

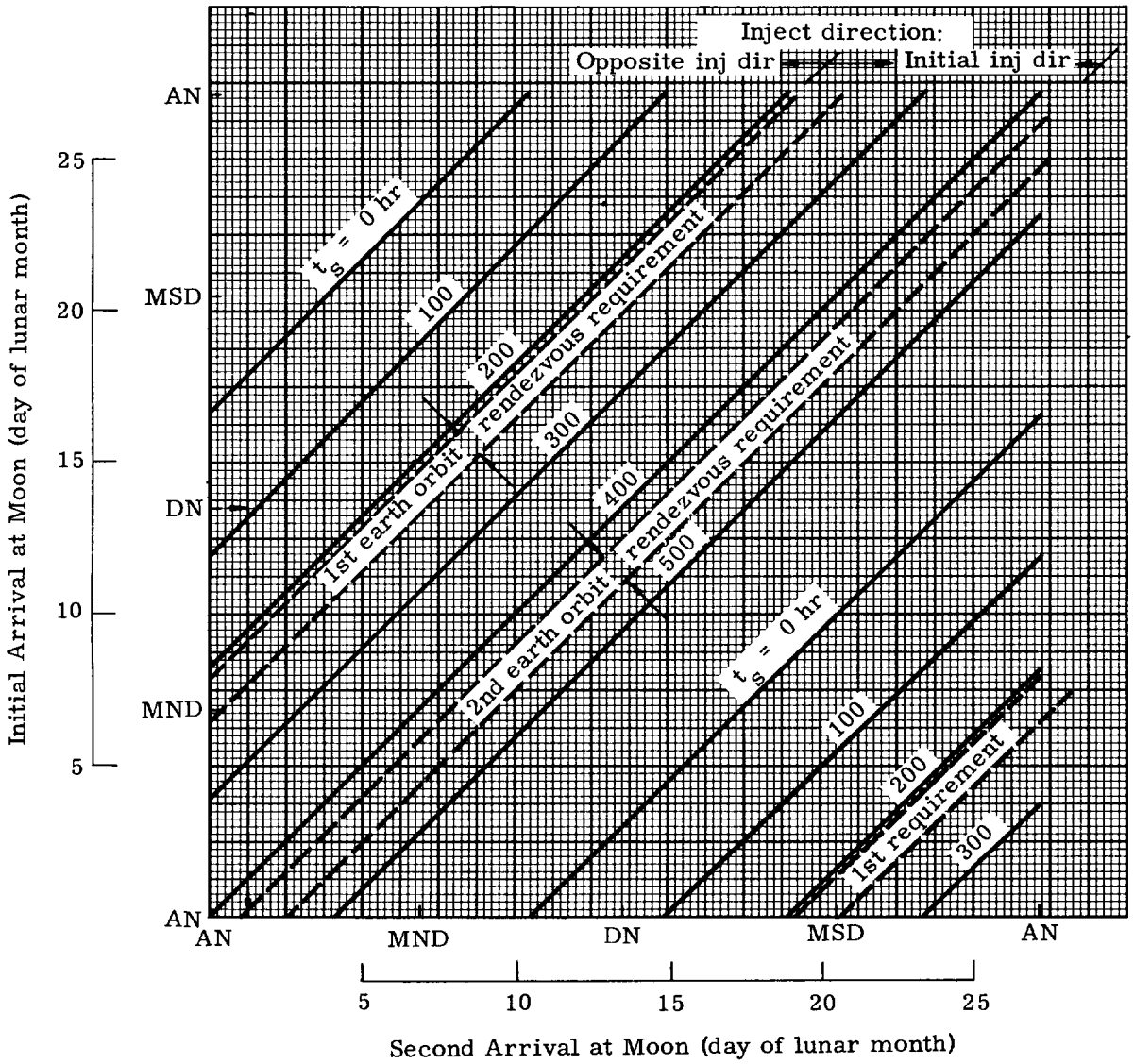


Fig. 27. Updating of Translunar Launch Date